Zooplankton-mediated carbon flux in the Southern Ocean: influence of community structure, metabolism and behaviour

Cecilia Liszka

A thesis submitted to the School of Environmental Sciences of the University of East Anglia in partial fulfilment of the requirements for the degree of Doctor of Philosophy

July 2018

Abstract

The biological carbon pump (BCP) exerts an important control on climate, exporting organic carbon from the ocean surface to interior. Zooplankton are a key component of the BCP and may enhance it through diel vertical migration (DVM) and faecal pellet production at depth. However, variability in these processes mean the zooplankton term is insufficiently constrained in global climate models. I investigated the role of zooplankton in the BCP at four locations in the Scotia Sea, Southern Ocean (SO), combining observations, in situ experiments and modelling.

I found that carbon flux is highly dependent on zooplankton structure, behaviour and community dynamics, with strong latitudinal variations. Zooplankton demonstrated a high degree of behavioural plasticity. Normal, reverse and non-migration modes were common within species and at the community level, with implications for seasonal export flux. Carbon export (faecal pellet and respiration flux) from migrants was generally higher north of the Southern Antarctic Circumpolar Current Front (SACCF), corresponding to greater species biomass and diversity, but could be highly variable. Faecal pellet attenuation depth, defined as the depth from which faecal pellet flux decreased from its maximal value, also corresponded to zooplankton biomass, being deeper in the north, and shallowest nearer the ice.

DVM may explain enhanced night-time fluxes which comprised a shallower input of dense, fast-sinking faecal pellets with high sinking velocities. Community-scale reverse migrations during summer reduced flux from migrants suggesting that at high latitudes, mode of migration may be important in determining zooplankton community carbon flux. Variability in water column temperature during DVM also affected carbon flux from respiration from *Euphausia triacantha*, a widespread SO euphausiid and interzonal migrant. The first comprehensive measurements of this kind showed short-term respiration rates to vary with a Q_{10} of ~4.7 between 0.2 and 4.7 °C. In model simulations, respiration flux accounted for two-thirds of total annual carbon flux from *E. triacantha*, dominating during summer when upper water column temperature was most variable.

Modelled carbon flux was also highly sensitive to feeding dynamics and migratory behaviour. Flux was enhanced during carnivorous feeding and asynchronous migration. However, when considering feeding dynamics and seasonal mixed layer depths, lower export was predicted from foray compared to 'classical' DVM. In summary, regions of high mesozooplankton biomass can generate large fluxes of carbon which penetrate the mid-mesopelagic but are also more difficult to predict due to variability in zooplankton behaviour and ecology. This will be improved with a deeper understanding of species-specific feeding and migration behaviours.

Contents

List of Tables 9
List of Figures 12
Acknowledgements 16
Chapter 1: Introduction 17
1.1 The oceans and biogeochemical cycling 17
1.1.1 The Biological Carbon Pump 19
1.1.2 The Southern Ocean and Scotia Sea 21
1.1.3 Zooplankton of the Southern Ocean 25
1.2 Zooplankton and the biological carbon pump 26
1.2.1 Zooplankton diel vertical migration 28
1.2.2 DVM and active flux 29
1.3 Motivation of the thesis 32
1.3.1 Specific aims of each chapter 33
Chapter 2: The influence of the Scotia Sea zooplankton community on diel vertical migration and carbon flux 36
2.1 Introduction 36
2.1.1 The Scotia Sea 36
2.1.2 Zooplankton of the Scotia Sea 37
2.1.3 Zooplankton and carbon flux 37
2.1.4 Purpose of the current study 38
2.2 Methodology 40
2.2.1 Physical environment and hydrography 40
2.2.2 Sampling strategy 40
2.2.3 Sample analysis 43
2.2.4 Data preparation and pre-treatment 43
2.2.5 Data analysis and statistics 44
2.2.6 Calculating biomass and carbon flux 46
2.3 Results 52
2.3.1 Physical environment and hydrography 52
2.3.2 Analysis of stations over depth and latitude 54
2.3.3 Taxonomic contribution to station groupings 59
2.3.4 Diurnal variability in species vertical migrations and distributions 66
2.3.5 Carbon flux from migratory zooplankton 74
2.4 Discussion 76

2.4.1 Zooplankton community structure across the Scotia Sea 76
2.4.2 Evidence for diel vertical migration at individual and community scale 78
2.4.3 Influence of vertical migration on carbon flux 81
2.4.4 Summary 85
Chapter 3: Zooplankton abundance and behaviour increases faecal pellet flux and remineralisation depth in the Southern Ocean 86
3.1. Introduction 86
3.1.1 Zooplankton faecal pellets and the biological pump 86
3.1.2 Uncertainty in faecal pellet-mediated export 86
3.1.3 Purpose of the study 88
3.2 Material and methods 89
3.2.1 Study area and sampling 89
3.2.2 Sample analysis 92
3.2.3 Data analysis and statistics 95
3.3 Results 97
3.3.1 Environmental and hydrographical context 97
3.3.2 Mesozooplankton analysis 98
3.3.3 Faecal pellet and sample analysis 101
3.4 Discussion 110
3.4.1 Is the mesozooplankton community a good predictor of faecal pellet export? 110
3.4.2 Race to the bottom: large, dense faecal pellets are the biggest contributors to flux 114
3.4.3 Attenuation of faecal pellet carbon is strongly modulated by zooplankton 115
3.4.4 Conclusion 119
3.4.5 Summary 119
Chapter 4: The effect of diel vertical migration on the respiration rate of a prominent Southern Ocean euphausiid, *Euphausia triacantha* 121
4.1 Introduction 121
4.1.1 *E. triacantha* distribution and ecology 121
4.1.2 Zooplankton vertical migrations and active flux 122
4.1.3 Metabolic theory 123
4.1.4 Purpose of the current study 124
4.2 Materials and methods 124
4.2.1 *Euphausia triacantha* distribution, abundance and environmental conditions 124
4.2.2 Measuring oxygen consumption 125
4.2.3 Determination of length, weight and carbon content 136

4.2.4 Data treatment 136
4.3 Results 138
4.3.1 Distribution and environment of *Euphausia triacantha* 138
4.3.2 Morphometric and elemental analysis 140
4.3.3 Statistical analysis 145
4.4 Discussion 147
4.4.1 Context of study 147
4.4.2 Overall response to temperature and size 147
4.4.3 Difference in response between years 149
4.4.4 Factors affecting variability in respiration rate 151
4.4.5 Overall findings in the context of other studies 155
4.4.6 Evidence for metabolic cold adaptation? 158
4.4.7 Summary and implications 159
Chapter 5: Modelling the active carbon flux from the sub-Antarctic krill, *Euphausia triacantha*, in the Atlantic sector of the Southern Ocean 161
5.1 Introduction 161
5.1.1 Purpose of the current study 162
5.2 Materials and methods 162
5.2.1 Model construction 162
5.2.2 Model inputs and assumptions 164
5.2.3 Scaling the model up 173
5.2.4 Sensitivity analyses 174
5.3 Results 176
5.3.1 Mixed layer depths 176
5.3.2 *E. triacantha* south Atlantic latitudinal distribution 177
5.3.3 Main ('BEST') model results 178
5.3.4 Results of sensitivity analyses 182
5.4 Discussion 188
5.4.1 Carbon export from respiration is affected by temperature and migrating population 190
5.4.2 Carbon export from egestion is highly sensitive to feeding behaviour 192
5.4.3 Summary 196
Chapter 6: Synthesis 197
6.1 Overview 197
6.2 Key findings 198
6.3 Concluding remarks 202
6.4 Directions for future work 206

Glossary 210
Appendix 1: Flow rate data 211
Appendix 2: Mesozooplankton abundance at individual stations 216
Appendix 3: Temperature variation in respiration experiments 218
References 220

List of Tables

Chapter 2

Table 2.1 Locations, dates and times of sampling and duration of MOCNESS deployments 42

Table 2.2 Parameters used in biomass flux calculation 48

Table 2.3 Dissimilarity statistics from SIMPER analysis carried out on the main groupings identified by multivariate analysis 61

Table 2.4 Taxa identified as cumulatively contributing to ≥50% difference between SIMPER groups 62

Table 2.5 Biomass fluxes over a diurnal period (mg DW m^{-2} d^{-1}) 68

Table 2.6 Diurnal fluxes of the species/ taxa driving biomass fluxes in at least one station 69

Table 2.7 Mean biomass (mg DW m^{-2}) averaged over each D and N sample per station 74

Table 2.8 Total active flux and maximum total C flux (mg C m^{-2} d^{-1}) for stations in S08 and A09 75

Chapter 3

Table 3.1 Details of 0 – 200 m Bongo nets with 200 µm mesh that were deployed during JR304 91

Table 3.2 Station name, date, time and geographical coordinates of experimental CTD deployments 91

Table 3.3 Semi-quantitative assessment of the most commonly observed diatom groups at ICE, P2 and P3 101

Chapter 4

Table 4.1 Details of the experiments carried out on JR304 and JR15002 135

Table 4.2 Regression coefficients for log wet, dry, carbon and nitrogen weight (WW, DW, C and N, mg) against log length (mm) 140

Table 4.3 Regression statistics for C and N content of *E. triacantha* as a function of WW and DW, and the %C, %N and C:N ratio as a function of DW (mg) 142

Table 4.4 Regression statistics for O_2 consumption as a function of temperature (°C) and weight (mg DW, C and N) for *E. triacantha* 145

Table 4.5 Regression statistics for weight specific respiration plotted against temperature for *E. triacantha* …… 146

Chapter 5

Table 5.1 Table of all the terms used in the construction and description of the model…… 165

Table 5.2 Table of chl-*a* (µg l^{-1}) values assigned to the model based on latitudinal zones of productivity …….. 167

Table 5.3 Description of all the model runs that were carried out …… 174

Table 5.4 Table of coefficients to explain the relationship between O_2 consumption and temperature for *E. triacantha*, reproduced from Chapter 4 …… 175

Table 5.5 Abundance of *E. triacantha* in the south Atlantic from the original Discovery expeditions of the 1920s and 1930s, reproduced from Mackey et al. (2012) …….. 178

Table 5.6 Contribution to C flux per degree of latitude in the south Atlantic sector of the SO for respiratory flux (C_R), egestory flux (C_E) and total C flux (C_{TOT}) as a % of the total C_R, C_E or C_{TOT} respectively …… 179

Table 5.7 Table showing the results of all sensitivity analyses, ranked alongside the results of the main model run ('BEST') in terms of size of difference …… 184

Appendix 1

Table A1.1 Volume of water filtered by MOCNESS deployments on JR177 based on flow rate data which was used to calculate volume filtered on a few occasions when the flowmeter failed …….. 211

Table A1.2 Volume of water filtered by MOCNESS deployments on JR200 (description as per previous) …….. 213

Appendix 3

Table A3.1 Mean temperature (°C) at T1 for every measuring point for each *Euphausia triacantha* respiration experiment …….. 218

Table A3.2 Mean temperature (°C) at T2 for every measuring point for each *Euphausia triacantha* respiration experiment …….. 218

Table A3.3 1 and 2 standard deviations for mean temperatures during each *Euphausia triacantha* respiration experiment …….. 219

Table A3.4 Percentage of measuring points for each year within 1 and 2 standard deviations 219

List of Figures

Chapter 1

Figure 1.1 Schematic of the global carbon cycle taken from Ciais et al. (2013) 17

Figure 1.2 Schematic of the three major ocean carbon pumps involving the regulation of atmospheric CO_2 changes by the ocean (taken from Heinze et al., 1991) 18

Figure 1.3 Schematic of the biological carbon pump, taken from Chisholm (2000) ... 20

Figure 1.4 Diagram illustrating a cross-section of the SO showing the principal water masses, fronts and zones (taken from Talley et al. (2011)). 22

Figure 1.5 The Southern Ocean including land masses and frontal features (taken from Talley et al. (2011)) 24

Figure 1.6 Schematic showing how zooplankton vertical migration can enhance the flux of respiration and faecal pellets to the deep ocean 30

Figure 1.7 Schematic illustrating two different modes of migration 32

Chapter 2

Figure 2.1 Map of the Scotia Sea showing the locations of sampling stations (adapted from Venables et al. (2012) 41

Figure 2.2 Schematic illustrating the steps taken to calculate the total biomass flux 51

Figure 2.3 Temperature and salinity profiles of stations R1, C3, P2 and P3 in S08 and A09 53

Figure 2.4 Chlorophyll fluorescence profiles for stations R1, C3, P2 and P3 in S08 and A09 54

Figure 2.5 nMDS plot of the S08 and A09 combined dataset 56

Figure 2.6 Ordination analysis on seasonally split data for S08 57

Figure 2.7 Ordination analysis on seasonally split data for A09 58

Figure 2.8 Bubble plots for S08 (A-D) and A09 (E-G) based on the 0.5% subset of taxa overlain on nMDS ordinations for each year 63

Figure 2.9 Diurnal population distributions of the six taxa exhibiting the largest biomass fluxes at each station 70

Figure 2.10 Schematic of main migrators at each station in S08 and A09 82

Chapter 3

Figure 3.1 Mean chlorophyll data for the month covering sampling (stations marked with filled blue circles) 90

Figure 3.2 Siphoning setup used to drain the contents of the carboys through a 53 µm mesh 92

Figure 3.3 Profiles of chl-*a* concentrations (µg l^{-1}) based on fluorescence measurements at ICE, P2 and P3 98

Figure 3.4 Group average cluster dendrogram of mesozooplankton samples taken with 0 – 200 m Bongo nets 99

Figure 3.5 Non-metric MDS plot of abundance by prosome length (PL) at each station with cluster analysis groups (determined by SIMPROF testing) superimposed 100

Figure 3.6 Mesozooplankton abundance and size spectra based on prosome length (PL) at ICE, P2 and P3 101

Figure 3.7 Left panel: Total abundance of faecal pellets at each station, stacked by contribution of different morphological type; Right panel: Total volume of faecal pellets at each station, stacked by contribution by different morphological type 103

Figure 3.8 Plot of the mean size (volume, mm^3) of faecal pellets across depth at ICE, P2 and P3 104

Figure 3.9 Area plots of predicted versus observed faecal pellet size distributions 105

Figure 3.10 Light microscope images of broken cylindrical, intact ovoid, spherical and partially broken ellipsoidal faecal pellets typical of those found in samples 107

Figure 3.11 SEM images of broken cylindrical, intact ovoid, spherical and partially broken ellipsoidal faecal pellets typical of those found in samples 108

Figure 3.12 Average faecal pellet sinking velocity (m d^{-1}) at ICE, P2 and P3 stations 109

Figure 3.13 faecal pellet flux (mg C m^{-2} d^{-1}) at ICE, P2 and P3 stations 110

Chapter 4

Figure 4.1 Photograph of the incubator setup on cruise JR304 128

Figure 4.2 Photograph showing the incubator set-up and insulation during JR15002 129

Figure 4.3 Photographs showing how the thermocirculator was stabilised and protected 130
Figure 4.4 Schematic showing the setup of the experiment in year 1 (JR304) and year 2 (JR15002) (not to scale) 132
Figure 4.5 Mean and SD of animal sizes in JR15002 experiments 133
Figure 4.6 Plots showing the day and night time abundances (individuals m^{-2}) of *E. triacantha* during summer and autumn at C3, P2 and P3 with station temperature data overlain 139
Figure 4.7 The relationship between log length (mm) and log wet (WW) and dry (DW) weight of *E. triacantha* (top panel); and between log length and log carbon (C) and nitrogen (N) (bottom panel) 141
Figure 4.8 Log C and N content (mg) plotted against weight (log WW and log DW, mg) 143
Figure 4.9 Elemental (CN) ratios: A) % C and % N plotted against DW and B) C:N ratio plotted against DW 144
Figure 4.10 Weight-specific oxygen consumption (µl O_2 mg DW^{-1} h^{-1}) plotted as a function of temperature (°C) 146
Figure 4.11 Published respiration rates from other authors for comparative species of euphausiid across temperatures ranging from -1.55 to 16 °C 157

Chapter 5

Figure 5.1 Schematic illustrating how the model was constructed, showing key inputs, variables and outputs 164
Figure 5.2 Temperature profiles for the vertical distribution of *E. triacantha* at representative latitudes of the Atlantic sector of the Southern Ocean deployed during JR161, JR177 and JR200 169
Figure 5.3 Schematic illustrating foray migration and the definition of feeding cycles 170
Figure 5.4 Variation of mixed layer depth (MLD, m) with latitude and time of year 177
Figure 5.5 Contour plot showing the total C flux (respiration and egestion) from the main model run ('BEST') across the full model extent (latitudes 50 to 65° S) in the Atlantic sector 180

Figure 5.6 Stacked bar plot of the relative contributions of C_R (orange) and C_E (green) to total C flux across the year at stations representative of different latitudes 181

Figure 5.7 Total C flux (kilotonnes) across latitude and month of year for sensitivity analyses 185

Figure 5.8 Plots of relative C_R (orange) and C_E (green) of selected sensitivity analyses that represent the maximum and minimum difference to C export 187

Chapter 6

Figure 6.1 Schematic showing how different sampling times or migration patterns may lead to incorrect conclusions when sampled only once during day and night 208

Appendix 1

Figure A1.1 Plots of haul duration (minutes) and volume filtered (m^3) with equations used to calculate missing volumes for JR177 (top) and JR200 (bottom) ... 215

Appendix 2

Figure A2.1 Average mesozooplankton abundance and size spectra based on prosome length at ICE 216

Figure A2.2 Average mesozooplankton abundance and size spectra based on prosome length at P2 216

Figure A2.3 Average mesozooplankton abundance and size spectra based on prosome length at P3 217

Acknowledgements

I would like to say a huge and heartfelt thank you to my entire supervisory team, Geraint Tarling, Clara Manno, Carol Robinson and Gabi Stowasser. You gave me the opportunity to pursue an ambition that has opened up a whole new world to me and have given me constant encouragement and support along the way. Thank you for all the time you have given me, for reading through countless drafts and for your thought-provoking and critical feedback that has undoubtedly made me a better and more critical scientist. In fact, thank you for making me a scientist! I am truly grateful. I am also indebted to Pete Ward for the many very happy hours spent learning taxonomy and putting the world to rights at the microscope. Without your teaching I would never know what I know now about Southern Ocean zooplankton, or probably be so enthusiastic about it. Your patience is also amazing!

Thank you to all the people at BAS who have helped me along the way, in particular Paul Geissler, Guy Hillyard and Elaine Fitzcharles for lab support; Laura Gerrish for help with mapping; Hugh Venables for mapping and interesting scientific discussions; and Ali Teague for being an incredible support throughout. Also to the many people in Cambridge that have made this such a great few years, including the original Gisborners, Ryan Patmore and Leyre Villota Nieva; Elise Biersma, for being a wonderful friend and for all the stimulating discussions (often over wine); and Vicky P, Vicky F, Clare, Jen, Ellen, Clara, Gabi and Anna for friendship and fun.

I would like to thank the Captains, Crew and fellow scientists on-board the RRS James Clark Ross for the amazing research cruises I was privileged to join, JR304 and JR15002, without which none of this would have happened. Those cruises and everyone on them instilled in me a love of polar research, during which I learnt all I know about shipboard science, and they have given me the most fantastic memories. Special shout-out to Jessie Gardner, for being my cabin mate and fellow inhabitant of the cold room at sea. I am particularly grateful to NERC, the University of East Anglia and the EnvEast DTP for funding this research. Thank you also to David Thomas and the School of Ocean Sciences at Bangor for hosting me during my last months, and the inhabitants of the Nautilus for being so welcoming.

A whole lot of love to my friends, for bearing with me whilst I went offline during the final months, and for your ‘krilliant’ jokes along the way. Also, my family, for being so incredibly supportive and encouraging, and for your interest in ‘napkin science’. Last but not least, Tim, my partner in crime and life. Thank you for keeping me going through the final few months, keeping me (relatively) sane and always in pizza. I won’t ask you to read any more!

Chapter 1: Introduction

1.1 The oceans and biogeochemical cycling

The oceans are a critical part of the global climate system (see Figure 1.1). They are responsible for the redistribution of heat from the tropics to the poles, the modification of cloud formation, and the exchange of carbon dioxide (CO_2) with the atmosphere (Bigg et al., 2003). The oceanic reservoir of CO_2 is 50 times greater than the atmospheric reservoir (Falkowski et al., 2000) such that the oceans exert a significant control on earth's climate over millennial timescales. Since industrial times, this has resulted in the oceans being responsible for the uptake of ~30% of anthropogenic CO_2 emissions (Stocker et al., 2013).

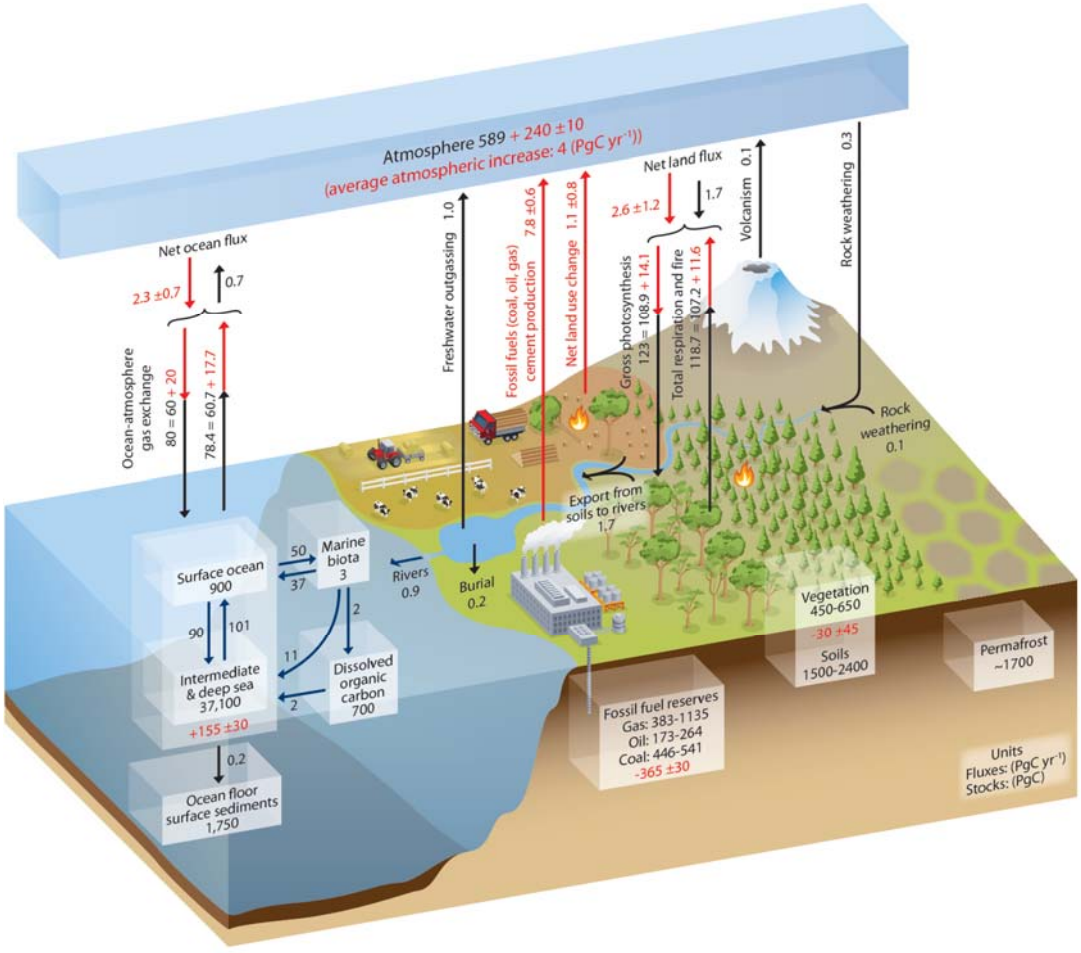

Figure 1.1: Schematic of the global carbon cycle taken from Ciais et al. (2013). The black and red numbers represent the size of carbon reservoirs during the pre-industrial and industrial period, respectively. The black and red arrows represent the size of the fluxes between reservoirs over the same respective time periods.

This uptake of CO_2 by the oceans is controlled mainly by three ocean pumps: the physically-driven solubility pump; and two biological pumps: the carbonate counter pump and the soft-tissue, or biological carbon pump (BCP) (Volk and Hoffert, 1985) (Figure 1.2). Together, these pumps maintain a gradient of CO_2 in the global ocean in which concentrations of dissolved inorganic carbon (DIC) are greater in deeper than shallower waters (Volk and Hoffert, 1985) and which keep CO_2 out of contact with the atmosphere for climatically significant time periods. The solubility pump is based on the equilibration of gaseous CO_2 in the atmosphere with aqueous CO_2 ($CO_{2\,aq}$) in the surface layer of the ocean. Due to the increased solubility of CO_2 in cold water, this pump is strongest at high latitudes and areas of deep water formation (Volk and Hoffert, 1985). The carbonate pump both lowers pCO_2 by removing carbonate ions from surface waters through the bioprecipitation of calcium carbonate ($CaCO_3$), and counteracts this by raising the pCO_2 of surface waters through the removal of calcium ions (Volk and Hoffert, 1985, Legendre et al., 2015). Both of these mechanisms contribute to the export and eventual sequestration of inorganic carbon.

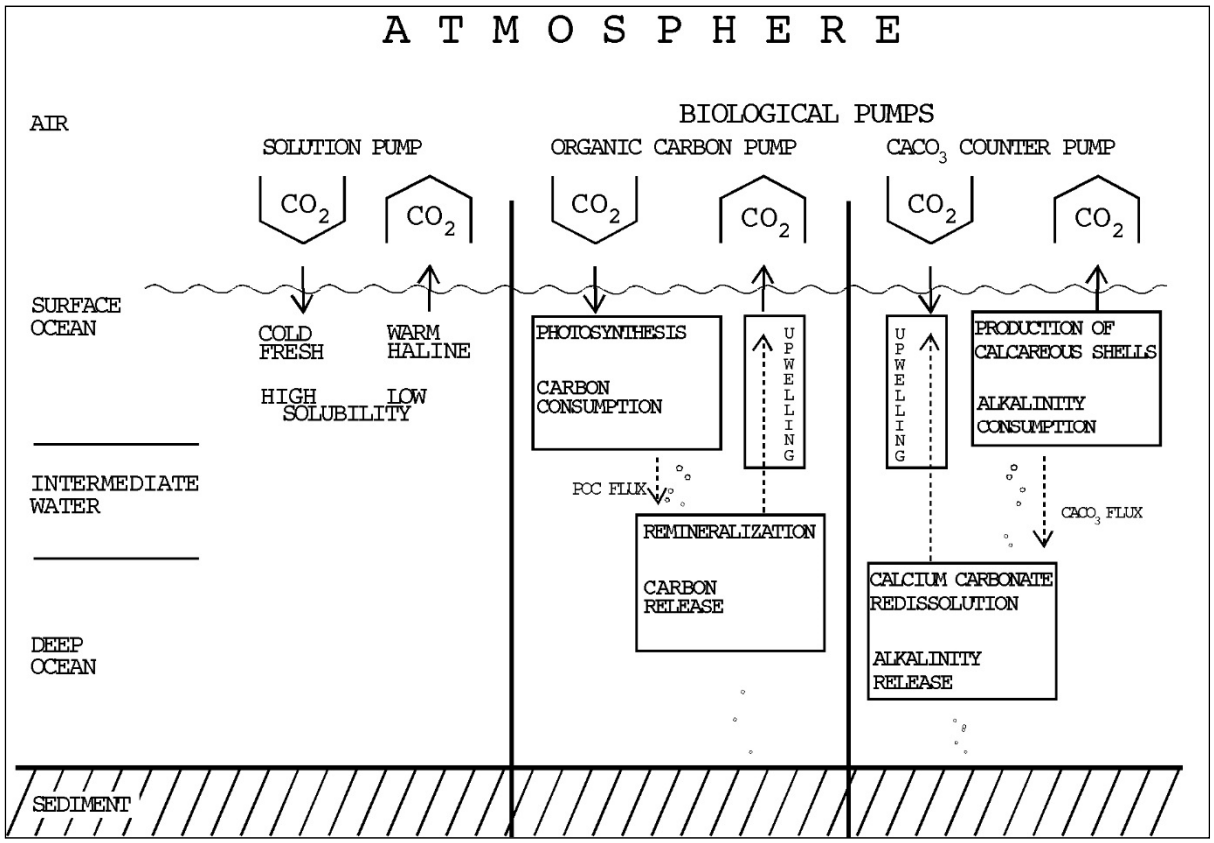

Figure 1.2: Schematic of the three major ocean carbon pumps involving the regulation of atmospheric CO_2 changes by the ocean (taken from Heinze et al., 1991)

1.1.1 The Biological Carbon Pump

The biological carbon pump (BCP) is the process by which inorganic CO_2 in surface waters is converted to organic carbon through photosynthesis and, through a series of interactions with the pelagic ecosystem, is exported from the euphotic zone (the depth above which ~1% photosynthetically active radiation (PAR) remains) to deeper waters (Longhurst and Harrison, 1989, Legendre et al., 2015) (Figure 1.3). The oceans are responsible for approximately half of all primary production (Chisholm, 2000) producing ~52 Pg C yr^{-1} (Westberry et al., 2008) with ~5-6 Pg C exported to the ocean interior each year (Henson et al., 2011, Siegel et al., 2014) via the BCP. Photosynthetic production lowers surface pCO_2, allowing more CO_2 to be taken up by the oceans, thus playing an important role in moderating atmospheric CO_2 concentrations. The gravitational sinking and remineralisation of organic matter contributes to the vertical gradient in DIC (Volk and Hoffert, 1985) and it is estimated that the BCP is responsible for approximately two thirds of this gradient (Passow and Carlson, 2012). However, atmospheric concentrations of CO_2 have also been shown to be highly sensitive to the depth of remineralisation, with a 24 m increase in remineralisation depth estimated to decrease CO_2 concentrations by 10-27 ppm (Kwon et al., 2009).

The BCP is primarily driven by the passive sinking of organic matter (including dead phytoplankton cells, larger phytodetrital aggregates or marine snow, faecal pellets produced by zooplankton feeding on lower trophic levels, and the moults and carcasses of dead organisms); and the physical mixing, advection and diffusion of carbon by water masses. Since much of this is controlled by the pelagic biota, it is also subject to the vertical gradient in biomass which decreases with approximately an order of magnitude with every kilometre of depth (Longhurst and Harrison, 1989) and the transformations of organic matter by the pelagic food web. The BCP exports >10 Pg of carbon from surface waters every year (Buesseler and Boyd, 2009). However, in contrast to the solubility pump which transports large quantities of dissolved CO_2 to depth, the BCP can be relatively inefficient if, for example, the supply of dissolved CO_2 to the surface exceeds the fixation and export of this material to depth. In addition, most of the exported carbon is remineralised before reaching sequestration depths >1000 m (Turner, 2015), resulting in less than 1% of POM estimated to ever reach the seafloor (Longhurst, 1990, Libes, 2009).

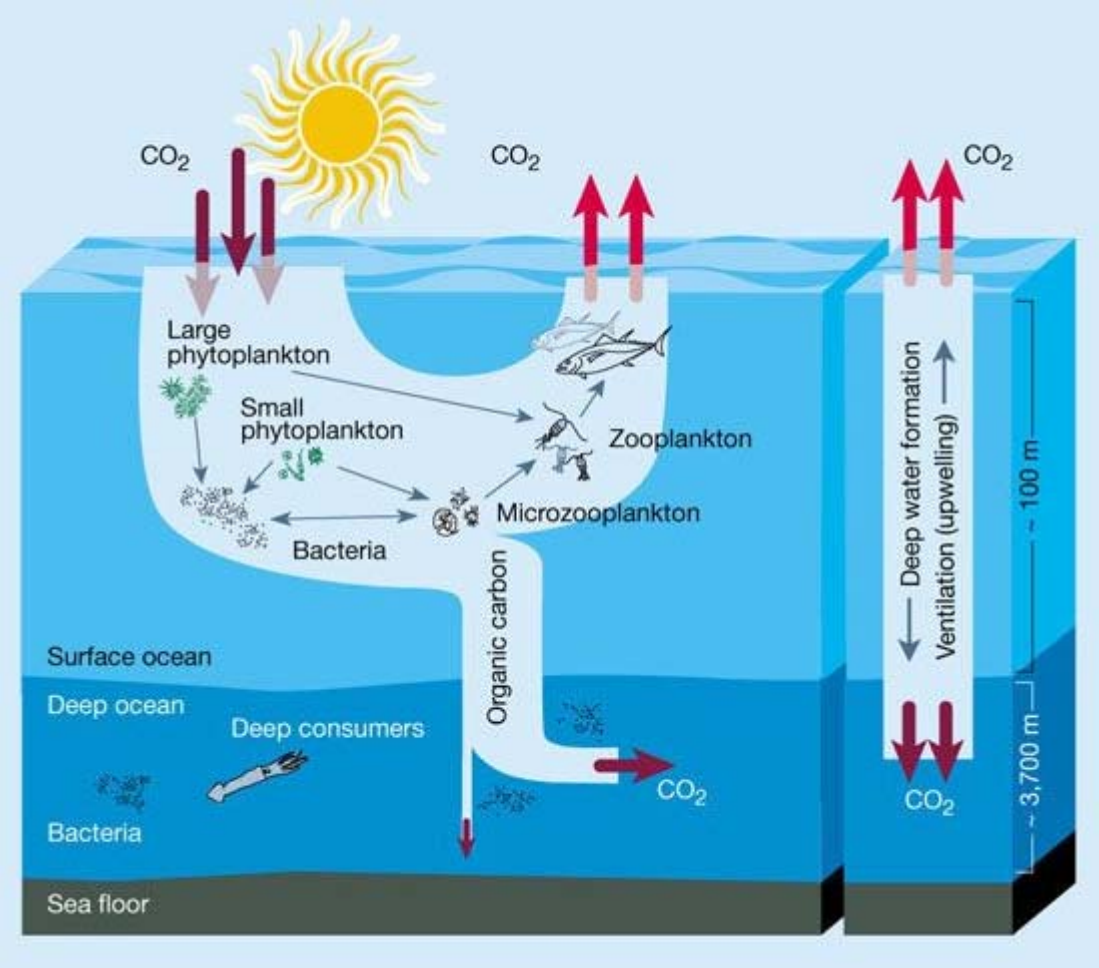

Figure 1.3: Schematic of the biological carbon pump, taken from Chisholm (2000).

Despite this inefficiency in sequestering carbon over geological timescales, the >10 Pg C exported each year by the BCP is consumed and respired by heterotrophic zooplankton and microbes, and converted into the dissolved pool, where it can remain over climatically important timescales (Legendre et al., 2015). There is, however, huge variability in the strength and efficiency of the BCP both over time and latitude, with differences in export related to variations in the remineralisation depth (Kwon et al., 2009), the overlying zooplankton community (Legendre and Rivkin, 2002) and physical processes of mixing that vary seasonally or interannually (Hauck et al., 2013).

Furthermore, climate change is likely to affect the strength of the BCP in the future. Warming oceans may become more saturated with CO_2 (Le Quéré et al., 2013) potentially altering phytoplankton production and community composition. In some places, warming may lead to increased stratification and the reduced mixing or upwelling of vital nutrients to the surface, whilst in others, stronger winds may have the opposite effect (Hauck et al., 2015).

Climate change is also likely to affect carbon cycling and trophic interactions between zooplankton (Steinberg and Landry, 2017) whilst the role of biology is projected to become more important as changes to ocean chemistry take place in response to CO_2 uptake (Hauck and Völker, 2015). This makes the task of understanding temporal and spatial variability in the BCP even more important, since the prediction of future changes to ocean uptake relies fundamentally on our understanding of processes as they currently operate.

1.1.2 The Southern Ocean and Scotia Sea

The Southern Ocean (SO) plays a particularly important role in global climate and in the uptake and sequestration of CO_2 since, whilst accounting for only 10% of global ocean area, it is responsible for >20% CO_2 uptake (Takahashi et al., 2002). Within the SO, areas of deep-water formation along the Antarctic Continental Shelf (Broecker et al., 1998, Clark et al., 2002) driven by cold temperatures and the dense, salty water left behind after ice formation, can sequester large quantities of CO_2. The strong Antarctic Circumpolar Current (ACC) is the prevailing current of the SO and separates sub-Antarctic waters to the north from Antarctic waters to the south. It comprises the three main fronts which represent transitions between water masses of different physical properties and which, particularly towards the surface, strongly influence the biogeography of the SO: the sub-Antarctic Front (SAF), the Polar Front (PF) and the Southern ACC Front (SACCF) (Figure 1.4). The ACC moves in a continuous easterly direction around the continent, connecting the worlds' oceans and transporting the deep, dense bottom water further north (Talley et al., 2011). This deep mixing and circulation means that much of the SO is nutrient rich, yet due to iron limitation (Martin, 1990, de Baar et al., 1995) is often low in productivity. As a result, the efficiency of the BCP is thought to be low (Hauck et al., 2015) although, with projected changes to climate, it is thought that this may increase.

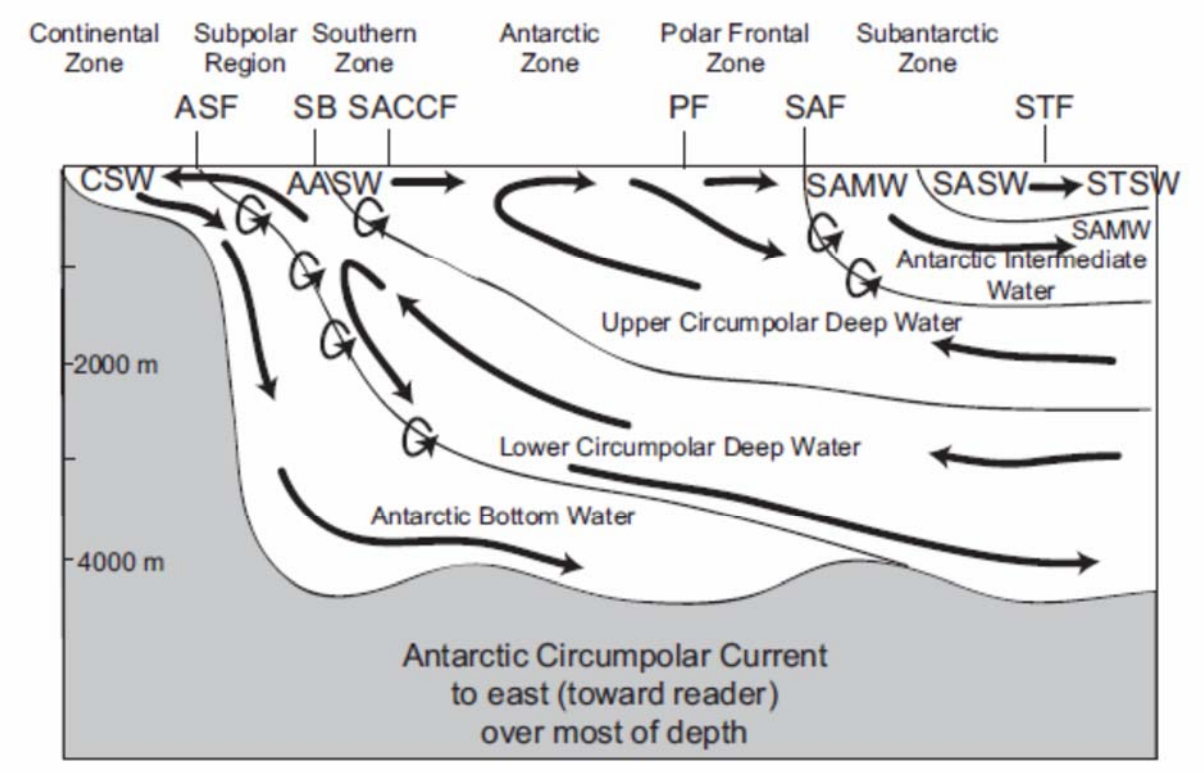

Figure 1.4: Diagram illustrating a cross-section of the SO showing the principal water masses, fronts and zones. Acronyms: Continental Shelf Water (CSW), Antarctic Surface Water (AASW), Sub-Antarctic Mode Water (SAMW), Sub-Antarctic Surface Water (SASW), Subtropical Surface Water (STSW), Antarctic Slope Front (ASF), Southern Boundary (SB), Southern ACC Front (SACCF), Polar Front (PF), Sub-Antarctic Front (SAF), Subtropical Front (STF). Taken from Talley et al. (2011).

Despite the high nutrient, low chlorophyll (HNLC) status of much of the SO, there are regions of exceptionally high productivity. The SO is heavily ice-influenced, with winter pack-ice extending as far as 60 °S, and it experiences large interannual variations in sea-ice cover (Talley et al., 2011). Sea-ice habitats can be highly productive: diatom-dominated ice-algae supports the overwintering development of post-larval krill (Quetin and Ross, 1991) as well as a substantial biomass of non-euphausiid macrozooplankton species (Flores et al., 2011). Changes in the extent of sea-ice have also been linked to altered dynamics between Antarctic krill and salps (Atkinson, 2004). The retreat of the seasonal ice-edge is also a period of high productivity, with the release of ice-algae, iron deposition and the influx of light combining to stimulate substantial ice-edge blooms with primary productivity reaching up to >2 mg C m^{-2} d^{-1} (Korb et al., 2005).

In the south Atlantic sector especially, where the ACC is funnelled through the narrowing Drake Passage and over complex bathymetry around island arcs (see Figure 1.5), turbulence and upwelling can combine to return nutrients and iron to the surface which, alongside lithogenic iron supply, stimulates primary production (Garabato et al., 2004, Kahru et al., 2007, Venables et al., 2012). Physical features may also play a role in determining the aggregation of euphausiids (Bernard et al., 2017) with accumulation zones arising in response to bathymetry, and particular tide and wind conditions. In the northern part of the Scotia Sea, where the ACC briefly wraps around the South Georgia and South Sandwich Island arc, extended summer blooms resulting from natural iron fertilisation support high levels of annual primary productivity (up to 40 mg C m^{-2} (Whitehouse et al., 1996)) and large populations of seabirds and mammals (Murphy et al., 2007). It was also recently suggested that the Scotia Sea ecosystem itself may represent a positive feedback on the supply of bioavailable iron through the digestive processes of euphausiids (Schmidt et al., 2016).

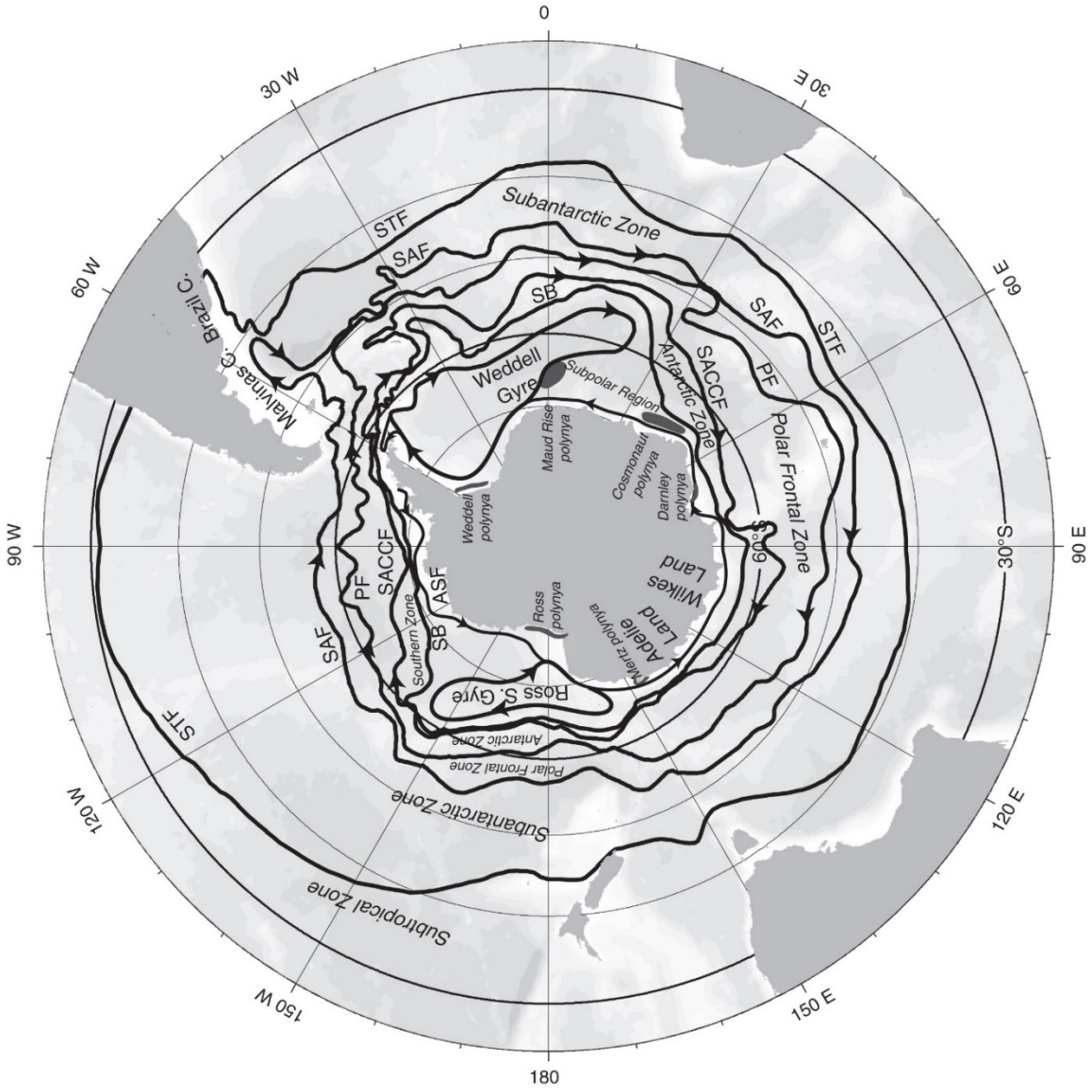

Figure 1.5: The Southern Ocean including land masses and frontal features (taken from Talley et al. (2011)). STF = Sub-Tropical Front; SAF = Sub-Antarctic Front; PF = Polar Front; SB = Southern Boundary; SACCF = Southern Antarctic Circumpolar Current Front; ASF = Antarctic Slope Front. Front locations are taken from Orsi et al. (1995).

Frontal features such as the Polar Frontal Zone (PFZ), positioned on average between 50 °S and 65 °S depending on topography (Moore et al., 1999) can also be areas of locally increased productivity. Previously considered a biogeographic barrier, it is in fact characterised by eddies and meanders which facilitate a mixing of phyto- and zooplankton, with higher productivity resulting from iron concentrations of nearly double the Antarctic average, entrained from sediments to the west (Longhurst, 1998). Ecologically, this dynamic productivity regime has been found to exert bottom-up controls on zooplankton community structure and abundance. Nutrient and iron-replete waters, characterised by higher chl-*a*

concentrations, longer bloom durations and a larger phytoplankton size-structure are associated with greater mesozooplankton abundance and biomass, whilst the opposite tends to be true of lower productivity, oligotrophic regions (Ward et al., 2005).

1.1.3 Zooplankton of the Southern Ocean

SO zooplankton biomass is dominated by euphausiids, salps and copepods which together comprise >90% the zooplankton, with <10% comprised of other groups such as polychaets, chaetognaths, molluscs, appendicularians, ostracods, amphipods and coelenterates (Schnack-Schiel and Mujica, 1994, Knox, 2007). Of the euphausiids, *Euphausia superba* (Antarctic krill), the 'keystone species' of the SO ecosystem (Murphy et al., 2007) is the largest and most well-studied. As the prey species for many higher predators (Trathan and Hill, 2016), it plays an important role in trophic transfer of energy but it is also of importance commercially (Atkinson et al., 2017). Despite this, estimates of its abundance are quite variable, due in part to its behaviour as a swarming species (Tarling et al., 2001, Klevjer et al., 2010) but also because of interannual variability and interspecific competition when salps may replace *E. superba* as the dominant species, with wide ranging ecological impacts (Loeb et al., 1997, Pakhomov et al., 2002, Atkinson, 2004). In addition to *E. superba*, four other principal species of euphausiid are regularly encountered south of the Polar Front (PF): *E. frigida*, *E. triacantha*, *E. crystallorophias* and *Thysanoessa macrura* (Cuzin-Roudy et al., 2014) of which all but *E. triacantha* are considered swarming species, and all but *E. crystallorophias* are considered vertical migrators.

Excluding swarming euphausiids, copepods have been estimated to comprise >75% of SO zooplankton biomass (Boysen-Ennen et al., 1991, Atkinson et al., 2012b) and, in contrast to euphausiids, they are generally more evenly distributed throughout the SO (Mackey et al., 2012) making them an important component of the SO ecosystem and one that potentially exerts a strong biological control on the recycling, repackaging and export of organic matter. Whilst copepod abundances are dominated by smaller copepods such as cyclopoids of the *Oncaea* and *Oithona* generas, copepod biomass in the SO tends to be dominated by a few large species, namely *Calanoides acutus*, *Calanus propinquus*, *C. similimus*, *Rhincalanus gigas* and *Metridia gerlachei* (Atkinson et al., 2012b). Nevertheless, the abundance of the smaller copepods, including *Oithona similis*, *Ctenocalaus citer* and *Microcalanus pygmaeus* has seen cyclopoid and smaller calanoid species increasingly recognised as important contributors to both biomass and the flow of energy through the SO ecosystem (Gallienne and Robins, 2001, Hansen et al., 2004, Turner, 2004). Most species exhibit a broadly circumpolar distribution and maintain a similar biomass across all sectors, yet variability in abundances, biomass and species distributions becomes more apparent over smaller temporal or spatial scales, as well

as latitudinally (e.g. Vervoort, 1965). This is typically due to bathymetry, currents and eddies which can result in the upwelling, mixing and advection of nutrients and biota, shifting the SO from a generally 'high nutrient, low chlorophyll' (HNLC) trophic status to one of locally significant productivity.

In terms of geographical distribution, the zooplankton of the SO is strongly affected by the ACC and the fronts incorporated within it (Ward et al., 2002). This results in community transitions largely following a north-south gradient, decreasing in biomass with increasing latitude (Ward et al., 2012b), although eddies and small scale turbulent mixing means that high productivity is also associated with the fronts themselves (Venables et al., 2012). In the Scotia Sea, the ecosystem can be broadly considered as being separated into two groups either side of the SACCF (Ward et al., 2012a, b), with the seasonal ice-zone affecting communities to the south of the front and warmer, sub-Antarctic surface waters influencing the region to the north. This is reflected in a less rich, generally biomass poor community at higher latitudes, and a more diverse and abundant community of mesozooplankton and macrozooplankton towards the north (Ward et al., 2012b). Many species of copepod also undertake seasonal and ontogenetic migrations with mating at depth, spawning taking place during the spring ascent, naupliar and copepodite development continuing throughout the ascent to the surface, followed by an autumnal descent to depth of the mature copepods (Longhurst, 1998). This pattern results in biomass tending to be higher in the surface during the spring/ summer and higher at depth during autumn/ winter, although timings and amplitudes vary between species, perhaps as a mechanism of reducing interspecific competition for food during the summer months (Longhurst, 1998). Angel (1984) notes the importance of such seasonal migrations prior to overwintering at high latitudes, in mediating a vertical transport of material to depth, and a supply of food to deeper dwelling predators such as syphozoans. To survive these periods of overwintering and diapause, Antarctic and sub-Antarctic species exhibit certain physiological differences to species from lower latitudes, including the development of carbon-rich seasonal lipid deposits (Hagen and Auel, 2001, Atkinson et al., 2012b) and such life cycle strategies may also contribute to seasonal carbon and nutrient fluxes which may differ from lower latitudes (Jónasdóttir et al., 2015).

1.2 Zooplankton and the biological carbon pump

Zooplankton are a numerically abundant, and phylogenetically and functionally diverse, component of the pelagic ecosystem. They form the link between phytoplankton and higher trophic levels, transferring carbon, energy and nutrients up the food chain. In feeding and producing faecal pellets (faecal pellets) they repackage phytoplankton and other organic matter into larger, denser and faster sinking particles (Steinberg and Landry, 2017). Copepod

and euphausiid faecal pellets can sink at rates of up to 862 m d^{-1} (Fowler and Small, 1972, Komar et al., 1981) whilst Bruland and Silver (1981) found pteropod and salp faecal pellets to sink at rates of up to 2,700 m d^{-1}. This makes them potential vectors of organic carbon flux to depth (Turner and Ferrante, 1979) and can enhance the strength of the BCP by increasing the depth at which organic carbon is remineralised and fuelling secondary production within the mesopelagic (~200-1000 m). The export of carbon through faecal pellets is supported by evidence of faecal pellets in deep-sea sediment traps, at times comprising the majority of particulate organic carbon (POC) at this depth, suggesting that faecal pellets are transported to depth either through direct sinking or by production in situ (Manno et al., 2015) and that they constitute an important component of the flux.

However, this may also be reduced by feedback effects from the zooplankton themselves: zooplankton are known to engage in coprophagy (faecal pellet ingestion), coprohexy (breaking up of faecal pellets) and coprochaly (faecal pellet loosening) (Lampitt et al., 1990, Iversen and Poulsen, 2007, Wilson et al., 2008) which can slow the sinking of faecal pellets. In particular, Iversen and Poulsen (2007) found copepods to primarily engage in coprohexy, but that by increasing the lability of faecal pellets during fragmentation, they became subject to further ingestion or breakdown by protozooplankton and microbes further down the water column (Poulsen and Iversen, 2008, Morata and Seuthe, 2014, Belcher et al., 2016). Microbial activity may also play a role in the degradation of faecal pellets, although the ability of microbe-associated faecal pellet degradation to slow the sinking of faecal pellet by any meaningful degree is dependent on both the size of the faecal pellet and the temperature of the water (Svensen et al., 2012, Marsay et al., 2015, Belcher et al., 2016). As a result of these zooplankton-mediated processes of retention and remineralisation in the upper water column, some doubt has been cast on the role of zooplankton faecal pellets as a vector of deep carbon export in recent years (Turner, 2015) with a suggestion that marine snow and sedimenting algal blooms may contribute more to deep sea carbon export and faecal pellets contribute more to sustaining zooplankton and microbial activity in the mesopelagic (Turner, 2015). However, substantial unresolved spatial and temporal variability still exists in in estimates of faecal pellet export flux which requires further constraining to be adequately represented in models of the BCP.

The role of the zooplankton community in the production and attenuation of faecal pellet and particulate organic carbon (POC) more generally, is also important. The changing size and morphology of zooplankton faecal pellets with depth demonstrates how zooplankton can exert a strong control on the type and magnitude of faecal pellet flux to the deep mesopelagic (Wilson et al., 2008, Belcher et al., 2017a). Dagg et al. (2014) were able to show

how high fluxes of faecal pellets could reach mid depth waters when euphausiids co-occurred with high concentrations of large diatoms, but were low when the diatom community was comprised of smaller cells. The ballasting effect of faecal pellets by mineral content shows that the magnitude of faecal pellet export is additionally dependent on what the zooplankton are eating, with diatom-based diets resulting in faster sinking faecal pellets than dinoflagellate based diets (Small et al., 1979, Frangoulis et al., 2001, Ploug et al., 2008). By incorporating phytoplankton-zooplankton trophic dynamics into a biogeochemical model of the SO, Le Quéré et al. (2016) were able to better reproduce phytoplankton dynamics and illustrate the dangers of simplifying zooplankton processes in large-scale ocean-atmosphere models.

1.2.1 Zooplankton diel vertical migration

Diel (or diurnal) vertical migration (DVM), is the phenomenon whereby planktonic animals generally dwell at depth during the day and migrate to surface waters to feed at night. It is considered to be the biggest migration on the planet in terms of biomass and is ubiquitous throughout all marine and freshwater pelagic communities (Brierley, 2014). It has a long history, thought to have first been described in a limnological context by Cuvier (1817), as described in the comprehensive review of Bayly (1986). DVM is considered primarily to be a feeding strategy driven by an external light stimulus, but as the complexity of the behaviour has become apparent, a number of hypotheses have been advanced to explain its ecological purpose. An early hypothesis was that of a predator-avoidance strategy when it was observed that copepods with no predation pressure did not migrate, whilst the same species in the presence of predators did (Gliwicz, 1986). The observation that downward migrations in the presence of predators conferred a survival advantage offsetting any energy or fecundity cost associated with the migration (Stich and Lampert, 1981) supported this theory. However, the depth that zooplankton in the sea migrate to is not fully consistent with this theory, since light levels may still be high enough to enable visual predation (Bayly, 1986). Another hypothesis proposes that there is a metabolic advantage to migrating to deeper depths, with a trade-off between slower growth and reproductive rates at lower temperatures, and lower metabolic costs of residing at depth during the day and fewer, but larger eggs (Enright, 1977). Hunger and satiation have also been found to modify DVM, with starved animals staying at the surface during daylight in times of food scarcity, even when this may result in a risk of predation, or descending during the night when satiation has been achieved (Pearre, 2003). Consequently, individual variation in hunger-satiation cycles may be able to introduce asynchrony to migrations that are synchronised to a greater degree by light cues at the start of the night (Pearre, 2003).

This has helped shape the view that, contrary to DVM being a simple upward migration at dusk and downward migration at dawn i.e. the 'classical' model of migration, migration may be much more variable than is understood from observations (Cushing, 1951, Bayly, 1986, Pearre, 2003). Pearre (1979b) discusses this with reference to sampling methodologies, showing how many of the ways in which DVM is sampled are inherently only a measure of synchronous changes at the population level, unable to capture differences in behaviour between individuals or to show whether different parts of the population migrate at different times. Observed variability in DVM that weakens the link between upward migration and night time feeding alone includes evidence for bimodal migration and feeding activity (Michael, 1911, Atkinson et al., 1992), 'midnight sinking' (Cushing, 1951), reverse migrations (Bayly, 1986) and asynchronous migrations of parts of the population at different times (Pearre, 1979b). Other factors can also influence DVM, including the size, developmental stage and buoyancy of an animal (Pearre, 2003) whilst all of these factors may additionally be superimposed upon seasonal or ontogenetic migrations (Angel, 1986). The hunger-satiation hypothesis (Pearre, 2003) has gained particular traction and it is thought that this 'foray' style of migration (see Figure 1.7) may be the predominant form of migration either during the night, or potentially throughout the whole day. Furthermore, the role of light has been found to be more complex still: Tarling et al. (1999), Berge et al. (2009), and Last et al. (2016) have shown how DVM may be related not only to changes in solar irradiation but also to lunar cycles, which are able to continue driving DVM during the polar night. In this context, light can be considered a synchroniser, or *Zeitgeber*, of DVM (Tarling, 2015). It is also thought that DVM is controlled by an underlying circadian rhythm (Gaten et al., 2008) with the behaviour linked to other circadian rhythms and clock genes (Teschke et al., 2016, Häfker et al., 2017), although work to establish a molecular basis for DVM is still at an early stage.

1.2.2 DVM and active flux

Far from just being an interesting biological phenomenon, DVM also adds to the complexity of our understanding of the BCP and fluxes of particulate and inorganic matter in the ocean. Central to this is the hypothesis that assessments of downward flux through the thermocline may be substantially underestimated due to the omission of vertical migrations (Angel, 1984) (see Figure 1.6). This permits a distinction between 'passive' and 'active' flux. Passive flux is defined as the passively sinking materials and processes that contribute to the BCP, whereas active flux constitutes the expedited transport of material to depth by processes such as zooplankton vertical migration. This builds on the 'ladder of migration' theory proposed by Vinogradov (1970) that explains how deep-sea communities are sustained with food from

above. Longhurst and Harrison (1988) first proposed that DVM from interzonal migrants represented an unaccounted for export of excreted nitrogen (N) from the euphotic zone, requiring an upward revision of estimates of new production to primary production (the *f*-ratio). DVM has more often been considered in terms of the contribution faecal pellets make to carbon export during such vertical traverses, and since the migration rates of micronekton may be as fast as the sinking rates of large faecal pellets (Angel, 1986), this may be a mediator of substantial additional export. Angel (1986) goes on to estimate that faecal pellet flux from euphausiids, decapods and nekton could contribute 25-65 % more to flux than what is caught in sediment traps. Longhurst (1990) developed this theory further, suggesting that the role of vertical migrants in active flux could not be limited to faecal matter alone but must also necessarily include the dissolved fraction of inorganic carbon respired as CO_2.

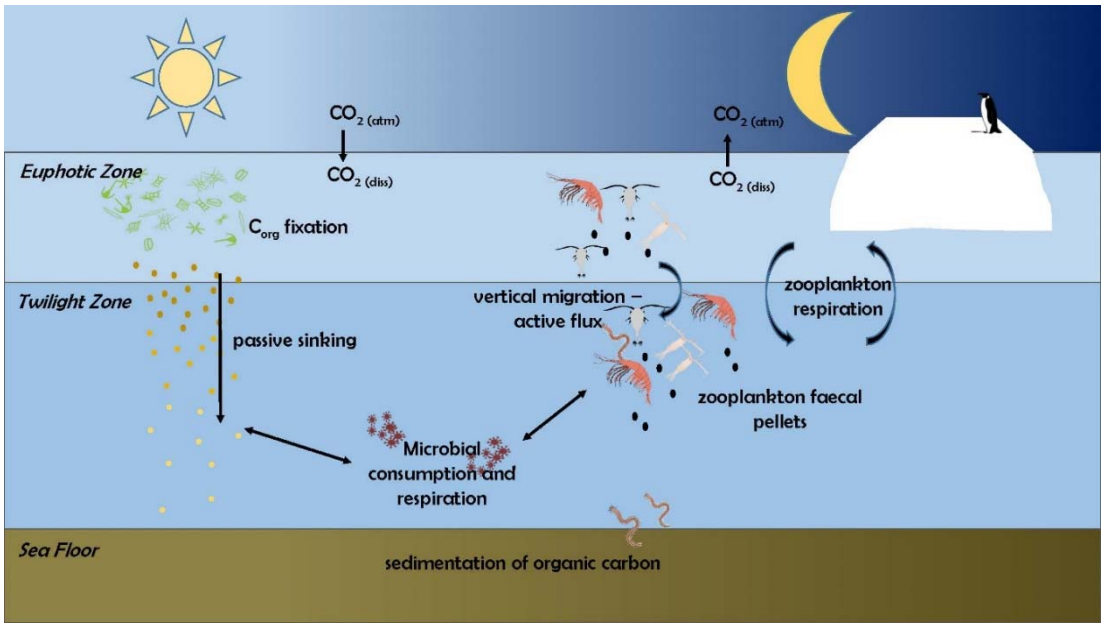

Figure 1.6: Schematic showing how zooplankton vertical migration can enhance the flux of respiration and faecal pellets to the deep ocean.

Since then, numerous studies, comprehensively reviewed by Turner (2015), have emerged focussing on particulate and dissolved matter fluxes from vertically migrating zooplankton, and their contributions to (or augmentation of) overall export flux. Driving these studies is the need to reconcile oceanic budgets of carbon, in particular in the mesopelagic or 'twilight' zone. This was underscored by Burd et al. (2010) who examined the emergent imbalance between inputs of organic material at the surface, and heterotrophic demand for carbon in the mesopelagic. They found bacterial growth efficiencies and cell carbon content

assumptions to be particularly important in determining the magnitude of the imbalance but considered that better accounting for lateral advection of particles and slowly sinking particles may help to close the gap. In another study, Steinberg et al. (2008) found that zooplankton vertical migration may account for the 'missing' POC at both a high latitude site where zooplankton and microbial demand for carbon in the mesopelagic were equally high, and at a low latitude, oligotrophic site where microbial respiration dominated. Taking a different approach, Giering et al. (2014) also found zooplankton processes, such as zooplankton-microbial synergies and DVM, to be fundamental to balancing the carbon budget of the twilight zone. In addition to POC, zooplankton DVM also has the potential to contribute substantially to the oceanic reservoir of DIC. By feeding in the surface at night and respiring at depth during the day, interzonal migrants can expedite the export of organic carbon from the surface layer and deposit it in dissolved form below the mixed layer. At the Bermuda Atlantic Time Series (BATS) station, it was estimated that vertical migration accounted for up to 20-30% sinking POC flux, such that the downward flux of carbon could be considered a lower bound on export production (Steinberg et al., 2000), whilst migratory respiratory flux in the northeast Atlantic was estimated to account for 23-71% of the gravitational flux of carbon measured at 150 m depth (Ariza et al., 2015).

A major challenge remaining in our understanding of zooplankton DVM in the context of carbon flux, is the nature of DVM itself, and changing our assumptions about the nature of DVM may also alter our estimations of the magnitude of the flux. This was shown by Tarling and Johnson (2006) when they examined the effect of satiation sinking on the active flux from *E. superba*. By performing 'foray' migrations in response to satiation and gut evacuation, carbon export was estimated to be 8% greater than that from a 'classical' single migration (illustrated with the schematic in Figure 1.7). Tarling and Thorpe (2017) also propose that this may substantially enhance downward fluxes from swarming krill, as satiated euphausiids sink to the bottom of the swarm to defecate, thus bypassing the region of most rapid degradation.

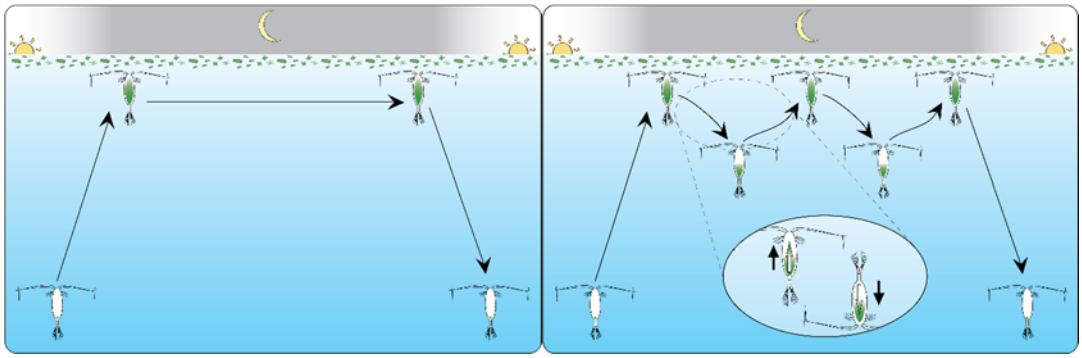

Figure 1.7: Schematic illustrating two different modes of migration. Left panel: the 'classical' migration with dusk ascent and dawn descent, with feeding in the euphotic zone throughout the night; Right panel: a 'foray' style of migration, in which the animal ascends and descends in response to hunger-satiation cues, evacuating their gut during the descent (taken from Pierson (2008)).

1.3 Motivation of the thesis

In light of the importance of the Southern Ocean in global climate and the productivity of much of the Scotia Sea ecosystem in particular, the purpose of this thesis is to explore the processes and magnitudes by which zooplankton affect the vertical flux of carbon in this region. In particular, I am interested in examining the influence of DVM on the active flux of particulate (faecal pellet, faecal pellet) and respiratory carbon, with both species-specific and whole community approaches. I address this through four chapters (Chapters 2-5) in which I apply a different methodology in each to answer different parts of the overall question, the aims of which are set out below. This was a multidisciplinary approach which included observations, the analysis of previously-collected samples, the personal collection and analysis of samples from two research cruises, on-board experiments, and modelling exercises. Laboratory analyses and experiments were carried out using a range of equipment including classical optical and scanning election microscropy (SEM), traditional taxonomy and semi-automated zooplankton imaging using the ZooScan, elemental analysis and oxygen optode respirometry.

In **Chapter 2** I analyse MOCNESS net samples from eight depths from day and night, at four stations within the Scotia Sea, over two years, for taxonomic composition and abundance. I then apply multivariate ecological analytical techniques to explore the diurnal and interannual change in vertical community structure, and determine the species responsible for driving patterns or groups. I develop metrics through which to distinguish species-specific and community diel vertical migrations, and apply empirical relationships to my results to estimate active community carbon flux at each station. In **Chapter 3**, I use a combination of

light and scanning electron microscopy to analyse faecal pellet samples I collected on board the RRS James Clark Ross, to determine the characteristics of faecal pellets found in the upper mesopelagic. I combine this with analyses of mesozooplankton samples I collected from Bongo nets during the same cruise, to consider processes responsible for different faecal pellet profiles. I quantify the faecal pellet flux at each station and relate this to the zooplankton processes influencing flux. In **Chapter 4** I conduct on-board experiments on Southern Ocean cruises across two years, to investigate the effect of DVM on the respiration rate of *E. triacantha* and the implications that this has for estimates of respiration flux. In **Chapter 5** I develop a model with which I estimate total active flux from *E. triacantha* and the relative contributions from respiration and egestion, using my own empirically determined respiration rates, and literature-derived estimates of faecal pellet export. I investigate the sensitivity of respiration and egestion carbon flux of *E. triacantha* to different environmental and behavioural parameters, and identify key uncertainties in the estimation of active flux from DVM. I conclude the thesis with a synthesis of my key findings and conclusions from this study, and I consider what questions it opens up for future work **(Chapter 6)**.

1.3.1 Specific aims of each chapter

Chapter 2: The influence of the Scotia Sea zooplankton community on diel vertical migration and carbon flux

The purpose of this chapter was to evaluate the diurnal and interannual variability of the mesozooplankton community at four sites in the Scotia Sea and to relate this to estimates of active community flux resulting from DVM of interzonal migrants. Specific aims were to:

1. Evaluate the structure of the Southern Ocean pelagic zooplankton community at time-scales ranging from the diurnal to the interannual, and at spatial scales ranging from the vertical (m) to the latitudinal (km)
2. Develop metrics through which to investigate DVM at the individual and community level
3. Produce estimates of active community flux from interzonal diel migrants and evaluate this in the context of the overlying zooplankton community

Chapter 3: Zooplankton abundance and behaviour increases faecal pellet flux and remineralisation depth in the Southern Ocean

The purpose of this chapter was to investigate how faecal pellet production and export flux in the upper mesopelagic varied between three contrasting sites in the Scotia Sea and how this was related to mesozooplankton in the upper mesopelagic. Specific aims were to:

1. Compare predicted mesozooplankton faecal pellet production with observed faecal pellet production in the upper 200 m to determine processes governing faecal pellet supply to the deeper ocean
2. Assess the morphological composition of faecal pellets observed over 400 m to determine the likely origin of faecal pellets
3. Quantify the magnitude of faecal pellet export flux across the upper 400 m in the Scotia Sea and relate this to controls exerted by the overlying zooplankton community

Chapter 4: The effect of diel vertical migration on the respiration rate of a prominent Southern Ocean euphausiid, *Euphausia triacantha*

The purpose of this chapter was to determine how temperature changes experienced during diel vertical migration would affect the respiration rate of a prominent Southern Ocean euphausiid, *E. triacantha*. Specific aims were to:

1. Determine the respiration rate of *E. triacantha* at temperatures experienced within its DVM and whether *E. triacantha* is able to compensate for short-term exposure to elevated temperatures
2. Evaluate the factors influencing the respiration rate of *E. triacantha* and the implications of this for determining its temperature-dependence
3. Assess whether *E. triacantha* shows any evidence for Metabolic Cold Adaptation (MCA)

Chapter 5: Modelling the active carbon flux from the sub-Antarctic krill, *Euphausia triacantha*, in the Atlantic sector of the Southern Ocean

The purpose of this chapter was to estimate the active flux resulting from the Southern Ocean euphausiid, *E. triacantha*, and evaluate the parameters that estimates of flux are most sensitive to. Specific aims were to:

1. Create a model that simulates DVM in *E. triacantha* and calculate the active egestion and respiration flux (flux below the mixed layer) in an overall 'BEST' model run

2. Determine the causes of latitudinal and seasonal variability in magnitudes and relative proportions of egestion and respiration flux from the 'BEST' model run
3. Run a series of sensitivity analyses to quantify the influence on estimates of flux of key parameters in the model and evaluate the importance of these parameters in determining accurate estimates of carbon flux from an important interzonal diel migrant

Chapter 6: Synthesis and future directions

In this chapter I synthesise the key findings of each chapter and draw some overarching conclusions in respect of zooplankton-mediated flux based on the entire study, including what questions this thesis has succeeding in answering. I also discuss potential areas of future work that I have identified in the course of this thesis.

Chapter 2: The influence of the Scotia Sea zooplankton community on diel vertical migration and carbon flux

2.1 Introduction

2.1.1 The Scotia Sea

The Scotia Sea, located in the South Atlantic sector of the Southern Ocean (SO), is bounded to the west by the Drake Passage and on the north, east and south by the undersea ridges and islands that make up the Scotia Arc. This combination of features and the complex bathymetry of the Scotia Sea make it a particularly dynamic region of the Southern Ocean. The predominant current, the Southern Antarctic Circumpolar Current Front (SACCF) is constricted as it moves in an easterly direction through the Drake Passage and is combined with high wind stress and a rough sea-floor topography that enhances turbulence and mixing (Garabato et al., 2004). The region around South Georgia is a particular hotspot of productivity within the Southern Ocean, with upwelling of iron to surface waters as the SACCF interacts with the shallow topography of the Scotia Arc stimulating long lasting blooms (de Baar et al., 1995, Korb et al., 2005). This supports a strong krill-based ecosystem (Murphy et al., 2007) which itself may act as a positive feedback on iron supply (Schmidt et al., 2016). In addition, the presence of dynamic frontal features (including the Sub-Antarctic Front (SAF), Polar Front (PF) and the SACCF) and the Marginal Ice Zone (MIZ) mean that the Scotia Sea is characterised by varying oceanographic regimes which include regions of high productivity that are uncharacteristic of the generally High Nutrient-Low Chlorophyll (HNLC) status of the Southern Ocean, as well as regions of lower productivity. These different productivity regimes result in quite different zooplankton communities and food web structures, which have been described by Ward et al. (2012b) in terms of functionally distinct 'bioregions' that are based on both ecological and physical features.

The Scotia Sea is one of the more well-studied regions of the Southern Ocean thanks in part to its abundant krill fishery which has in turn supported important communities of higher predators. Comprehensive sampling programmes date back to the original *Discovery Investigations* of the early 20th century, driven by the need for whale stock management information, and have been continued with programmes including the BIOMASS Investigations (Biological Investigations of Marine Antarctic Systems and Stocks) (El-Sayed, 1994), the British Antarctic Survey (BAS) Western Core Box time-series, which has been instrumental in collecting krill biomass and associated data since 1981 and, more recently, BAS's multidisciplinary DISCOVERY 2010 Programme (Tarling et al., 2012).

2.1.2 Zooplankton of the Scotia Sea

Such in-depth study of the Scotia Sea has resulted in a large body of literature describing the structure, composition and seasonal change of zooplankton communities that reside there, albeit with particular geographic, depth or seasonal foci, and notwithstanding the significant inter-annual variability that can characterise the region (Constable et al., 2003). Southern Ocean (SO) zooplankton biomass is broadly dominated by small euphausiids and copepods (Atkinson and Peck, 1988, Ward et al., 1995) and, in some SO regions, copepods can comprise >75% of zooplankton biomass (Boysen-Ennen et al., 1991, Atkinson et al., 2012b). They are therefore capable of exerting a significant influence on the BCP through the recycling, repackaging and export of organic carbon.

The Scotia Sea is also characterised by a strong physical-biological coupling and, although subtly differing zones have been proposed over time, a partitioning of zooplankton communities along frontal zones such as the SAF and PF appear most supported in the literature (Ward et al., 2002, 2003, Longhurst, 2010), along with clear differences between on- and off-shelf communities (Ward and Shreeve, 1999). Furthermore, contrary to the idea of frontal positions being considered a barrier, they have been found to be associated with the highest zooplankton abundance and diversity (e.g. Ward et al., 2003) possibly due to the turbulent mixing that occurs where frontal boundaries meet, with inter-annual variability as the positions of fronts shift from year to year.

Latitudinally, zooplankton community structure appears to be governed in part by seasonality, and in part by the position of the SACCF (Ward et al., 2012a, b), both of which are intricately linked with temperature and the seasonal location of sea-ice. With regards to season, the naturally later spawning times of many species occupying regions south of the SACCF have been observed to lead to their relatively greater abundance in autumn compared to summer, whilst abundance between summer and autumn is less variable north of the front (Ward et al., 2012a). Atkinson and Peck (1988) also found evidence of a pronounced seasonal migration of some species, in which copepod volume in winter in the top 250 m was 26% that of summer, yet below 250 m was markedly higher than in summer.

2.1.3 Zooplankton and carbon flux

Many zooplankters are thought to carry out diurnal vertical migrations (DVM) in which animals residing deeper in the water column during the day, migrate to the surface at night to feed. Reasons for such migrations include endogenous (Gaten et al., 2008) and exogenous drivers (Angel, 1986) but species-specific behaviours can also be modified by changes to environmental conditions or predator-prey dynamics (Bayly, 1963, Neill, 1990, Ohman,

1990). Since it represents arguably the biggest migration of biomass on the planet, DVM is considered instrumental in driving an export of carbon and nutrients from the epipelagic to deeper layers of the ocean, enhancing the strength of the Biological Carbon Pump (BCP) (Longhurst, 1990, Steinberg et al., 2000, Buesseler et al., 2007). Estimates of how much this so-called 'active flux' contributes as a proportion of sinking particulate organic carbon (POC) flux vary greatly dependent on oceanic regime and season (see Turner, 2015 and refs therein) but range from 3% (Hernández-León et al., 2001, Putzeys et al., 2011) to 70% (Dam et al., 1995). In addition to natural variability, DVM is a complex phenomenon to study and many challenges identified by Pearre (1979b) remain today. A central idea is that what is measured at the population level is unlikely to be representative of individual behaviours. Various hypotheses of DVM have been proposed that suggest a more complex pattern of behaviour than that of a 'classical' dusk ascent, dawn descent, model (Tarling et al., 2002, Pearre, 2003, Last et al., 2016). Secondly, a degree of behavioural plasticity has been observed, in which migrations may reverse or cease entirely. Hypothesised as a predator evasion tactic or linked to changing environmental conditions, animals are able to switch to spending daylight hours at the surface and migrate to depth at night, challenging current understanding of the extent, role and impact of DVM on carbon and nutrient fluxes.

Globally, we are still some way from a complete understanding of the processes controlling surface to deep water carbon flux (Burd et al., 2010), yet models suggest that small changes in the depth of sinking carbon respiration could alter atmospheric CO_2 concentrations by 10-27 ppm (Kwon et al., 2009). The SO in particular is one of the world's biggest carbon sinks and SO zooplankton have been implicated as an efficient vector of organic carbon via sinking faecal pellets (faecal pellets) (Cavan et al., 2015, Manno et al., 2015, Belcher et al., 2017a). Furthermore, Le Quéré et al. (2016) have shown that global biogeochemical models linked to climate change projections are significantly improved when taking account of Southern Ocean plankton processes and interactions, warranting a deeper understanding of the role of DVM in SO zooplankton.

2.1.4 Purpose of the current study

Most studies of zooplankton in the Southern Ocean have been restricted to surface or near-surface waters (Ward et al., 1995, Pakhomov et al., 1997, Ward et al., 2003, Ward et al., 2012a), with depth-integrated studies often comprising taxonomic or life-cycle accounts (Voronina, 1972, Park, 1978, Atkinson, 1991, Park, 1993). A number of studies have addressed vertical community structure and distribution of zooplankton and nekton to as deep as 1000 m in the ice edge and nearby open water in (Hopkins et al., 1993, Hopkins and Torres, 1988, Lancraft et al., 1989) the Weddell and southern Scotia Seas (Hopkins and

Torres, 1988, Lancraft et al., 1989, Hopkins et al., 1993), and more recent studies have also addressed vertical community structure around the Western Antarctic Peninsula (Marrari et al., 2011, Wiebe et al., 2011). However, the vertical distributions and migratory dynamics of zooplankton have also been shown to exhibit potential controls on the active transport of carbon and other nutrients (e.g. Longhurst and Harrison, 1988, Longhurst and Harrison, 1989, Steinberg et al., 2000, Steinberg et al., 2002) with implications for the efficiency of the BCP (Kwon et al., 2009). This is of particular interest in regions of high carbon sequestration such as the Southern Ocean and especially in the Scotia Sea, where productivity is especially high but, to date, the influence of vertical community structure on carbon flux has received little attention.

In this study, I analyse MOCNESS (Multiple Opening and Closing Net with Environmental Sensing System) mesozooplankton data taken at consecutive 125 m sampling intervals from the surface to 1000 m total depth, during day and night in two consecutive years. Samples were taken at four stations in the Scotia Sea, representing a spatial gradient moving from a most southerly ice-influenced region, to two open water and putatively oligotrophic regions on either side of the SACCF, to the most northerly and naturally iron-fertilised region downstream of South Georgia. Day and night time sampling to 1000 m was conducted at each station, allowing a comprehensive analysis of the biomass-structured zooplankton community across a broad geographical scope, and the diurnal variation in vertical distribution. Through this, the diurnal migratory dynamics of biomass dominant taxa within the Scotia Sea ecosystem are evaluated, enabling the first considerations of community-scale active flux to be considered across contrasting regions within the Scotia Sea, and across season.

I investigate the question of how the vertically distributed zooplankton community drives carbon fluxes between the epipelagic and mesopelagic zones in different regions of the Scotia Sea by:

i. Describing the vertical structure across stations in relation to environmental characteristics and how well conserved that structure is between years
ii. Investigating whether shifts in the vertical range or depth of biomass maxima of particular taxa occur over a diurnal period
iii. Identifying characteristics of the vertical zooplankton community structure in relation to the drivers of downward fluxes of carbon

2.2 Methodology

2.2.1 Physical environment and hydrography

An SBE9Plus CTD, set up with instrumentation including a dual SBE 3Plus temperature sensor and SBE4C conductivity sensor, was deployed. Temperature and salinity data were averaged for every 2 m from the surface to 1000 m for plotting.

2.2.2 Sampling strategy

Zooplankton sampling was carried out by colleagues who deployed MOCNESS nets on board the RRS James Clark Ross on two Southern Ocean research cruises forming part of the DISCOVERY 2010 Programme. The two cruises correspond to the austral summer 2008, called S08 from hereon in (Dec 2007-Feb 2008) and austral autumn 2009, called A09 from hereon in (Mar-April 2009) sampling seasons (cruises JR177 and JR200 respectively).

In both seasons, double oblique deployments were made at four pre-defined stations that formed part of an established sampling programme along a north-south transect in the Scotia Sea. The stations include R1 (an ice edge station), C3 (an open water, oligotrophic region), P2 (a putative oligotrophic region, upstream of the South Georgia & South Sandwich Island archipelago) and P3 (a naturally iron-fertilised and productive region, downstream of the archipelago) (see Figure 2.1). At each station, nets were deployed as close as possible to midnight and midday, resulting in two sets of samples for each station. Full details of stations and sampling are given in Table 2.1.

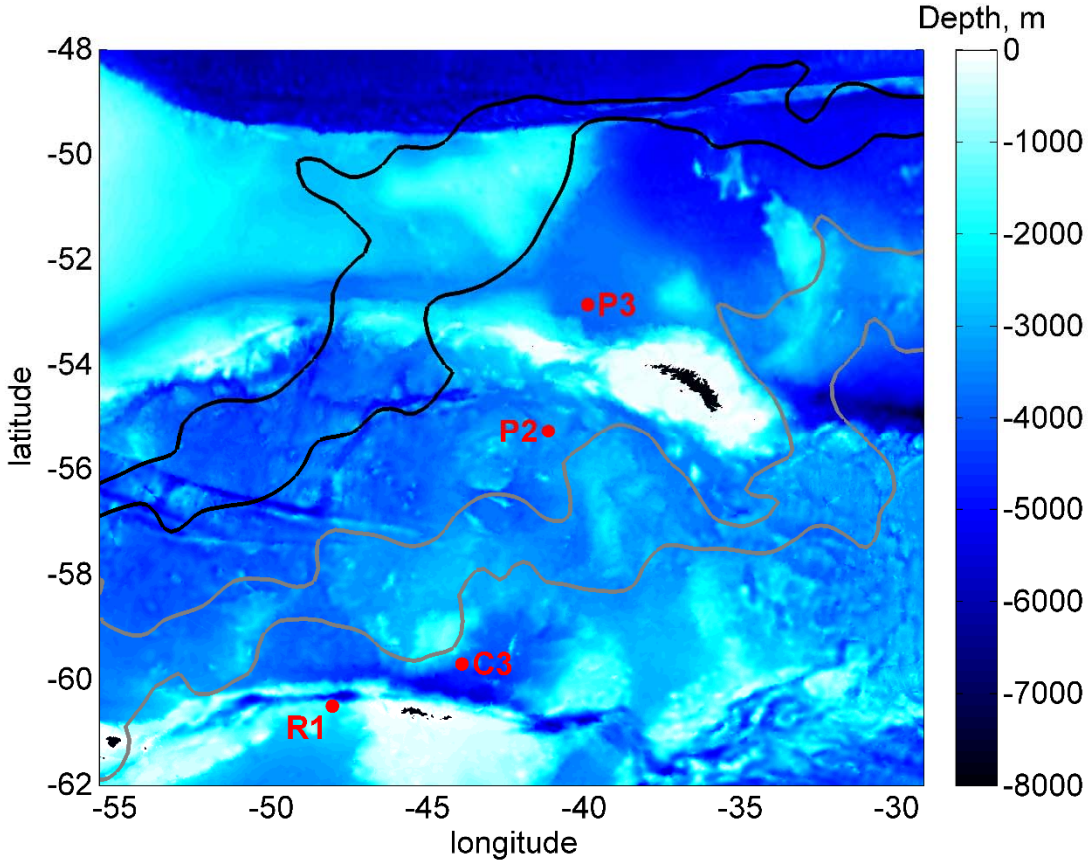

Figure 2.1: Map of the Scotia Sea showing the locations of sampling stations. The black lines represent the northern and southern edges of the Polar Front and the grey lines represent the northern and southern edges of the Southern Antarctic Circumpolar Current Front (SACCF) (adapted from Venables et al. (2012).

To obtain the samples, a 1 m^2 MOCNESS, with a 330 µm mesh net, was deployed to 1,000 m with Net 1 opened (wire-out rate of 30 m/min). The MOCNESS comprises nine nets which sample the water column sequentially in 125 m depth intervals, resulting in a series of depth-discrete samples over a depth of 1,000 m. Once at 1,000 m the net was then hauled back in at an average rate of 20 m/min with nets 2 to 9 being sequentially closed at 125 m intervals throughout the water column. Depth intervals were as follows: 1,000 to 875 m (Net 2), 875 to 750 m (Net 3), 750 to 625 m (Net 4), 625 to 500 m (Net 5), 500 to 375 m (Net 6), 375 to 250 m (Net 7), 250 to 125 m (Net 8), 125 to 0 m (Net 9).

Table 2.1: Locations, dates and times of sampling and duration of MOCNESS deployments. D and N refer to deployments predominantly conducted during daylight and night time hours, respectively. S08 refers to sampling conducted during summer 2008 and A09 to autumn 2009. *This set of samples was in too poor a condition to analyse so has been omitted from the analysis.

Station	Latitude	Longitude	Year/Season	Event ID	D/N	Date	Start time	End time	Haul duration (hrs)
R1	-60.48	-48.24	S08	57	D	04/01/08	18:42	21:29	2.8
R1	-60.48	-48.24	S08	61	N	05/01/08	00:14	02:31	2.3
C3	-59.68	-44.07	S08	137	D	14/01/08	17:02	19:28	2.4
C3	-59.68	-44.07	S08	143	N	15/01/08	00:08	02:30	2.4
P2	-55.24	-41.29	S08	249	D	27/01/08	12:08	14:21	2.2
P2	-55.24	-41.29	S08	260	N	29/01/08	00:38	02:53	2.3
P3	-52.86	-40.10	S08	292	D	01/02/08	18:39	21:28	2.8
P3	-52.86	-40.10	S08	276	N	01/02/08	00:13	02:32	2.3
R1	-60.49	-48.20	A09	26	D	16/03/09	17:52	20:34	2.7
R1*	-60.49	-48.20	A09	12	N	14/03/09	22:32	01:24	2.9
C3	-59.69	-44.08	A09	72	D	21/03/09	17:44	20:34	2.8
C3	-59.69	-44.08	A09	75	N	22/03/09	00:25	03:25	3.0
P2	-55.27	-41.35	A09	152	D	31/03/09	13:03	15:43	2.7
P2	-55.27	-41.35	A09	146	N	31/03/09	00:50	03:49	3.0
P3	-52.83	-40.05	A09	167	D	02/04/09	17:06	19:38	2.5
P3	-52.83	-40.05	A09	183	N	03/04/09	23:21	02:10	2.8

Once the net had been recovered, cod ends were detached, brought into the laboratory and decanted into labelled buckets. Some specimens were removed immediately from the buckets for other experiments or analysis and this was recorded with the preservation of the sample. Once all experimental specimens had been removed, the remaining catch was preserved, with some samples being preserved in formalin and a small number in 95% ethanol if molecular work was anticipated on specimens. Samples were then transported back to the Cambridge site where they were stored at ambient temperature until later analysis.

2.2.3 Sample analysis

Sample analysis was carried out by myself and a colleague, P. Ward, in 2015. Samples were first sorted as a whole, enumerating all individuals of larger and less abundant taxa such as larger euphausiids, chaetognaths, fish and gelatinous organisms. Samples were then split to sequentially smaller subsamples using a Folsom Plankton Splitter. Splits ranged from 1/2 to 1/1024 depending on the number of organisms present. Organisms were then identified to the lowest possible taxonomic level and counted under a stereo-microscope. More common copepods and euphausiids were identified to species and, where possible, stage. Other taxa and less common copepods were identified to the lowest possible taxonomic level above species.

Raw counts were multiplied by split to give a count for the whole sample, and converted to abundance m^{-2} by dividing by the volume of water filtered by the net (m^3) and multiplying by the depth interval (125 m). Flow rate data were taken from the flowmeter attached to the MOCNESS where possible. On occasions the flowmeter failed so the volume filtered was calculated using the equation given by plotting duration of individual net haul against volume filtered from observed flowmeter readings. Details of this are in Appendix 1.

One set of samples from the autumn cruise (JR200, R1, Night) and an individual sample from P3, Night (Net 7, 250 – 375 m) were in too poor a condition to analyse (due to evaporation of the preservative) or lost entirely so are not incorporated in this analysis.

2.2.4 Data preparation and pre-treatment

Data analysis and statistical treatment was performed by myself. Data were first combined into one sample (net) by variable (taxa/ stage) matrix and variables assigned to their respective higher taxonomic categories. Any variables that totalled zero across the entire dataset were removed. An initial summary analysis was conducted on the entire abundance

dataset to determine contribution to abundance from particular levels of taxonomic classification and overall patterns within the dataset.

Since number of taxa (including stages) totalled up to >230 in some datasets, the dataset was reduced before further analysis. Stages were generally combined to their respective species, the exceptions being *Metridia* copepodites which comprised a significant number but could not be accurately speciated, and euphausiid calyptopis and furcilia stages. Less common species were aggregated to genus (spp.). Finally, since some taxa, including *Chaetognatha*, *Polychaeta*, *Salpa*, and *Ostracoda* were of too coarse a taxonomic classification, thus hiding species-specific variation, they were excluded from quantitative analysis but considered qualitatively.

The resulting abundance (individuals m^{-2}) dataset was converted to biomass (mg dry weight (DW) m^{-2}) using published body size to weight ratios (Ward et al., 2012a). The biomass dataset was analysed first as a combined 'two-year' dataset, then separated into summer (JR177, S08) and autumn (JR200, A09).

2.2.5 Data analysis and statistics

Multivariate analyses were conducted on biomass data in PRIMER 7 (v7.0.13, Primer-E) (Clarke and Gorley, 2015). Data were imported as a sample-variable matrix where samples represented each depth sampled and variables represented taxa. There were 64 samples in total for summer (4 stations, 8 depths, day and night at each station) and 55 samples for autumn (the same sampling regime minus the lost samples explained earlier).

For all station by station analyses, sample data were transformed using a log(x+1) transformation. This transformation was selected as the most appropriate after shade plots confirmed that this reduced the extreme dominance of heavily abundant taxa to similarity matrices relative to square root or fourth root transformations. For station by station analyses, resemblance matrices based on the log(x+1) transformed data were created, calculating Bray-Curtis similarities between samples. For analyses of contribution by taxa, data were standardised so that all variables per sample totalled 100. Bray-Curtis similarities were calculated between variables.

Hierarchical cluster analysis (group average clustering) was performed, first on the two-year dataset (S08 and A09 combined) and subsequently on the annually separated data. A Type 1 SIMPROF (similarity profiling) test was carried out during the analysis, resulting in clusters which showed significant between-group differences, but where no further within-group

structure could be statistically shown. A new factor was produced representing the cluster groupings.

A non-metric multidimensional scaling (nMDS) analysis (Kruskal stress formula 1) was also performed on all three datasets. This produces an ordination in multidimensional space with distances between the samples representative of the similarities between samples in the underpinning resemblance matrix. The new cluster group factors were overlaid on their respective nMDS plots to illustrate the spatial ordination of samples in terms of groups of samples that showed particular within-group similarities.

To investigate whether particular taxa or groups of taxa could be identified as driving the observed latitudinal and vertical patterns, or of describing a community trait gradient, a series of analyses using resemblances between variables as well as between samples were run. The following analyses were applied separately to each seasonally separated dataset. The list of taxa was first reduced to incorporate only those that contributed ≥0.5% biomass to at least one station, an approach described by Field et al. (1982) to reduce the risk of associating species based on shared absences, and to ensure that analyses are not biased by the most dominant taxa overall. A Type 2 SIMPROF test was first run, rejecting the hypothesis of no underlying structure within the retained list of taxa and encouraging further analysis. This resulted in a reduced dataset of 34 taxa in S08 and 32 in A09.

Sample data were then transformed, followed by classification and ordination as described above. Variable data were standardised, a resemblance matrix created and cluster analysis with Type 3 SIMPROF testing carried out between variables. Based on these cluster groups, coherent species curves were created as a first means of identifying groups of species that demonstrated some level of within-group association, or single taxa that formed no associations with other taxa. Shade plots were then created, ordering variables by coherent species groupings, thus illustrating relative abundance of taxa in the coherent species groupings, and indicating whether a reduced number of species could be seen to drive variability in observed patterns.

To aid statistical discrimination of influential taxa between cluster groups, SIMPER (similarity percentage) analysis was carried out. A similarity statistic for each group and a dissimilarity statistic for every pair of groups was produced, based on relative contribution, presence or absence of taxa. Abundance and contribution to dissimilarity statistics were calculated for highest contributing taxa. SIMPER analysis groups were determined by merging SIMPROF groups produced by cluster analysis on the 0.5% datasets according to appropriate branches of the dendrogram (see Figures 6 and 7, bottom panels).

Since there was a strong vertical component to the clustering of sample groups, subtle differences in biomass change between nearby depths may not have been fully reflected in resulting clusters. The shade plot thus had the additional advantage of allowing interrogation of the relative abundances of particular taxa within groups, identification of subtle shifts in the centre of biomass of selected taxa from one depth to another and inference of vertical migrations within the water column.

2.2.6 Calculating biomass and carbon flux

To investigate diurnal shifts in the range and distributions of biomass within the 0.5% subset, the biomass flux between day and night for each station was calculated. The parameters used in the calculation are listed in Table 2.2. The process taken is set out in Figure 2.2 and described in the following text. R1 A09 was excluded as there was no night time net to act as a comparison.

In order to calculate biomass flux for each station, step 1 was to calculate three different metrics of biomass distribution through the water column, representing the main body of the population: (i) the depth of the modal peak biomass (D_{Modal}), (ii) depth of the 25th percentile in biomass (D_{25th}) and (iii) 75th percentile in biomass (D_{75th}) for each taxon (*x*) in both *day* and *night* hauls at each station (*S*).

Step 2 was to calculate the modulus difference in depth of these three biomass distribution metrics between day and night according to Equations 2.1, 2.2 and 2.3:

$$\Delta_{Modal,S,X} = \left| D_{Modal,day,S,X} - D_{Modal,night,S,X} \right| \quad \text{Equation 2.1}$$

$$\Delta_{25th,S,X} = \left| D_{25th,day,S,X} - D_{25th,night,S,X} \right| \quad \text{Equation 2.2}$$

$$\Delta_{75th,s,x} = \left| D_{75th,day,S,X} - D_{75th,night,S,X} \right| \quad \text{Equation 2.3}$$

In step 3, the average of b_{day} and b_{night} (mg DW m^{-3}) at the respective depth was derived to determine the mean biomass undergoing vertical flux (*B*, mg DW m^{-3}) (Equations 2.4-2.6):

$$B_{Modal,S,X} = \frac{b_{Modal,day,S,X} + b_{Modal,night,S,X}}{2} \quad \text{Equation 2.4}$$

$$B_{25th,S,X} = \frac{b_{25th,day,S,X} + b_{25th,night,S,X}}{2}$$ Equation 2.5

$$B_{75th,S,X} = \frac{b_{75th,day,S,X} + b_{75th,night,S,X}}{2}$$ Equation 2.6

For Step 4, *Flux* (mg DW m^{-2}) was calculated by multiplying *B* by *Δ* (Equations 2.7-2.9)*:*

$$Flux_{Modal,S,X} = B_{Modal,S,X} \cdot \Delta_{Modal,S,X}$$ Equation 2.7

$$Flux_{25th,S,X} = B_{25th,S,X} \cdot \Delta_{25th,S,X}$$ Equation 2.8

$$Flux_{75th,S,X} = B_{75th,S,X} \cdot \Delta_{75th,S,X}$$ Equation 2.9

Step 5 was to average the three biomass distribution metrics to derive a mean estimate of flux ($\overline{Flux}$, mg DW m^{-2}) (Equation 2.10):

$$\overline{Flux}_{S,X} = \frac{Flux_{Modal,S,X} + Flux_{25th,S,X} + Flux_{75th,S,X}}{3}$$ Equation 2.10

For Step 6, the flux across all taxa making more than a 0.5% contribution to station biomass was summed to derive a community level flux (*Comm_flux*, mg DW m^{-2}) (Equation 2.11):

$$Comm\_flux_S = \sum_{X=1}^{X=n} \overline{Flux}_{S,X}$$ Equation 2.11

Where *n* is the total number of taxa making greater than a 0.5% contribution to station biomass

Table 2.2: Parameters used in biomass flux calculation

Symbol	Definition	Unit
S	Station	
X	Taxon	
n	Total number of taxa making more than a 0.5% contribution to station biomass	
night	Night time haul	
day	Daytime haul	
Modal	Mean modal biomass	mg DW m^{-3}
25^{th}	25th percentile biomass	mg DW m^{-3}
75^{th}	75th percentile biomass	mg DW m^{-3}
D	Depth of biomass distribution metric (i.e. *Modal*, 25^{th} or 75^{th})	m
Δ	Modulus of the difference in *D* between *night* and *day*	m
b	Biomass	mg DW m^{-3}
B	Biomass undergoing flux	mg DW m^{-3}
Flux	Movement of biomass between D_{day} and D_{night}	mg DW m^{-2}
$\overline{Flux}$	Mean flux across the mode, 25th and 75th percentiles	mg DW m^{-2}
Comm_flux	Community level flux derived from all taxa making more than 0.5% contribution to station biomass	mg DW m^{-2}

Two measures of carbon flux were subsequently calculated as resulting from the migratory biomass (the portion of the population crossing 125 m between D and N): (i) a minimum estimate of active carbon flux, and (ii) a maximum zooplankton-derived carbon flux.

The first was estimated by summing, for the migratory biomass, respiratory C produced below 125 m and egestory FPC produced during the hour post-feeding. This represents a minimum estimate, with only faecal pellets produced during active descent contributing to flux.

The second was estimated by summing, for the migratory biomass, respiratory C produced below 125 m and egestory FPC produced over the entire feeding period i.e. hours of darkness for normal DVM and hours of light for reverse DVM (rDVM) (see later discussion). This assumes that the migratory biomass is not static but comprised of individuals that

periodically replace each other as they become satiated, sink and empty their guts. This therefore represents a maximum zooplankton-derived carbon flux (both passive and active), some of which will be remineralised or consumed before sinking out.

As a first step, for individual species in the 0.5% biomass subset, the amount of biomass (mg DW m^{-2}) undergoing flux across 125 m was calculated through the following steps:

1. The % of total individual biomass occupying the top 125 m for D and N was calculated
2. The difference in biomass (%) between D and N was calculated
3. The average total individual biomass was calculated as follows: $(b_{tot}(D) + b_{tot}(N))/2$
4. The % difference (step 2) was multiplied by average biomass (step 3) to calculate the biomass change in the top 125 m between D and N
5. The total individual biomass change was summed for all migrating species at each station/ season

where b_{tot} is total individual species biomass.

Secondly, the number of hours of darkness and light was calculated for each station, for the given latitude and date of sampling, by determining sunrise and sunset times. These were calculated using the sunrise.set function in the StreamMetabolism package in RStudio (V.1.0.136) (R Core Team (2016).

Respiratory flux (R_{flux}) was calculated by applying a mean O_2 consumption rate (based on a representative range of Antarctic species from Ikeda and Fay (1981)) to the migratory biomass and converting it from O_2 to C using the relationship in Equation 2.12:

$$R_{flux} = \text{ml } O_2 \text{ mg DW } h^{-1} \text{ x RQ x } (12/22.4) \qquad \text{Equation 2.12}$$

using an RQ of 0.99 (weighted mean of values for copepods and euphausiids (Mayzaud et al., 2005)).

The derived respiration rate was applied to the migrating biomass at each station, and multiplied by the number of hours the animals were below 125 m (light hours for DVM and dark hours for rDVM).

Egestory flux (E_{flux}) was calculated using the relationship of FPC to chl-*a* derived by Wexels Riser et al. (2007) for *Calanus* spp. (Equation 2.13):

$$E_{flux} = 0.0547x + 0.0658 \qquad \text{Equation 2.13}$$

Where E_{flux} is µg FPC $copepod^{-1}$ h^{-1} and x is measured chl-*a* over the top 125 m at respective stations.

Station-specific FPC copepod^{-1} h^{-1} was calculated using *in situ* measured chl-*a* values and converted to FPC mg DW $^{-1}$ h^{-1} by dividing by the mean weight of representative *Calanus* spp. from the study region, as representative of the mean size of the migrating biomass. This was applied to the biomass undergoing flux at each station and multiplied by either one hour or the number of hours the migrating biomass was at the surface (for active flux or total carbon flux respectively).

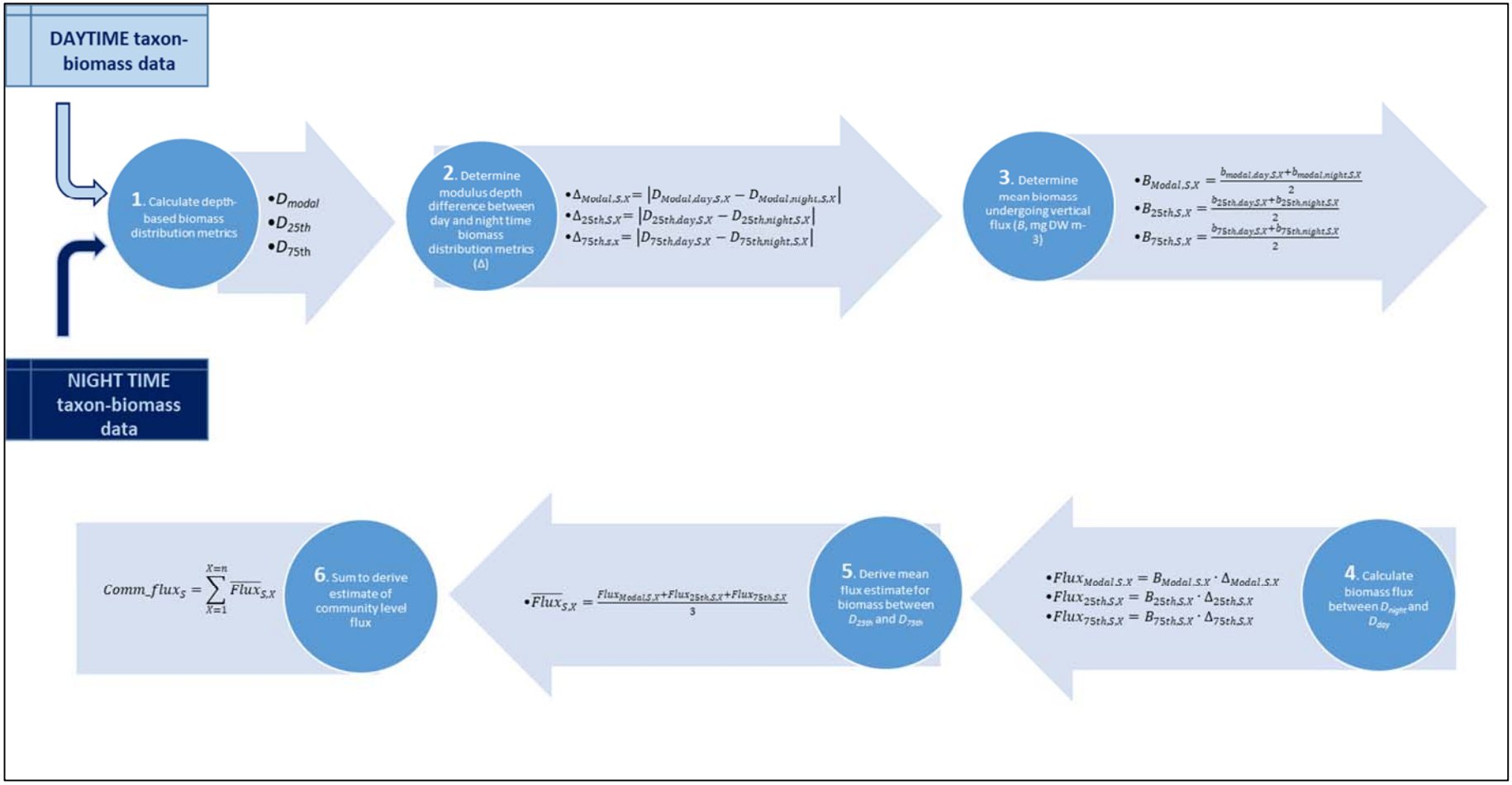

Figure 2.2: Schematic illustrating the steps taken to calculate the total biomass flux (mg DW m^{-2}), between day and night, of all taxa that comprised ≥0.5% biomass at each station

2.3 Results

2.3.1 Physical environment and hydrography

Temperature and salinity profiles, and chlorophyll profiles, are shown in Figure 2.3 and Figure 2.4 respectively. In summer 2008 (S08), R1 was characterised by a shallow and unstable (~20 m) mixed layer with relatively high chl-*a* (1.1 µg l^{-1} in the top 15 m). The autumn 2009 (A09) mixed layer was warmer (by up to 2.5 °C), deeper (~100 m, with higher salinity and lower chl-*a*) and more stable.

The water column at C3 in S08 had a sharp thermocline beneath a thin subsurface (~10 m) layer of warmer water, which developed into a deep and stable (~80 m) mixed layer in A09. At C3 the top 100 m also warmed by up to 2.5 °C and surface (~0-20 m) salinity increased by ~0.4 PSU. Both years exhibited quite low chl-*a* profiles although A09 increased slightly (by 0.2-0.4 µg l^{-1}) with a sub-surface maximum of 0.65 µg l^{-1} at 35 m.

P2 and P3 had similar temperature and salinity profiles in both years, the main difference being the temperature of the top ~80 m in A09 which was 1-1.5 °C warmer. By ~200 m at R1/C3, and ~120 m at P2/ P3, the S08 and A09 profiles had become almost identical. The S08 mixed layer at P2 was characterised by a deep and relatively stable chl-*a* layer (mean 1.0 µg l^{-1} in top 60 m) whilst the mixed layer at P3 had a more variable vertical profile with numerous peaks, with a maximum of 1.1 µg l^{-1} at 45 m. In A09 the mixed layer of each station had approximately equivalent chl-*a* profiles with a mean of 0.3 µg l^{-1} over the top 60-80 m.

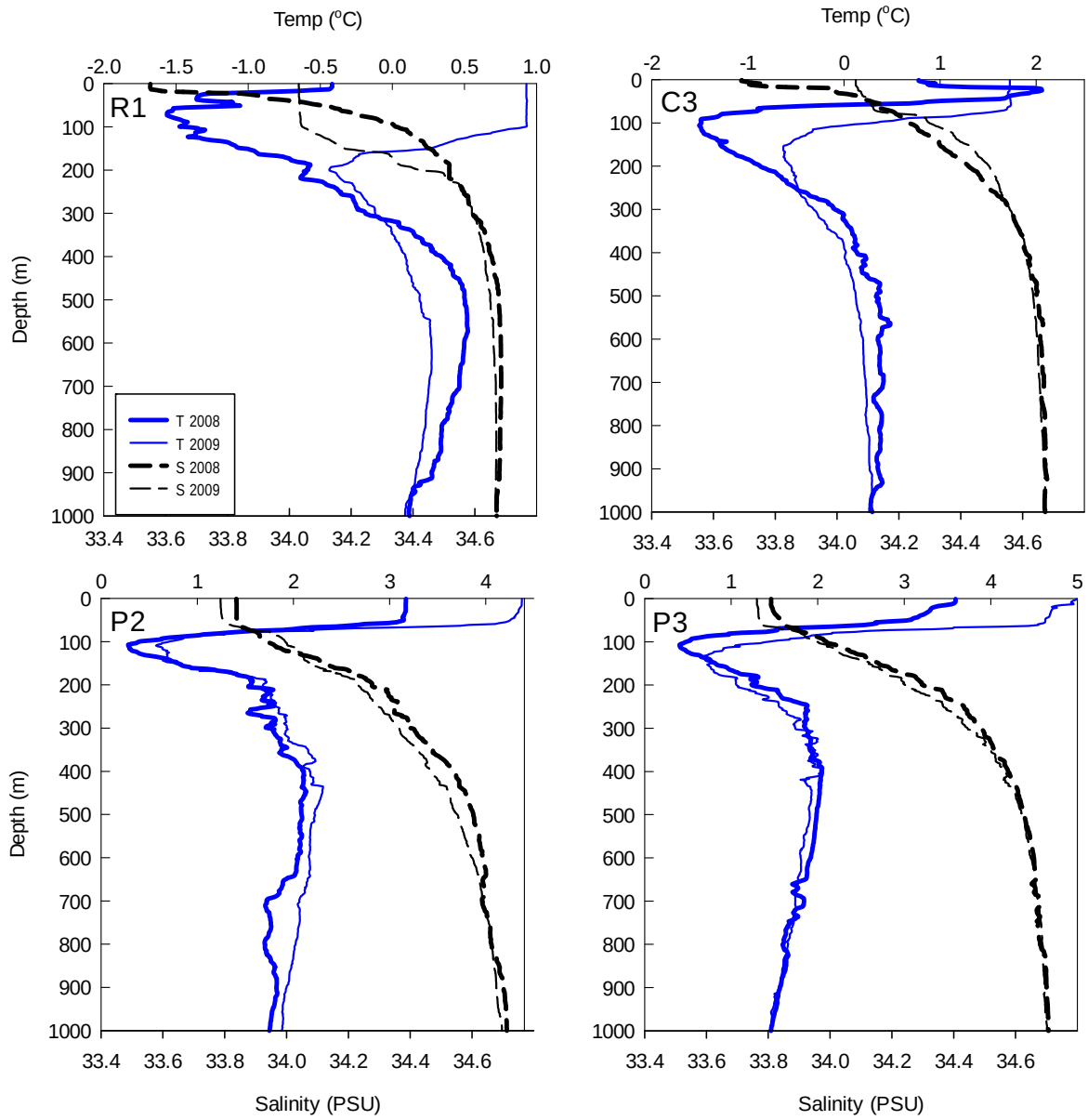

Figure 2.3: Temperature (blue) and salinity (dashed grey) profiles of stations R1, C3, P2 and P3 in summer 2008 (bold) and autumn 2009 (fine). Note different temperature scales on each graph (salinity scale remains the same).

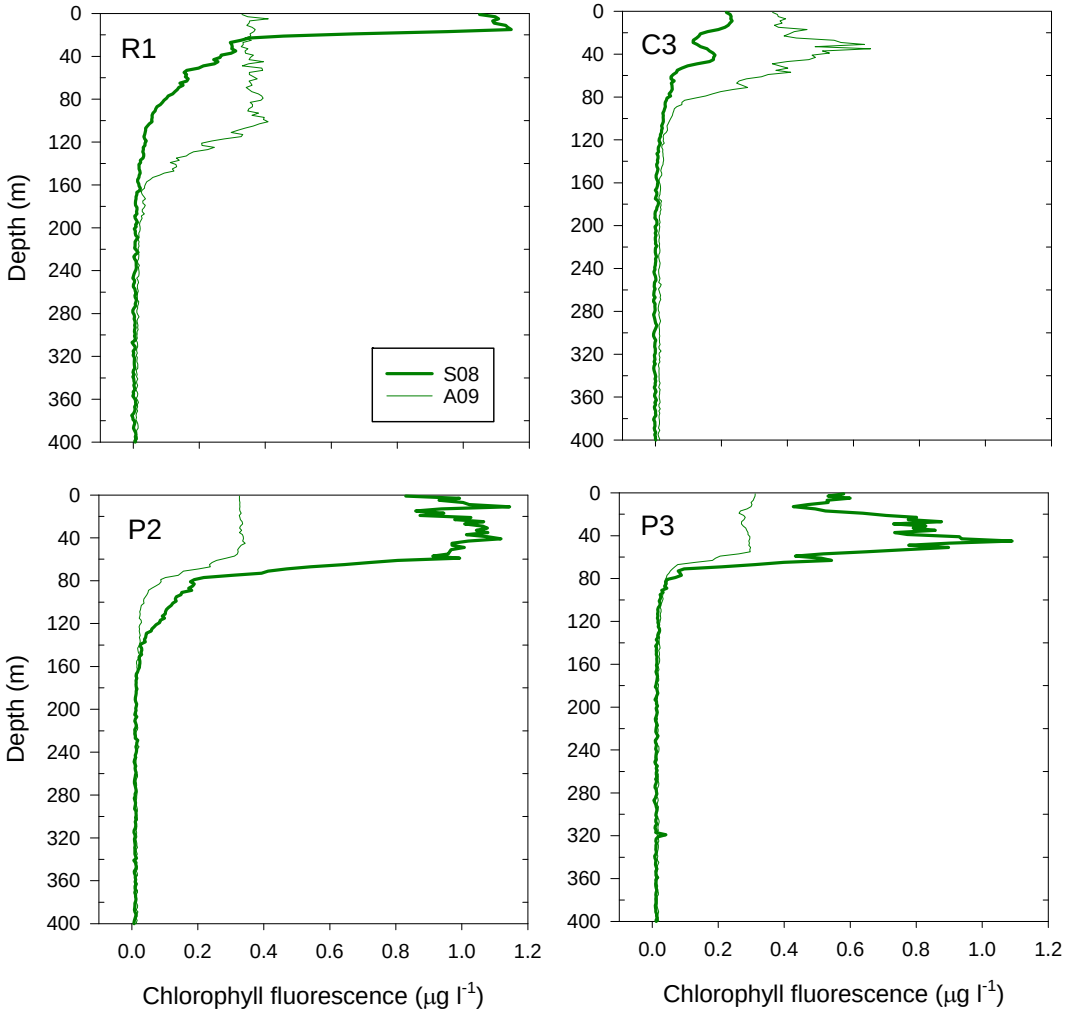

Figure 2.4: Chlorophyll fluorescence profiles for stations R1, C3, P2 and P3 in summer 2008 (bold) and autumn 2009 (fine).

2.3.2 Analysis of stations over depth and latitude

Multivariate analysis on the full (two-year) dataset showed the separation of the stations into two broad groups: a 'South' station grouping comprised of R1 and C3, and a 'North' station grouping comprised of P2 and P3. Cluster analysis produced two initial branches, one of which comprised solely the samples from 625-0 m from the North group. On the second node, one branch comprised deep samples from across South (most 1000-500 m samples) and North (selected 1000-500 m samples) stations, another comprised the remaining samples (spread across all depths) from the North group, and two samples (C3 (N), 1000-875 m, and R1 (D), 250-125 m) branched off separately. Additional groups were created within all of these nodes, with within-group similarity of final groups being explained primarily on the basis of depth.

The nMDS plot showed a similar pattern of North/South separation, additionally showing deeper samples to be positioned closer together than shallower samples which increasingly diverged with shoaling (Figure 2.5).

The same broad North/South grouping was retained when the dataset was split by year (Figure 2.6 and 2.7, top panels) although the distinction between latitudinal groups was significantly clearer in A09 (Figure 2.7). In A09, the first branching positioned R1/C3 and P2/P3 samples on opposite nodes of the dendrogram, with no evidence of increased homogeneity between deeper samples across the SACCF. In contrast, in S08 (Figure 2.6) a degree of homogeneity amongst deeper (generally 1000-375 m) samples was observed. Shallower (500 –0 m) samples increasingly diverged and broadly reproduced North/South groupings seen in Figure 2.5. This same structure was further reproduced when individual year datasets were reduced to contain only those taxa which contributed ≥0.5% to at least one sample (Figure 2.6 and 2.7, bottom panels). In S08, the first level split of the dendrogram separated deeper from shallower samples and the second level split between north and south. In A09, the first level split separated north from south, with depth determining the second level split.

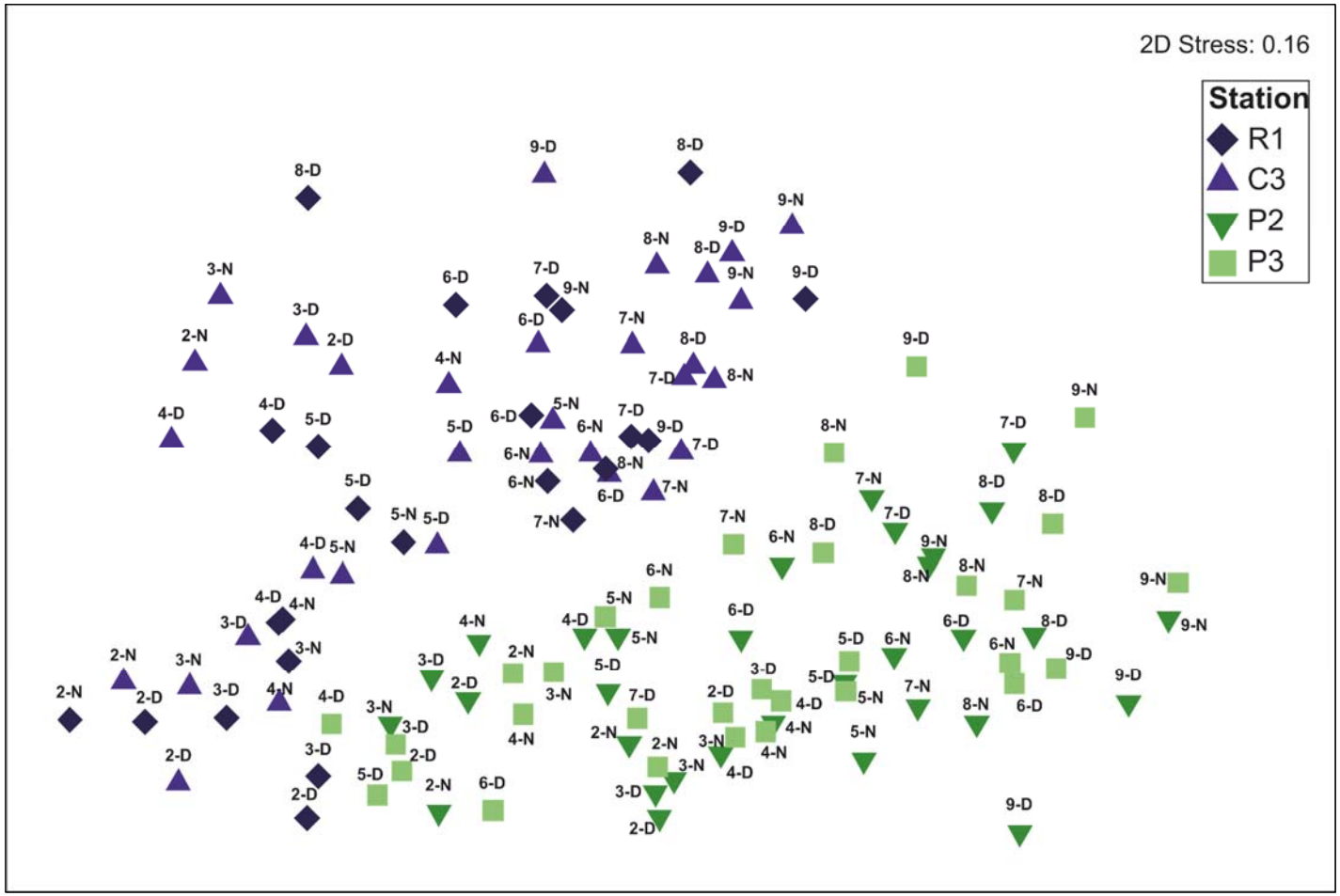

Figure 2.5: nMDS plot of the S08 and A09 combined dataset. Numbers refer to 125 m net intervals, where 2 is the deepest (1000-875 m) and 9 is the shallowest (125 m to surface). D and N refer to Day and Night. Analysis is based on the full (55) taxa list.

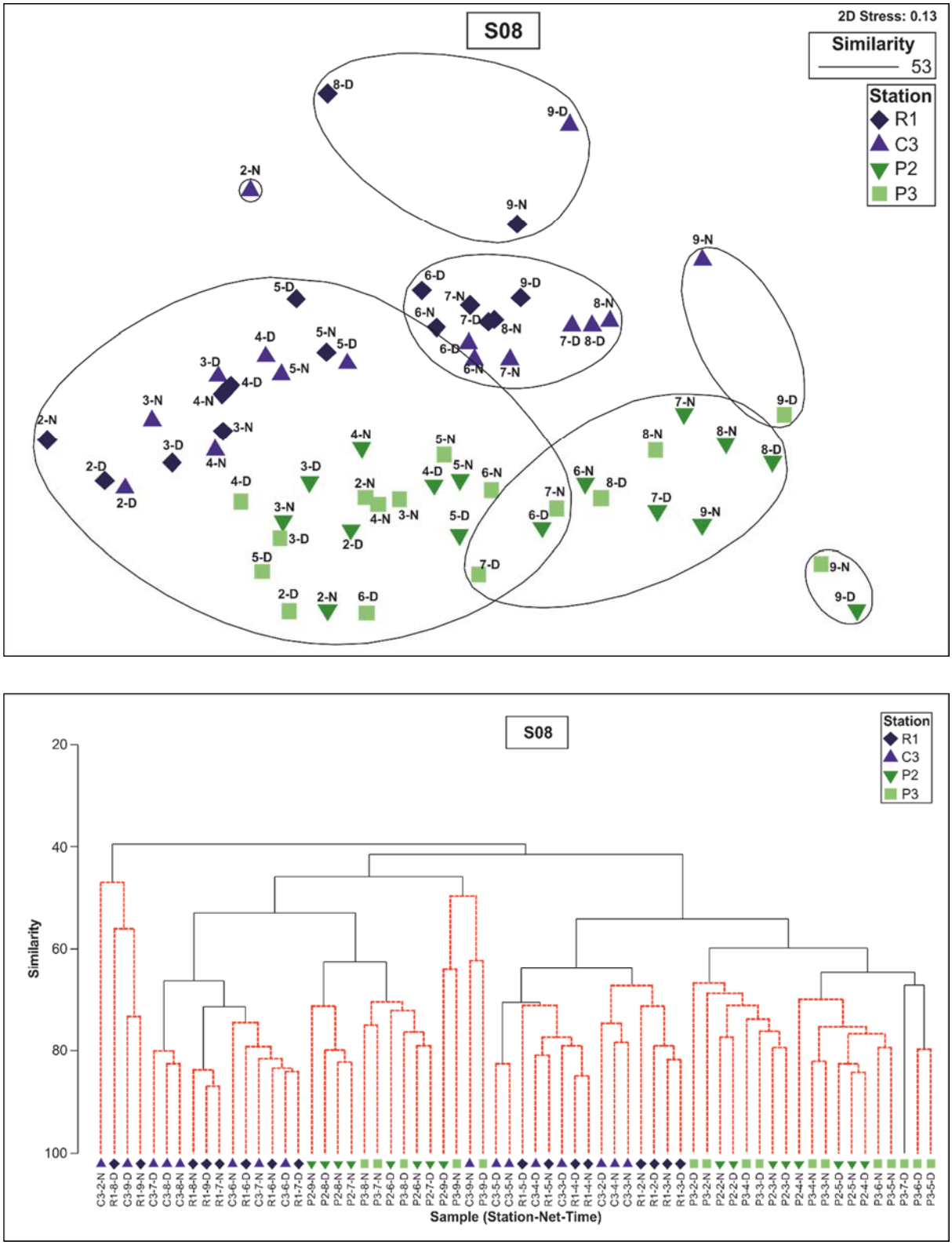

Figure 2.6: Ordination analysis on seasonally split data for S08. Top panel: nMDS plots based on full (55) taxa list with clusters overlain at the 53% similarity level. Bottom panel: cluster analysis based on the reduced dataset (taxa contributing ≥0.5% to at least one sample). Sample labelling follows the same convention as the previous figure.

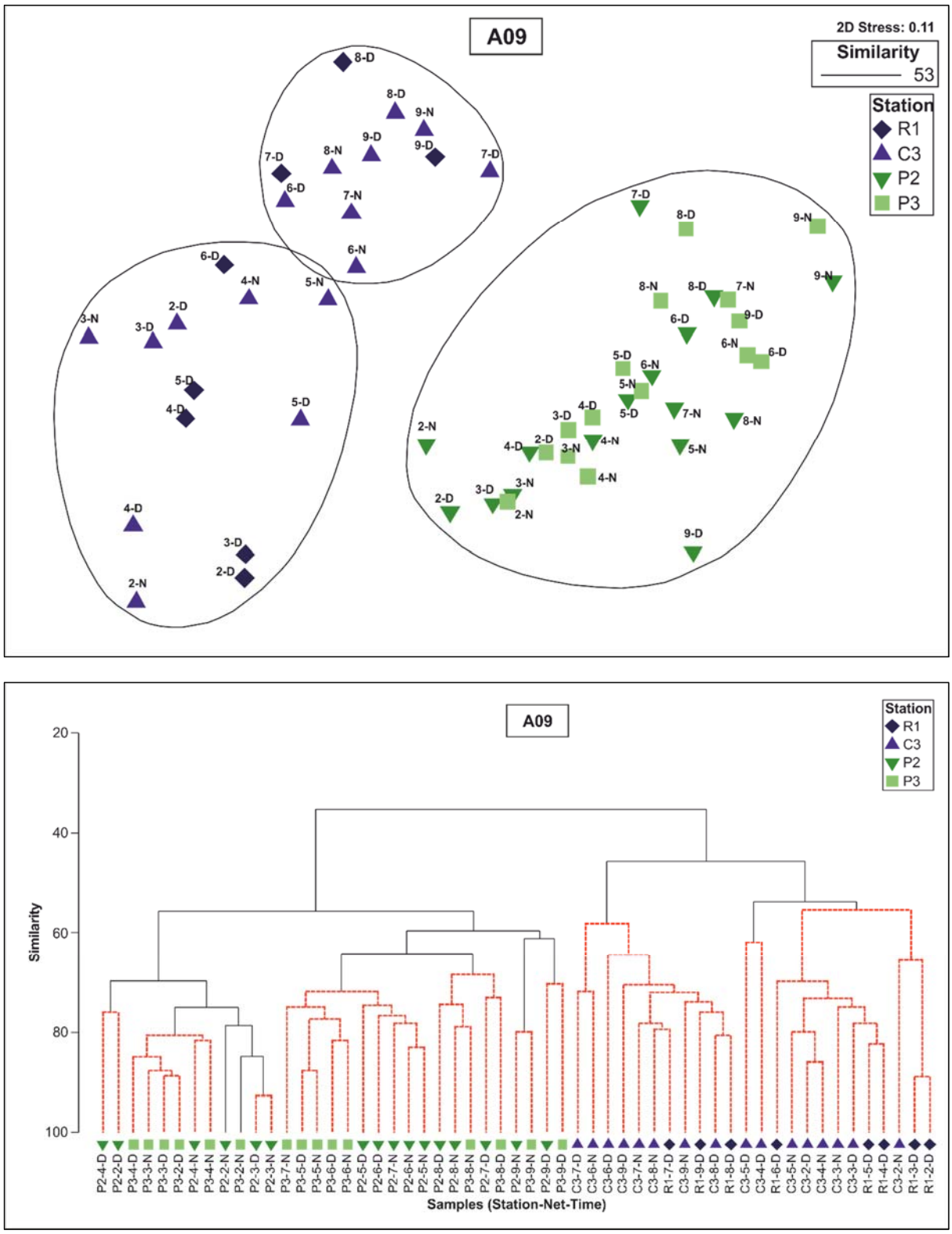

Figure 2.7: Ordination analysis on seasonally split data for A09. Top panel: nMDS plots based on full (55) taxa list with clusters overlain at the 53% similarity level. Bottom panel: cluster analysis based on the reduced dataset (taxa contributing ≥0.5% to at least one sample). Sample labelling follows the same convention as the previous figure.

2.3.3 Taxonomic contribution to station groupings

Between both years/seasons, there was a large degree of overlap in taxonomic contribution to SIMPER dissimilarities (Table 2.3), defined as those which cumulatively contributed ≥50% to between group dissimilarities. Out of 16 taxa in S08 and 12 in A09, 10 were found to be important in both years, with six and two unique taxa in S08 and A09, respectively. The full list of taxa is given in Table 2.4.

In general, no single taxon disproportionately influenced dissimilarities in a particular group, with 7-8 taxa in S08, and 5-9 in A09, together comprising the ≥50% individual between group dissimilarities. Mild exceptions to this were *Euphausia superba*, which contributed 12% of the difference between shallow (500-0 m) and surface (top 125 m only) samples in summer, and 18% between deep and shallow samples in autumn (most abundant in surface and shallow samples respectively), and *Calanus simillimus*, contributing >12% to differences between north and south in autumn with high biomass in northern and correspondingly low biomass in southern samples.

Many of the most important taxa i.e. those identified as most contributory by SIMPER, were found to occupy broad depth ranges with relatively few being wholly absent from a particular group. The only taxa entirely absent from the main SIMPER groups in Table 2.3 were *Ctenocalanus* spp and *Calanus simillimus* (absent from shallow samples in C3/R1 in summer but relatively abundant in shallow waters of P2/P3). *Metridia curticauda*, *Lucicutia* spp. and *Eucalanus* spp. were the only taxa limited to deeper waters. For most other taxa, differences between groups were generally driven by variations in the distribution of biomass within a wide depth distribution rather than absolute presence or absence.

As well as similarities in taxa driving inter-group differences between years, there were also some key differences. Firstly, in S08, the major division occurred between shallow and deep water samples, with *M. curticauda* defining deep samples and *Euchaeta antarctica* and *Thysanoessa* spp. characterising shallower samples (Figure 2.8 A). In A09 the first level split was between north and south, the differences largely being determined by the absence of *Rhincalanus gigas*, *C. simillimus* and *Thysanoessa spp.* at C3/R1 (Figure 2.8 E). Secondly, the sub-groups (N/S) that formed from second level dendrogram splits in S08 were defined by more subtle variations in taxonomic abundance (Figure 2.8 C & D) than the A09 sub-divisions (deep/shallow), where high abundances of typical deeper dwellers (*M. curticauda* and *Eucalanus* spp.) separated deep from shallow sub-groups (Figure 2.8 F & G). Finally, in S08, there was a marked distinction between the bulk of the shallow samples (500-125 m) and the 125 m to surface layer. This was driven largely by very high abundances of euphausiids

(*E. superba* and *Thysanoessa* spp.) and high abundances of *C. simillimus* in the surface, which together explained 28% of the dissimilarity (Figure 2.8 B).

Table 2.3: Dissimilarity statistics from SIMPER analysis carried out on the main groupings identified by multivariate analysis. Branching refers to the level of the split on the dendrogram, Comparison gives the descriptions of groups of samples that were being compared, and Dissimilarity is the average dissimilarity statistic based on cumulative species contributions to difference between groups. For S08 Shallow encompassed nets from 500-0 m (North and South) and Deep encompassed nets from 1000-375 m (North) 500-100 m (South). For A09 Shallow encompassed nets 625-0 m (North) and 500-0 m (South) and Deep encompassed nets 1000-750 m (North) and 1000-375 m (South).

	S08	
Split level	**Comparison**	**Dissimilarity**
Level 1	Shallow v Deep	58.62
Level 2	Shallow v surface	54.2
Level 2	Deep: North v South	45.96
Level 3	Shallow: North v South	47.16

	A09	
Split level	**Comparison**	**Dissimilarity**
Level 1	North v South	64.69
Level 2	North: Deep v Shallow	44.29
Level 2	South: Deep v Shallow	54.36

Table 2.4: Taxa identified as cumulatively contributing to ≥50% difference between SIMPER groups. S08 refers to austral summer 2008/09; A09 refers to austral autumn 2009.

Taxon	**Present**
Calanoides acutus (Copepoda)	S08
Calanus propinquus (Copepoda)	S08
Calanus simillimus (Copepoda)	S08, A09
Ctenocalanus spp. (Copepoda)	S08
Euchaeta antarctica (Copepoda)	S08, A09
Euchaeta biloba (Copepoda)	S08
Euchaeta rasa (Copepoda)	S08
Euphausia frigida (Euphausiacea)	S08, A09
Euphausia superba (Euphausiacea)	S08, A09
Lucicutia spp. (Copepoda)	S08
Metridia curticauda (Copepoda)	S08, A09
Metridia gerlachei (Copepoda)	S08, A09
Metridia lucens (Copepoda)	S08, A09
Pleuromamma robusta (Copepoda)	S08, A09
Rhincalanus gigas (Copepoda)	S08, A09
Thysanoessa spp. (Euphausiacea)	S08, A09
Eucalanus spp. (Copepoda)	A09
Metridia copepodites (Copepoda)	A09

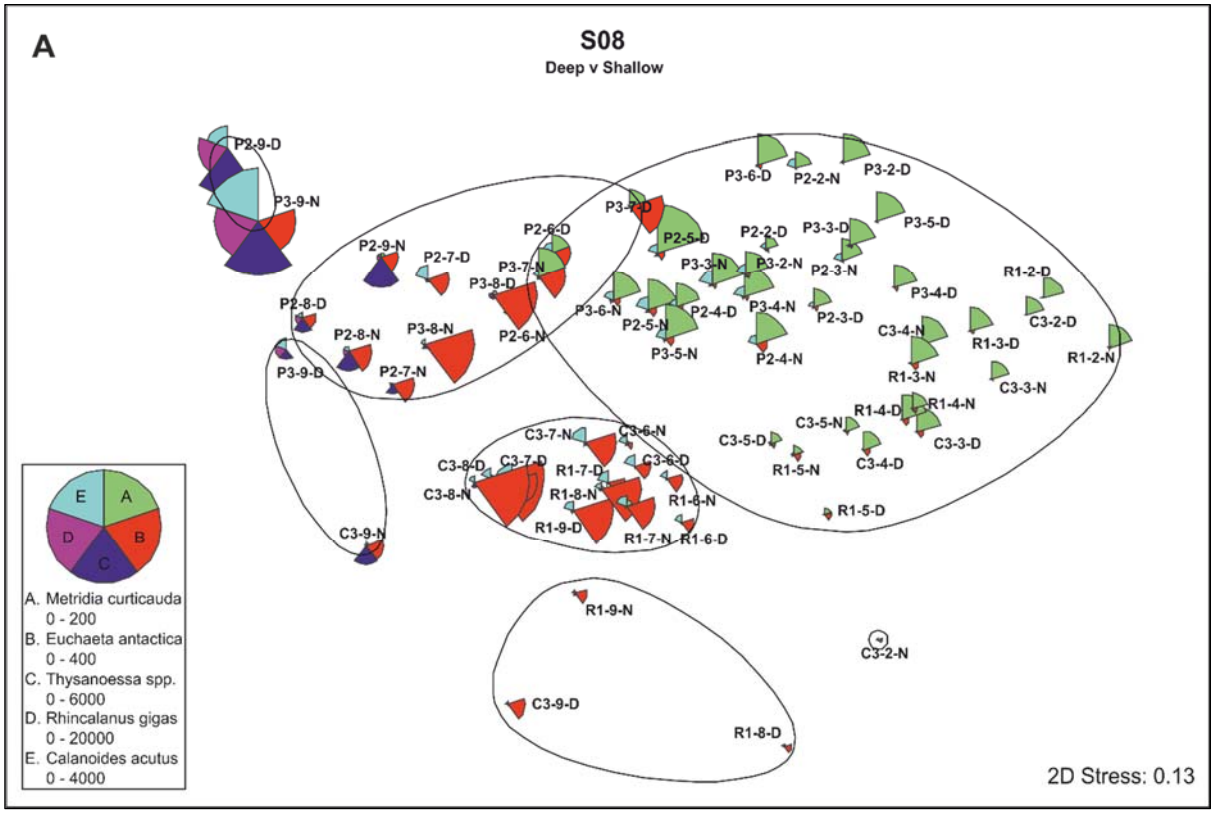
A
S08
Deep v Shallow
A. Metridia curticauda
0 - 200
B. Euchaeta antactica
0 - 400
C. Thysanoessa spp.
0 - 6000
D. Rhincalanus gigas
0 - 20000
E. Calanoides acutus
0 - 4000
2D Stress: 0.13

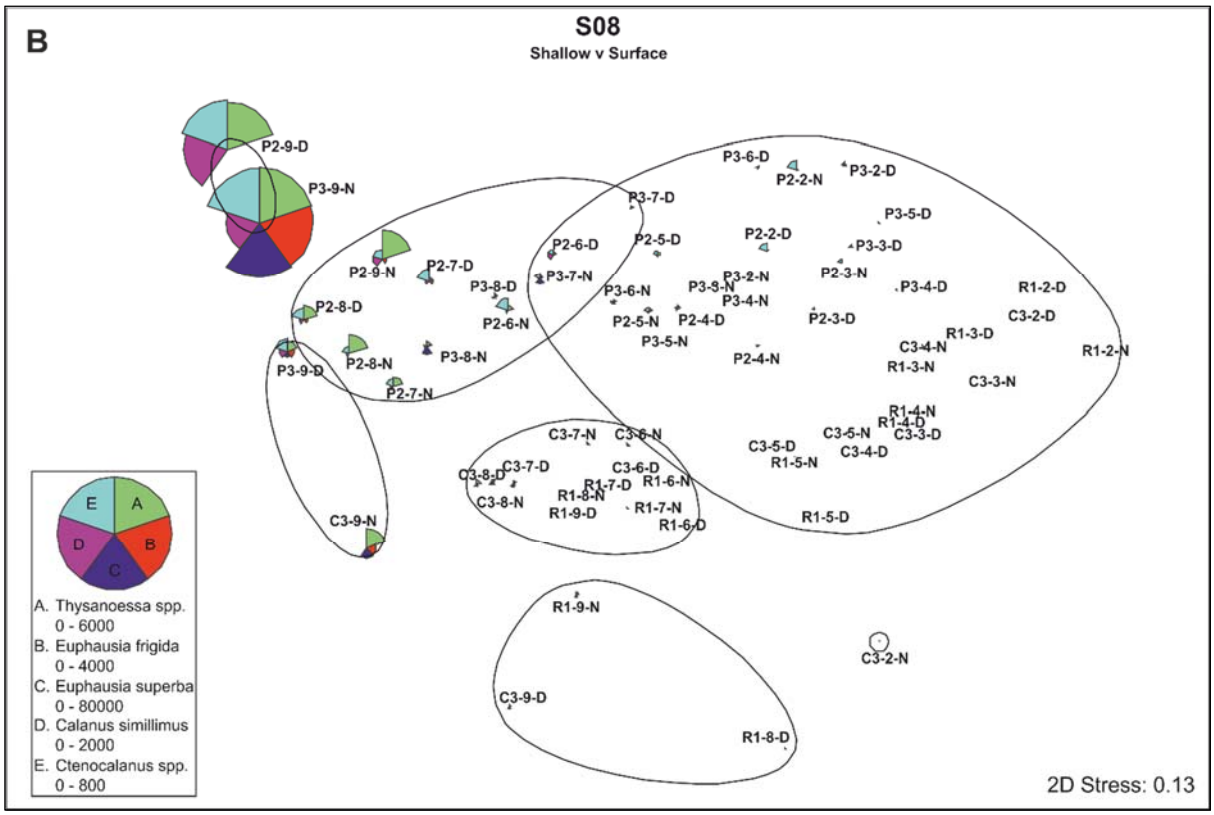
B
S08
Shallow v Surface
A. Thysanoessa spp.
0 - 6000
B. Euphausia frigida
0 - 4000
C. Euphausia superba
0 - 80000
D. Calanus simillimus
0 - 2000
E. Ctenocalanus spp.
0 - 800
2D Stress: 0.13

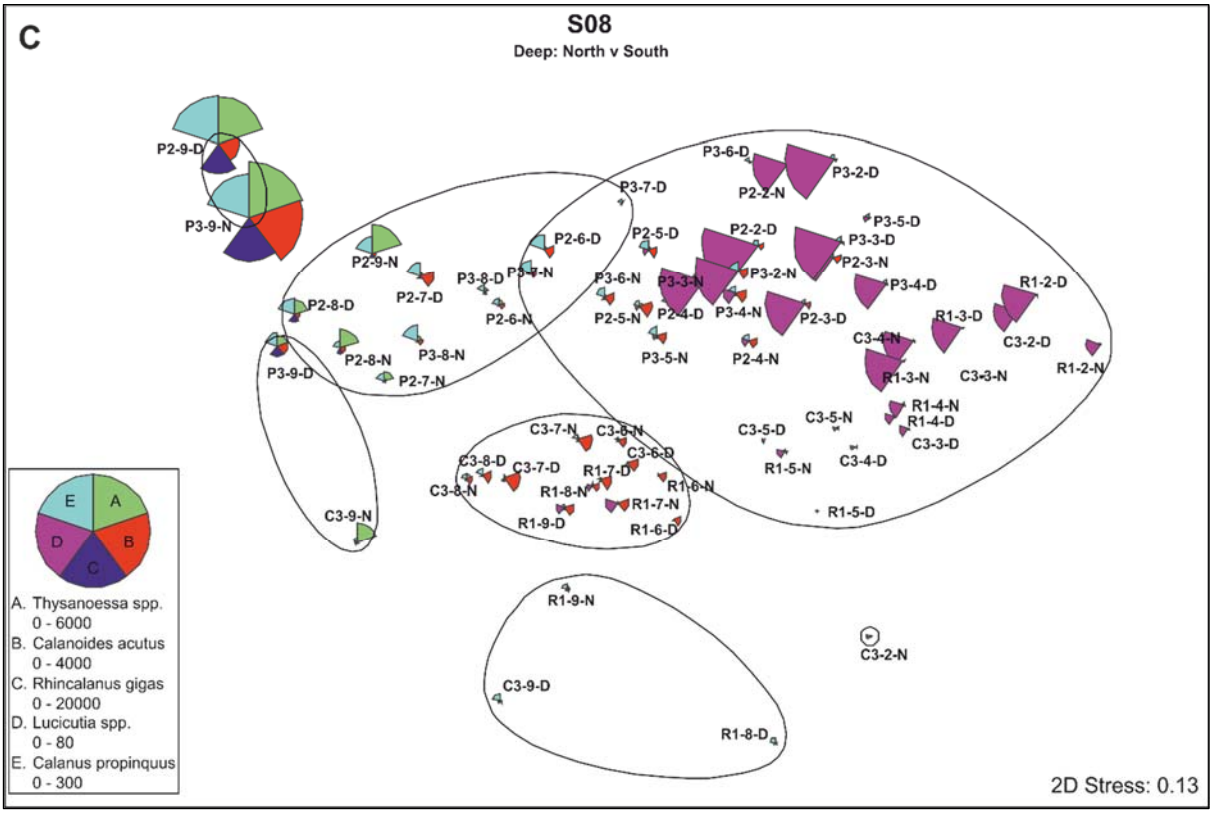
C
S08
Deep: North v South
A. Thysanoessa spp.
0 - 6000
B. Calanoides acutus
0 - 4000
C. Rhincalanus gigas
0 - 20000
D. Lucicutia spp.
0 - 80
E. Calanus propinquus
0 - 300
2D Stress: 0.13

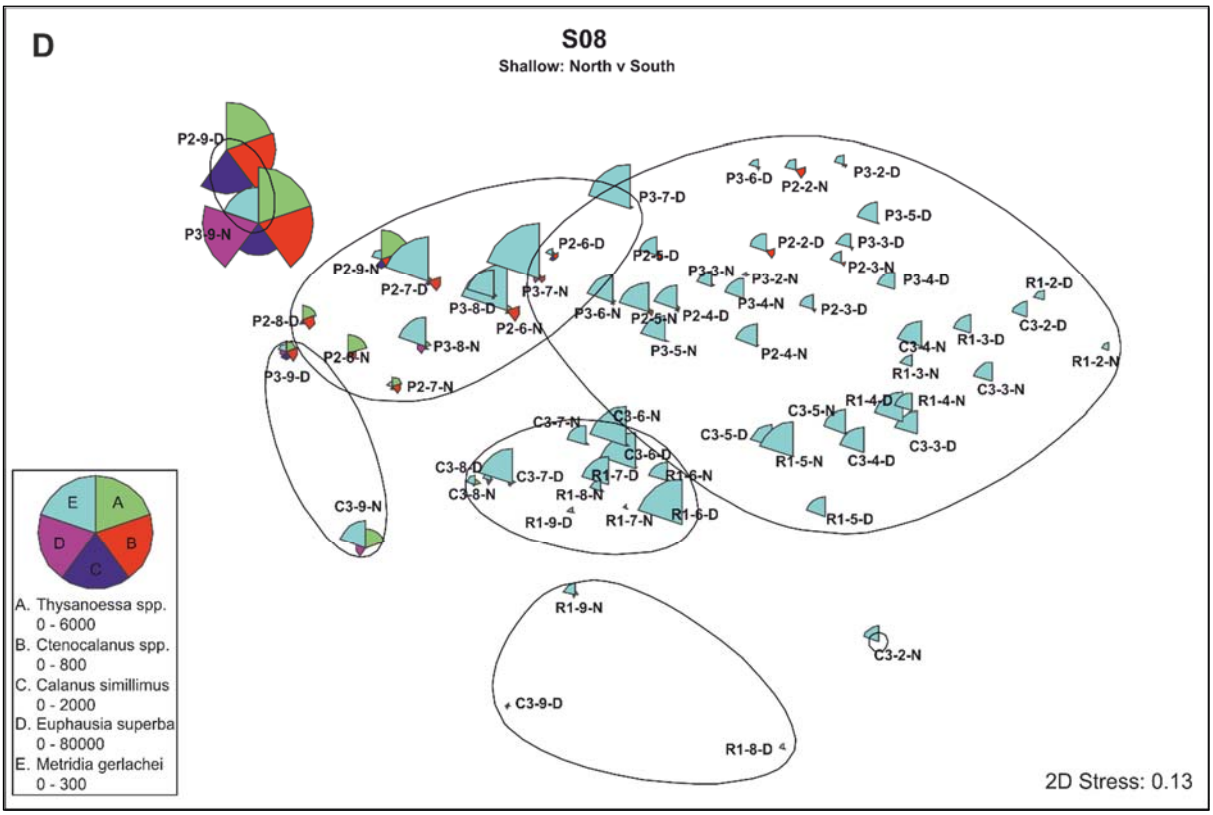
D
S08
Shallow: North v South
A. Thysanoessa spp.
0 - 6000
B. Ctenocalanus spp.
0 - 800
C. Calanus simillimus
0 - 2000
D. Euphausia superba
0 - 80000
E. Metridia gerlachei
0 - 300
2D Stress: 0.13

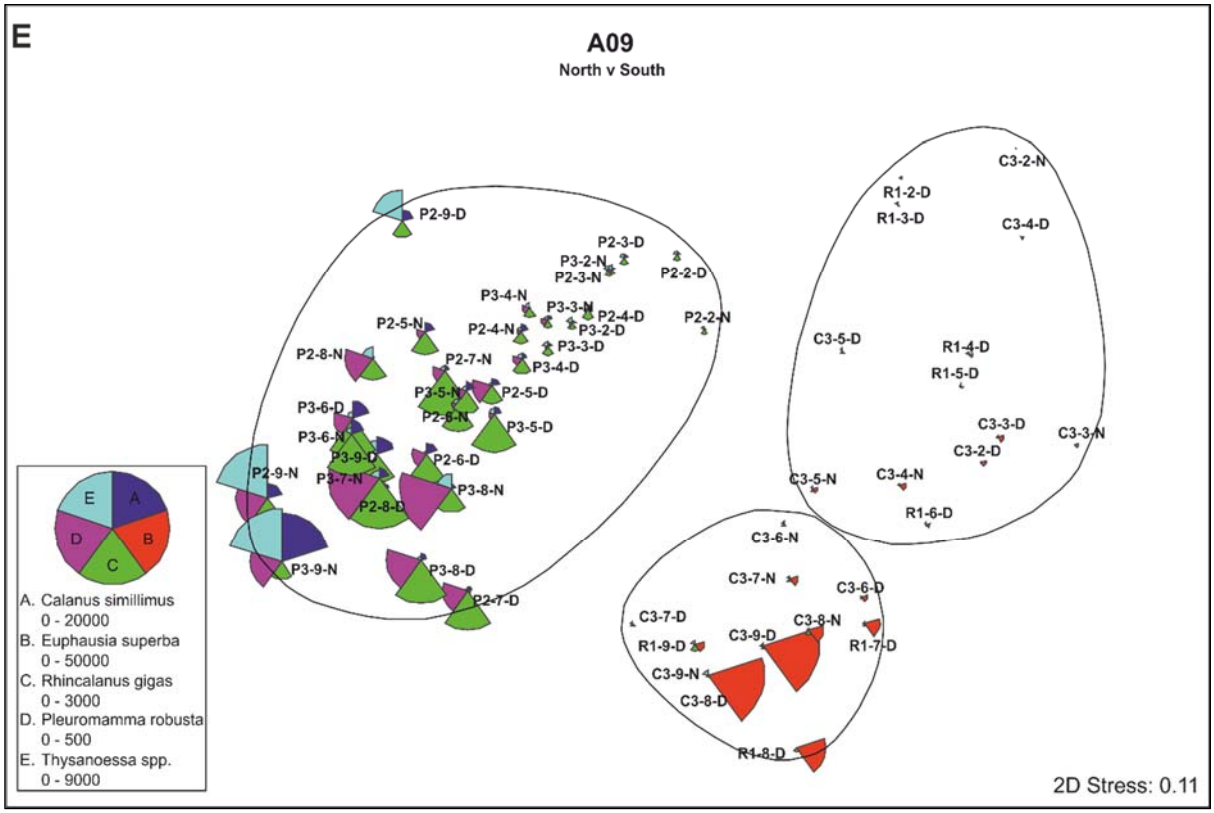
E
A09
North v South
P2-9-D
P2-3-D
P3-2-N
P2-3-N
P2-2-D
P3-4-N
P3-3-N
P2-4-D
P2-5-N
P2-4-N
P3-2-D
P2-2-N
P3-3-D
P2-8-N
P2-7-N
P3-4-D
P3-5-N
P2-5-D
P3-6-D
P2-6-N
P3-6-N
P3-5-D
P3-9-D
P2-6-D
P2-9-N
P3-7-N
P3-8-N
P2-8-D
P3-9-N
P3-8-D
P2-7-D
C3-2-N
R1-2-D
R1-3-D
C3-4-D
C3-5-D
R1-4-D
R1-5-D
C3-3-D
C3-3-N
C3-2-D
C3-5-N
C3-4-N
R1-6-D
C3-6-N
C3-7-N
C3-6-D
C3-7-D
C3-8-N
R1-9-D
C3-9-D
R1-7-D
C3-9-N
C3-8-D
R1-8-D
A
B
C
D
E
A. Calanus simillimus
0 - 20000
B. Euphausia superba
0 - 50000
C. Rhincalanus gigas
0 - 3000
D. Pleuromamma robusta
0 - 500
E. Thysanoessa spp.
0 - 9000
2D Stress: 0.11

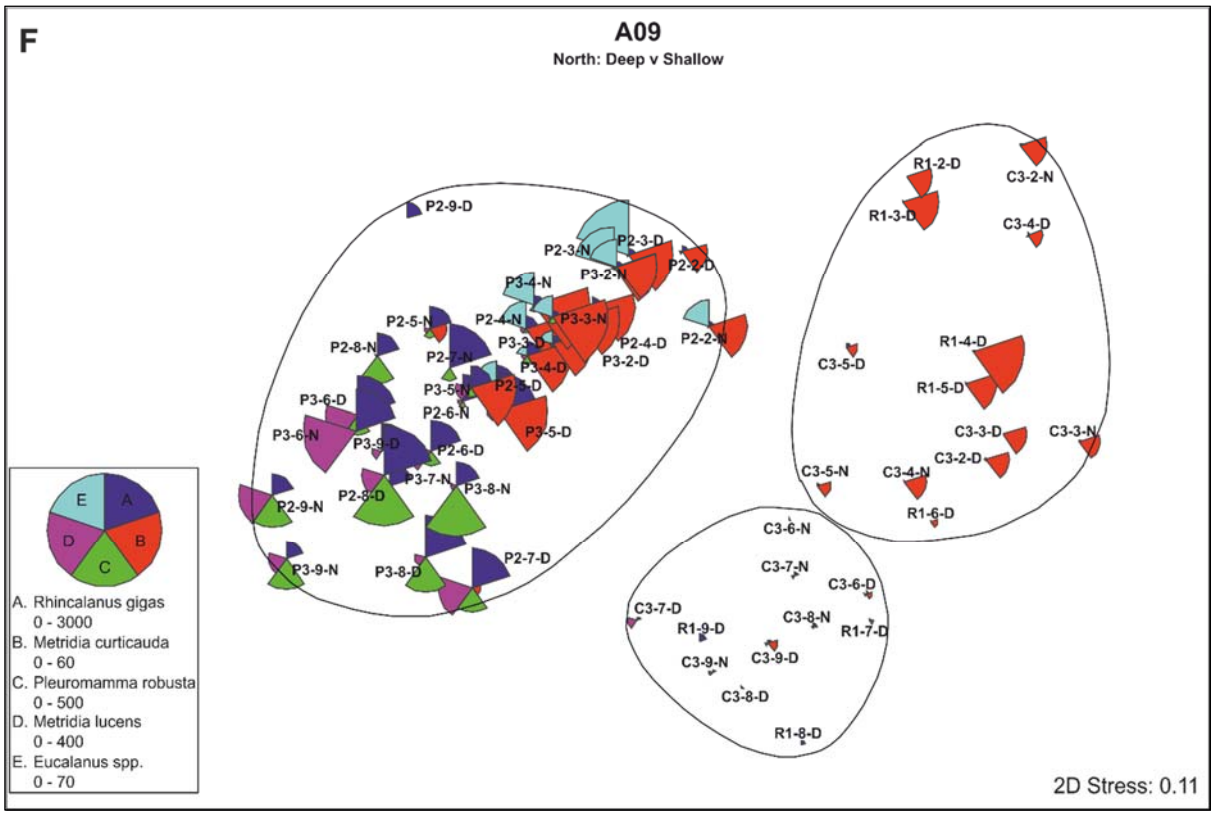
F
A09
North: Deep v Shallow
P2-9-D
P2-3-D
P2-3-N
P3-2-N
P2-2-D
P3-4-N
P2-5-N
P2-4-N
P3-3-N
P2-8-N
P3-3-D
P2-4-D
P2-2-N
P2-7-N
P3-4-D
P3-2-D
P3-5-N
P2-5-D
P3-6-D
P2-6-N
P3-6-N
P3-5-D
P3-9-D
P2-6-D
P3-7-N
P3-8-N
P2-9-N
P2-8-D
P3-9-N
P3-8-D
P2-7-D
R1-2-D
C3-2-N
R1-3-D
C3-4-D
C3-5-D
R1-4-D
R1-5-D
C3-3-D
C3-3-N
C3-2-D
C3-5-N
C3-4-N
R1-6-D
C3-6-N
C3-7-N
C3-6-D
C3-7-D
C3-8-N
R1-9-D
R1-7-D
C3-9-N
C3-9-D
C3-8-D
R1-8-D
A
B
C
D
E
A. Rhincalanus gigas
0 - 3000
B. Metridia curticauda
0 - 60
C. Pleuromamma robusta
0 - 500
D. Metridia lucens
0 - 400
E. Eucalanus spp.
0 - 70
2D Stress: 0.11

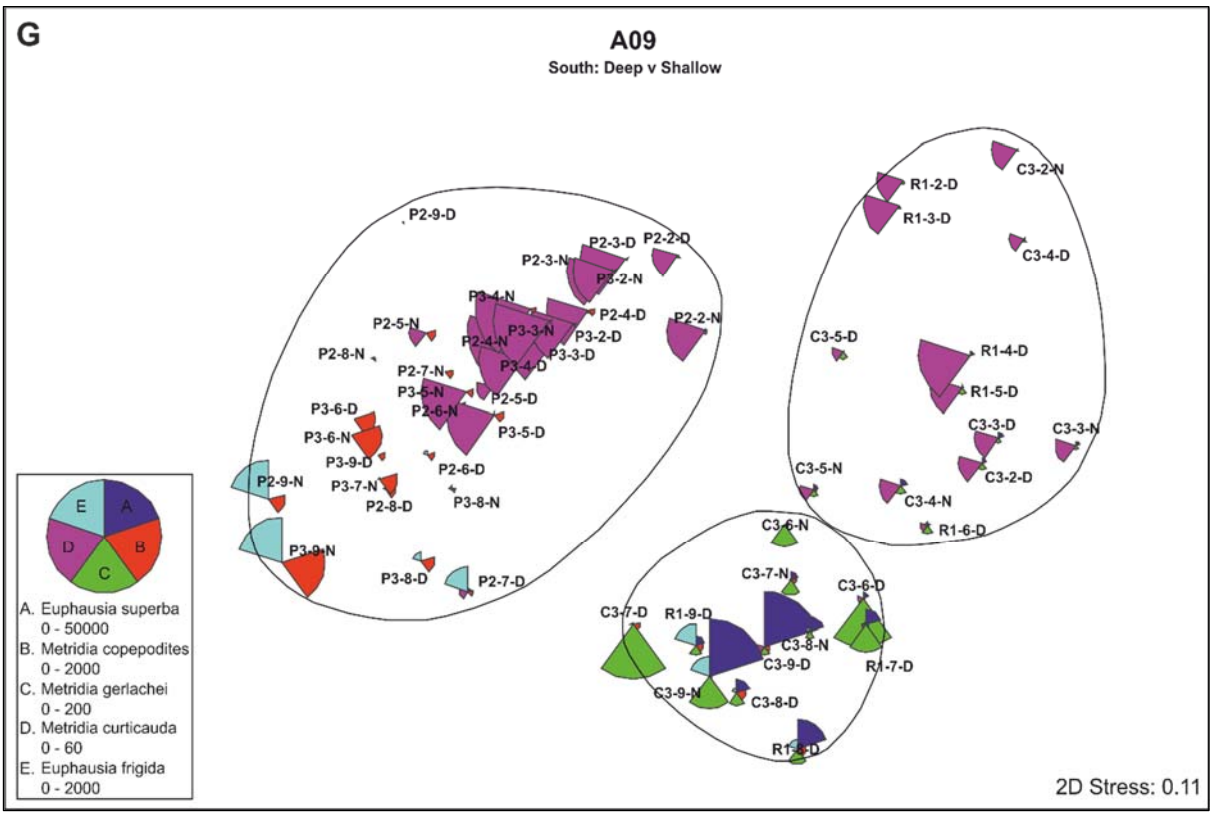

Figure 2.8: Bubble plots for S08 (A-D) and A09 (E-G) based on the 0.5% subset of taxa overlain on nMDS ordinations for each year. Bubbles on each plot correspond to the top five taxa contributing to dissimilarities between a particular group. Segments of the bubbles represent the relative biomass of each taxa. Values are given in biomass (mg DW m^{-2}). Plots correspond to the SIMPER groups in Table 2.3. 'South' refers to samples labelled R1 and C3; 'North' refers to samples labelled P2 and P3. For S08 Shallow encompassed nets from 0-500 m (North and South) and Deep encompassed nets from 375-1000 m (North) 500-100 m (South). For A09 Shallow encompassed nets 0-625 m (North) and 0-500 m (South) and Deep encompassed nets 750-1000 m (North) and 375-1000 m (South). Black circles group samples at an arbitrary 53% similarity level to illustrate the greater degree of separation between groups of samples in A09.

2.3.4 Diurnal variability in species vertical migrations and distributions

Total biomass fluxes (mg DW m^{-2}) and individual species fluxes are shown in Table 2.5 and Table 2.6. At the oligotrophic station, C3, and the station upstream of South Georgia P2, either side of the SACCF front, total fluxes show a positive (migrating up from day to night) overall biomass shift over the diurnal period in both S08 and A09, representative of normal DVM. At C3 this was driven largely by euphausiids in S08 and *Metridia gerlachei* and *E. frigida* in A09, although this was countered by a negative flux (downward from day to night) of *C.*

propinquus (-216 mg DW m^{-2}), where a negative flux indicates a reverse migration. At P2, *E. frigida*, *Euchaeta antarctica*, *M. lucens* and *P. robusta* drove the biomass movement, although *E. superba* also exhibited a negative flux corresponding to -390 mg DW m^{-2}. There was a significant positive total flux of biomass at P3 in A09, driven largely by *C. simillimus* and *Thysanoessa* spp. with contributions from *Metridia* copepodites and *E. frigida*. However, in S08, a negative flux was observed, driven largely by the amphipod *Themisto gaudichaudii* (-809 mg DW m^{-2}) although all members of the *Metridia* genus exhibited negative fluxes of between -60 to -138 mg DW m^{-2}. At R1 in S08, the only year for which data at this station were available, there was an overall negative movement of biomass, primarily driven by *E. antarctica*, *C. acutus* and *R. gigas*. Of all the taxa in the top five SIMPER groups, only one (*Eucalanus* spp.) did not exhibit a significant biomass flux.

Overall, considering the entire 0.5% datasets, the majority of taxa exhibited some diurnal movement of biomass. Out of the minority that remained at the same depth, there was no consistency in behaviour between taxa, with many being taxa that had exhibited minor to significant shifts in their centre of biomass at other stations or times. The distributions of the taxa exhibiting the largest biomass fluxes are presented in Figure 2.9. These largely coincided with the taxa that drove the latitudinal and vertical patterns. Only two (*Drepanopus* and *Themisto gaudichaudii*) that were not significant contributors to defining community structure showed large diurnal shifts in biomass (Table 2.6).

Whilst the centre of biomass for most taxa (defined as the depth between the 25^{th} and 75^{th} biomass percentiles) varied from compact (≤ one 125 m depth strata) to relatively wide (up to 4 depth strata), the range of their entire distribution was often very wide, in many cases the depth of the entire 1000 m water column. *Euphausia frigida* was the exception and consistently had the narrowest depth distribution of between 125 and 500 m. Furthermore, in general the centres of biomass of most taxa either contracted or occupied the same depth range between day and night, although there was intra-specific and inter-station variability with some expanding in range. In particular, *C. acutus* and *M. gerlachei* were found to exhibit all three behaviours. There was no apparent link between this behaviour and whether daytime samples were taken comparatively late in the day.

Table 2.5: Biomass fluxes over a diurnal period (mg DW m^{-2} d^{-1}). Positive fluxes represent movement of biomass from deeper to shallower water from day to night (normal DVM). Negative fluxes represent movement of biomass from shallower to deeper water from day to night (rDVM). Values are summed across all taxa comprising ≥0.5% biomass in at least one sample.

	S08				A09		
Total diurnal biomass flux	**R1**	**C3**	**P2**	**P3**	**C3**	**P2**	**P3**
From 25th %ile	-522	2099	1740	-1031	272	2169	-426
From modal depth	-444	2493	5258	-1378	236	2224	746
From 75th %ile	-85	4523	7317	-1426	-301	1921	43665
Mean diurnal biomass flux	-350	3038	4771	-1278	69	2105	14662

Table 2.6: Diurnal fluxes of the species/ taxa driving biomass fluxes in at least one station. A dash indicates a species that was not present at this station; a zero indicates no biomass flux at this station. Positive fluxes represent movement of biomass from deeper to shallower water from day to night (normal DVM). Negative fluxes represent movement of biomass from shallower to deeper water from day to night (rDVM). Taxa highlighted yellow contributed to SIMPER dissimilarity in S08 only; blue, to A09 only; green, to both; and grey did not contribute significantly to SIMPER differences. Species are listed in hierarchical order of how many SIMPER groups they contributed to.

	S08				**A09**		
Mean diurnal flux of species biomass	**R1**	**C3**	**P2**	**P3**	**C3**	**P2**	**P3**
***Thysanoessa* spp. (Euphausiacea)**	0	699	776	0	4	0	5412
***Euphausia superba* (Euphausiacea)**	0	2137	-	0	0	-390	0
***Rhincalanus gigas* (Copepoda)**	-44	0	1854	0	16	0	-853
***Metridia curticauda* (Copepoda)**	-29	29	46	22	-4	15	-33
***Calanus simillimus* (Copepoda)**	-	0	204	0	-	0	8191
***Pleuromamma robusta* (Copepoda)**	0	3	-51	-101	0	260	76
***Metridia gerlachei* (Copepoda)**	-19	0	109	-61	164	-3	-
***Euphausia frigida* (Euphausiacea)**	3	62	-39	0	122	1337	670
***Calanoides acutus* (Copepoda)**	-132	71	1102	0	-28	0	86
***Ctenocalanus* spp. (Copepoda)**	-	-	792	0	-	-	-
***Calanus propinquus* (Copepoda)**	2	-1	5	-8	-216	117	-35
***Eucalanus* spp. (Copepoda)**	-	-	-4	-	-	0	9
***Euchaeta antarctica* (Copepoda)**	-149	0	-40	-138	28	322	-47
***Lucicutia* spp. (Copepoda)**	21	37	0	-18	-5	0	4
***Metridia* copepodites (Copepoda)**	0	-7	58	-62	-30	73	903
***Metridia lucens* (Copepoda)**	5	0	-66	-79	11	300	0
***Drepanopus* spp. (Copepoda)**	-	-	-	-	-	-	217
***Themisto gaudichaudii* (Amphipoda)**	-	-	14	-809	2	15	0

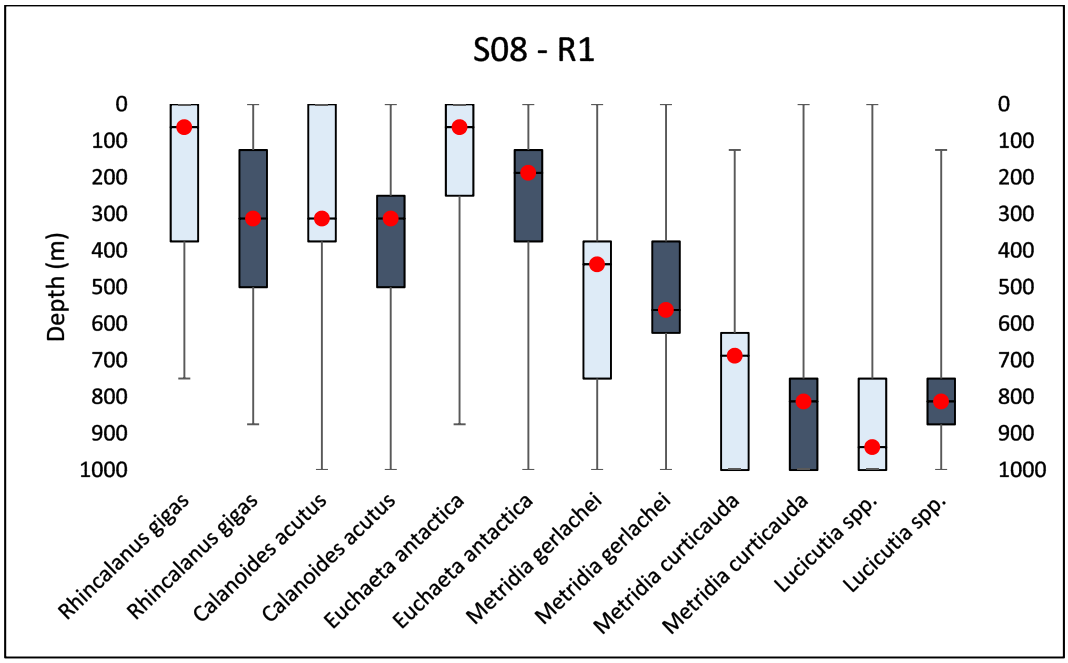
S08 - R1
Depth (m)
0
100
200
300
400
500
600
700
800
900
1000
Rhincalanus gigas
Rhincalanus gigas
Calanoides acutus
Calanoides acutus
Euchaeta antactica
Euchaeta antactica
Metridia gerlachei
Metridia gerlachei
Metridia curticauda
Metridia curticauda
Lucicutia spp.
Lucicutia spp.

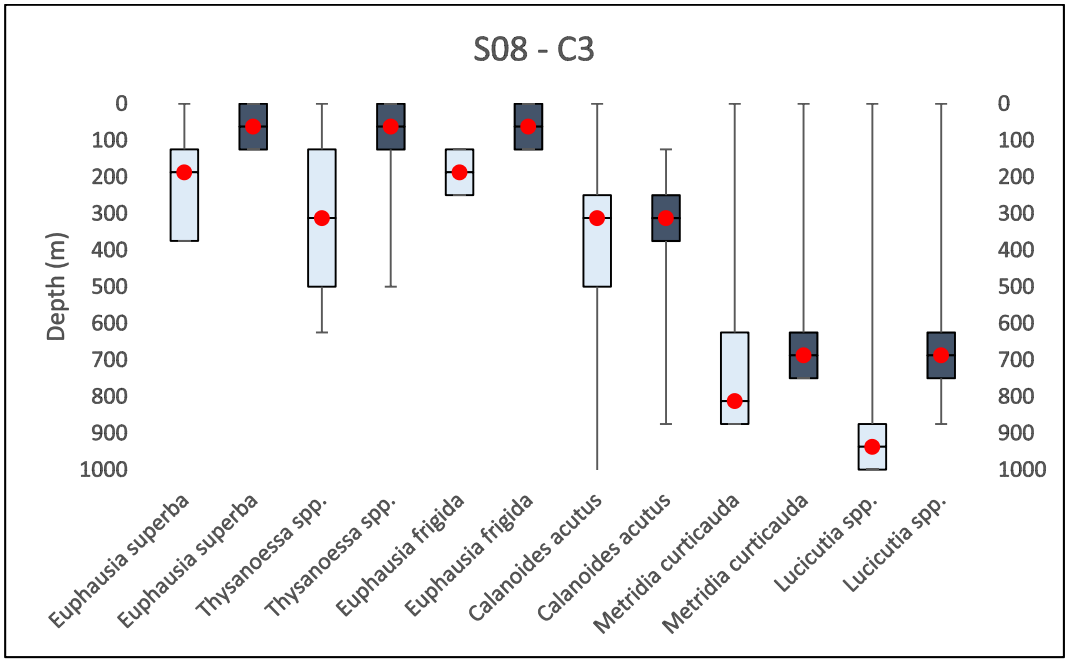
S08 - C3
Depth (m)
0
100
200
300
400
500
600
700
800
900
1000
Euphausia superba
Euphausia superba
Thysanoessa spp.
Thysanoessa spp.
Euphausia frigida
Euphausia frigida
Calanoides acutus
Calanoides acutus
Metridia curticauda
Metridia curticauda
Lucicutia spp.
Lucicutia spp.

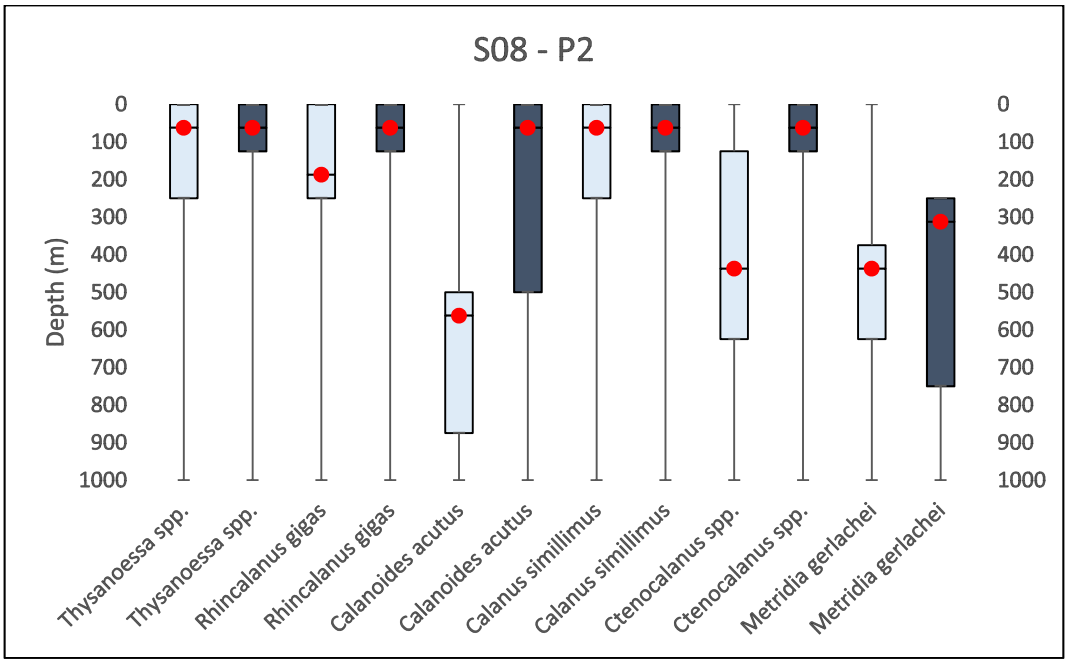
S08 - P2
Depth (m)
0
100
200
300
400
500
600
700
800
900
1000
Thysanoessa spp.
Thysanoessa spp.
Rhincalanus gigas
Rhincalanus gigas
Calanoides acutus
Calanoides acutus
Calanus simillimus
Calanus simillimus
Ctenocalanus spp.
Ctenocalanus spp.
Metridia gerlachei
Metridia gerlachei

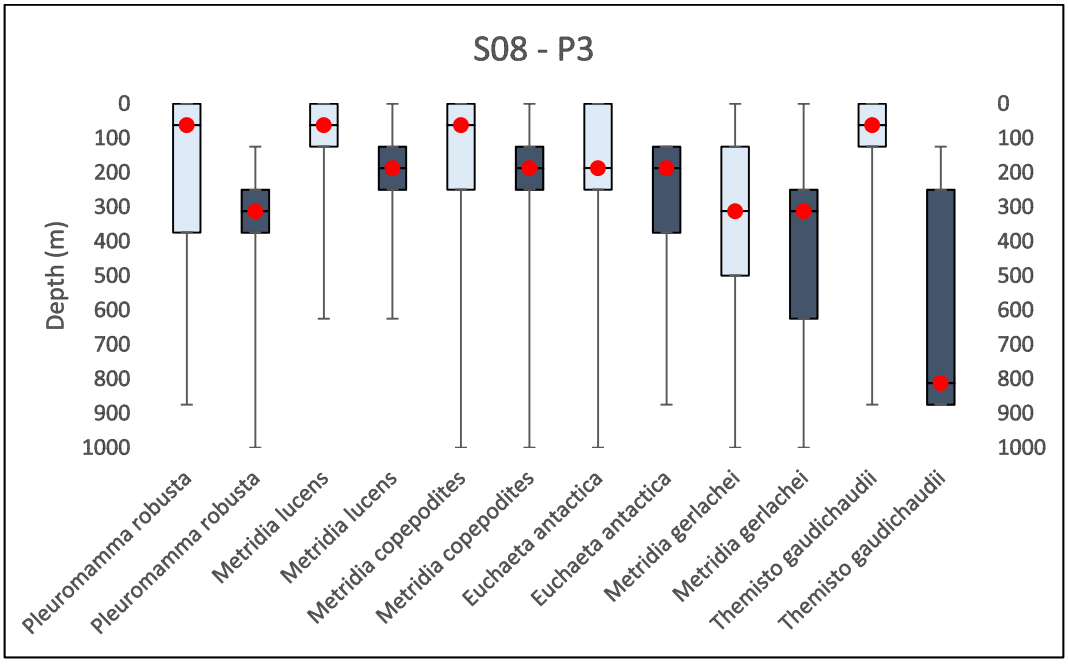
S08 - P3
Depth (m)
0
100
200
300
400
500
600
700
800
900
1000
Pleuromamma robusta
Pleuromamma robusta
Metridia lucens
Metridia lucens
Metridia copepodites
Metridia copepodites
Euchaeta antactica
Euchaeta antactica
Metridia gerlachei
Metridia gerlachei
Themisto gaudichaudii
Themisto gaudichaudii

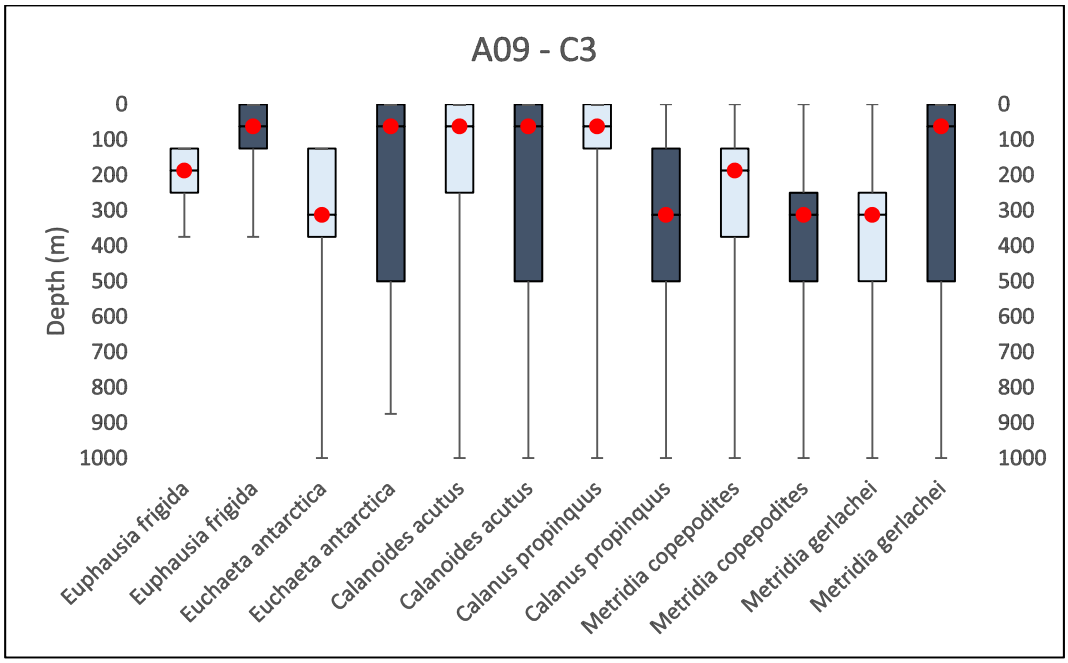
A09 - C3
Depth (m)
0
100
200
300
400
500
600
700
800
900
1000
Euphausia frigida
Euphausia frigida
Euchaeta antarctica
Euchaeta antarctica
Calanoides acutus
Calanoides acutus
Calanus propinquus
Calanus propinquus
Metridia copepodites
Metridia copepodites
Metridia gerlachei
Metridia gerlachei

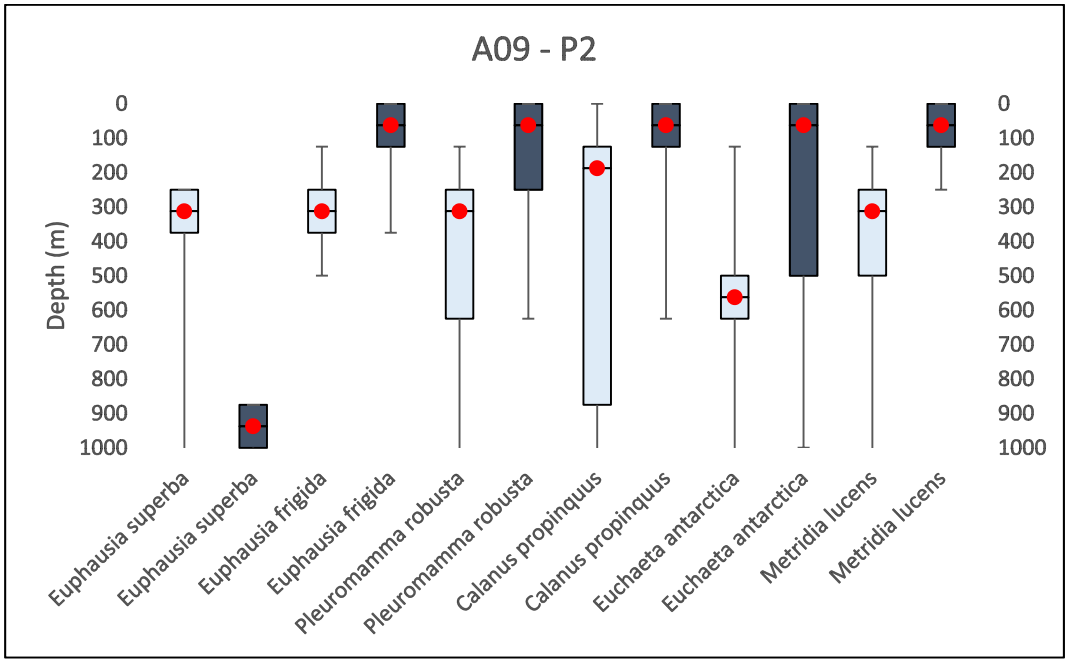
A09 - P2
Depth (m)
0
100
200
300
400
500
600
700
800
900
1000
Euphausia superba
Euphausia superba
Euphausia frigida
Euphausia frigida
Pleuromamma robusta
Pleuromamma robusta
Calanus propinquus
Calanus propinquus
Euchaeta antarctica
Euchaeta antarctica
Metridia lucens
Metridia lucens

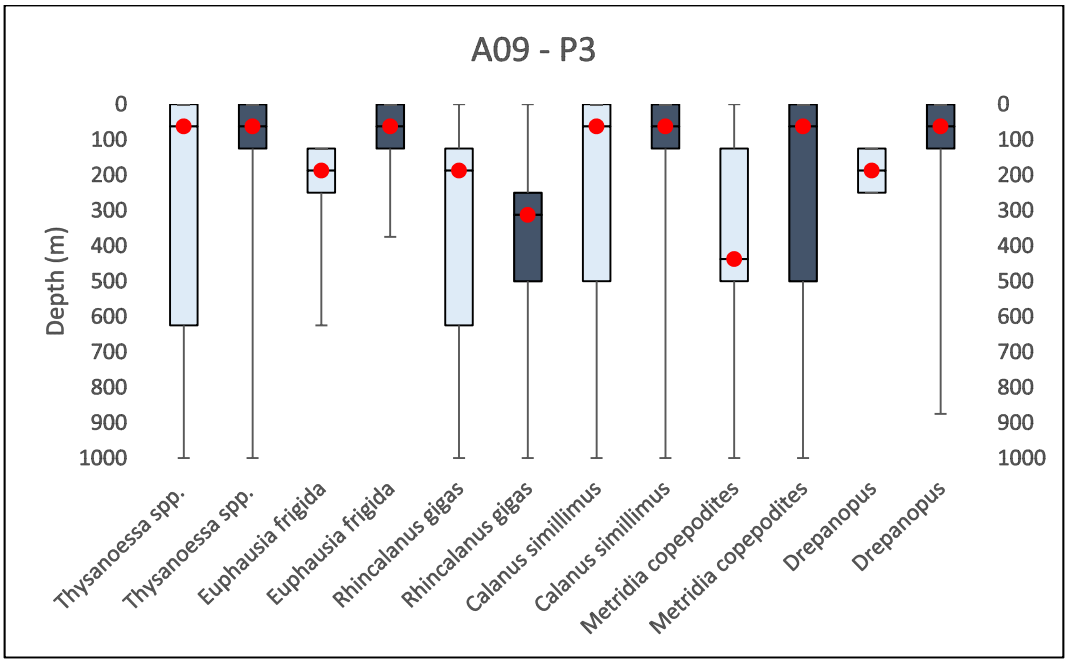

Figure 2.9: Diurnal population distributions of the six taxa exhibiting the largest biomass fluxes (positive or negative) at each station (top 4 panels: S08; bottom 3 panels: A09). Red dots are the median depth of the 125 m strata of maximum biomass. Boxes represent the full spread of the 25th to 75th percentile of the population and whiskers represent the full depth range. Boxes coloured in light blue represent daytime populations; dark blue represents night time populations. R1 A09 was excluded as there was no night time net from which to calculate diurnal fluxes.

The depth gradient was also characterised by a decrease in biomass with depth (Table 2.7) in which surface biomass ranged from a mean of 95 times greater than at 1000 m in S08 to 289 times greater in A09. This represented a decrease of one order of magnitude at more southerly stations, to up to four orders of magnitude at P3. By 1000 m in both years biomass across stations was approximately equivalent, although the depth that this was reached was significantly shallower (375-250 m) in S08 than in A09 (1000-625 m).

Table 2.7: Mean biomass (mg DW m^{-2}) averaged over each D and N sample per station.

	Mean biomass at each station (mg DW m^{-2})							
	S08				**A09**			
Depth (m)	R1	C3	P2	P3	R1	C3	P2	P3
0-125	345	1936	7032	52599	1938	48871	7703	14913
125-250	169	896	1052	1486	13351	3315	987	2200
250-375	327	746	731	965	3570	713	2247	4010
375-500	247	318	437	289	195	396	1681	4774
500-625	124	86	417	248	131	259	1091	1890
625-750	111	132	244	221	362	350	520	657
750-875	113	98	159	311	99	401	310	521
875-1000	63	56	224	226	89	223	185	352

2.3.5 Carbon flux from migratory zooplankton

Active carbon flux (respiration at depth + faecal pellet flux during final descent) and total zooplankton-derived carbon flux (respiration at depth + faecal pellet production during entire surface feeding period) are presented in Table 2.8. In both years, active respiration flux was the greatest contributor to total active flux with active egestion flux contributing between 2-8% during normal DVM and 12-21% during rDVM. In A09, respiration and egestion flux contributed approximately equal amounts to total maximum carbon flux at all stations, but in S08 this was more variable and egestion flux ranged from 0.3 (at C3) to >5 (R1) times that of respiration flux.

Table 2.8: Total active flux and maximum total C flux (mg C m^{-2} d^{-1}) for stations in S08 and A09. Total active flux is the sum of active respiration (R) flux and active egestion (E) flux. Max total flux is the sum of active respiration (R) flux and total egestion (E) flux. Values in red represent fluxes from rDVM. Note C3 A09 had a weakly positive (normal) DVM signal overall and in the top 25th percentile but within the top 125 m alone was negative (reverse). There was no night time net at R1 in A09.

	S08					**A09**				
Station	Active R flux	Active E flux	**Total active flux**	Total E flux	**Max total C flux**	Active R flux	Active E flux	**Total active flux**	Total E flux	**Max total C flux**
R1	0.258	0.070	**0.328**	1.323	**1.580**	**N/A**				
C3	8.760	0.156	**8.916**	2.362	**11.121**	2.743	0.225	**2.968**	2.726	**5.469**
P2	13.190	1.075	**14.265**	8.617	**21.807**	5.133	0.410	**5.543**	5.200	**10.332**
P3	3.506	0.461	**3.967**	7.128	**10.634**	20.560	1.581	**22.141**	20.157	**40.717**

2.4 Discussion

2.4.1 Zooplankton community structure across the Scotia Sea

Considering all nets from both S08 and A09 together, depth and latitude emerged as the two variables primarily driving sample structure, resulting broadly in four groups of samples. In terms of latitude, samples from R1 and C3 (South) tended to group together, and samples from P2 and P3 (North) did likewise. Considering depth, shallow (500 m to surface) samples from P2 and P3 formed one cluster entirely separately to the rest whilst deeper P2/P3 samples (1000 m to 250 m) formed another. Similarly, shallow R1/C3 samples (500 m to surface) formed one group, and another was comprised of the deeper samples along with a couple of outliers. However, neither depth nor latitude emerged as the principal driver of sample grouping and, in agreement with Ward et al. (2014), deep (1000-500 m) samples in particular demonstrated a large degree of homogeneity across all stations.

When years/ seasons were considered independently the same four groups emerged, although with some notable differences. Firstly, an opposite response of samples to each variable is observed, that is where depth was the primary driver one year, latitude was the primary driver in the other and vice versa; secondly, in shallower samples particularly, different species (or groups of species) were found to drive the response in different years; and thirdly, the S08 North/ South groupings were notably less distinct than in A09. In S08, samples were initially separated by depth, with a high biomass of *M. curticauda* defining samples deeper than 500 m from all stations, and higher biomass of E. *antarctica*, *C. acutus* and *Thysanoessa* spp. more common in 500 m to surface samples. Broad North and South groups then emerged within the deep and shallow groups, with greater species diversity and higher biomass more characteristic of samples from the northern stations. In contrast, in A09 there was a very clear latitudinal separation at all depths, in which stations to the north of the SACCF during the year of sampling (Venables et al., 2012) were characterised by presence of the copepods *C. simillimus*, *R. gigas*, *P. robusta* and the euphausiid *Thysanoessa* spp., whilst C3 and R1 to the south of the boundary current were almost devoid of these species and were typified instead by the euphausiid *E. superba*. However, on both sides of the front, a depth-driven gradient emerged as the secondary variable of influence, leading to an increasing divergence of groups with shoaling. This was in part driven by the presence or absence of particular species or groups of species: in deeper (1000-500 m) samples, *M. curticauda* was abundant in both North and South groups, with *Eucalanus* spp. additionally found in the North. Shallower samples were more distinct from one another: *R. gigas*, *P. robusta* and, in the shallowest samples, *M. lucens*, characterised the North group whereas

the South group was defined by the copepod *M. gerlachei* (particularly in mid-depths) and euphausiids *E. superba* and *E. frigida*.

Southern Ocean ecosystems are related across a latitudinal gradient to the physical positions of frontal water masses (Ward et al., 2002, 2012b, 2014) and the ontogenetic development of species in relation to latitude (Ward et al., 2012a). In studies of the top 400 m of the Scotia Sea, the Southern Antarctic Circumpolar Current Front (SACCF) has been found to separate mesozooplankton communities of warmer areas to the north from colder, ice-influenced, regions to the south (Ward et al., 2012a), with seasonal variations in species composition and biomass related to the later spawning of higher latitude communities. In another study based on the early 20th century Discovery expeditions to the west of Drake Passage, zooplankton community groups were related to the positions of Antarctic, Polar Frontal and sub-Antarctic water masses (Ward et al., 2014). As the only known study to consider zooplankton to depths of up to 1000 m in this region, this also found the influence of frontal positions in community groupings to reduce with depth.

In considering explanations for the different structuring of sample groups between the two years it must first be noted that sampling in S08 took place in January (early summer) whereas A09 was in March (early autumn). Significant interannual variability, as well as A09 being an anomalously warm year (Venables et al., 2012) make a direct seasonal comparison impractical. Nevertheless, the later sampling of A09 means that zooplankton populations would have been at a more advanced stage of development, with older stages likely contributing to a relatively greater biomass. Older stages may also have been starting their seasonal descent, and there is a suggestion that this may be the case with the expansion of the main body of biomass in some species, e.g. *R. gigas* and *C. simillimus*, although this could also be reflecting the fact that (with the exception of *Metridia* spp.) both copepodites and adults are incorporated in the population. It is clear that the structure of the top 60 to 120 m in particular varied across stations, with A09 profiles generally exhibiting deeper and more stable mixed layers. Deeper than ~200 m however, the physical hydrography of stations was almost identical in both years, likely representing the transition from Antarctic Surface Water to Antarctic Deep Water and accounting for the greater homogeneity between deeper samples across North and South. Specifically, deeper samples in both years are differentiated largely by three key species: *M. curticauda*, *Lucicutia* spp. and *Eucalanus* spp., whilst significantly more variability in both hydrography and biology characterised the upper water column between year and station.

Although chl-*a* over the top 60-80 m was approximately equal at all stations in A09, this appeared to have little direct bearing on the intermediate (0-500 m) vertical structure of the communities between latitudinal groups which were more distinct from each other than in S08. In A09 the copepods *R. gigas*, *P. robusta* and *M. lucens* were more important in the North whilst the euphausiids *E. superba*, *E. frigida* and the copepod *M. gerlachei* were more characteristic of the South group. In contrast, with the exception of the surface samples, there was greater overlap between North and South in S08 with a relatively high biomass of *E. antarctica* and *M. gerlachei* common to both groups. A09 was unusually warm with much reduced ice extent in the South and higher chl-*a* concentrations in the North (Korb et al., 2012, Borrione and Schlitzer, 2013), possibly contributing to the more diverse and abundant copepod community in the north. Korb et al. (2012) linked the absence of an ice-edge bloom in A09 to the low abundance of cryptophytes in the phytoplankton, with the reduced diversity perhaps being reflected in the less diverse zooplankton community dominated by euphausiids. Greater ice extent the previous year may have allowed the development of a more diverse copepod community in the South in S08, whilst high chl-*a* dominated by large diatoms in the North likely provided plentiful food for a diverse ecosystem dominated in biomass terms by larger copepods *R. gigas*, *C. acutus* and *C. simillimus* and euphausiids *Thyssanoessa* spp. and *E. frigida*.

2.4.2 Evidence for diel vertical migration at individual and community scale

In neither year did samples form clear associations based on time of sampling (day or night), indicating that DVM did not sufficiently alter the composition of samples at a 125 m sampling interval. However, that day and night time samples of the same depth were further apart on ordination plots did suggest differences of a more subtle nature which was confirmed by species-specific biomass on shade plots and subsequent calculations of total biomass flux of taxa in the 0.5% subset. Substantial fluxes of biomass were evident at every station, apart from C3 in A09 at which a positive but small flux occurred. Fluxes were not however wholly consistent in direction across year and station, with R1 and P3 in S08 exhibiting negative fluxes i.e. a reverse DVM (rDVM) trend. Within individual stations, species-specific biomass fluxes were a mixture of positive, negative and neutral, regardless of the overall flux at that station, whilst within species themselves, there was generally a high degree of variability in both sign and amplitude of movement. For example, *P. robusta*, a known large-amplitude migrator (Atkinson et al., 1996), exhibited negative (rDVM) fluxes of 51 and 101 mg DW m^{-2} in P2 and P3 respectively in S08, a negligible positive flux at C3 in the same year, and positive (classic DVM) fluxes of 260 and 76 mg DW m^{-2} at P2 and P3 respectively in A09. *C. acutus* exhibited similarly variable fluxes, ranging from a positive flux of 1102 mg DW m^{-2} at P2 in

S08 to a 132 mg DW m^{-2} negative flux at R1 in the same year whilst the deeper dweller, *M. curticauda*, ranged from a 33 mg DW m^{-2} reverse migration to a 46 mg DW m^{-2} normal migration. On the other hand, the euphausiid, *Thysanoessa* spp., only exhibited positive or neutral night time migrations (ranging from 0 to 5412 mg DW m^{-}). Atkinson and Peck (1988) similarly found a high degree of inter-station variability in abundance and the shape of their vertical distribution profile, although they noted that this variability was reduced for larger and more abundant species, a pattern not seen so clearly here.

It has long been hypothesised that alternative patterns of DVM may be exhibited other than the 'classical' mode of a single upward migration at dusk and downward sinking at dawn. Hypotheses of 'midnight sinking' (Cushing, 1951, Tarling et al., 2002) and 'satiation sinking' (Pearre, 2003, Tarling and Johnson, 2006) both propose modes of migration in which animals undergo a bimodal or 'foray' style of behaviour: multiple migrations a night in response to exogenous cues of satiation, predator arrival or food concentration/ availability. Pearre (1979b, 2000) discusses many of the problems involved in detecting and characterising DVM, including how net samples from single depth and single time points may mask much of the variability inherent within a population and conceal anything other than entirely synchronous or simultaneous migrations. I address the first problem with a full water column sampling approach, in which the population distribution and its associated diurnal change can be visualised, an approach which illustrates how variable both distributions and movements of individual species populations can be. For example, in S08 *C. propinquus* exhibits a classical upward night time movement and expansion of the main body (and range) of the population at R1, a deepening of the base of the main body and range at night at C3 and P3, and a contraction of depth of the main body of population and deepening of range at P2 (S08). One limitation of this study however, is that there is only one day and one night time sampling point such that variability occurring around these sampling points may not be fully represented. Within the taxa responsible for the greatest biomass fluxes at each station, variable diurnal patterns of movement are observed both at an individual species level and at the scale of the whole community. In the first case, species including *E. superba*, *R. gigas*, *C. acutus*, *C. propinquus*, *P. robusta*, *M. gerlachei* and *M. curticauda* all display both positive and negative migrations over time and space, with reverse migrations also occurring, even where the overall station signal was of positive flux e.g. C3 A09.

At the community level, a generally normal signal of DVM is observed at four stations, a reverse DVM (rDVM) signal at two stations (R1 and P3 in S08), and a mixed signal at A09 C3. At the stations displaying rDVM, there was a near universal reverse migration of the species that dominated the biomass flux, including those that otherwise undertook normal

migrations. In their reviews on the adaptive and demographic value of zooplankton migration, Lampert (1989) and Ohman (1990) describe the adoption of reverse migration as a response to larger invertebrate predators such as chaetognaths and euphausiids. Sims et al. (2005), in linking the reverse migration of *Calanus* spp. to that of sharks, have also shown how predator-prey dynamics can have wide-reaching ecosystem impacts. Diurnal fluxes from euphausiids in the study are trivial at both stations. At R1, euphausiid biomass is negligible during the day, however a large biomass (232 mg DW m^{-3}) of *Euphausia superba* occurs in the surface of the night time sample. It is possible that this represents a passing swarm whose arrival may have triggered the nocturnal descent of smaller zooplankton in the water column. Additionally, a large number of chaetognaths was found between 625 and 750 m of the daytime sample (pers. obs). Whilst a species-specific analysis of chaetognath distribution was not possible due to insufficient taxonomic resolution, total abundances at the other stations in S08 decreased with depth with no evidence of DVM, in agreement with the published description of one of the more abundant species, *Sagitta gazellae* (David, 1965). Of other common species, *S. marri* is known to be abundant in mid-depth waters (250-500m) and to mature between 750-1000 m (David, 1965) whilst *Eukrohnia hamata* and juvenile *Eukrohnia* are found to be abundant between 500-1000 m (Kruse et al., 2009). The large numbers present at depth during the day in S08 may therefore represent these species exerting predatory pressure on zooplankton, stimulating a reverse migration and explaining the near surface daytime presence of *R. gigas*, *C. acutus* and *E. antarctica*. However, an entirely different situation is observed at P3. Here, a substantial euphausiid biomass (comprised of *Thysanoessa* spp, *E. superba* and *E. frigida*) is present in the surface during both day and night and no movement of the populations below 125 m is observed. Whilst a night time presence alone may explain night time sinking of other zooplankers, the large daytime biomass invalidates this theory. Simultaneously, a deep daytime population of chaetognaths or other large predators is not seen, although in the daytime net, an incursion of salps between 250 - 375 m is observed (pers. obs). Whether this is sufficient to act to 'compress' copepod populations towards the surface and stimulate a reversal of their normal migration, or whether some other factor is responsible for rDVM here cannot be readily determined, but it is nonetheless clear that, in the study location, rDVM is both possible and not uncommon at both a species and community level. Furthermore, this discussion is focussed on only those taxa which demonstrated the largest biomass fluxes at each station and neglects the presence of other taxa (such as the euphausiids discussed above) which may be present yet exhibit no variability in depth.

Other factors can obscure the true signal of DVM. Limited food availability can result in animals spending longer feeding in surface layers (Johnsen and Jakobsen, 1987) although chl-*a* levels at rDVM stations are high enough to cast doubt on this being the case here. Sampling methodologies can also hide variability linked to asynchrony or the effect of simultaneous seasonal or ontogenetic migrations (Pearre, 1979b). There is additionally an increasing body of work discussing the role of moonlight as an exogenous driver or synchroniser of migration both within and outside the polar night (Tarling et al., 1999, Berge et al., 2009, Tarling, 2015, Last et al., 2016) which opens up the possibility of a lunar influence on zooplankton movements that has hitherto not been fully understood. It is also possible that observed patterns or magnitudes may be affected by patchiness, a well-known phenomenon but one that is inherently difficult to study (Haury et al., 1978). Whereas phytoplankton patches are considered to have a strong physical basis, for example arising from discontinuities in temperature, salinity or density (Mackas et al., 1985), zooplankton patchiness is understood to be scale dependent (Levin, 1992, Garçon et al., 2001) and often driven by biological factors which have the potential to override physical factors (Folt and Burns, 1999, Trudnowska et al., 2016). As DVM itself is one cause of zooplankton patchiness, it is to some degree controlled for in this methodology, suggesting also that the scale of sampling is sufficient for the scale of analysis. Although the effects of smaller scale processes e.g. food location and predator avoidance may remain hidden, Wiafe and Frid (1996) found that, over relatively short timescales, the short-term spatial structure of a zooplankton community was not affected by periods of turbulent physical mixing, suggesting that advective or turbulent processes alone are not sufficient to alter zooplankton community structures.

2.4.3 Influence of vertical migration on carbon flux

Out of the seven stations, substantial diurnal biomass fluxes, integrated over the 1000 m water column, were observed at six of them, four of which via normal DVM (>2,100 to >4,700 mg DW m^{-2} d^{-1}), and two via reverse migration (-350 to >-1,270 mg DW m^{-2} d^{-1}). Within the total fluxes, there were also significant and highly variable vertical movements (in both directions) of individual populations throughout the diurnal period, evident in almost all taxa to some degree, including almost all the biomass-dominant taxa characterising latitudinal and vertical groupings. The relative contributions of the different taxa to overall migratory biomass at each station and year/season is summarised schematically in Figure 2.10. Where zooplankton vertical migrations involve incursions to the euphotic zone and sinking below the base of the mixed layer, they can be responsible for an active export of dissolved organic and inorganic carbon and nitrogen (e.g. Steinberg et al., 2000, Al-Mutairi and Landry, 2001, Steinberg et al., 2002) and organic particulate carbon via faecal pellet production (e.g. Dagg

et al., 2014, Turner, 2015 and references therein) from the surface to the interior of the ocean.

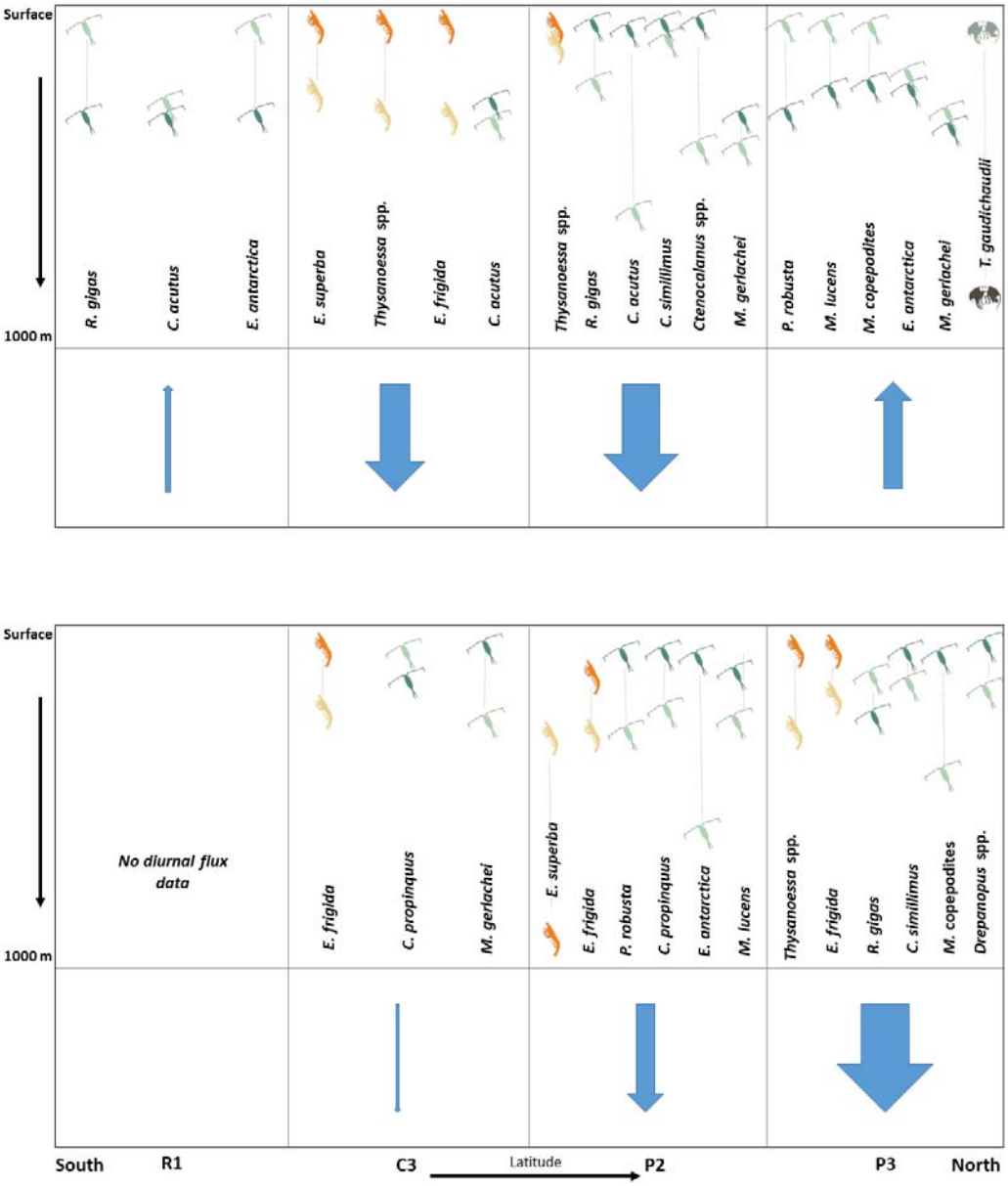

Figure 2.10: schematic of main migrators at each station in S08 (top panel) and A09 (bottom panel). Species contributing most to migrating biomass are illustrated in the top part of each panel, at their approximate daytime (light colour) and night time (dark colour) depths. The arrows in the bottom part of the panel represent the relative size and direction of biomass flux.

Since these biomass fluxes are integrated over the full 1000 m water column, resulting active carbon flux cannot be directly extrapolated. However, in agreement with predicted gradients

(Longhurst and Harrison, 1989) biomass is heavily biased towards the surface (in S08 a mean 34% biomass at southern stations (range 23-45%) and a mean 81% at northern stations (range 68-93%) and in A09 50% and 52% (ranges 10-90% and 51-52%, respectively). Examining only the top 125 m, migratory biomasses were found to range from 53% to >100% of total integrated migratory fluxes over 1000 m, with active flux from these migrations ranging from 0.3 to 14.3 mg C m^{-2} d^{-1} (S08) and 3.0 to 22.1 mg C m^{-2} d^{-1} (A09). Most of this (79-98%) came from respiratory flux occurring below 125 m, suggesting faecal pellet contribution to active flux to be minimal. However, this is a highly conservative estimate, based on a classical view of DVM and assuming that only faecal pellets produced during the hour post-feeding contribute to active flux. Instead, it is likely that the animals contributing to the migratory surface biomass have more complex behaviours than remaining statically at the surface. Under this assumption of constant population turnover as a result of feeding-satiation-sinking cycles, this first calculation ('Active E flux') can be viewed as a minimum estimate, and 'Total E flux' can represent an upper bound on carbon flux produced during feeding hours, ranging from 1.6 to 21.8 mg C m^{-2} d^{-1} (S08) and 5.5 to 40.7 mg C m^{-2} d^{-1} (A09). Although much of this carbon would constitute passive flux, under foray behaviour more would be actively transported down with each sinking cycle, thus enhancing estimates of active flux.

In comparable locations in the Scotia Sea during summer 2013, Belcher et al. (2016) found POC flux at ~160 m to range from 145 – 181 mg C m^{-2} d^{-1}. Based on this, active flux from the main migratory biomass in summer could range from 0.2% (ICE) to 8% (P2) with the majority of this coming from respiration. Whilst respiration estimates are based on empirically determined rates and subject only to variability in day length, FPC estimates are additionally dependent on levels of chl-*a*. This means that inherent in the calculation is the assumption that, under low chlorophyll levels, FPC production decreases, whereas this neglects the contribution of omnivorous or detritivorous feeding under different life strategies (Atkinson, 1995, Metz and Schnack-Schiel, 1995).

On the other hand, with respiration flux being subject to day length, the mode of migration becomes important. At P3, active flux represented only 3% of Belcher et al. (2016)'s POC flux, yet the mode had reversed meaning that 8.6 hours of darkness were spent at depth and 15.5 hours of light at the surface. Under normal migration, active flux from the same biomass would have been 5% of POC flux due to a near doubling of respiration flux, illustrative of how temporal variability in behaviour may influence the magnitude of organic carbon that is exported from the mixed layer. It is especially noteworthy that some normally migratory species e.g. *C. acutus*, and *C. simillimus*, were static at this point in time, whereas if they had

been exhibiting migrations akin to those of P2 or P3 in autumn (where normal DVM occurred), active flux would have contributed as much as 21% of Belcher et al. (2016)'s POC flux. An interesting feature is that, in A09, where hours of dark and light are approximately equal, R flux and total E flux are also approximately equal. Under these conditions, a reversal in mode would not alter fluxes. In S08 however, total E flux can vary between 0.3 to >5 times that of R flux, with higher values driven more by hours spent at the surface than levels of chlorophyll. This suggests that having a better understanding of the migratory behaviour of individuals, both in terms of reversals and forays, is important for an accurate estimation of active flux, particularly in summer.

In addition to shallow fluxes, diurnal fluxes of biomass occur over the entire 1000 m water column blurring the boundaries of separation between species over depth. In shallower to mid depth waters, euphausiids and copepods including *R. gigas*, *C. propinquus*, *M. gerlachei*, *M. lucens* and, in A09, *Metridia* copepodites, resided at and migrated to often variable depths, resulting in overlapping distributions of biomass dominant taxa. The three main deeper dwelling taxa, *M. curticauda*, *Lucicutia* spp. and *Eucalanus* spp. all exhibited both normal and reverse migrations. These deeper fluxes were of similar magnitudes within year, with the exception of *Eucalanus* spp. which was only found in the northern group. Although magnitude of flux varied between years, this may be due to A09 being in a later stage of succession or the unusually warm environmental conditions of A09. These deeper migrations transport carbon and nutrients across depth and illustrate how Vinogradov (1962)'s 'ladder of migration' fuels deeper layers of zooplankton and bacterial production.

What we do not see is smaller scale variability within the top 125 m, so it is possible that finer-scale, previously reported epipelagic migratory dynamics are being missed (e.g. Atkinson et al., 1992, Ward et al., 1995, Atkinson et al., 1996). Nevertheless, the data confirm significant movements of biomass within the water column over the diurnal period, with a number of animals being found in the topmost layer even if the main body of the population resides deeper, indicating wide distributional and migratory ranges. The variability in fluxes observed supports the idea that DVM is not a single, synchronous movement of a population but in fact a continuous and individually-determined behaviour. The implication is of an episodic or periodic foray, and/or the migration of only a part of the population at any one time, such that significant individual variability within an overall population actually masks the full extent of DVM. This has implications for carbon fluxes in that actual fluxes based on wide ranges and multiple forays are likely to be higher than were they based on the shift of the mean population alone. These results also show that, despite quite different latitudinal and vertical zooplankton community structure, clear diurnal fluxes of biomass occur

between the epi- to mesopelagic under most conditions, and that these fluxes are driven by a relatively small number of taxa that define community groups. They also show that reverse migrations are possible, indeed common, amongst many normally migrating species. This has been shown to occur both at an individual level and at a whole community level where it is hypothesised that the presence of predators may temporarily change the normal pattern of migration.

2.4.4 Summary

- Two variables dominate in determining community structure across the Scotia Sea: latitude, with a North/South separation occurring in the region of the SACCF; and depth, with samples becoming more homogenous with depth, indicative of incursion of Antarctic Deep Water.
- Interannual variability in (i) extent of sea-ice and (ii) characteristics of bloom influence the complexity of the zooplankton community.
- DVM is apparent in a number of species that make substantial contributions to the biomass at each station and drive differences in community between stations, resulting in large fluxes of biomass and a vertical cascade of carbon across the entire water column.
- Species performing DVM demonstrate behavioural plasticity, switching to reverse migration at one station, putatively as a predator avoidance tactic, as well as species-specific variability within and between stations and years/ seasons.
- Significant fluxes of biomass can occur on both sides of the SACCF, in oligotrophic regions and productive regions, although are generally higher north of the SACCF.
- Active carbon flux driven by near-surface DVM and rDVM can supply a considerable quantity of DIC to the upper mesopelagic but supply of POC can be highly variable and dependent on mode and behaviour of migration.
- The ratio of R to E flux varies significantly more in S08, with R:active E ranging from 4 to 56 vs ~13 at all stations in A09. Similarly, the R:max E ratio ranges from 0.2-4 in S08 and is ~1 at all stations in A09.

Chapter 3: Zooplankton abundance and behaviour increases faecal pellet flux and remineralisation depth in the Southern Ocean

3.1. Introduction

3.1.1 Zooplankton faecal pellets and the biological pump

The biological carbon pump (BCP) is the mechanism through which photosynthetically derived organic material is transformed by the pelagic food web and delivered from the euphotic zone to the deeper ocean (Legendre et al., 2015), largely via the sinking of phytoplankton cells and detrital aggregates including moults, feeding webs and carcasses, sequestering carbon and driving the uptake of atmospheric CO_2 by the oceans. This pump is also driven by the passive sinking of faecal pellets (faecal pellets) produced by zooplankton and micronekton feeding in the epi- and upper mesopelagic, effectively converting small, slow-sinking phytoplankton cells into larger, faster-sinking agglomerates (Turner, 2015 and references therein). Zooplankton also act as important mediators of flux throughout the water column, transforming faecal pellets via processes of ingestion (coprophagy), fragmentation (coprohexy) and loosening (coprochaly) (Lampitt et al., 1990, Noji et al., 1991, e.g. Iversen and Poulsen, 2007). Faecal pellets are repackaged as they sink (Urrère and Knauer, 1981), contributing both to the sequestration of carbon in the deep ocean and supporting the metabolism of mesopelagic biota (Buesseler et al., 2007, Steinberg et al., 2008, Robinson et al., 2010). It is hypothesised that this flux is further enhanced by diel vertical migration (DVM), a process whereby zooplankton migrate vertically within the water column in response to feeding and survival cues (e.g. Angel, 1986, Emerson and Roff, 1987, Longhurst and Harrison, 1989). Such migrations are thought to expedite the passage of organic carbon, nitrogen and phosphorous to meso- and bathypelagic depths (Urrère and Knauer, 1981), with resulting deep faecal pellet production effectively bypassing the region of greatest zooplankton abundance and most rapid remineralisation.

3.1.2 Uncertainty in faecal pellet-mediated export

Factors affecting faecal pellet sinking and attenuation include temperature (Bendtsen et al., 2015, Marsay et al., 2015), season (Urban et al., 1993, Frangoulis et al., 2001), food type or availability and resulting faecal pellet composition or ballast (Francois et al., 2002, Ploug et al., 2008, Atkinson et al., 2012a, Dagg et al., 2014), microbial colonisation and degradation (Turner, 1979, Sampei et al., 2009, Belcher et al., 2016), and the mechanical degradation of faecal pellets by physical and biological processes (e.g. Sampei et al., 2009). However, whilst

zooplankton faecal pellets can contribute significant amounts of carbon to intermediate and deep-sea fluxes, the amount of faecal pellet material that is eventually exported to the deep ocean is still subject to a wide degree of both spatial and temporal variation (González, 1992, González et al., 2000, Turner, 2002). Consequently, estimates of the contribution of faecal pellet carbon to export flux are highly variable, ranging from <1 % to ~100 % (Turner, 2015, Steinberg and Landry, 2017), dependent on geographic region, trophic structure (Peinert, 1989) and oceanic regime. Partly because of this uncertainty, there still exist wide discrepancies in the amount of material reaching the "twilight" zone (Buesseler et al., 2007, Burd et al., 2010). Furthermore, it is thought that regional differences may be reflected in the efficiency with which faecal material is transferred to depth, with recent work in the Southern Ocean (SO) challenging established ideas of primary productivity being linearly related to export efficiency in all cases (Maiti et al., 2013, Cavan et al., 2015). This has a direct impact on our understanding of what fuels biological activity in this zone, as well as our understanding of the ocean's role in atmospheric CO_2 drawdown and the parameterisation of climate models. Recent work sheds light on the complexities of zooplankton-microbial interactions (e.g. Steinberg et al., 2008, Giering et al., 2014) and zooplankton trophic dynamics (Le Quéré et al., 2016) in resolving discrepancies between estimated surface production and carbon demand in the mesopelagic, with the latter drawing particular attention to the need for improved understanding of zooplankton-faecal pellet interactions in the SO.

Material collected in sediment traps has demonstrated the importance of zooplankton mediated faecal pellet flux in the oceans, with well-preserved faecal pellets being found at depths much greater than expected purely from sinking from the surface (e.g. Wilson et al., 2013, Manno et al., 2015) suggesting a more complex picture of zooplankton-faecal pellet dynamics. Furthermore, studies on the morphology of faecal pellets have provided insight into the likely origin of faecal pellets and their repackaging by different types of zooplankton throughout the water column (Turner, 2002, Wilson et al., 2008, Belcher et al., 2017a). Whilst food type, concentration and species can influence the shape and size of faecal pellets (Mauchline, 1998), some generalisations have been drawn: spherical faecal pellets are considered likely to originate from smaller copepods, naupliar stages and amphipods (González, 1992, Yoon et al., 2001), cylindrical faecal pellets from euphausiids, and ellipsoidal or ovoid faecal pellets from larger copepods, pteropods and chaetognaths (González, 1992, Gonzalez and Smetacek, 1994, Manno et al., 2010).

3.1.3 Purpose of the study

The purpose of this study is to investigate the distribution and vertical flux of faecal pellets over the top 400 m at three different locations of the Scotia Sea, SO, that represent different oceanographic regimes. The Scotia Sea is a region which experiences locally high primary productivity (PP) and zooplankton abundances such as in areas of natural iron fertilisation downstream of South Georgia where phytoplankton blooms can last up to 4 months (Whitehouse et al., 2008), and in regions close to the ice edge where seasonal ice retreat stimulates substantial diatom blooms (Korb et al., 2005). This contrasts with areas of lower PP and shorter bloom conditions that are more characteristic of the high nutrient-low chlorophyll (HNLC) status of much of the Southern Ocean. This is an important region where the attenuation of faecal pellet carbon produced in the epipelagic has the potential to be very high as faecal pellets undergo biological and physical transformations over their passage to depth. However, whilst the potential roles of zooplankton versus other controls of ballasting, temperature and bacterial respiration are now becoming better understood in this region (Manno et al., 2015, Belcher et al., 2017a), processes of export, remineralisation and particle repackaging in the mesopelagic are temporally and spatially variable and require continued efforts to fully resolve. Estimates of particle transport efficiency are highly variable, particularly at high latitudes (Buesseler et al., 2007, Maiti et al., 2013, Marsay et al., 2015) with two- to four-fold differences in efficiency between *in-situ* and modelled results (Maiti et al., 2013). Although recent work in the Southern Ocean suggests a low transfer efficiency and correspondingly high mesopelagic remineralisation in this region (Cavan et al., 2015), our knowledge remains hampered by a paucity of measurements at intermediate depths.

This study will provide higher resolution insight into the fate of faecal pellets in the epi- and upper mesopelagic, particularly to the relatively under-sampled depths below the mixed layer (300 to 400 m). It will advance our understanding of the intermediate-depth processes that control export and sequestration flux. Recent work has suggested that, where species of euphausiid are abundant and consume a diatom-rich diet, they exert a strong control on export flux (Dagg et al., 2014), although this may be affected by the variable diets of Southern Ocean euphausiids (Mauchline, 1980). *Euphausia superba* is a central component of the Southern Ocean ecosystem, comprising the link between primary productivity and higher predators for which they constitute a major prey item (Murphy et al., 2007). This is particularly true for the Scotia Sea where larval recruitment is high (Hopkins and Torres, 1988, Loeb et al., 1997) and where up to half the population of *E. superba* occurs (Atkinson, 2004). This work therefore aims to i) establish the role of the zooplankton community in

faecal pellet flux to depth by comparing observed faecal pellet profiles with predicted profiles across contrasting stations; and ii) quantify the flux of faecal pellet carbon across the upper mesopelagic, from the surface to 400 m, to improve our understanding of zooplankton processes affecting flux through the mesopelagic.

3.2 Material and methods

3.2.1 Study area and sampling

This study was conducted at three time-series stations in the Scotia Sea: P3, P2 and ICE, which I sampled once each at six depths over the top 400 m (Figure 3.1). The stations encompass different oceanic regimes which is reflected in zooplankton community compositions. P3 is situated downstream of South Georgia where it benefits from natural iron fertilisation and is characterised by high levels of biological productivity and a diverse zooplankton community. P2 is situated upstream of South Georgia and receives low natural iron inputs. Its zooplankton community is similar in composition to P3 but often reduced in abundance. ICE is situated close to the ice edge where seasonal ice advance and retreat is an important feature and where euphausiids typically dominate the zooplankton.

All samples were collected by me on board Southern Ocean research cruise JR304 (Watkins et al., 2015) on the RRS James Clark Ross. The expedition took place in the austral spring/ summer season, from 15 November 2014 to 17 December 2014. Samples were subsequently analysed by me.

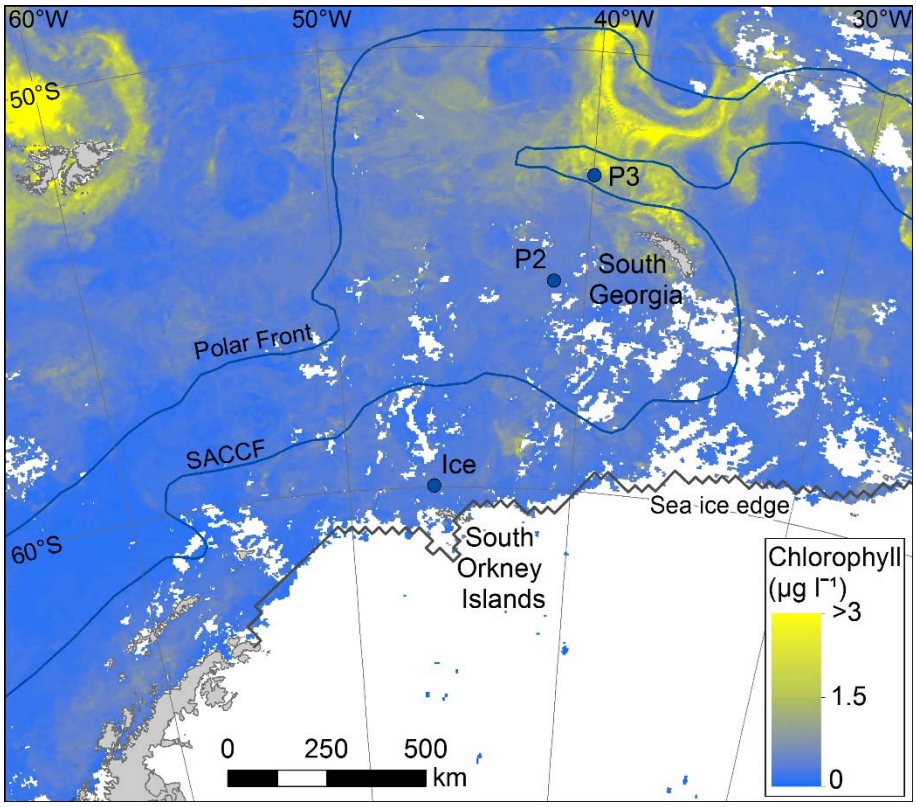

Figure 3.1: Mean chlorophyll data for the month covering sampling (stations marked with filled blue circles). Data were taken from NASA MODIS website https://oceandata.sci.gsfc.nasa.gov/MODIS-Aqua/Mapped/Monthly/4km/chlor_a/

3.2.1.1 Environmental and hydrographic data

An SBE9Plus CTD was set up with instrumentation including a dual SBE 3Plus temperature sensor, SBE4C conductivity sensor and a fluorometer. Fluorescence was converted from volts into chl-*a* (µg l^{-1}) using the manufacturer's calibration. Chl-*a* concentrations were used as a proxy for the relative primary productivity of each station.

Aqua MODIS 4 km, 32 day mean chlorophyll data were also obtained from NASA's Ocean Colour Data website (https://oceandata.sci.gsfc.nasa.gov/MODIS-Aqua/Mapped/Monthly/4km/chlor_a/) for the study area to provide additional environmental context and indicate mean productivity conditions around the stations before, after and during the period of sampling.

3.2.1.2 Mesozooplankton

Mesozooplankton samples were collected in order to predict the abundance and size spectra of faecal pellet produced from within the upper 200 m for comparison with direct observations of faecal pellets from bottle samples. Motion-compensated Bongo nets with a 200 µm mesh net (57 cm mouth diameter, 2.8 m long) were deployed at all time-series

stations throughout the cruise (see Table 3.1 for details). Nets were deployed to 200 m depth during morning and evening, as close as possible to 12 hours apart, in order to sample populations as they went through their diurnal cycle. Samples were passed through a stacked sieve onto a 200 µm mesh and immediately frozen and stored at -80 °C. Once back at the BAS laboratories they were defrosted and immediately fixed in 100 % ethanol in preparation for analysis.

Table 3.1: Details of 0 – 200 m Bongo nets with 200 µm mesh that were deployed during JR304 and analysed for mesozooplankton abundance and size spectra at ICE, P2 and P3

Station	Date	Time (GMT)	Latitude	Longitude
ICE, Night	25/11/2014	21:18	59.96231 S	46.15973 W
ICE, Day	26/11/2014	07:20	59.9624 S	46.16011 W
P2, Night	28/11/2014	19:44	55.24843 S	41.26397 W
P2, Day	29/11/2014	09:05	55.24777 S	41.26484 W
P3, Day	13/12/2014	06:26	52.81209 S	39.97234 W
P3, Night	13/12/2014	21:17	52.81178 S	39.97261 W

3.2.1.3 Faecal pellets

An SBE 32 carousel water sampler holding 24 12 litre Niskin bottles and attached to an SBE11Plus deck unit was deployed and water for sample analysis was collected at the three stations, ICE, P2 and P3 (see Table 3.2). Six bottles were fired at each station, one at each of the following depths: 5 m, 20 m, 40 m, 100 m, 200 m and 400 m.

Table 3.2: Station name, date, time and geographical coordinates of experimental CTD deployments

Station	Date	Time (GMT)	Latitude	Longitude
ICE	26/11/2014	17:29	59.9629 S	46.1602 W
P2	29/11/2014	03:41	55.2476 S	41.2661 W
P3	13/12/2014	22:56	52.8118 S	39.9726 W

Once on deck, water was gently siphoned out of the Niskin bottles via a piece of silicone tubing, which had been pre-rinsed three times with 0.22 µm filtered seawater (FSW), into pre-rinsed 20 L carboys. To ensure collection of all possible faecal material from the funnelled

base of the Niskin bottles, the base of each bottle was opened, rinsed with FSW, and the water collected in separate sterile 250 ml Nalgene bottles.

The contents of the carboys and Nalgene bottles were then gently filtered through a 53 µm mesh (see Figure 3.2) and bottles rinsed through with FSW. The contents of the mesh were backwashed into a 250 ml sterile Nalgene bottle using a 5% borax-buffered formalin-seawater solution.

Formalin-preserved samples were stored in the shipboard chemical cupboard until arrival back at the British Antarctic Survey, Cambridge, where they were stored in the dark at ambient temperature until analysis within 21 months.

Figure 3.2: Siphoning setup used to drain the contents of the carboys through a 53 µm mesh.

3.2.2 Sample analysis

3.2.2.1 Mesozooplankton

Mesozooplankton samples were split using a Folsom Plankton Splitter, according to the density of the sample, and final splits were analysed using two methods. In the first, half of the final fraction split was analysed for size spectra using ZooScan, a semi-automated software package for digital zooplankton analysis (CNRS and Hydroptic). This was the method used for all quantitative and comparative analysis.

ZooScan analysis allows the rapid numerical and size spectra analysis of zooplankton samples, whilst the combination of digital image classification with a manual verification step

reduces error and biases compared to fully automated methods (Gorsky et al., 2010). To improve the accuracy of the dimensions given by the ZooScan, it was calibrated with type material of known size belonging to BAS.

The split was transferred to a beaker and topped up to 500 ml with tap water. Once a preparatory background scan had been run, the sample was gently mixed and a 25 ml aliquot removed from the beaker. The ZooScan tray was prepared with a small amount of fresh water, the frame was inserted, the 25 ml sample was added to the tray and the scan was run. This was repeated for two further aliquots from the 500 ml sample. Once scanned, images were processed using the ZooScan software and analysed with Ecotaxa (Picheral et al., 2017). Items were broadly classified into groups of Copepoda, Amphipoda, Euphausiacea and 'other' (including chaetognaths, polychaetes, ostracods, pteropods, phytoplankton cells and detritus). Finally, for the purposes of this analysis, all Copepoda and Amphipoda, including juvenile and nauplius stages, were grouped together as mesozooplankton. Although some euphausiids and their furcilia stages were present in the samples, these were excluded from analysis as Bongo nets are known to under-sample macro-zooplankton and nekton abundance due to their ability to outswim the net. Zooplankters in the 'other' category were also excluded from analysis due to poor image resolution, varying orientations and subsequent difficulties in estimating faecal pellet size. Abundance of these zooplankters in the samples was low (<4 % of all zooplankton identified) so they would likely not have been large contributors to the flux overall.

The other half of the final split was preserved in 35 ml 95% ethanol and analysed by the Plankton Sorting and Identification Center Morski Instytut Rybacki, Poland. This method was used to provide contextual insight into taxonomic composition but did not form part of the quantitative or comparative analysis. The zooplankton aliquot was sorted according to the taxonomic categories as follows:

1. All specimens belonging to the "Major Copepoda Taxa" identified and enumerated to species and stage.
2. All specimens belong to the "Euphausiacea Taxa" identified to species where possible and life stages identified as Euphausiacea.
3. Chaetognatha and Pteropoda identified to species/ genus where possible.
4. All specimens belonging to "Non- Major Copepoda Taxa" or "Other Zooplankton Taxa" if present, counted and identified to the low taxonomic level where possible.

3.2.2.2 Faecal pellets

The contents of the Nalgene bottles (generally between 100 ml and 200 ml) were filtered onto a 53 µm mesh, gently rinsed and backwashed into petri dishes. The contents of the petri dishes were examined under a light microscope (Olympus SZX16 with SDF PLAPO 0.5XPF and 1.6XPF objectives) for whole or fragmented faecal pellets, whole or fragmented 'ghost pellets' (white pellets with little organic material visible inside the peritrophic membrane), and other organic matter (e.g. diatoms, protozoa and marine snow). Faecal pellets were photographed using a Canon EOS 70D camera. In many cases, specimens of marine snow, diatoms and other organic material were photographed, but where the sample contained a lot of similar sized or type of items, counts or estimations e.g. to the nearest ten, were made of the number of items. For all photographs, observations related to type and abundance of sample content, lens and magnification were recorded. Images were visually examined and measured using the scale bar with the imaging software, Image J (Rasband, 1997-2016).

faecal pellets were categorised into morphological type: cylindrical, spherical, ovoid or ellipsoidal. In Image J, length (L) and width (W) of items were measured. Where the item was an irregular shape e.g. wider at the top than the bottom, measurements of each part were made and an average taken. The measurement scale was calibrated using the 'Set Scale' function in Image J to a millimetre graticule measured at different permutations of magnification. The volume of each item was calculated using the geometric formulae for sphere, cylinder and ellipsoid/ovoid (González et al., 2000, Manno et al., 2015). Since spherical items included some that were a slightly irregular shape, the volumetric conversion used, as the radius, half of the average of both the L and W measurements. The carbon content of faecal pellets was calculated using mean conversion factors specific to the Scotia Sea for spring-early autumn calculated by Manno et al. (2015): 0.052 mg C mm^{-3} for ovoid/ ellipsoidal; 0.035 mg C mm^{-3} for spherical; and 0.030 mg C mm^{-3} for cylindrical faecal pellets.

A number of faecal pellets, including many small, spherical items that were too small to identify clearly with the magnification of the light microscope alone, were examined further with Scanning Electron Microscopy (SEM). Samples were filtered onto 53 µm mesh, rinsed to remove formalin and backwashed into a petri dish. They were then pipetted gently onto PELCO double coated carbon conductive tabs, excess water was pipetted off and the stub was allowed to air dry. Samples were analysed with a Hitachi TM3000 SEM and associated software.

Estimates of faecal pellet numbers are likely to represent a minimum per sample due to unavoidable losses incurred at every transfer stage (from Niskin to carboy; carboy to filter; filter to Nalgene bottle; Nalgene bottle to petri dish), despite care taken to minimise this.

3.2.2.3 Semi-quantitative analysis of phytoplankton

A semi-quantitative analysis of phytoplankton species present in each sample was carried out. Samples were visually assessed and where possible the most common species were identified. Species were assigned to one of three categories based on a visual analysis of comparative abundances within samples: present; moderately abundant; and highly abundant, with 'present' and 'highly abundant' defining the comparative extremes within which abundance was determined.

3.2.3 Data analysis and statistics

3.2.3.1 Mesozooplankton

Following Ecotaxa image processing and verification, data were exported and analysed in RStudio (V.1.0.136) (R Core Team (2016), converting object length in pixels (estimated with ZooScan as the object's major axis (Gorsky et al., 2010)) to prosome length (PL) in mm and using this value to classify zooplankton into 0.1 mm size spectra bins, ranging from 0 - 0.1 mm to 5.9 - 6.0 mm. The object_major classification measures the primary axis of the best fitting ellipse for the object whilst feret diameter gives the longest dimension between any two points along the object boundary. Object_major was thus chosen as it appeared less sensitive to interspecific differences in length, or the orientation, of antennules (Gorsky et al., 2010). Calibration of the ZooScan with known type material confirmed that the dimensions given by object_major represented the size of the prosome of the animal rather than the full body length.

Counts per sample were achieved by multiplying up to the 500 ml subsample that the aliquots came from and then by the relevant split. Counts per sample were converted to individuals m^{-2} by dividing by the volume filtered (m^{-3}, calculated from the net mouth area and depth of haul) and multiplying by sample depth interval.

A multivariate analysis in PRIMER 7 (v.7.0.13) (PRIMER-e) was carried out on the station abundance data to assess how samples varied from one another. Data were arranged in a sample-variable matrix, where variables were median prosome length classes (median of size bin calculated previously e.g. 0 – 0.1 became 0.05). This resulted in 50 body length variables and six samples (day and night nets for each station). Data were first square root transformed and a resemblance matrix based on Bray-Curtis similarity calculated. A hierarchical cluster

analysis of the resulting resemblance matrix with clustering based on group averages was first performed. This incorporated a SIMPROF Type 3 test on each node of the dendrogram to identify the level below which no statistically significant multivariate structure was identified. This method identifies clusters of samples which demonstrate internal association but between which there is statistical separation. Secondly, a non-metric Multi-Dimensional Scaling (nMDS) analysis was carried out on the same resemblance matrix, upon which plot the cluster groups identified in the previous analysis were overlaid. The MDS results in an ordination of stations along axes of abundance and station based on the rank similarities of samples to one another.

In addition, an Anderson-Darling *k* sample test was performed on pairs of day/ night samples to examine whether the distributions of prosome size spectra differed statistically. Day/ night abundances from each station were then averaged for each size class and a one way ANOVA was used to compare the abundance-size distribution for the three stations.

The predicted faecal pellet size from these animals was calculated as a function of prosome length (PL) following equation 3.1:

$$log_{10}FPV = \theta\ log_{10}(PL) + n \qquad \text{Equation 3.1}$$

where θ of 2.58 and n of 5.4 have been taken from known relationships derived and adapted from Mauchline (1998) and Stamieszkin et al. (2015).

Predicted faecal pellet size was compared with actual faecal pellet size by comparing the frequency distributions of each using an Anderson-Darling *k* sample test.

3.2.3.2 Faecal pellets

faecal pellet abundance per m^3 was calculated by dividing by the volume of the Niskin sampling bottle (12 L) and multiplying by 1000. The same calculation was used to calculate the volume and carbon of faecal pellets per m^3.

To investigate a difference in faecal pellet volume over depth, ANOVA tests were carried out for each station (Shapiro-Wilks and Kruskal-Wallace). Volumes of faecal pellets from 5 m, 20 m, 40 m and 100 m were also combined into a 0 – 100 m depth bin and 200 m and 400 m were combined into a 200 – 400 m depth bin to investigate whether faecal pellet volume changes significantly from the upper to lower mesopelagic and the same ANOVA tests were applied.

faecal pellet flux was calculated following the methodology set out in Dagg et al. (2014) according to Equation 3.2:

$$FP\ flux\ (g\ C\ m^{-2}\ d^{-1}) = \frac{\sum(w_s \times C)}{V}$$ Equation 3.2

where w_s is the faecal pellet sinking velocity, C is faecal pellet carbon content (g C) and V is the sample volume (m^3).

faecal pellet sinking velocity (w_s, $m\ d^{-1}$) was calculated using an empirically derived relationship adapted from Komar et al. (1981), Equation 3.3, which has been shown to represent the settling velocities of mixed copepod and euphausiid faecal pellets of different dimensions from a number of datasets.

$$w_s = (1.21 \times 10^3) \times L^2 \left(\frac{L}{W}\right)^{-1.664}$$ Equation 3.3

Where L is the faecal pellet length (cm) and W is the faecal pellet diameter (cm).

Statistics were carried out in SigmaPlot V.13.0.0.83 (Systat Software Inc.) and RStudio (V.1.0.136) (R Core Team (2016).

3.3 Results

3.3.1 Environmental and hydrographical context

Chlorophyll profiles obtained from CTD instrumentation (see Figure 3.3) illustrate the relative productivity at and differences between stations. The highest values were observed at P3 (CTD017) where a chl-*a* maximumof 2.7 µg l^{-1} was observed at ~30 m. The lowest values were observed at the ICE station where peak values at ~35 m were 0.5 µg l^{-1}, followed by a secondary peak of ~0.4 µg l^{-1}at ~70 m. At P2, fluorescence in the top 100 m was generally quite low (~0.5 µg l^{-1}) with sharp peaks >1.5 µg l^{-1}at ~10 and 45 m and 0.9 µg l^{-1} at ~80 m.

Overall, all three stations exhibited subsurface chl-*a* maxima and deep profiles (up to 100 m) of chl-*a* biomass. Whilst the ICE station exhibited low chl-*a* biomass at 5 m, chl-*a* rapidly increased to its 35 m peak of ~0.5 µg l^{-1} and remained between 0.1 – 0.4 µg l^{-1} as deep as 120 m. Similarly, at P3 chl-*a* was consistently >2 µg l^{-1} between 0 – 50 m, remaining at >0.5 µg l^{-1} as deep as 80 m and only reaching a minimum below 120 m. Chl-*a* biomass at P2 was relatively constant at ~0.5 µg l^{-1} from 0 – ~65 m, with a narrow peak occurring in between the 40 m and 100 m sample depths, possibly indicating some surface-level disruption to the water column from wind or storm turbulence.

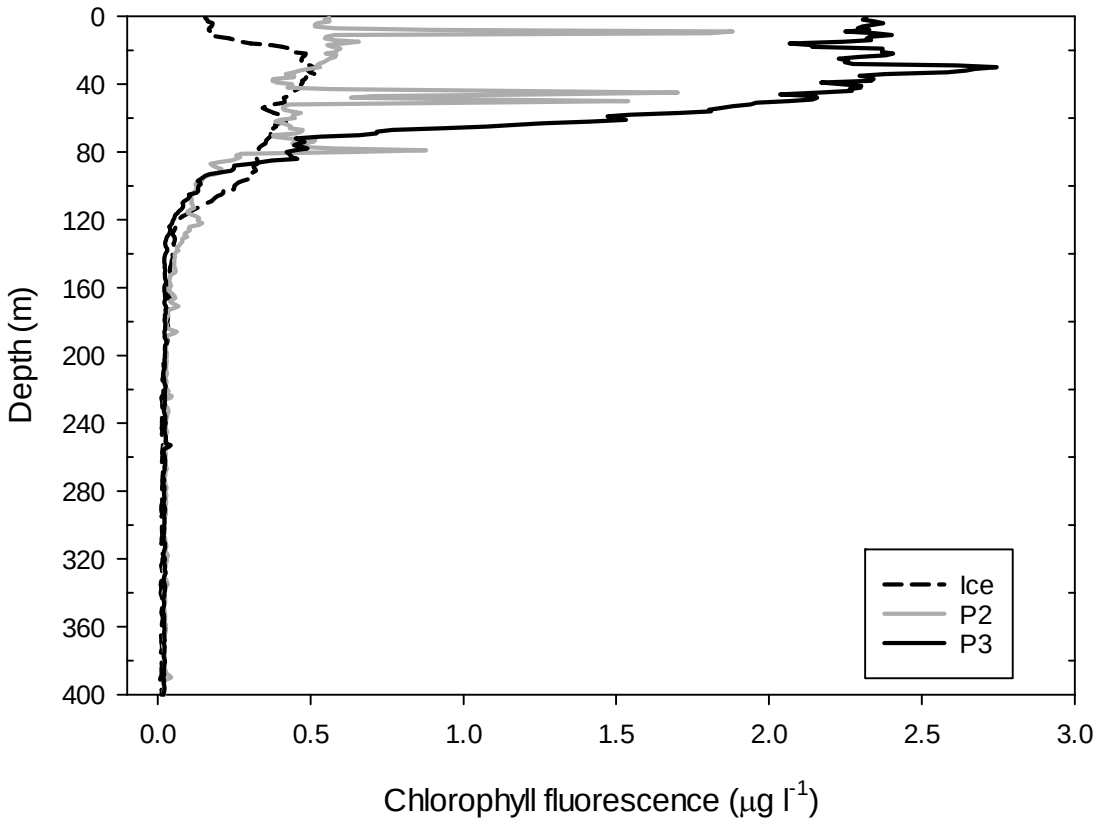

Figure 3.3: Profiles of chl-*a* concentrations (µg l^{-1}) based on fluorescence measurements at ICE, P2 and P3. Measurements were taken with CTD casts from which water samples were obtained.

3.3.2 Mesozooplankton analysis

Total mesozooplankton abundance (Figure 3.6) across the upper 200 m water column at P2 (>180,000 inds m^2) was over 12 times greater than at the ICE station (<15,000 inds m^2) and P3 abundances (>510,000 inds m^2) were almost three times greater than at P2 (individual station plots are in Appendix 2). The two multivariate analysis methods employed showed abundances per size class to be the most significant factor determining differences between the stations. Hierarchical cluster analysis (Figure 3.4) resulted in an initial clustering of ICE station samples forming one cluster and P2/ P3 samples forming the second. This second cluster was further broken down into separate clusters of P2 and P3 samples. No significant differences in size spectra distribution between Day and Night samples were found at any station. nMDS analysis (Figure 3.5) illustrated a clear separation of the three sets of station samples along the axis of abundance. A separation of Day and Night samples at ICE and P2

suggests a shift in the size spectra of species between the two samples, although this was not deemed significant by SIMPROF analysis.

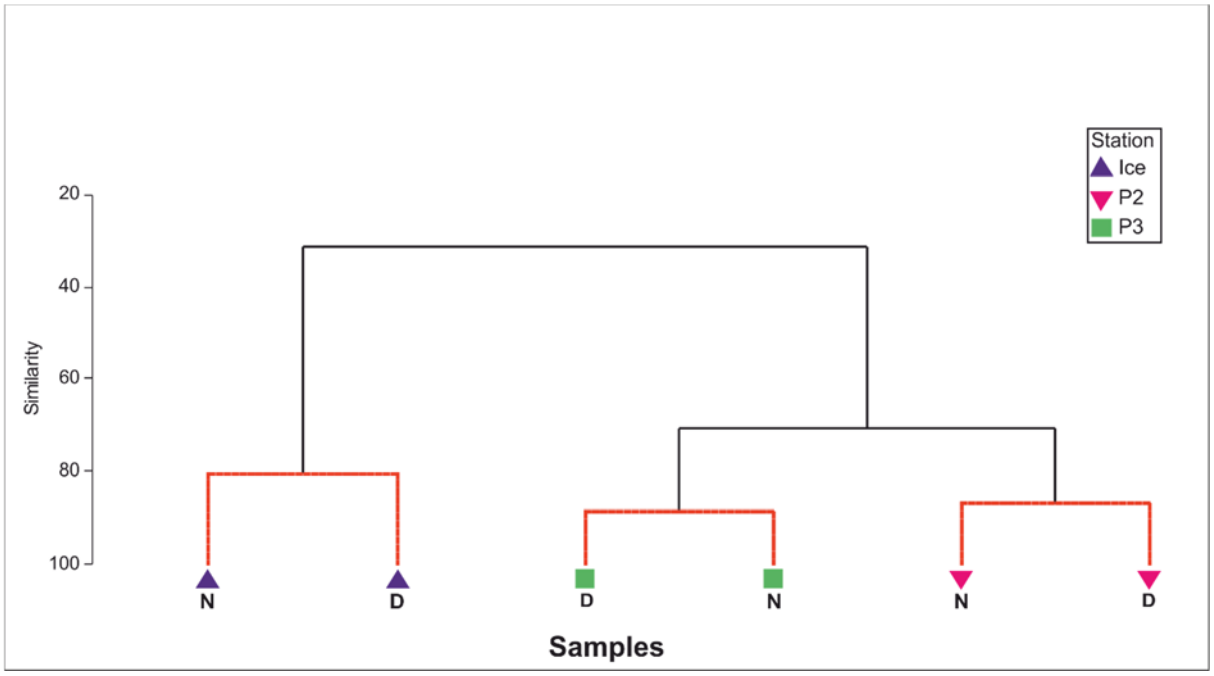

Figure 3.4: Group average cluster dendrogram of mesozooplankton samples taken with 0 – 200 m Bongo nets. Groups of samples within which no significant multivariate structure is determined (determined by SIMPROF testing) are illustrated by the red lines. Night and Day samples are represented on the plot by N and D, respectively.

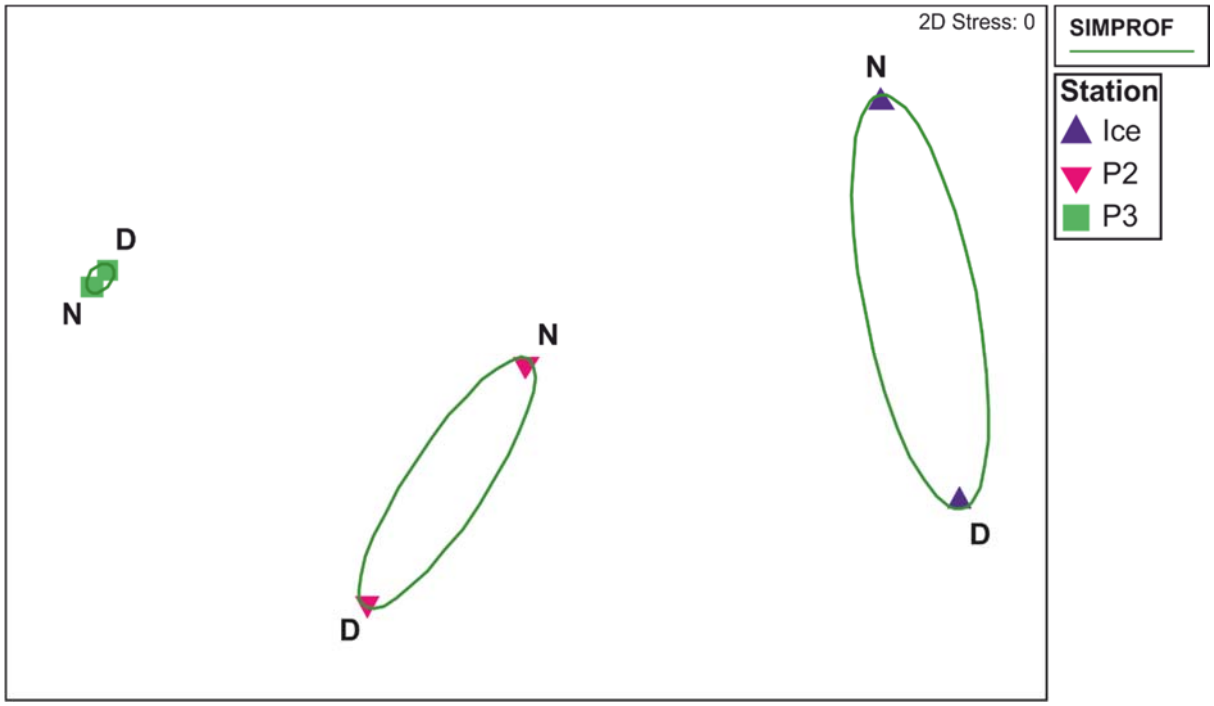

Figure 3.5: Non-metric MDS plot of abundance by prosome length (PL) at each station with cluster analysis groups (determined by SIMPROF testing) superimposed. Night and Day samples are represented on the plot by N and D, respectively.

An Anderson-Darling *k* sample test found no significant difference between the day and night nets ($p > 0.05$). Combined with the SIMPROF groups, this supported combining the two nets into an average for each station. A subsequent ANOVA on the averaged abundance data (Shapiro-Wilk's and Kruskal-Wallace) found a significant difference between the three stations ($p = 0.047$) and a Tukey test found a significant difference between ICE and P3 ($p = 0.049$).

Mesozooplankton size range (PL, mm) did not vary substantially between stations (median PL 0.35 – 5.15 mm at ICE, 0.35 – 5.05 at P2 and 0.35 – 5.25 mm at P3). On the whole however, animals at P3 were found to be smallest and animals at P2 the largest (peak abundance, x0(P3) = 0.60 mm, x0(ICE) = 0.62 mm and x0(P2) = 0.64 mm).

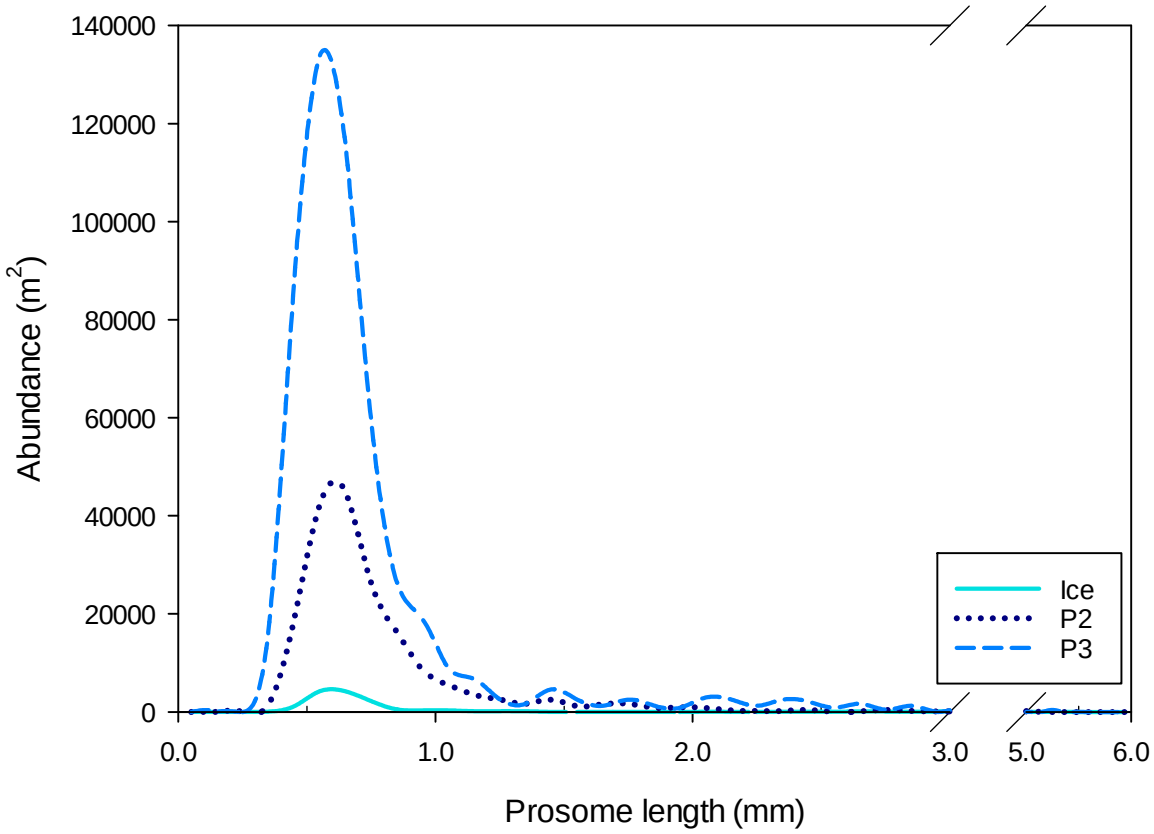

Figure 3.6: Mesozooplankton abundance and size spectra based on prosome length (PL) at ICE, P2 and P3.

3.3.3 Faecal pellet and sample analysis

A semi-quantitative analysis revealed some obvious differences in phytoplankton flora between stations, although at all stations the phytoplankton was dominated by diatoms. The most commonly observed groups are presented in Table 3.3.

Table 3.3: Semi-quantitative assessment of the most commonly observed diatom groups at ICE, P2 and P3. The scale is * = present, ** = moderately abundant, *** = highly abundant.

	ICE	**P2**	**P3**
Corethron spp.	*		*
Fragilariopsis spp.		**	**
Eucampia spp.			***
Pseudo nitzschia			**
Thalassiothrix spp.		*	
Thalassiosira spp.		*	*

Diatoms and other organic material were sparsest at the ICE station across all depths. At P2, diatoms were observed as deep as 100 m but in greatest abundance at 20 and 40 m. In addition, occasional zooplankton and other specimens were observed within the samples, including copepods and their nauplii, euphausiid larvae, pteropods, polychaete worms, foraminifera and egg masses. The highest concentration of material was encountered at P3 where diatoms, marine snow and other organic and non-organic items were abundant to 40 m. Copepods of varying sizes were the most abundant type of zooplankton observed, although pteropods were also found. Below 40 m material became sparser but zooplankton, diatoms and marine snow were still evident at 100, 200 and 400 m.

3.3.3.1 Faecal pellet abundance and volume

The total abundance of faecal pellets (Figure 3.7, Left panel) throughout the upper water column (0 – 100 m) differed between stations, although at all stations there was some attenuation between 100 - 200 m and then an increase at 400 m. In terms of total faecal pellet volume (mm^3) (Figure 3.7, Right panel), faecal pellet volume increased at ICE to a 40 m maximum, decreasing slightly at 100 m and substantially thereafter; a bimodal peak in volume was exhibited at 20 m and 100 m at P2; whilst at P3 faecal pellet volume increased substantially to a 100 m peak before attenuating.

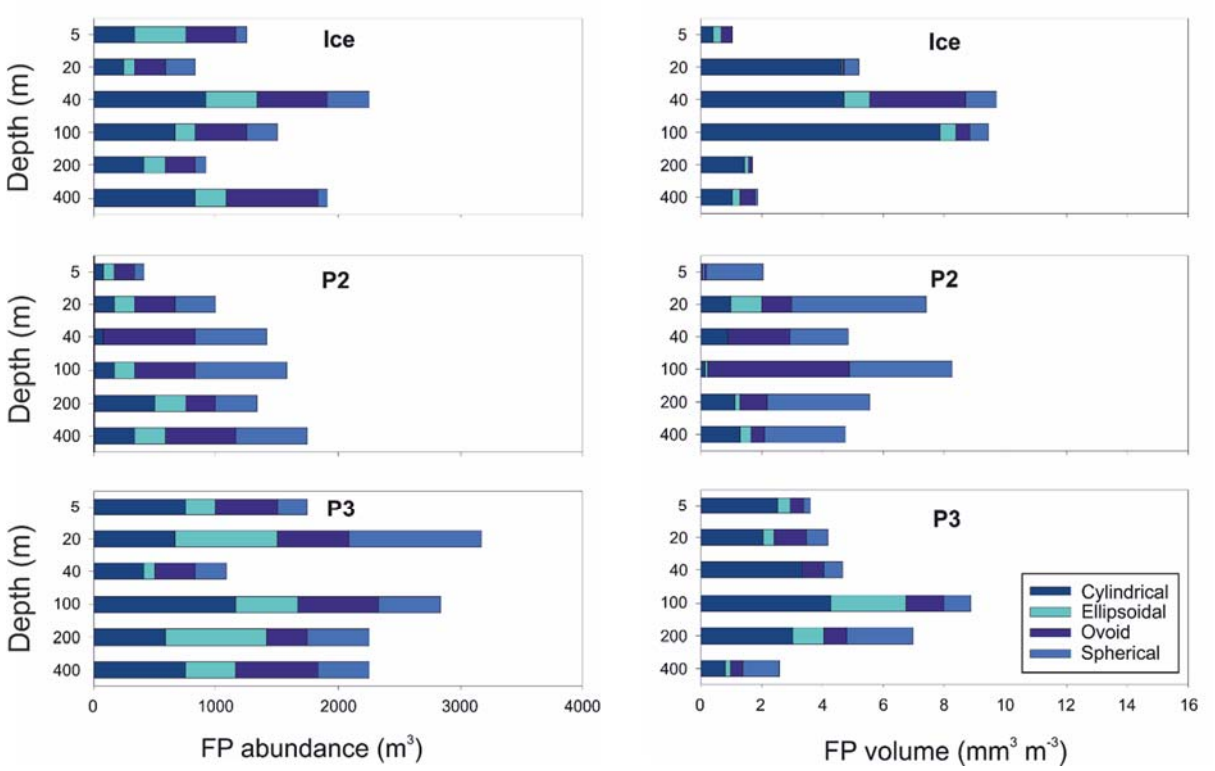

Figure 3.7: Left panel: Total abundance of faecal pellets at each station, stacked by contribution of different morphological type; Right panel: Total volume of faecal pellets at each station, stacked by contribution by different morphological type.

The mean size of faecal pellets (measured in volume, mm^3) at each depth across stations is shown in Figure 3.8. At ICE, faecal pellet size was greatest at 100 m (0.0063 mm^3) although a similar size peak occurred at 20 m (0.0062 mm^3). This was comprised mainly of faecal pellets of a cylindrical morphology. At P2, mean size was greatest at 20 m (0.0074 mm^3), comprised largely of ovoid and spherical faecal pellets, with a secondary peak at 100 m before decreasing to a 400 m minimum. At P3 faecal pellet size peaked at 40 m (0.0043 mm^3) before decreasing slightly to 200 m and more substantially at 400 m.

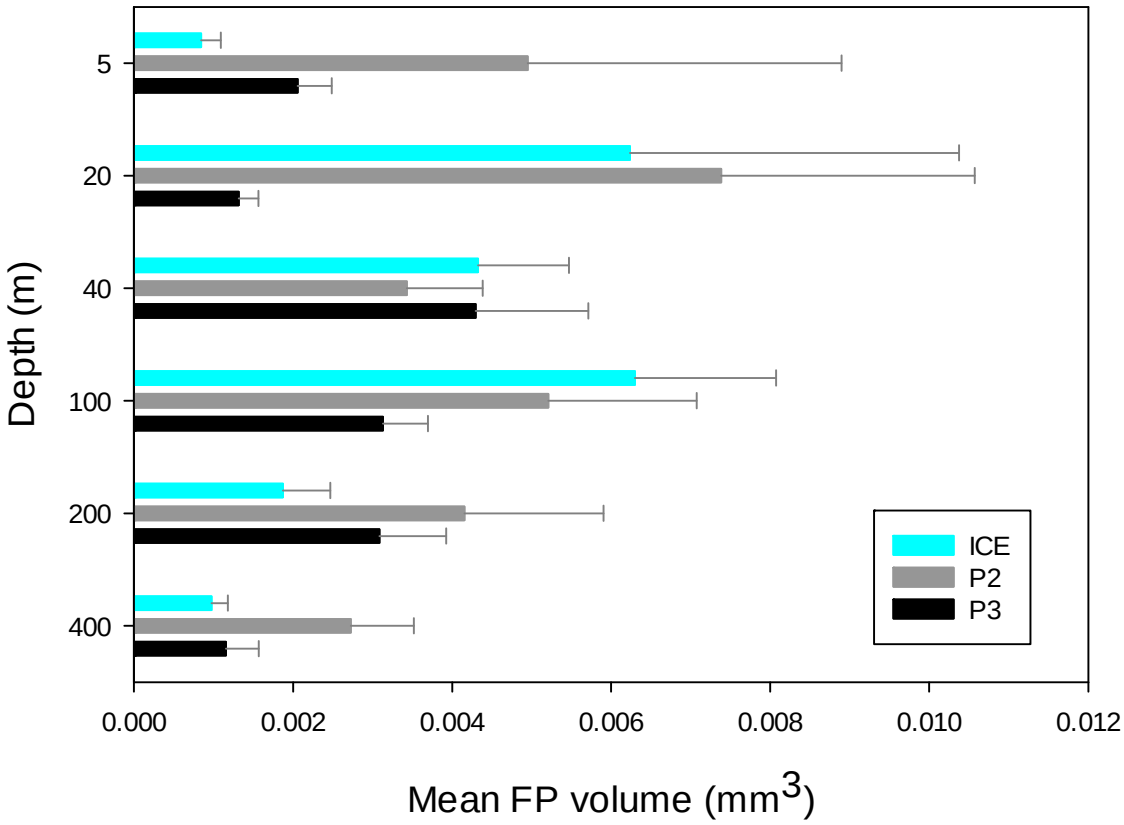

Figure 3.8: Plot of the mean size (volume, mm^3) of faecal pellets across depth at ICE, P2 and P3.

The size spectra (volume, mm^3) of faecal pellets encountered at each station ranged from <0.0001 - 0.045 (ICE), <0.0001 - 0.043 (P2) and <0.0001 - 0.018 (P3). No significant difference (Shapiro-Wilk's and Mann-Whitney U-statistic) was found in faecal pellet volume between those found in the 0 to 100 m depth range and those from 200 to 400 m. Predicted faecal pellet size spectra ranged from <0.0001 - 0.016 (ICE), <0.0001 - 0.015 (P2) and <0.0001 - 0.017 (P3). At all three stations the majority (> 80 %) of predicted faecal pellets occurred in the 0 – 0.0001 mm^3 size range.

Distributions of predicted faecal pellet size spectra, based on the mesozooplankton community in the top 200 m, and actual faecal pellet size spectra of faecal pellets encountered in the top 200 m at each station are shown in Figure 3.9. Anderson-Darling k sample tests revealed significant differences ($p < 0.0001$) between predicted and actual faecal pellet size spectra (based on volume), both between 0 and 200 m and 0 and 400 m depth (total faecal pellet sampled depth).

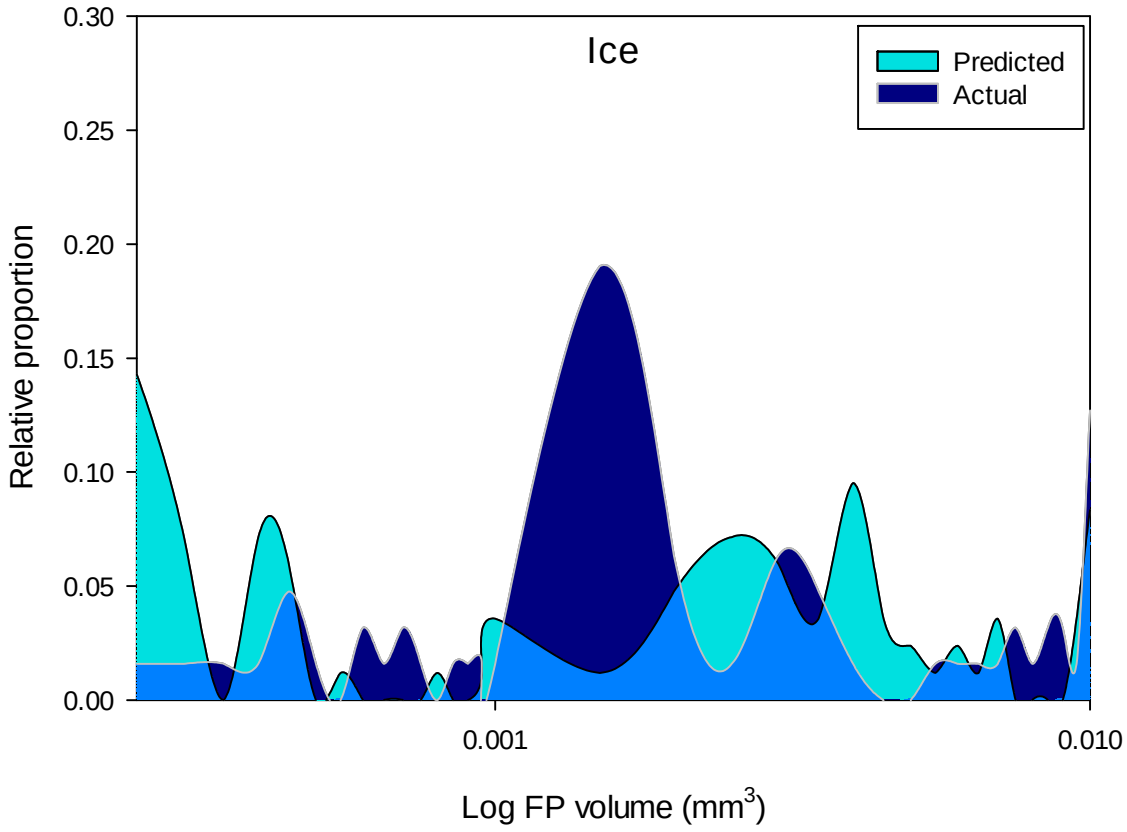
Ice
Predicted
Actual
Relative proportion
0.30
0.25
0.20
0.15
0.10
0.05
0.00
0.001
0.010
Log FP volume (mm3)

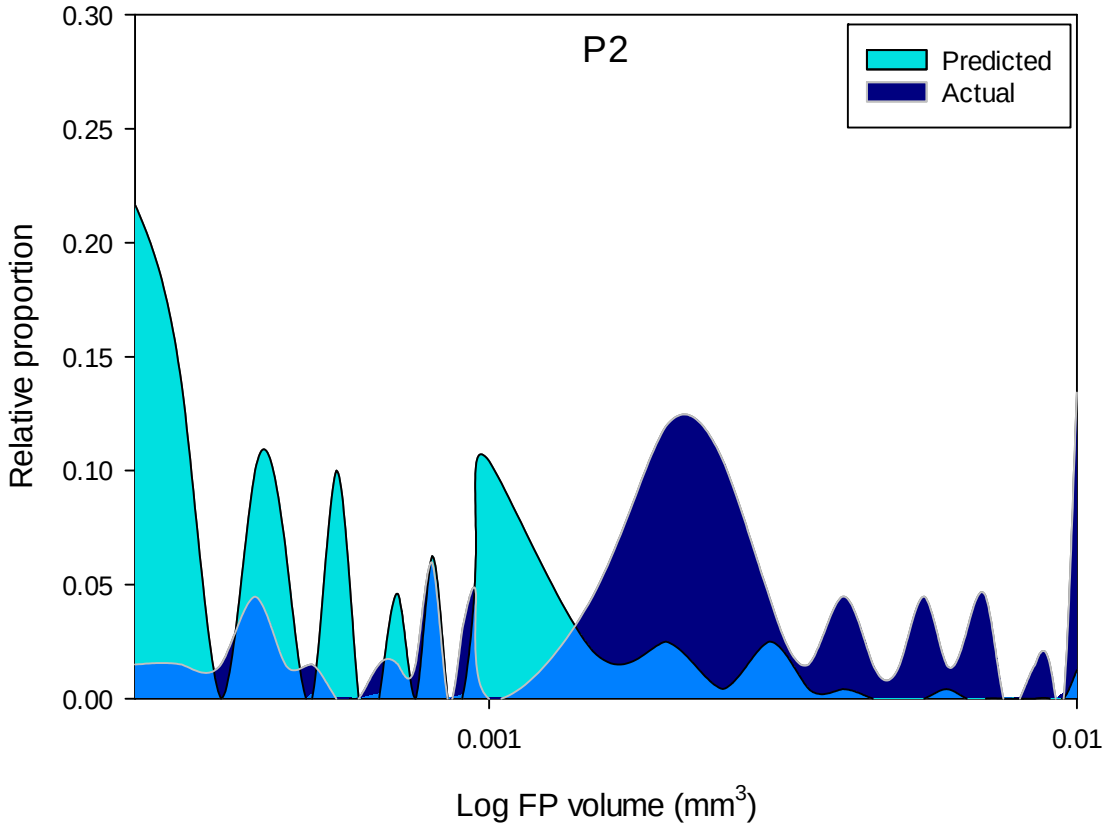
P2
Predicted
Actual
Relative proportion
0.30
0.25
0.20
0.15
0.10
0.05
0.00
0.001
0.01
Log FP volume (mm3)

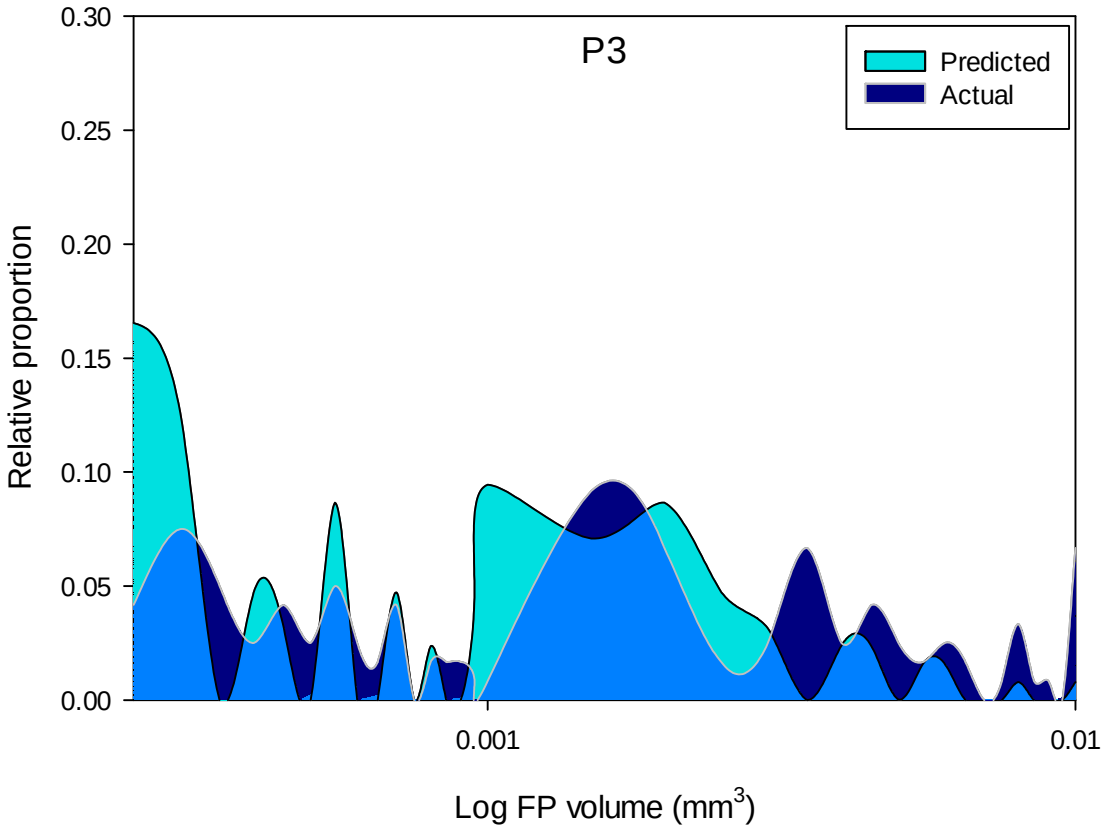

Figure 3.9: Area plots of predicted versus observed faecal pellet size distributions. Faecal pellets ≥0.0002 mm^3 are plotted as the log faecal pellet volume (mm^3) against the proportion of the total for each faecal pellet size class (as a percentage)

3.3.3.2 Faecal pellet morphology

Examples of the different morphological types identified as seen under the light microscope and SEM microscope are shown in Figures 3.10 and 3.11 respectively. The contribution of faecal pellets of different morphological type both to overall faecal pellet biomass and as a proportion of total faecal pellet biomass also varied across depth and between stations. At the ICE station, cylindrical faecal pellets dominated the flux in both abundance and volume over all depths, contributing most to the flux at 20 m (89% of total volume), remaining the dominant contributor until 400 m despite attenuation. Ellipsoidal and ovoid faecal pellets were also important contributors, together contributing over 50% at 5 m and ≥ 40% at 40 m and 400 m but demonstrating no clear pattern. Spherical faecal pellets were most prominent at 40 m in both number and volume although they only contributed 10% of flux, attenuating rapidly below this depth.

At P2, ovoid and spherical faecal pellets strongly dominated in abundance and volume at all depths (≥73% in the top 200 m, 65% at 400 m), with only small contributions from cylindrical or ellipsoidal faecal pellets. Despite this, the contribution of cylindrical faecal pellets to faecal pellet volume increased with depth, increasing from 3% at 5 m to 27% at 400 m (except for 100 m), although there was no apparent pattern to ellipsoidal faecal pellets.

At P3, the contribution of cylindrical faecal pellets dominated in both number and volume over the top 200 m, although the overall mix was much more heterogeneous. Both ovoid and ellipsoidal faecal pellets were fairly significant contributors, on average contributing 27% to total volume over all depths. Spherical faecal pellets tended to increase in importance with depth however and, by 400 m, had become the greatest contributor to total volume (47%).

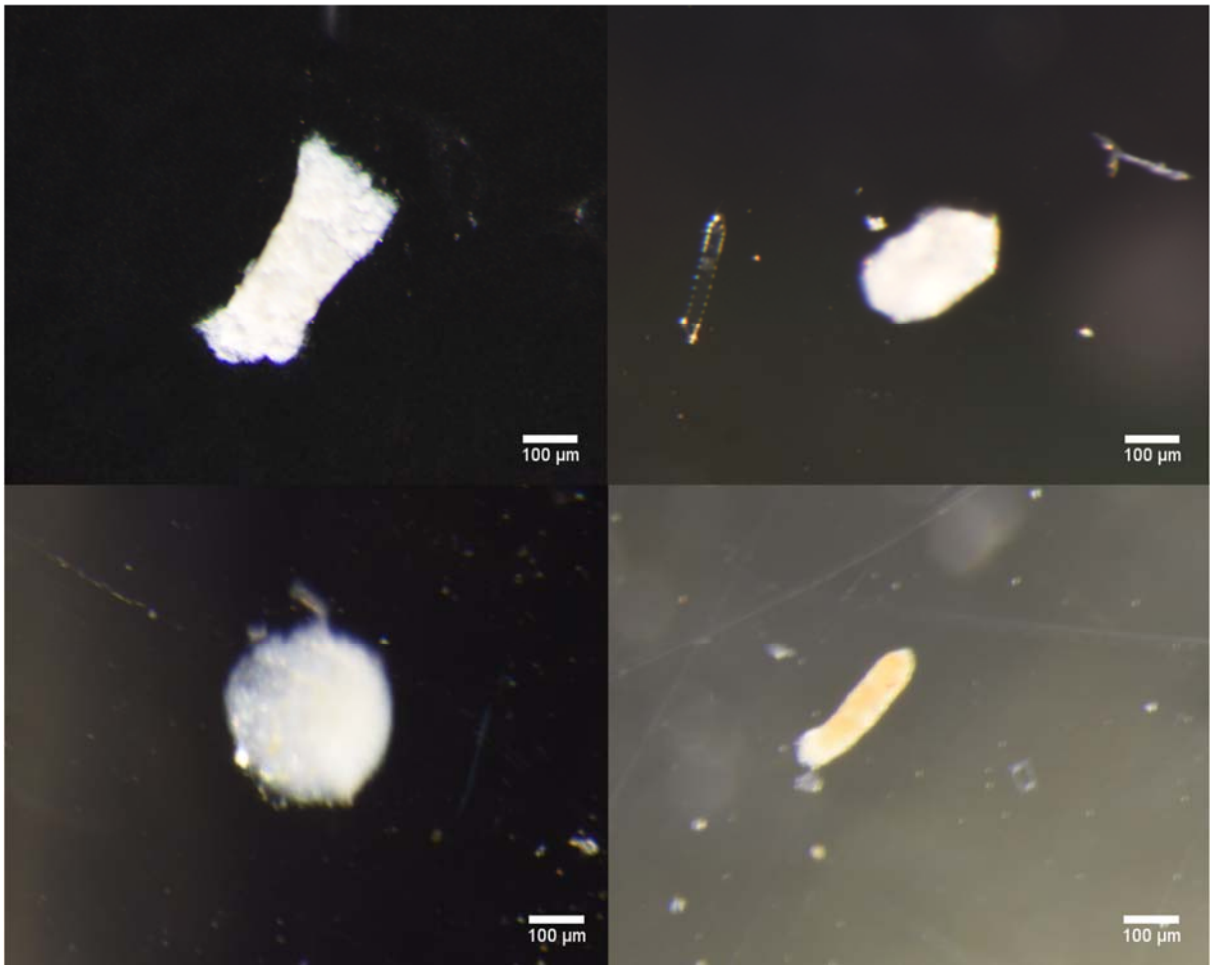

Figure 3.10: Clockwise from top left: Light microscope images of broken cylindrical, intact ovoid, spherical and partially broken ellipsoidal faecal pellets typical of those found in samples.

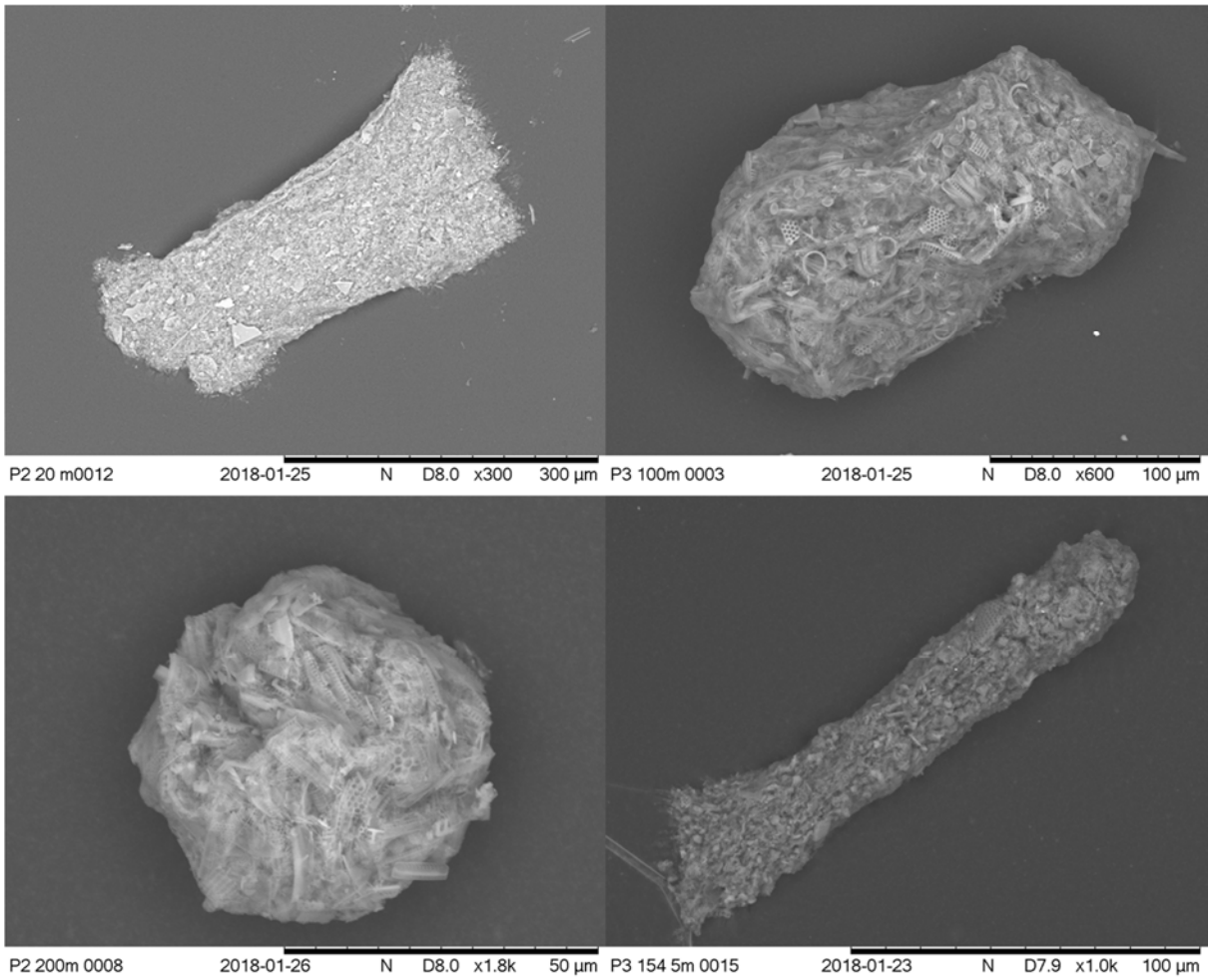

Figure 3.11: Clockwise from top left: SEM images of broken cylindrical, intact ovoid, spherical and partially broken ellipsoidal faecal pellets typical of those found in samples. Images show evidence of organic material, peritrophic membrane (on ovoid and spherical faecal pellets) and diatom fragments.

3.3.3.3 Faecal pellet sinking rates and flux

The mean sinking velocities of faecal pellets at each depth, as calculated from the relationship derived by Komar et al. (1981), are presented in Figure 3.12. Sinking rates are generally highest at P2 and lowest at P3. At ICE there is an increase in average sinking speed to 270 m d^{-1} at 100 m, followed by a decrease to 82 m d^{-1} at 400 m. At P2, there is a strong decrease in sinking velocity with depth from 437 m d^{-1} at 20 m to 192 m d^{-1} at 400 m. At P3, there is a slight increase in sinking rate to 218 m d^{-1} at 40 m followed by a steady decrease to 115 m d^{-1} at 400 m.

This is reflected in the flux of carbon over depth (mg C m^{-2} d^{-1}) as calculated from faecal pellet sinking rates, shown in Figure 3.13. Overall, P2 exhibits the greatest attenuation and P3 the

least, although by 400 m, the station with lowest flux is ICE (9 mg C m^{-2} d^{-1}) and P2, despite strong attenuation, exhibits the greatest 400 m flux (67 mg C m^{-2} d^{-1}). Stations differ in the depth of peak flux: at ICE, flux peaks at 40 m before attenuating strongly; at P2 the peak occurs at 20 m followed by a rapid attenuation; whilst at P3 flux gradually increases to 100 m before a gradual attenuation to 400 m.

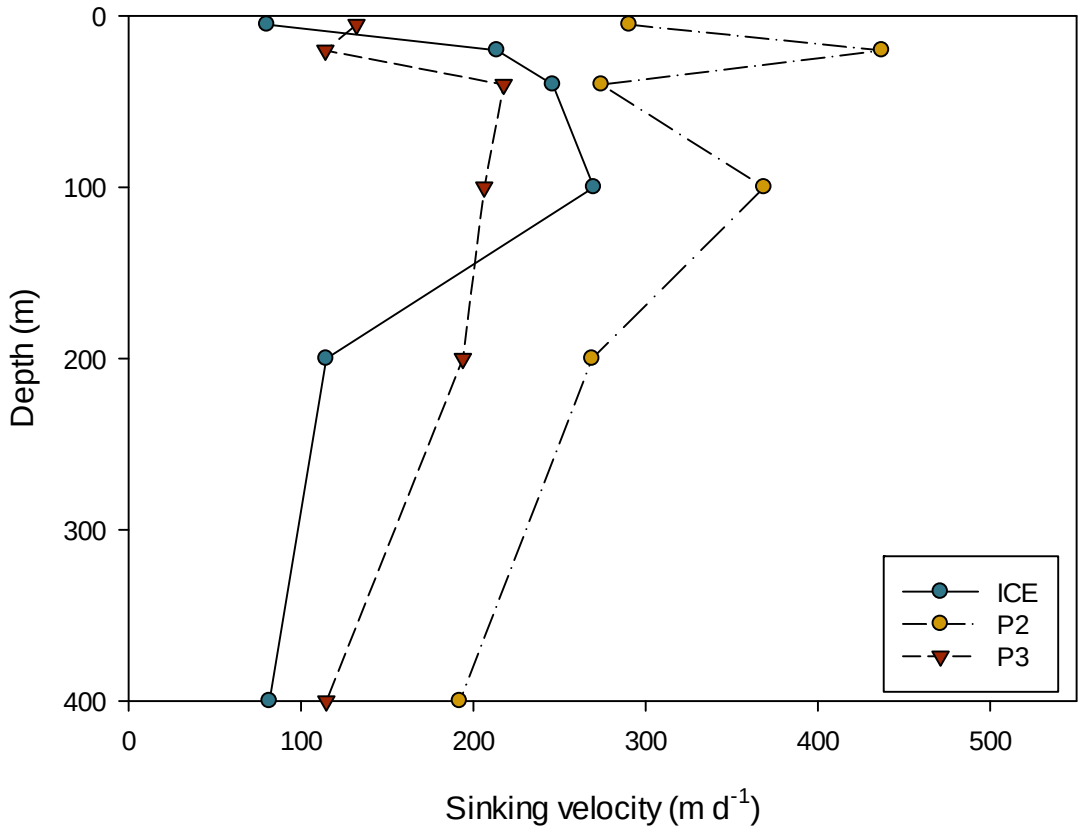

Figure 3.12: Average faecal pellet sinking velocity (m d^{-1}) at ICE, P2 and P3 stations

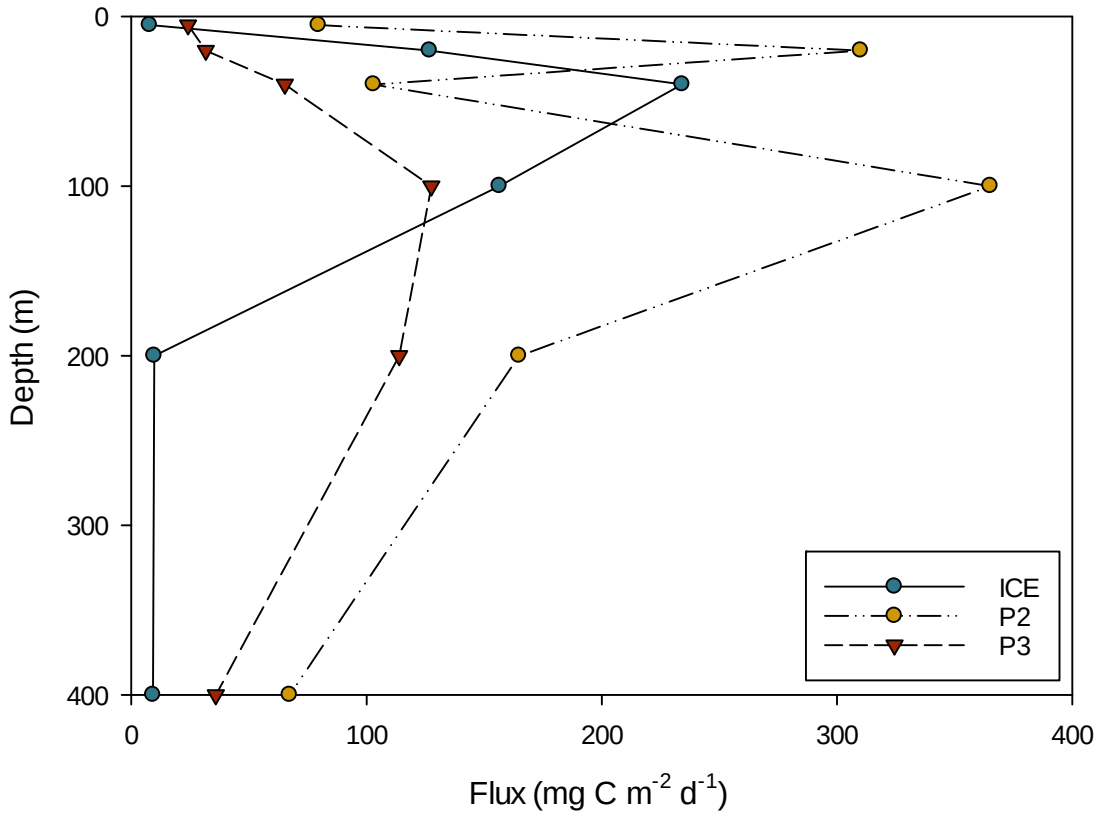

Figure 3.13: Faecal pellet flux (mg C m^{-2} d^{-1}) at ICE, P2 and P3 stations

3.4 Discussion

3.4.1 Is the mesozooplankton community a good predictor of faecal pellet export?

At all stations, the size spectra of faecal pellets in the top 200 m deviated strongly from that predicted based on the mesozooplankton community sampled over the same depth. Whilst observed faecal pellets generally fell within the same size range as those predicted, distributions were markedly different, especially at the smallest end of the spectrum. In particular, the smallest size fractions were significantly under-represented in the observations across all stations, whilst relative proportions of larger faecal pellets were higher in the observations than in the predictions. Based on the predictions, I expected >85 % of faecal pellets produced to be ≤0.0002 mm^3 at all stations, yet found 78% (ICE) to 97% (P2) of faecal pellets to be >0.0002 mm^3, up to nine times greater than expected. Faecal pellets with volumes of ~0.0001 mm^3 often corresponded to those with one dimension <60 µm suggesting that one reason for not observing the very smallest faecal pellets was the

choice of mesh size. However, considering how few of the very smallest faecal pellets were observed, it is unclear whether a reduction in mesh size would alter this result to any meaningful degree. Nevertheless, removing faecal pellets ≤0.0001 mm^3 from consideration still left between 6% (ICE) and 14% (P2) of the smallest faecal pellets unaccounted for. In addition, the amount of small faecal pellets rapidly remineralised may be even greater than suggested by this mismatch, as predicted faecal pellet sizes were based on zooplankton caught in a 200 µm mesh Bongo net and all zooplankton enumerated were ≥300 µm. This implies that the highly abundant smaller zooplankton such as copepods of the genus *Oithona* spp. (Gonzalez and Smetacek, 1994, Dahms et al., 2015) and their faecal pellets are underrepresented. Since conventional sampling with a 200 µm mesh may also underestimate mesozooplankton between 200 and 800 µm in length (Gallienne and Robins, 2001), it is likely that the actual proportion of faecal pellets in the smaller size fraction is higher still.

Whilst there was no significant difference in the size distribution in observed faecal pellets between the upper four depths and bottom two depths at each station, mean faecal pellet volume by depth did show an initial tendency to increase over the shallowest depths (the depth of which varied from 100 m at ICE, to 20 m at P2 and 40 m at P3) followed by a decreasing trend from peak depth to 400 m. The suggestion is that the rate of production of smaller faecal pellets in the surface waters exceeded the loss of this fraction, whether to zooplankton-mediated mechanisms of coprophagy, coprohexy and coprochaly due to a relatively greater abundance of phytoplankton as a food source, or due to the microbial or physical breakdown of particles as they sink. Conversely, as depth increases and light penetration and chlorophyll decreases, faecal matter is likely to increase in importance as a food source leading to an increase in the ingestion and breakdown of smaller faecal pellets by other biota. Furthermore, smaller faecal pellets produced in the mixed layer (between 40 and 80 m in this study) would likely benefit from greater retention than larger ones that can sink out of the mixed layer into deeper waters, leading to an enhanced encounter rate of smaller particles in shallower waters.

Similar patterns have been observed elsewhere: Lane et al. (1994) found that the larger faecal pellets of the copepod species *Calanus finmarchicus* were important mediators of downward flux in the North Atlantic Bight, and the faecal pellets of smaller copepods such as *Centropages typicus* were, on the whole, recycled. More recently, in a study in the same region of the Scotia Sea, Belcher et al. (2017a) used Marine Snow Catcher (MSC) and sediment trap data to conclude that the smallest faecal pellets were not efficiently transferred from meso- to bathypelagic depths and that they would represent a small

contribution to the flux of carbon. The present data represents the portion of the water column above their MSC data (from 110 m below the mixed layer) and an intermediate depth of 400 m and suggests that, as well as not being transferred from meso- to bathypelagic depths, the smallest particles are in fact remineralised almost immediately after production, regardless of depth or oceanographic regime. The importance of the microbial flora of zooplankton faecal pellets, whether in breaking down the organic content of faeces or as a direct food source for other biota has long been appreciated (Johannes and Satomi, 1966, Poulsen and Iversen, 2008, Svensen et al., 2012), yet Svensen et al. (2012) also found that degradation of faecal pellets by the microbial community and biota <200 µm is unlikely to retard the sinking rates of larger copepod faecal pellets sufficiently to retain them at the surface. Since temperature is also a key determinant of microbial breakdown (Mauchline, 1998), larger faecal pellets will sink further and faster before sustaining microbial damage relative to smaller ones.

When considering only those faecal pellets >0.0002 mm^3 some interesting patterns and notable differences between the three stations emerge. Firstly at ICE, there is a peak in observed faecal pellets in the 0.0015 – 0.002 mm^3 size range which is not predicted from the mesozooplankton community, and more deviation in general from the expected distribution than is seen at P2 or P3. The majority of the missing peak is comprised of cylindrical faecal pellets that are typical of euphausiids. Due to the ability of euphausiids to outswim the Bongo nets they are not effectively captured by this method, although taxonomic analysis found two to eight times as many euphausiid calyptopes at ICE than at P2 or P3. Euphausiids are known to be an important component of the macrozooplankton community in much of the Scotia Sea (e.g. Ward et al., 2012b) and to have large, fast sinking faecal pellets (Fowler and Small, 1972). Additionally, the abundance of mesozooplankton in the top 200 m, and chl-*a* over 100 m, were up to one order of magnitude lower at ICE when compared to P2 and P3. A study identifying bioregions of the Scotia Sea suggested that communities in the colder waters to the south of the SACCF and close to the ice edge are typified by a greater proportion of smaller zooplankton, including copepods of the *Oithona* and *Oncaea* generas, cyclopoid nauplii, as well as the large *Euphausia superba* (Ward et al., 2012b). This is consistent with the present results which show the faecal pellet community to be largely comprised of cylindrical faecal pellets with few small faecal pellets. This also suggests that, for this region, the mesozooplankton community alone is an insufficient predictor of faecal pellet export in the upper mesopelagic and instead euphausiids play a more influential role in faecal pellet carbon transport over intermediate depths.

Secondly, at P2 and, to a lesser degree at P3, a number of faecal pellets in the 0.001 - 0.0015 mm^3 range were predicted but not observed. This corresponds to mesozooplankton with a prosome length of 1.8-2.1 mm, equivalent to, for example, early copepodite stages of *Calanoides acutus*, *Scolecithricella* spp., and *Euchaeta* spp., as well as older stages of *Metridia* spp. Taxonomic analysis revealed the presence of most of these species, to differing degrees, at both stations, so reasons for the absence of their faecal pellets from the samples is intriguing. A simple explanation could be that the model is predicting what should occur in the absence of any biological or physical changes, yet faecal pellets also become subject to processes which act to reduce their size. Looking more closely at the distributions, at both stations there are faecal pellets just below the expected peak, whilst higher up the log scale, the expected and actual peaks, whilst correlated, become increasingly offset from one another. The implication is that physical, mechanical and biological processes, including the degradation of faecal pellets by bacteria (enteric and free-living) and protozooplankton (Poulsen and Iversen, 2008, Morata and Seuthe, 2014), play an important role in reducing faecal pellet size. This has the effect of decoupling expected and observed faecal pellet size ranges, with proportionally more observed faecal pellets at the larger end of the size spectrum and more predicted faecal pellets at the smaller end.

Finally, at P2 a large number of predominantly ovoid and spherical faecal pellets were observed across the upper 200 m in the size range 0.002 - 0.003 mm^3, as well as increased numbers in sizes up to 0.007 mm^3, something not reflected to the same degree in the prediction. SEM analysis showed many of these faecal pellets to be densely packed, often comprised of diatom fragments, and with fully or partially intact membranes. This corresponds to zooplankton with a prosome length of 2.3 - 3.8 mm such as *C. acutus* CIV and CV, *C. propinquus* CIV and CV and *Euchaeta* spp. Examination of sampling times revealed that the P2 CTD sample had been collected four hours after sunset, whilst ICE was collected in the middle of the day and P3 one hour prior to sunset. This raises the possibility that faecal pellets captured at P2 were the result of recent production from vertically migrating zooplankton feeding on diatoms, hence were fresher and more labile, but also ballasted with mineral content. A proportionately greater than predicted amount of faecal pellets of this size may therefore be the result of a diel pulse of new faecal pellet production, and captured as other smaller faecal pellets were preferentially remineralised. The mismatch may also reflect the fact that the mesozooplankton analysis is based on the average abundances of mesozooplankton encountered in the top 200 m approximately four hours prior to sunset and two hours after sunrise, thus missing the migratory zooplankton that were dwelling deeper than 200 m during the day. At an oceanic station in the Scotia Sea, the proportion of

the population in the top 100 m was found to increase from 45% to 60% from midday to midnight, with an additional secondary biomass peak between 150 to 300 m found at midnight (Ward et al., 1995). Larger copepods such as *C. acutus* and *C. propinquus* undertake deeper DVMs than smaller species or younger stages (Atkinson et al., 1992, Ward et al., 1995) and data presented in Chapter 2 confirms that these species have migratory amplitudes of up to 500 m. This supports the theory that zooplankton not captured by the daytime Bongo nets were responsible for an additional pulse of faecal pellet production during the night between 20 and 100 m. It also illustrates that estimates of faecal pellet flux may be affected by diel variability in zooplankton distribution and that more work is required to understand the importance of short-term (diel) variability of faecal pellet flux.

3.4.2 Race to the bottom: large, dense faecal pellets are the biggest contributors to flux

Mean sinking rates calculated in this study ranged from 80 to 437 m d^{-1} across all stations (range 5 - 1919 m d-1). P3 had the slowest mean sinking rates, although they were also similar to ICE. Faecal pellets at P2 consistently displayed the fastest sinking rates, thus also contributing to the greatest calculated carbon fluxes. Faecal pellet sinking rates have been observed to be highly variable, ranging from 36–376 m d^{-1} (mixed zooplankton faecal pellets, Smayda (1969)), 20–101 m d^{-1} (mixed copepods, Small et al. (1979)) and 15–862 m d^{-1} (euphausiids, Fowler and Small (1972), (Belcher et al., 2017b)). Komar et al. (1981)'s relationship is based on a water temperature of 13 °C, and seawater viscosity is most strongly affected by temperature (Sharqawy et al., 2010). It must therefore be considered that sinking velocities in the more viscous water of the Scotia Sea may result in slower sinking speeds of up to ~55% (Taucher et al., 2014). However, sinking velocity is also related to faecal pellet density which is affected by food type (Bienfang, 1980) or concentration (Dagg and Walser, 1986), the level of faecal pellet compaction (Fowler and Small, 1972, Small et al., 1979) and ballast (Ploug et al., 2008). Since diets naturally high in mineral ballast and diatom frustules tend to produce denser, faster-sinking faecal pellets (Small et al., 1979, Bienfang, 1980, Ploug et al., 2008), faecal pellets originating from the characteristic diatom community of the Scotia Sea, and based on a herbivorous diet, should be faster-sinking than those of similar dimensions and originating from a flagellate or omnivorous diet (Frangoulis et al., 2001) and this should offset the loss of sinking speed associated with the viscosity effect. Indeed, the fastest sinking faecal pellets were those found at P2, where the faecal pellet assemblage was dominated by ovoid and spherical faecal pellets, typical of those in Figure 3.11 and in agreement with the observation by Cadée et al. (1992) of a number of fast-sinking, oval faecal pellets in the size range 0.002 - 0.013 mm^3. Many of the faecal pellets found at P2

were densely packed with the silica frustules of diatoms, the mineral ballasting of which is likely to significantly increase sinking and subsequently flux rates. Considering also that a threefold variation in sinking rates can manifest in faecal pellets of the same size originating from the same diet (Turner, 1977) and that the extent of mineral ballasting of faecal pellets may significantly alter flux rates (Armstrong et al., 2001, Francois et al., 2002), the sinking velocities calculated here are within the range of calculated values and variability.

Based on the calculated rates, it would take a small faecal pellet typical of the copepod genus *Oithona* 12 days to sink 100 m, whilst it could take as little as 2.5 hours for a faecal pellet from the *Calanus* genus to sink over the same depth. This implies a much greater residence time in the water column of smaller faecal pellets relative to larger ones, whilst the larger surface area to volume ratios of smaller faecal pellets provide greater opportunity for mechanical and microbial degradation to combine to result in the preferential breakdown and removal of smaller faecal pellets. Extrapolating this further, for an *Oithona* faecal pellet to sink from 400 to 1500 m would take 130 days. Conversely, a faecal pellet typical of *Calanus* or *Metridia* spp. could sink to this depth over between 1 to 6 days, respectively, illustrating how the more rapid sinking rates of faecal pellets produced by larger zooplankton can contribute disproportionately more to deeper fluxes as evidenced by sediment traps (Manno et al., 2015), and explain the absence of small spherical faecal pellets from bathypelagic depths.

3.4.3 Attenuation of faecal pellet carbon is strongly modulated by zooplankton

At all stations, faecal pellet associated carbon flux initially increased from the surface (5 m) to a mid-depth maxima: this occurred at 40 m at ICE and 100 m at P3, whilst at P2 an initial peak at 20 m was followed by a second peak at 100 m. Fluorescence profiles indicated a below-surface chlorophyll maximum between 40 and 70 m at ICE suggesting that most faecal pellets resulted from zooplankton production above the chl-*a* maximum (Pearre, 2003). At P3, a deep and stable (~60 to 80 m) mixed layer was observed and at P2 chl-*a* peaks occurred throughout an ~80 m mixed layer. Here, chl-*a* was up to >2.0 µg l^{-1} higher, and zooplankton abundances over the top 200 m, were at least an order of magnitude higher than at ICE (1.5 x 10^4 inds m^{-2} at ICE versus 1.8 x 10^5 to 5 x 10^5 inds m^{-2} at P2 and P3 respectively). This supports the *in situ* production of faecal pellets from autotrophic feeding to at least 80 m at P2 and P3 but possibly deeper if vertically migrating animals make brief forays through the chl-*a* maximum to feed, with faecal pellets either sinking down or being produced at depth. The greater abundances of zooplankton at P2 and P3 may also explain why, by 400 m, fluxes at P2 and P3 were up to 7 times higher than at ICE. Despite this, faecal pellet carbon fluxes at all stations demonstrated a high degree of attenuation, with flux maxima of between 0.13

gm^{-2} d^{-1} at P3 and 0.37 g m^{-2} d^{-1} at P2 decreasing by an order of magnitude by 400 m which suggests efficient processes of remineralisation in the intermediate depths.

At ICE, cylindrical faecal pellets typical of euphausiids dominated the flux, comprising 83% of total faecal pellets at 100 m, with relatively little contribution from copepod faecal pellets. Below this, flux decreased strongly to a minimum of 9 mg m^{-2} d^{-1} at 400 m. This finding is in agreement with a previous study by Cavan et al. (2015) who observed 82% of faecal pellets in the seasonal ice zone (SIZ) to be of euphausiid origin as well as a large decrease in flux with depth. In a separate study, Dagg et al. (2014) found their faecal pellet samples to be comprised almost entirely of cylindrical types and for euphausiids to comprise almost half of the abundance in net samples. They identified two types of flux event: HI, where faecal pellet concentrations peaked at around 100 m and then rapidly declined, and LO, where faecal pellet abundance and carbon flux was generally low. They concluded that, where euphausiids were episodically abundant and had a diet rich in diatoms, they became the dominant contributor to faecal pellet flux, but that where food quality was lower, the flux was much reduced. Whilst direct adult euphausiid abundances were not available, the findings at ICE, along with the elevated number of calyptopes in the zooplankton samples, confirm that where the community is euphausiid dominated, they contribute proportionately more to the export of organic material from the surface. Nevertheless, the strong attenuation of flux between 100 and 400 m also shows that, despite these pellets being an important component of export out of the mixed layer, only a small fraction eventually reaches the deeper mesopelagic. Iversen and Poulsen (2007) found that zooplankton were more likely to fragment or loosen faecal pellets than ingest them directly, breaking faecal pellets into smaller fragments that would then be more susceptible to enhanced degradation by bacteria or protozooplankton (Poulsen and Iversen, 2008). Since microbial breakdown of intact pellets is considered insufficient to explain the degree of faecal pellet attenuation seen in this region (Marsay et al., 2015, Belcher et al., 2016) and chl-*a* levels are comparatively low, it is likely that coprohexy by the zooplankton community plays an important role making faecal pellet carbon available to the microbial and microzooplankton community. Nevertheless, despite the SO being known for its high euphausiid abundances, the fluxes obtained in the present study were still lower than Dagg et al. (2014) found during their HI flux events. This perhaps illustrates how faecal pellet production by passing swarms can result in patchy or episodic fluxes (Belcher et al., 2017b, Tarling and Thorpe, 2017) that can overwhelm remineralisation processes sufficiently to drive export to depth.

Higher fluxes were observed at P2 and P3, which were also characterised by a more diverse and abundant zooplankton community. At P3, cylindrical faecal pellets were still an

important component of the flux, although overall there was a more heterogeneous mix of morphologies with ovoid and spherical faecal pellets becoming increasingly important with depth. This agrees with the relatively constant presence of ovoid faecal pellets found throughout the water column and in deep-sea sediment traps (González, 1992, Manno et al., 2015), suggesting that ovoid faecal pellets are most likely to consistently contribute to carbon export and sequestration fluxes, whilst cylindrical faecal pellets have the potential to make short term, episodic contributions to export fluxes through the mesopelagic. The deepest (100 m) peak in flux was observed at P3, with more gradual attenuation below this depth than at P2, and a greater contribution from ovoid and spherical faecal pellets at 400 m relative to ICE. Since larger faecal pellets can sink 100 m in as little as 2.5 hours, whilst smaller faecal pellets would take >12 days to cover the same distance, the accumulation of faecal pellet material at 100 m from a combination of *in situ* production and sinking from above is feasible. The zooplankton community at P3 was abundant, with high levels of chl-*a*. In addition, sampling occurred during the day, when vertically migrating zooplankton would be more dispersed throughout the water column. Thus, the slower attenuation at P3 may be explained by a rain of particles from above, reduced remineralisation by upper mesopelagic plankton due to high levels of primary productivity, and the *in situ* production of faecal pellets by omnivorous, detritivorous and migratory zooplankton.

Attenuation was equally deep at P2, although there was also a shallower peak in flux at 20 m. The fact that faecal pellet sampling at P2 occurred four hours after sunset suggests that DVM may be playing a role in the production of fresher, denser faecal pellets both at this shallower peak and at least as deep as 100 m. Zooplankton composition at P2 is similar to P3 yet abundances are almost three times lower. However, a substantial part of the community is likely to have ascended to feed prior to the time of faecal pellet sampling and been missed by the daytime zooplankton sampling. Assuming that the animals are actively feeding, this would explain the production of fresh, high volume faecal pellets, many of which still had intact or partially intact peritrophic membranes. Since both chl-*a* and zooplankton abundances were greater at P3 than P2, such high faecal pellet fluxes at P2 are somewhat surprising. This may be reconciled by considering that this represents a diel input of faecal pellet material which is quickly subjected to zooplankton mediated processes of remineralisation and attenuation. Further work is therefore required to understand how profiles of flux and particle attenuation vary over short, daily, timescales as a result of DVM. Another question that must be considered is whether faecal pellets that are largely comprised of diatom material contribute to carbon flux in the same way as those that contain

more organic material, and whether different types of faecal pellet need to be considered differently in their contribution to carbon flux.

An additional feature of the faecal pellet flux profile at P2 is a reduction in flux at 40 m, followed by a subsequent increase at 100 m. The chl-*a* profile from the same CTD shows spikes in chl-*a* biomass throughout a deep mixed layer, suggesting a previous disturbance of the water column which is becoming re-stratified. The reduction in flux at 40 m corresponds to low chl-*a*, whilst the peaks in flux at 20 m and 100 m are directly below peaks in chl-*a* , suggesting active feeding within chl-*a* layers which resulted in the densely packed, labile faecal pellets observed at these depths. The presence of a diversity of zooplankton specimens in bottle samples supports the presence of a mid-depth community at 100 m, which may be feeding on faecal pellets raining down from above and further contributing to the secondary peak in flux observed at 100 m. Despite differences between stations in terms of absolute fluxes, at 100 m carbon flux from faecal pellets was the dominant contributor to export flux at all stations. Faecal pellet fluxes were compared to sinking particulate organic carbon (POC) fluxes from Marine Snow Catcher (MSC) data obtained for the same stations at comparable times during the same cruise (Belcher et al., 2017a). The MSC data was obtained at the mixed layer depth + 110 m, thus varying between stations. Therefore, as a first approach the equation and *b* coefficient given in Martin et al. (1987) was applied to calculate faecal pellet fluxes at the comparable depth. Based on this, faecal pellets were found to comprise between 78% (at P3) and 132% (at ICE) of the POC flux whilst, at P2 faecal pellets comprised approximately 100% of the POC flux, a plausible finding given the substantial flux from fresh faecal pellets at this station, discussed in more detail in previous sections. However, Martin's *b* does not fully describe the variability in Southern Ocean regions (Francois et al., 2002, Cavan et al., 2015), resulting in overestimated and underestimated fluxes at ICE and P3 respectively. When faecal pellet fluxes were estimated from the flux attenuation curves in Figure 3.13, faecal pellets were found to comprise 92% of POC flux at ICE and ≥110% POC flux at P2 and P3. Whilst a >100% contribution seems contradictory, it is likely illustrative of short-term spatial or temporal variability, methodological differences between the MSC and Niskin bottle sampling approaches, and the fact that a single large pellet may be sufficient to increase calculated fluxes quite considerably. Nevertheless, similarly high (>90%) faecal pellet contributions to deep POC have been reported previously for P3 (Manno et al., 2015) and, as discussed in earlier sections, the larger than expected fluxes at P2 may represent short-term temporal variability that may exceed normally sinking POC flux.

3.4.4 Conclusion

Despite the low temperature variability of the SO in general, ICE is separated from P2 and P3 by the SACCF, representing a difference in surface water temperatures of up to 5 °C. In contrast to other models where POC remineralisation is set to increase with temperature (e.g. Marsay et al., 2015), these results show that the shallowest remineralisation occurs at ICE, where zooplankton abundances are lowest and dominated by euphausiids, and that deepest remineralisation occurs at P3 where there is a diverse, abundant zooplankton community dominated by copepods. This illustrates the strong modulation by the zooplankton community on the supply and transfer of faecal pellets between the epi- and upper mesopelagic in the SO. In fragmenting and consuming faecal pellets, the zooplankton community is sustaining further zooplankton production and microbial respiration in the twilight zone and contributing to a deep pool of DOC, enhancing deeper remineralisation by the microbial community. Zooplankton faecal pellets were also the dominant contributor to total POC flux out of the mixed layer at all stations in the Scotia Sea, regardless of regime or depth of attenuation. I also find evidence to show that DVM enhances faecal pellet flux across the upper mesopelagic, producing a shallower pulse of fresh, dense faecal pellets during the night. This is important as greater fluxes were observed at P2 under the putative DVM hypothesis than at a nearby station, P3, with comparatively greater zooplankton abundance. Repeat sampling to quantify the variability in faecal pellet fluxes on short e.g. diel timescales, as well as longer seasonal scales, is imperative to understand more about the processes delivering carbon to the meso- and bathypelagic ocean and to adequately represent these processes in global carbon models.

3.4.5 Summary

1. Within the top 200 m, smaller faecal pellets are lost preferentially whilst larger faecal pellets remain in proportions greater than predicted from the mesozooplankton community structure. This suggests that rapid remineralisation of the smallest faecal pellets occurs soon after production and that they do not contribute significantly to mesopelagic production or faecal pellet carbon export.
2. In ice-influenced regions where the community is euphausiid-dominated, mesozooplankton contribute little to faecal pellet flux. Euphausiids are an important mediator of faecal pellet flux out of the mixed layer but high fluxes to the deep sea are more likely to be driven by episodic, swarm events.
3. Despite lower zooplankton abundances relative to P3, higher flux at P2 was observed which may be due to DVM and the production of high volume, dense faecal pellets

at shallower depths. This suggests that flux is sensitive to both spatial community gradients, and events over short temporal-scales as well as seasonal timeframes.

4. Deep flux attenuation at P2 and P3 compared to ICE suggests that flux is strongly modulated by the zooplankton community, and remineralisation depth cannot be predicted by temperature alone. In particular, larger zooplankton contribute faster-sinking, more labile faecal pellets; the physical breakup of faecal pellets by zooplankton in the mesopelagic enhances deeper microbial remineralisation; and smaller zooplankton such as *Oithona* repackage fragments into smaller, more refractory faecal pellets in the mesopelagic. This is especially important to consider when representing POC attenuation processes in global ocean carbon models.
5. The carbon content of faecal pellets may exhibit greater variation than is currently assumed, as faecal pellets comprised largely of diatom fragments were observed alongside pellets of a predominantly organic nature. Whilst mineral ballasted faecal pellets may result in a large flux of material to depth, this may not necessarily result in an equivalent flux of carbon, illustrating how food availability and type can affect the role of faecal pellets in carbon flux.

Chapter 4: The effect of diel vertical migration on the respiration rate of a prominent Southern Ocean euphausiid, *Euphausia triacantha*

4.1 Introduction

4.1.1 *E. triacantha* distribution and ecology

Euphausia triacantha (Holt and Tattersall, 1906) is one of 85 known species of krill from the family Euphausiidae (Mauchline and Fisher, 1969b, Horton et al., 2017) and one of the five principal species of Antarctic or sub-Antarctic distribution (Kirkwood, 1982). It is a large species of euphausiid, the adult stage ranging from 24 to 41 mm, and has a relatively long life span of up to three years (Baker, 1959, Siegel, 1987). *E. triacantha* is a predominantly sub-Antarctic species, most commonly found between 50 °S and 60 °S, from the south of the Antarctic Convergence to the northerly limits of the East Wind and Weddell Drifts (Mauchline and Fisher, 1969a, Kirkwood, 1982), although has been found as far south as 66 °08 ’ S in the waters off the Antarctic Peninsula (Piatkowski, 1985).

E. triacantha is a common component of Southern Ocean zooplankton. It has a circumpolar distribution, can be locally highly abundant and, since it does not swarm, contrary to the most well-known of Southern Ocean euphausiids, *E. superba*, has a more consistent distribution in the areas it occurs. *E. triacantha* was found to be the most abundant crustacean in a study in the oceanic Scotia Sea, and the most abundant euphausiid on the north-west shelf of South Georgia, contributing 6% to overall nekton biomass (Piatkowski et al., 1994). It is also one of the most important contributors to abundance and biomass in the sub-Antarctic Front-Antarctic Polar Front (SAF-APF) and APF-Antarctic Divergence (AD) inter-frontal zones of the SO Pacific sector and replaces *E. superba* as the dominant euphausiid in that region (Pakhomov and McQuaid, 1996).

Because of its sub-Antarctic distribution, *E. triacantha* is thought to be thermally restricted to waters of approximately 2 to 8 °C (Mauchline and Fisher, 1969a, Kirkwood, 1982), although occasionally considerable occurrences in the colder waters of the Antarctic Peninsula (Piatkowski, 1985) suggest a relatively wide thermal tolerance. In addition, *E. triacantha* displays a pronounced and consistent diel vertical migration (DVM) with a near absence from the surface during the day (Piatkowski et al., 1994). It has a wide migratory amplitude, having been recorded at daytime depths of up to 750 m and in surface waters at

night (Baker, 1959), thus experiencing temperatures across the most thermally variable parts of the water column.

4.1.2 Zooplankton vertical migrations and active flux

Diel migrant zooplankton have been considered agents of active carbon flux for well over four decades, although early attention was focussed on the contribution made from faecal pellets alone (Angel, 1986). Longhurst (1990) broadened the question to additionally consider the role of respiratory flux, suggesting that the flux of dissolved inorganic carbon (DIC) could be considerable, and range from 13-58 % of estimated particulate flux sinking across the pycnocline. This becomes particularly important when it is assumed that the majority of carbon being respired is consumed at the surface, thus expediting the transport of DIC into the comparatively unmixed waters of the deeper ocean. The question has remained an important one, with a recent study suggesting that DOC and respiratory carbon associated with vertical migration could account for up to 20-30% sinking POC flux in some locations (Steinberg et al., 2000). A recent study estimated that respiratory flux from migrators alone could account for 23-71% of the gravitational flux of carbon measured at 150 m depth (Ariza et al., 2015).

The mesopelagic zone is assumed to be characterised by high levels of heterotrophic activity, which rely upon inputs of carbon from above. Total oceanic respiration is highly variable in both time and space, and may exceed primary production (del Giorgio and Duarte, 2002), and estimates of carbon demand within the twilight zone are not fully balanced by inputs from the surface (Burd et al., 2010), requiring a better understanding of the biota to constrain this. del Giorgio and Duarte (2002) conservatively estimated the contribution of zooplankton to oceanic respiration to be 5% of total plankton respiration, or ~3 Gt C y^{-1}, although when carnivorous feeding was taken into account, Hernández-León and Ikeda (2005a) found mesozooplankton respiration to account for 13 Gt C y^{-1}, potentially augmenting the imbalance even further. However, the accuracy of this estimate relies upon data on specific respiration rates, which can vary widely at large and small-scale spatial and temporal scales, and estimates of biomass which vary seasonally and may be difficult to obtain (Hernández-León and Ikeda, 2005a). The authors suggest that, to improve the accuracy of the global estimate, an urgent goal should be the acquisition of respiration and biomass data for zooplankton in the southern hemisphere for which there is currently a lack (Hernández-León and Ikeda, 2005a). Behaviours such as diel vertical migration (DVM) may also complicate the role of zooplankton, with DVM hypothesised to help reconcile some of the 'missing' carbon by providing inputs of organic carbon to the mesopelagic (e.g. Giering et al., 2014) and by respiring material at depth that was consumed in the photic zone.

4.1.3 Metabolic theory

To properly address this, one of the questions that needs to be answered is how metabolism varies as a response to changing physical and chemical conditions as the zooplankton migrate within the water column. Whole animal metabolism can be defined as the sum of all cellular processes that provide an organism with the energy it requires to survive, feed, grow, move and reproduce. Since this is complicated to measure at the cellular level, for organisms where aerobic respiration is the primary means of supplying the oxygen required for cellular metabolism, its measurement is most commonly achieved by measuring oxygen consumption (Lampert, 1984). The Metabolic Theory of Ecology (MTE) (Kleiber, 1932, West et al., 1997, Gillooly et al., 2001) formalises our understanding of how metabolic rate varies with both body size and temperature, and attempts to provide a unifying model through which ecology can be explored through metabolism. It remains a useful framework for considering the links between organisms, ecology and ecosystem productivity, although its universality has been more recently called into question (O'Connor et al., 2007). Amongst the contentions against it include the fact that the principle of allometric scaling is both unfeasible in nature and unmechanistic, and that the reliance on the Boltzmann relationship is insufficient to explain physiological variability and processes of acclimation over different temporal scales, especially in ectotherms (O'Connor et al., 2007). Despite this, some of the most influential works on zooplankton metabolism have proposed similar global relationships (e.g. Ikeda, 1970, 1985, and Ikeda et al., 2001). Underlying these relationships is firstly the idea that respiration increases as a function of size, described by the relationship $R = aW^b$, where a and b are proportional constants and the exponent b is generally between 0.7-0.9 (Hernández-León and Ikeda, 2005b). Secondly for temperature, activation energy (E_a) is fundamental to defining the thermodynamic relationship between temperature and reaction rate (Clarke, 2017) and is described according to the Arrhenius relationship, $k = Ae^{-Ea/RT}$. In physiological studies this is often described as the van't Hoff rule, with reference to the Q_{10} coefficient, $Q_{10} = (R_1/R_2)^{10/(T1-T2)}$, where R_1 and R_2 are the reaction rates at two temperatures, T_1 and T_2. This is a measure used to describe the sensitivity to temperature of a species' respiration rate, defined as the increase in rate with a 10 °C rise in temperature.

An additional consideration for the polar regions is the hypothesis of Metabolic Cold Adaptation (MCA) in which it was proposed that animals living in cold regions have a higher basal metabolic rate than would be predicted by global temperature relationships alone (Ege and Krogh, 1914, Scholander et al., 1953, Wohlschlag, 1960). This is a controversial theory, with opponents suggesting that elevated rates are artefacts induced during the experimental process such as handling stress or lack of acclimation time, or due to difficulties in obtaining

a ‘true’ basal metabolic rate (e.g. Holeton, 1974, Clarke, 1980, Steffensen, 2002). It has also been argued that assessing cold adaptation or temperature compensation through integrated processes of growth or respiration is too coarse to understand potential compensatory processes at the molecular level (Clarke, 1991). However, the majority of studies on MCA have been focussed on the benthos or fish, with relatively little attention given to this subject for the pelagic zooplankton.

In light of this, it is hypothesised that the temperature change experienced by zooplankton over their DVM may be reflected in alterations to their metabolic rate. This may in turn be of fundamental importance in determining the contribution of zooplankton to both the dissolved carbon pool and also in understanding the temporal and spatial variability in estimations of plankton respiration in the open ocean.

4.1.4 Purpose of the current study

To date, many studies have addressed the role of temperature on zooplankton respiration through global or interspecific studies yet, with some notable exceptions, such as *E. superba*, *E. pacifica* and *Meganyctiphanes norvegica*, detailed studies of individual species are still relatively few. Due to its deep migratory behaviour, abundance throughout the sub-Antarctic region and subsequent biomass, *E. triacantha* has the potential to be a significant contributor to the active flux of carbon, especially in areas of high abundance. Whilst it is clearly able to cross sharp thermal gradients, the effect of temperature on its metabolic rate remains unknown. The purpose of this study is to investigate the respiration rate of *E. triacantha* over a range of temperatures within the range it is likely to experience, and to determine whether there is a change in respiration rate as a response to temperature experienced during a vertical migration.

4.2 Materials and methods

4.2.1 *Euphausia triacantha* distribution, abundance and environmental conditions

Day and night time MOCNESS samples were collected by colleagues at four stations encompassing the sub-Antarctic to Antarctic zones in the Scotia Sea, Southern Ocean, during the DISCOVERY 2010 sampling program (see description in Chapter 2). The stations sampled were R1 (an ice influenced station), C3 (an open water, oligotrophic region), P2 (a putative oligotrophic region, upstream of the South Georgia & South Sandwich Island archipelago) and P3 (a naturally iron-fertilised and productive region, downstream of the archipelago) (see Chapter 2, Figure 2.1). Samples were sorted and analysed by myself and P. Ward, as described in Chapter 2, section 2.2.3 with the difference that most counts were obtained from the whole sample, with only a few being obtained from splits of a half or quarter.

Where counts were obtained from a split they were multiplied by the split to give a count for the whole sample. The whole sample count was converted to abundance m^{-2} by dividing by the volume of water filtered by the net (m^3) and multiplying by the depth interval (125 m). Flow rate data were taken from the flowmeter attached to the MOCNESS where possible. Where this failed (<25% nets), the volume filtered was calculated using the equation given by plotting duration of individual net haul against volume filtered from observed flowmeter readings (see Chapter 2, section 2.2.3 and Appendix 1).

Temperature data were obtained by separately deploying an SBE9Plus CTD with a dual SBE 3Plus temperature sensor. Data were averaged for every 2 m from the surface to 1000 m.

4.2.2 Measuring oxygen consumption

4.2.2.1 On-board oxygen consumption experiments

Oxygen consumption experiments were conducted on board two Southern Ocean research cruises with the British Antarctic Survey, JR304 (Nov/ Dec 2014) and JR15002 (Nov/ Dec 2015).

Non-invasive oxygen measurements were taken using a PreSens Fibox 4 fibre-optic oxygen transmitter with temperature sensor Pt100 and PSt3 sensor spots (PreSens, Precision Sensing GmbH, Germany). The device is based on the principle of dynamic luminescence quenching by molecular oxygen, following the Stern-Volmer equation (Klimant et al., 1997, Demas et al., 1999). A chemical complex fixed in an oxygen-permeable matrix (the sensor spot) is excited by a blue light that responds to the level of oxygen present in the medium, returning an oxygen-quenched red luminescence (Tengberg et al., 2006). The more oxygen present, the greater the luminescence quenching and the lower the level of luminescence returned by the indicator molecule.

4.2.2.2 Justification for choice of method

Optodes are considered to be amongst the most reliable methods of determining oxygen consumption in aquatic systems (Tengberg et al., 2006). Traditionally, metabolism has been measured directly by the Winkler titration method, as described in Omori and Ikeda (1984) or by Clark-type electrodes (Clark, 1956); or indirectly by enzymatic approaches (Packard, 1971, King and Packard, 1975, Martínez-García et al., 2009). Disadvantages of these approaches include the need for a long incubation time, potentially inducing starvation effects, and a more laborious experimental procedure requiring hazardous chemicals and associated waste disposal in the case of the Winkler method; oxygen consumption at the cathode, inducing potential sensor drift, and detection problems at low temperatures, with electrodes; and variation in the respiration/Electron Transport System (R/ETS) ratio when

using enzymatic methods in zooplankton (Hernández-León and Gómez, 1996). In contrast, oxygen optodes are non-invasive; give rapid, accurate results after short incubation times (Warkentin et al., 2007); are capable of detecting small changes in oxygen at low temperatures (Technical Data, Presens GmbH, 2014); and consume no oxygen over long periods of use in extreme conditions (Mock et al., 2002).

4.2.2.3 Calibration of sensor spots

For the JR304 cruise, experiments were carried out on newly calibrated (to 0% and 100% saturated water) sensor spots received directly from the manufacturer. Prior to JR15002, all sensor spots were user calibrated (again to 0% and 100% saturation) to correct for any sensor drift, as described below.

To achieve the 0% calibration point, oxygen-free water was produced first by filtering seawater through a 0.22 µm filter (500 ml bottle top filter, Ultra Cruz) into an autoclaved glass media bottle and then by adding a sodium sulphite and cobalt nitrate mixture (1 g Na_2SO_3 and 50 µl $Co(NO_3)_2$ per 100 ml seawater). 100% oxygen saturated water was produced by filtering seawater as before into an autoclaved glass media bottle, filling to three quarters full, and leaving the bottle to equilibrate with the air overnight at the calibration temperature. Calibration bottles were filled from these bottles.

Sensor spots were calibrated at ~3.5 °C. Bottles were filled with filtered seawater (FSW) as described above and allowed to acclimate to calibration temperature for 48 hours prior to calibration. The calibration was carried out using the calibration routine on the PreSens device, with the temperature probe in another bottle of water acclimated in the same tank to the same temperature.

The 100% saturation calibrations were repeated on board, as per the manufacturer's recommendation. Water was prepared as described above, with the exception being that underway seawater was filtered through a three-step filtration pump (smallest pore size 0.22 µm). Whilst my calibrations were carried out in seawater, the manufacturer's calibrations were carried out in freshwater; however this has no effect on calibration values since the calibrations are based on partial pressure which does not differ between the two. However, the salinity value in the device was altered to 34 ‰ prior to taking measurements as the unit µmol l^{-1} is sensitive to salinity.

Upon return from the field, a preliminary analysis of the respiration data found that the JR304 data appeared to be systematically offset below that of JR15002 and that this was likely due to the different calibration conditions between the two years. This was corrected for by retrospectively calibrating the raw JR304 data with JR15002 calibration constants, in

accordance with advice from the manufacturers. This was done using the PreSens Oxygen Calculator v3.0.0.0 and PreSens Oxygen Calculator Software Instruction Manual V3.0.0 (Presens GmbH, 2016). To carry out the retrospective calibration, the type of sensor spot (PSt3) was selected which pre-loaded the relevant sensor constants, and the new calibration data were entered into the software. Calibration data required were phase angle (°), temperature (°C) and O_2 saturation (% a.s.) for the 0% and 100% calibration points, along with pressure (mbar) and mode (humidity) related to the calibration environment. Once the new calibration settings were entered, temperature (°C), pressure (mbar) and phase angle (°) from the raw JR304 data were entered into the software and corrected O_2 values were calculated. This new calibration raised estimated respiration rates by 0.04 ± 0.01 µl O_2 mg DW h^{-1}.

4.2.2.4 Incubator set-up and experimental design

Incubation experiments were conducted in the Cool Specimen Room (cool room) on the RRS James Clark Ross, in tanks set to different temperatures designed to simulate the temperature of the approximate range of depths experienced by *E. triacantha* during their diurnal vertical migration in the Scotia Sea. The intention was to conduct incubations at ~1 °C and ~4 °C. However, as a result of technical problems on board during the first year (JR304), resulting in difficulties in maintaining an identical temperature throughout the cruise, experiments during this year were conducted at multiple temperatures within the range experienced by *E. triacantha* ranging from 0.2 - 4.7 °C. For the second year (JR15002), an improved incubator setup was used. Experiments in both years involved the incubation of euphausiids concurrently at two different temperatures.

For the first year, JR304, a purpose-built incubator (Spartel Temperature Gradient Incubator) was used (Figure 4.1). This had a C-400 circulator unit at the warm end and an FC-500 in-line cooler unit and C-85D circulator unit at the cold end, with temperature at each end controlled by ethylene-glycol anti-freeze being circulated through the end block. The temperature of the cold end was set by the chiller cooling the antifreeze and the circulator unit heating against it. The circulator unit at the other end then warmed against the cooled water within the tank to create a gradient of temperature that reached ~3 °C at the warm end (see Figures 4.1 and 4.4). The temperature of the circulator units had to be set slightly lower or higher than the respective temperature required; the cold end was initially set at -2.5 °C to achieve an internal temperature of 1 °C and the warm end was set at 4 °C to achieve 3 °C. In addition, realisation of the desired temperatures was affected by the ambient room temperature. At times, the temperature control was compromised when the thermostatic control of the cold room failed, causing the ambient temperature to increase,

or for the cooling component of the thermostatic room control to overcompensate and over-cool the room. This was countered by adjusting the temperature setting of the cooler and circulator units. This resulted in the low temperature experiments (T1) being set at mean temperatures of between 0.2 ± 0.68 °C to 2.2 ± 0.05 °C and the high temperature experiments (T2) set at between 2.57 ± 0.1 °C to 3.35 ± 0.16 °C (Table 4.1). 52% of T1 and 62% of T2 measurements were within 1 s.d. and 97% of both were within 2 s.ds (see Appendix 3).

Figure 4.1: Photograph of the incubator setup on cruise JR304

To overcome these issues, for JR15002 the temperatures of two separate tanks (plastic Alibert boxes) were maintained with a thermostatically controlled water bath set-up (Figure 4.2). This comprised a chiller unit (Julabo FL300 chiller) and a thermocirculator unit with cooling coil for each tank (ED Heating Immersion Circulator and Julabo Cooling Coil). As before, the system was kept in the cool room which was thermostatically controlled at ~4 °C. To provide additional insulation for the 1 °C tank against the temperature of the room, the tank was externally covered with a layer of bubble wrap and a second layer of closed cell foam on all sides and the bottom of the tank. To achieve the desired temperature, the chiller unit was filled with approximately 5 L of ethylene-glycol anti-freeze which was circulated through tubing sequentially connected to the cooling coils fitted to each thermocirculator (see Figures 4.2 and 4.4). One length of tubing connected the outlet pipe of the chiller unit to the inlet of the first thermocirculator; a second length connected the outlet of the first

thermocirculator to the inlet of the second thermocirculator; a final length connected the outlet of the second thermocirculator back to the chiller unit. Improved precision of temperature control was achieved by using the chiller unit to excessively cool the water and using the thermocirculators to warm against this lower temperature. The chiller unit was therefore set to -10 °C and the thermocirculator units were set to 4 °C or 1 °C respectively, achieved by the heating element of the thermocirculator sitting inside the cooling coil. This resulted in 67% of T1 and T2 measurements being within 1 s.d. and 100% within 2 s.ds (see Appendix 3).

Figure 4.2: Photograph showing the incubator set-up and insulation during JR15002. The chiller unit was placed to the left of the left hand tank (outside the picture).

Each thermocirculator was fixed to a hard plastic bracket, cut to the correct height to keep the cooling coil and automatic cut-off float submerged just below the surface of the water. The brackets were placed in the top right and left hand corners of the 4 °C and 1 °C tanks, respectively, so that both thermocirculators could be easily connected to one another. To reduce the likelihood of water splashing or entering the units during times of rough weather, the backs of the units were enclosed in Tupperware boxes, with large gaps padded out with foam and small gaps closed up with electrical tape. A flexible plastic 'skirt' was attached to the bottom of the unit to sit on the water and limit splash-back. Figure 4.3 shows how the units were encased.

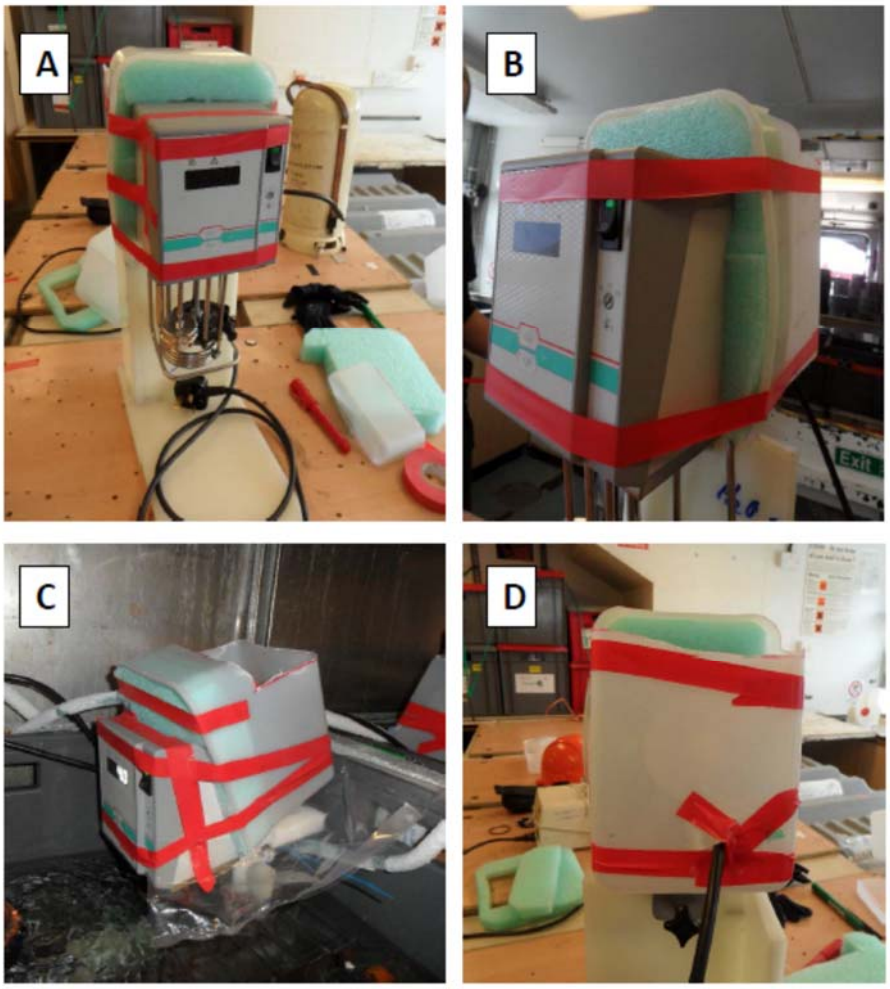

Figure 4.3: Photographs showing how the thermocirculator was stabilised and protected by A) being affixed to a hard plastic bracket; B) the front view showing the Tupperware container and foam padding enclosing the unit; C) the plastic skirt attached to the bottom of the unit; and D) the back view showing smaller holes taped up to prevent water ingress

Despite these precautions, water ingress via condensation on the backs of the circulators still occurred. The main issue as a result of this was that one thermocirculator suffered a repeated electrical error, requiring regular resetting, although once reset it still operated effectively. Towards the end of the cruise, the chiller unit was affected by water splashes during a particularly stormy period and eventually failed.

For the future use of this setup, it is recommended firstly to use waterproof coverings around vulnerable points e.g. heat vents or panels of the units. Given the cold temperature of the room, heat escape from the system was not viewed by engineers to be significant, so covering the heat vents was not deemed likely to be a problem. Secondly, the cooling coil of the circulator should be lengthened or removed and replaced with tubing. This would allow

the anti-freeze to circulate and the chiller units to be kept further away from any potential splashback. With such modifications, this setup would be made moisture resistant and hence more suitable for shipboard operations. The better control of temperature between experiments in JR15002 and the increased numbers of individuals per incubation provided superior replication of results compared to that in JR304. These data were therefore considered separately as well as part of the entire dataset in subsequent analyses.

4.2.2.5 Animal capture and experiment set-up

Healthy specimens of *E. triacantha* were selected from three RMT8 and five MOCNESS net catches during cruise JR304 and two RMT8 net catches during cruise JR15002. Details of experiments are in Table 4.1 and the setup is illustrated in Figure 4.4. Selected animals were transferred from buckets of seawater to two consecutive containers of 0.22 µm Filtered Sea Water (FSW) to rinse them as well as possible whilst causing minimal stress before incubation. Animals were transferred to incubation bottles that had been filled and left to acclimate to temperature in the incubator for at least an hour prior to experimental set-up. One animal was incubated per 60 ml bottle in JR034, five per 250 ml bottle in JR15002 Experiment 1 and four per 250 ml bottle in JR15002 Experiment 2. It was not possible to incubate five euphausiids per bottle in Experiment 2 due to insufficient numbers of healthy animals at the time of experiment set-up. The mean length of euphausiid in Experiment 1 was 27.0 ± 1.6 mm (range 21.9 – 39.4 mm) and for Experiment 2 was 27.7 ± 1.2 mm (range 23.9 – 36.6 mm) (Figure 4.5). Overall, mean length was 27.3 ± 2.9 mm (range 21.9 to 39.4 mm) and mean weight was 33 ± 13 mg (range 15 to 96 mg).

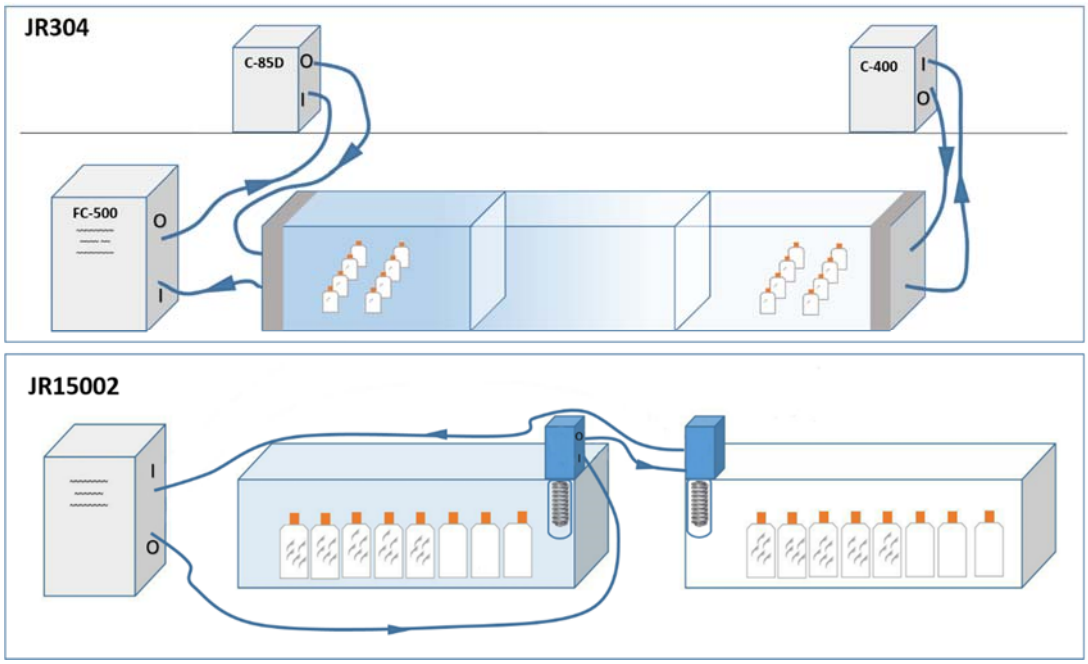

Figure 4.4: Schematic showing the setup of the experiment in year 1 (JR304) and year 2 (JR15002) (not to scale). In JR304 the water was cooled by one unit and pumped by the other. In JR15002 the water was cooled by the chiller (external) and heated and pumped by the circulators (internal). I = In; O = Out.

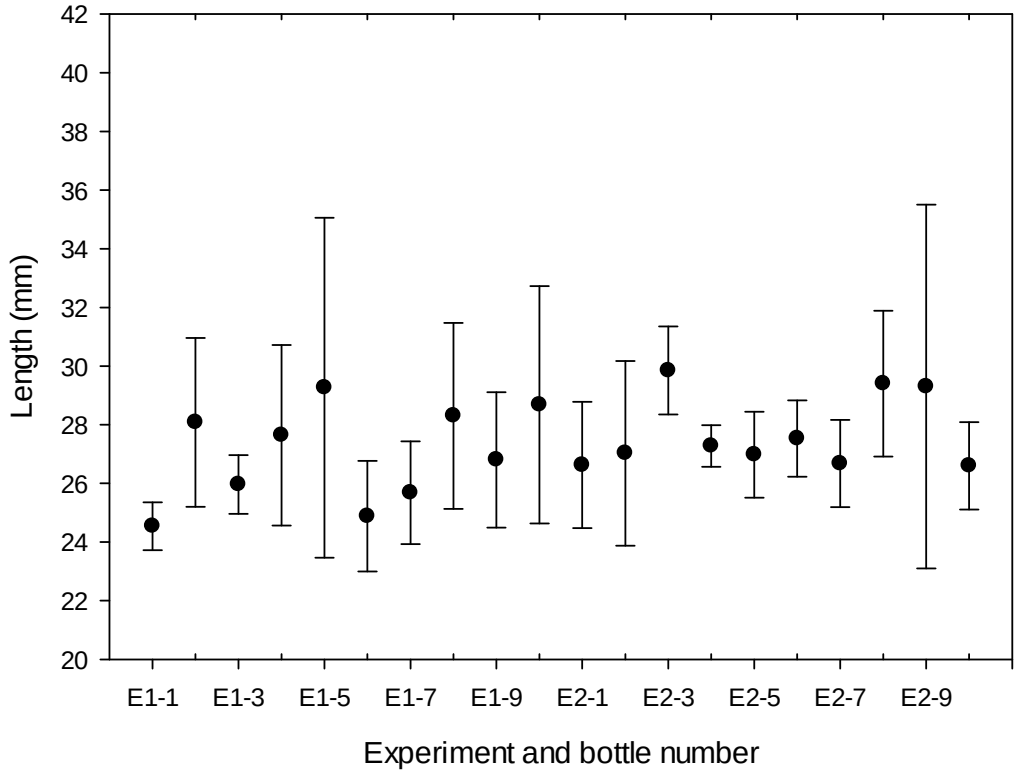

Figure 4.5: Mean and SD of animal sizes in JR15002 experiments. E1 and E2 represent Experiment 1 and Experiment 2, respectively. The number represents the bottle number. In Experiment 1, there were five animals per bottle; in Experiment 2 there were four.

For each temperature, there were six experimental replicates and two controls in JR304 (six experiments in total), and five experimental replicates and three controls in JR15002 (two experiments). A drop of water from the same container as the euphausiids, equivalent to what would have accompanied the animals in experimental bottles, was placed into each of the control bottles. At least 2 hours elapsed between capture and introduction to the experimental bottles during which animals were kept in water acclimated to the temperature of the experiment. Approximately a further 30 minutes elapsed between experiment set-up and the first measurement.

Bottles were topped up with FSW which had also been acclimated to the same temperatures and a stopper inserted. Bottles were tapped and tipped gently to encourage any air bubbles to rise to the surface. Any remaining air was let out, the bottles were topped back up with FSW and re-stoppered. Bottles were gently inverted to test for any remaining air which was removed following the procedure above. Once all air had been removed, bottles were left for ~30 minutes at their respective temperature to allow animals to settle and an initial (T0)

reading was then taken by holding the fibre optic cable (Polymer Optical Fibre, POF) flush against the sensor spot for at least 30 consecutive seconds. Readings were then taken every 1 to 4 hours.

Whilst taking readings, the animals were inspected for general activity and health. The oxygen saturation of the water in the bottles was also carefully monitored. It is considered that the critical concentration of oxygen below which respiration rates of marine animals markedly decline is 50% (Ikeda, 1970) although this varies between species. In this study, measured oxygen saturation (% a.s.) at the end of incubations was >70%.

Bottles containing dead or deteriorating animals were discarded. Bottles containing a full set of healthy animals were terminated together, after at least three readings. Upon termination, the animal was removed from the incubation bottle, inserted into an Eppendorf tube and frozen immediately at -80 °C to prevent degradation of the specimen during storage and transport back to the United Kingdom.

Although in general, mortality was low and showed no association with temperature, one experiment was discarded due to a high mortality rate which may have been related to damage incurred by the animals as the net was brought up. A further experiment had to be discarded due to a break in the polymer optical fibre (POF) which caused all readings to be obtained with a low amplitude (<3,000) (see later discussion on amplitude in Section 3.2.4.1). The results from both years were first investigated as a whole (full dataset) and subsequently investigated independently, and they are discussed as such in the following sections. The justification for this is that there were some methodological differences and improvements between the two years which necessitate both a discussion in their own right and a discussion in terms of their impact on the results.

Table 4.1: Details of the experiments carried out on JR304 and JR15002. T1 and T2 and SD T1 and SD T2 refer to the mean temperature and standard deviation of the temperatures experienced by animals during each experiment. Animals were exposed either to T1 or to T2 for the duration of the experiment. Animals at start refers to the number of animals exposed to each temperature. Animals at end refers to the number of healthy animals remaining at the end of each experiment.

Cruise	Exp #	Duration (h)	T1 (°C)	T2 (°C)	Animals per bottle	Animals at start	Animals at end	SD T1 (°C)	SD T2 (°C)
JR304	INC3	27.9	0.80	3.28	1	6	3	0.12	0.15
JR304	INC4	4.0	1.20	2.92	1	12	10	0.13	0.06
JR304	INC5	6.4	0.20	3.35	1	12	11	0.68	0.16
JR304	INC6	3.7	1.81	3.14	1	12	11	0.04	0.01
JR304	INC7	6.2	1.56	2.57	1	12	9	0.10	0.05
JR304	INC8	4.0	2.20	3.19	1	12	12	0.05	0.12
JR15002	EXP1	2.1	1.43	4.66	5	50	50	0.00	0.00
JR15002	EXP2	2.2	1.74	4.73	4	40	40	0.11	0.08

4.2.3 Determination of length, weight and carbon content

Animals were removed from the -80 °C freezer in batches of 15-20 individuals. Once thawed, they were measured (L, mm) from the front of the rostrum to the tip of the telson. Wet weight (WW, g) was taken immediately after length measurement, within 2 minutes of being removed from the Eppendorf, in pre-weighed weighing boats. Animals were quickly dabbed on paper to remove excess water.

Animals were transferred in these weighing boats to the drying oven where they were dried at 65 °C for at least 48 hours, after which they were re-weighed for dry weight (DW, g) in the same weighing boats as for wet weight. Wet and dry weights were made using a Sartorius GENIUS ME weighing balance. A subsample of weighing boats was weighed before and after drying to check for any alteration of weight during the drying process of which there was none.

Following DW measurement, animals were homogenised using a ceramic pestle and mortar and transferred to tin capsules for elemental (CHN) analysis. Only animals from JR15002 were analysed for CHN content. Capsules were filled to between 1 and 5 mg as quantities above 5 mg were expected to exceed measurement thresholds for samples with a high carbon content. CHN capsules were weighed using a Mettler Toledo MT5 Microbalance.

Between DW and homogenisation, animals were kept in a desiccator containing silica beads which had also been heated to 65 °C. After preparation, capsules were kept in sealed 96 well plates in a cool dry place in a box containing silica beads until analysis.

Animals were analysed for CHN content in a CE440 Elemental Analyser (Exeter Analytical Limited).

4.2.4 Data treatment

Data from each incubation experiment were collected on the Fibox 4 device and exported from the device to the accompanying PreSens Data Manager software in .csv format. This was converted to .xlsx for analysis.

4.2.4.1 Quality control and correction of oxygen consumption data

Prior to analysis the data were checked and quality controlled. This consisted of checking the data for errors and removing associated 'bad' data. Two Error codes, Error 2 and Error 4, were identified. Error 2 was the more common, although both were rare.

Error 2 corresponded to no O_2 data being recorded and a correspondingly very low amplitude (≤1,000 µV) as a result of the Polymer Optical Fibre (POF) not being connected to the sensor spot. Error 4 corresponded to a low amplitude of between >1,000 - ≤3,000 µV, whereby the

polymer optical fibre (POF) was at an angle such that it wasn't able to perceive an accurate light excitation response. Since the light excitation is directly related to the phase angle received and hence the O_2 values calculated, any values containing these errors were removed. There were also a very small number of readings with amplitudes between 3,000 and 15,000 µV. Since the majority of readings were >17,000 µV, I set a threshold of 15,000 µV and removed readings corresponding to an amplitude <15,000 µV to ensure no questionable data remained.

4.2.4.2 Data analysis and statistics

O_2 consumption per bottle was calculated by subtracting the mean O_2 consumption of control bottles from the O_2 consumption of experimental bottles. O_2 consumption values were then converted from µmol l^{-1} to µl l^{-1} by multiplying by 22.391 (ICES, 2018) in order to be comparable with other studies. O_2 consumption per individual per hour (µl O_2 ind^{-1} h^{-1}) was then calculated through the following steps:

(i) Divide by the duration (h) of the experiment

(ii) Divide by the number of individuals per bottle

(iii) Multiply by 1 litre divided by bottle volume (ml)

µl O_2 ind^{-1} h^{-1} was then converted into weight-specific oxygen consumption (µl O_2 mg W^{-1} h^{-1}) by dividing by WW, DW, C or N weight (mg).

To test for the effect of size on O_2 uptake, temperature-normalised weight-specific O_2 consumption was regressed against DW. Multiple regressions were also run, with both µl O_2 ind^{-1} h^{-1} and weight-specific O_2 consumption as response variables, and weight and temperature as independent variables, to investigate the extent to which temperature or size determined O_2 consumption rates.

When weight was found to have negligible effect on weight-specific O_2 consumption rates, further investigations were carried out on weight-specific O_2 consumption as a function of temperature alone. The equation $y = a * b^x$ was found to give the best fit and curves were fitted to both the full dataset (both years) and the second year (JR15002) alone, as described above.

To investigate the sensitivity of *E. triacantha*'s respiration rate to increases in temperature, the Q_{10} was calculated by following the van't Hoff rule (Equation 4.1).

$$Q_{10} = \left(\frac{R_2}{R_1}\right)^{\left(\frac{10}{T_2 - T_1}\right)} \qquad \text{Equation 4.1}$$

where T_1 is the lower temperature, T_2 is the higher temperature and R_1 and R_2 are the respiration rates at T_1 and T_2 respectively.

Length-weight coefficients were determined first by log transforming all data and then by regressing WW, DW, C and N against length with a linear fit. A linear model was also fitted to log C and N data against log WW and DW.

To examine the effect of size on elemental composition, both the percentage content of C and N, and the C:N ratio, were regressed linearly against log DW.

Statistics were carried out in SigmaPlot V.13.0.0.83 (Systat Software Inc.) and RStudio (V.1.0.136) (R Core Team (2016).

4.3 Results

4.3.1 Distribution and environment of *Euphausia triacantha*

Euphausia triacantha were found at three stations across the Scotia Sea from the sub-Antarctic (52.83 S) to Antarctic zones (59.68 S), both in summer and autumn, where surface temperatures varied from 5 to <1 °C (Figure 4.6). They displayed a large vertical distribution at all stations in both seasons, from the surface to as deep as 1,000 m. They also displayed clear evidence of diurnal vertical migration, with a total absence of animals in the top 250 to 275 m in C3 and P2 during the day in both seasons. At P3, animals were found between 125 and 250 m during the day in summer, followed by an ascent by the majority of the population to the surface at night. In autumn, a small number of animals was found in the surface during the day but this markedly increased at night. Across their vertical migratory ranges, the temperatures experienced by the animals ranged from -1.5 to 2.1 °C at the most southerly station, and from 0.4 to 5.0 °C at the most northerly, with the species therefore experiencing a total temperature range of 6.5 °C. The strongest temperature gradient experienced was over the thermocline, between ~60 to 100 m, which animals crossed during their migrations to the surface across which the mean temperature change was 3.5 °C (range 2.5 °C to 4.5 °C).

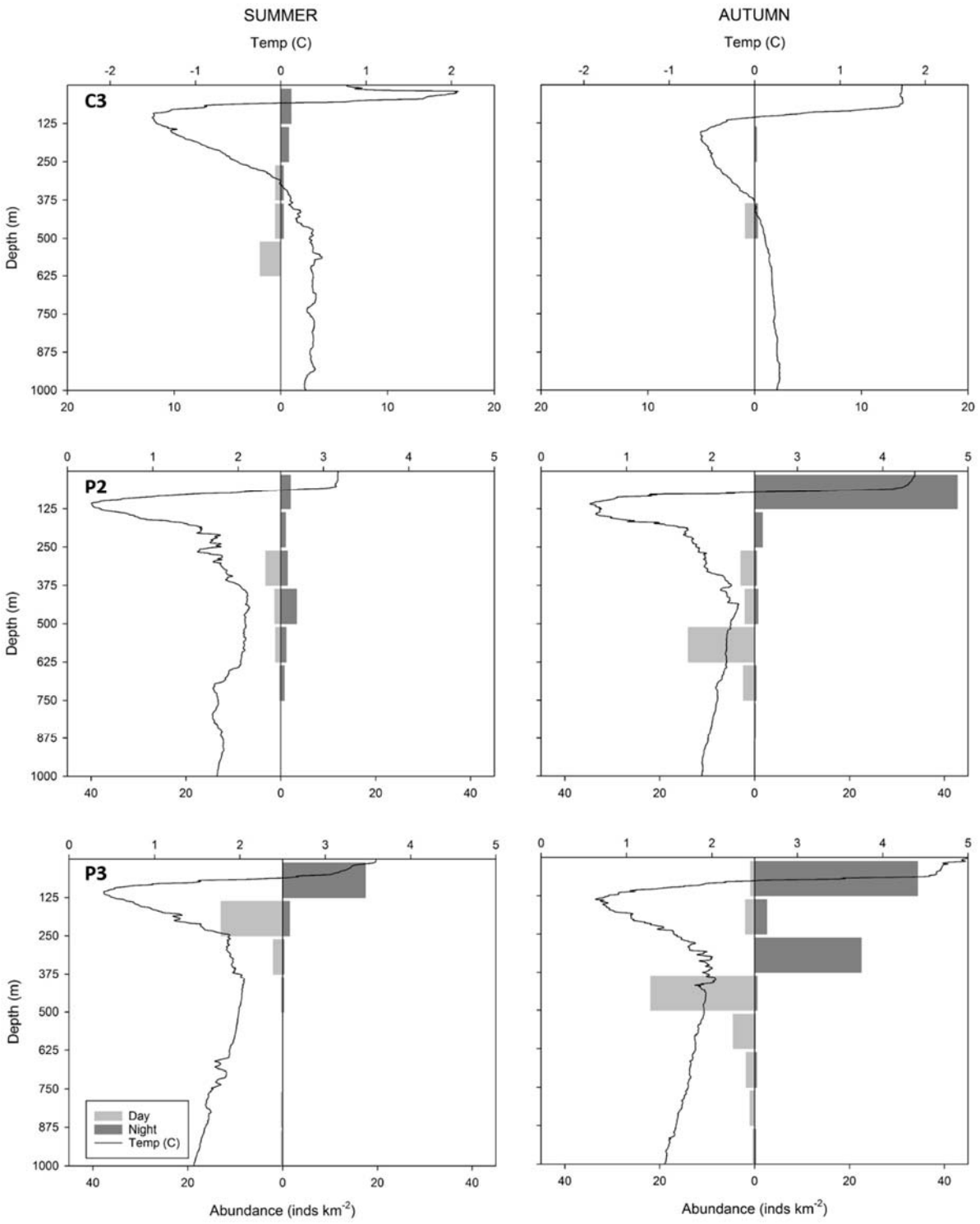

Figure 4.6: Plots showing the day and night time abundances (individuals m^{-2}) of *E. triacantha* during summer and autumn at C3, P2 and P3. No *E. triacantha* were recorded at R1 in the years sampled. Temperature data recorded from the CTD at each station at the same time is overlain. Note the different scale axes for abundance and temperature at C3.

4.3.2 Morphometric and elemental analysis

In total, 159 animals were measured and weighed. Animals ranged in size from 20 to 39.4 mm. This likely represents animals from at least two age cohorts, the sub-adult population (<24 mm) and the adult population (>24 mm) (Baker, 1959, Siegel, 1987). Wet weights ranged from 60.31 to 427.32 mg and dry weights ranged from 12.49 to 96.01 mg. Animals were on average comprised of 78% water. 90 animals were analysed for elemental composition. Carbon (C) content ranged from 37.89% to 45.01% whilst nitrogen (N) content ranged from 8.76% to 10.11%. The mean C:N ratio was 4.39 but this ranged between 3.93 and 4.90.

Since morphometric relationships are generally expressed as a power law, measurements were converted to log values and linear regressions were plotted as shown in Figure 4.7. There was a significant relationship ($P < 0.0001$) between length and WW, DW, C and N mass. Likely due to the greater numbers of individuals in the length-weight measurements than elemental analyses, the regression was stronger ($R^2 > 0.9$) for WW and DW than for C and N ($R^2 > 0.8$). The regression coefficients and R^2 values are given in Table 4.2.

Table 4.2: Regression coefficients for log wet, dry, carbon and nitrogen weight (WW, DW, C and N, mg) against log length (mm). n = 159 for WW and DW; n = 90 for C and N.

	logY = a + b*logX		
Log weight (mg)	**a**	**b**	**R2**
WW	-2.062 ***	2.943 ***	0.963
DW	-3.066 ***	3.172 ***	0.949
C	-3.332 ***	3.100 ***	0.820
N	-3.697 ***	2.907 ***	0.832

*** P < 0.001

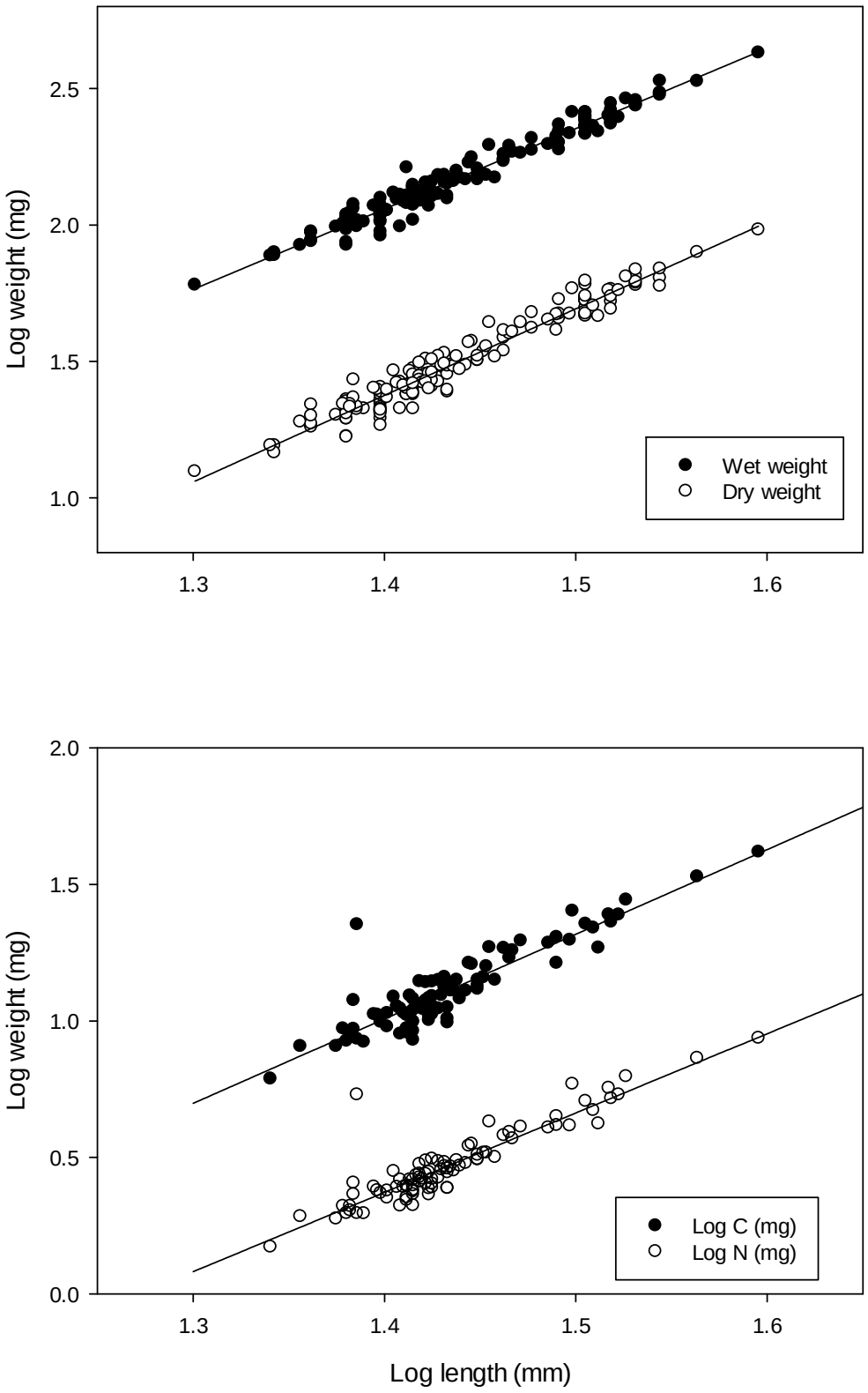

Figure 4.7: The relationship between log length (mm) and log wet (WW) and dry (DW) weight of n = 157 specimens of *E. triacantha* (top panel); and between log length and log carbon (C) and nitrogen (N) of n = 90 specimens (bottom panel).

Log-log regressions of C and N against WW and DW found significant relationships in all cases, with absolute C and N content increasing with size (expressed as weight) (see Figure 4.8 and Table 4.3). In addition, the % C, % N and therefore, the C:N ratio, were found to vary weakly with DW (Figure 4.9 and Table 4.3). Although C:N ratios increased significantly with DW, there was substantial variability, with high (>43%) C found in animals as small as 27 mg and relatively low (<40%) C in animals between 41-58 mg. Similarly, the relatively low (9%) N content was found in a 29 mg animal, whilst the smallest animal contained 9.6% N.

Table 4.3: Regression statistics for C and N content of *E. triacantha* as a function of WW and DW, and the %C, %N and C:N ratio as a function of DW (mg)

		logY = a + b*logX		
Log weight (mg)	**Log elemental weight (mg)**	**a**	**b**	**R2**
WW	**C**	-1.273***	1.104***	0.901
WW	**N**	-1.767***	1.036***	0.915
DW	**C**	-0.442***	1.042***	0.992
DW	**N**	-0.976***	0.970***	0.992

		Y = a + b*logX		
Log weight (mg)	**Elemental composition**	**a**	**b**	**R2**
DW	**C (%DW)**	35.783***	4.080***	0.166
DW	**N (%DW)**	10.502***	-0.646**	0.097
DW	**C:N**	3.296***	0.736***	0.224

*** P < 0.001; ** P < 0.01

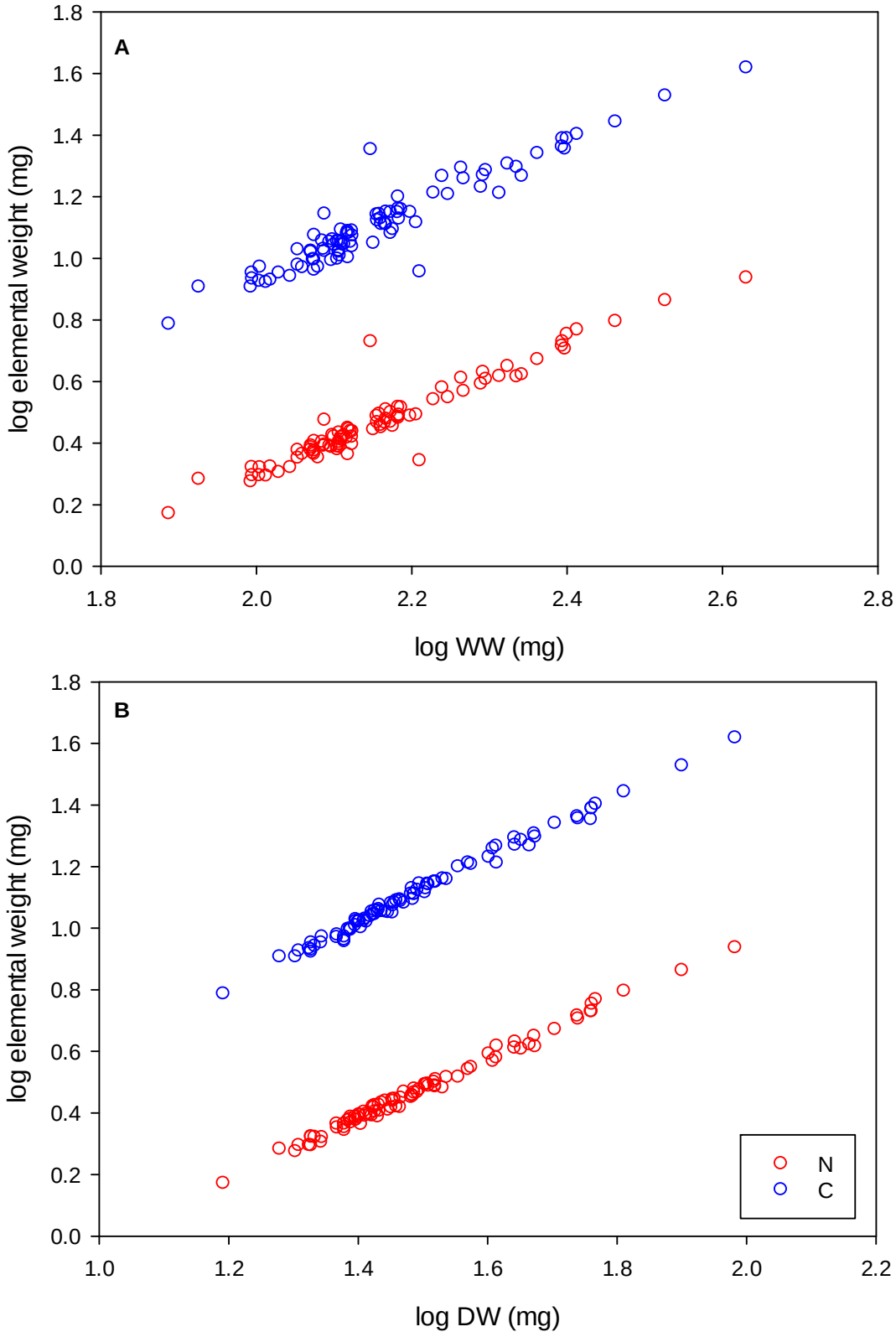

Figure 4.8: Log C and N content (mg) plotted against weight (log WW and log DW, mg)

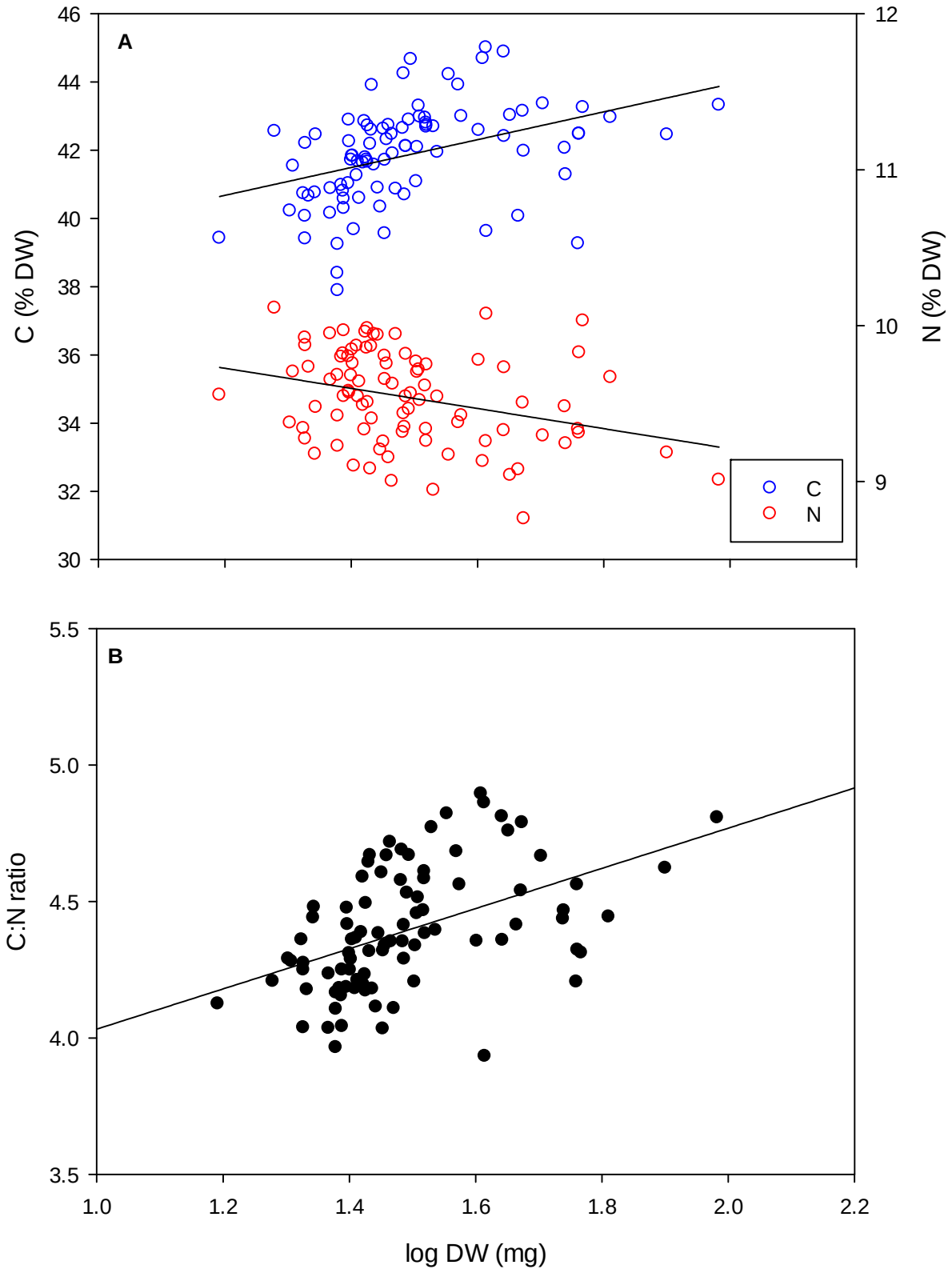

Figure 4.9: Elemental (CN) ratios: A) % C and % N plotted against DW and B) C:N ratio plotted against DW

4.3.3 Statistical analysis

4.3.3.1 Effect of size and temperature on respiration rate

Multiple regression of O_2 consumption per individual against temperature (°C) and weight (mg) (Table 4.4) indicated a significant relationship with temperature and DW. When JR15002 was considered alone, there was a significant effect of both temperature and WW, DW, C and N, with the relationship becoming marginally stronger from C to DW, to N respectively. Considering weight specific respiration, a significant relationship was found only with temperature with no effect of DW both in the full dataset and JR15002 alone. The same was found with C and N for JR15002, although for weight specific respiration, the regression marginally strengthened from C to N to DW.

The lack of effect of DW on weight-specific respiration was confirmed with linear regression of log weight-specific oxygen consumption against log DW, which showed a slight but non-significant ($P > 0.05$) trend of decreasing weight-specific oxygen consumption with increasing size.

Table 4.4: Regression statistics for O_2 consumption (y = O_2 ind^{-1} h^{-1} or O_2 mg DW^{-1} h^{-1}) as a function of temperature (°C) and weight (mg DW, C and N) for *E. triacantha*

		logY = a0 + a1X1 + loga2X2			
Oxygen consumption rate (µl O_2)	**Unit mass (mg)**	**a0**	**a1**	**a2**	**R^2**
ind^{-1} h^{-1}	DW (full data)	-0.279*	0.056***	0.843***	0.677
ind^{-1} h^{-1}	DW (JR15002)	0.004	0.0660***	0.682*	0.563
ind^{-1} h^{-1}	C	0.312	0.066***	0.637*	0.553
ind^{-1} h^{-1}	N	0.685***	0.065***	0.720*	0.578
$weight^{-1}$ h^{-1}	DW (full data)	-0.279*	0.056***	-0.158*	0.264
$weight^{-1}$ h^{-1}	DW (JR15002)	0.006	0.066***	-0.319	0.522
$weight^{-1}$ h^{-1}	C	-0.039	0.039***	-0.189	0.488
$weight^{-1}$ h^{-1}	N	0.686***	0.065***	-0.28	0.519

* $P < 0.05$; ** $P < 0.01$; *** $P < 0.001$

4.3.3.2 Model fit of oxygen consumption to temperature

When considered independently, weight specific O_2 consumption was found to vary significantly ($P < 0.001$) with temperature with a positive response (see Figure 4.10 and Table 4.5). This was the case both when all data were considered together and with JR15002 alone.

Calculated Q_{10} values (Table 4.5) were higher for the full dataset (6.5) than JR15002 alone (4.5) when weight specific O_2 consumption rates were taken at 1 and 4 degrees. The difference is due to the same absolute difference in O_2 consumption yet lower absolute values for the full dataset, leading to a greater ratio between respiration rates (R2/R1) at the higher (T2) and lower (T1) temperatures respectively, for the full dataset.

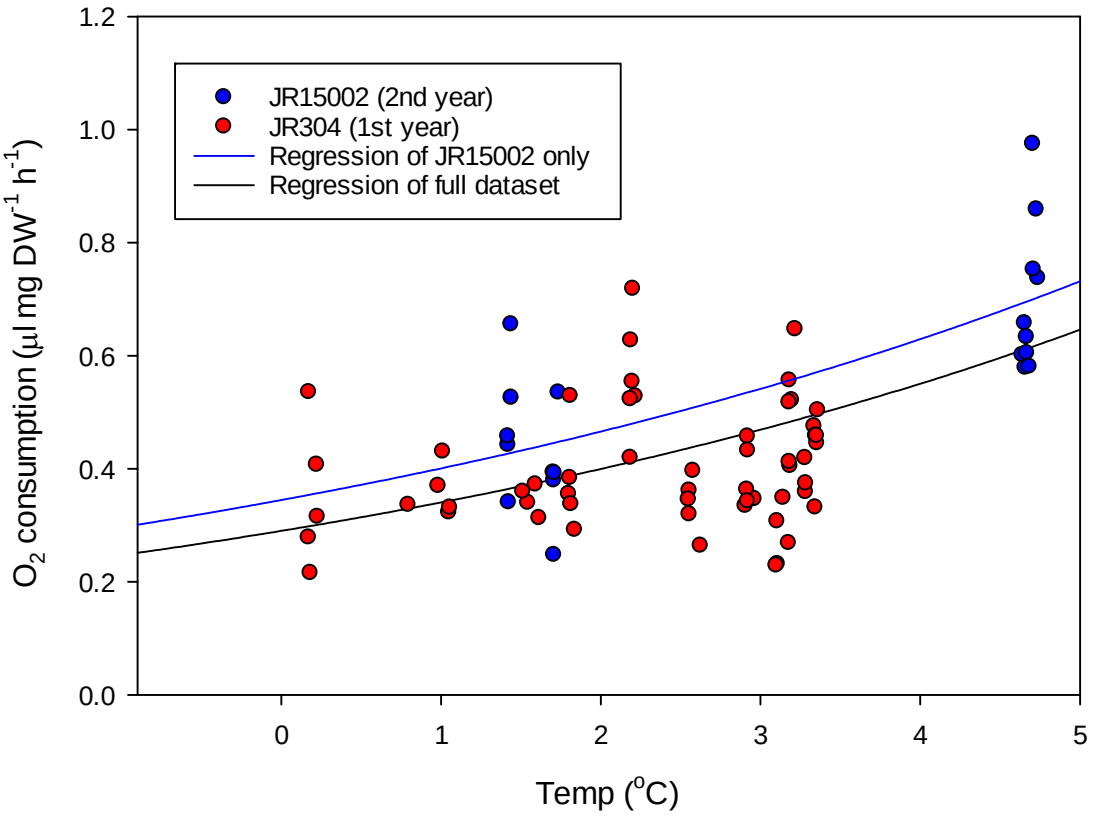

Figure 4.10: Weight-specific oxygen consumption (µl O_2 mg DW^{-1} h^{-1}) plotted as a function of temperature (°C). Red and blue circles correspond to JR304 and JR15002 respectively whilst regressions are plotted for all data (JR304 + JR15002) and for JR15002 only.

Table 4.5: Regression statistics for weight specific respiration plotted against temperature

Regression of O_2 mg DW^{-1} h^{-1} against temp

	$y = a * b^X$			
Oxygen consumption rate (µl O_2)	**a**	**b**	**R^2**	**Q_{10}**
Full dataset	0.290	1.174	0.310***	4.97
JR15002 only	0.345	1.163	0.547***	4.51

*** P < 0.001

4.4 Discussion

4.4.1 Context of study

Analysis of depth-discrete zooplankton samples taken across the Scotia Sea showed *E. triacantha* to be both abundant and to be distributed over a wide latitudinal gradient in both summer and autumn, from the colder waters south of the Southern Antarctic Circumpolar Current Front (SACCF) to the warmer, more productive region of the north Scotia Sea, north of the front. Abundances were greater north of the SACCF in both summer and autumn yet, at all stations, *E. triacantha* displayed a prominent diel vertical migration (DVM) with daytime depths ranging from the 125-250 m depth strata to 825-1000 m, and night time depths from 0-125 m to 825-1000 m, and within which a significant shift of biomass towards the surface at night was observed. This confirms previous observations of the species exhibiting a wide vertical and latitudinal distribution, and a consistent absence of *E. triacantha* in surface waters during the day compared with their presence at night (Baker, 1959). Temperatures experienced by the animals over this DVM spanned up to 4.5 °C in our study, with the most rapid and substantial changes occurring in the region of 50 to 100 m and corresponding to the depth the euphausiids would cross during their upward and downward migrations. This study was therefore justified in investigating the effect of short-term changes in temperature on the respiration rate of *E. triacantha*. The ultimate purpose of this was to determine whether temperature-dependent changes in respiration rate over short timescales could be sufficient to alter carbon export associated with vertical migrations.

4.4.2 Overall response to temperature and size

Overall, when the individual or weight specific respiration of *E. triacantha* (measured as O_2 consumption ind^{-1} h^{-1} or O_2 consumption mg DW^{-1} h^{-1}, respectively) was regressed against temperature, a response of increasing respiration with increasing temperature was observed. The relationship was best described by an exponential curve, and the rate of weight-specific respiration rose with a calculated Q_{10} of 4.97 for the full dataset. The Q_{10} coefficient is a measure often used to describe the sensitivity to temperature of a species' respiration rate, although it has been criticised for only adequately describing the central portion of the relationship (Clarke, 2017) and not characterising variation in rate at the extremes of the range adequately. For this geographical region, a Q_{10} from 1 to 4 is considered within the 'normal' range (Clarke and Peck, 1991). Values outside that may be indicative of some sort of stress (Hirche, 1984), too short an acclimation period (Ivleva, 1973) or indeed whether routine or active metabolism is being measured (Conover, 1978). Despite

this, Q_{10} values >5 have been observed both in intra-specific (e.g. Siefken and Armitage, 1968, Holopainen and Ranta, 1977, Lampert, 1984) and inter-specific (e.g. Alcaraz et al., 2013) studies. In the present study, animals were acclimated to their incubation temperature for at least two hours prior to incubation and a ~30 minute period of adjustment given before the first measurement so as to avoid an undue stress response. However, since the purpose of the experiment was to simulate the short-term response of *E. triacantha* to temperature change as experienced during a typical DVM, this was deemed a sufficient acclimation period. Another feature of the Q_{10} is that it is both inversely related to the temperature range over which it is calculated, and to temperature itself (Clarke, 2017), with lower temperatures and temperature ranges yielding relatively higher values. Considering this, a Q_{10} of 4.97 is a reasonable reflection of the increase in physiological rate exhibited by *E. triacantha* over the short timescale of its migration, although it is also prudent to consider that it may also represent an element of the variability in weight-specific respiration rate observed at a given temperature (Figure 4.10).

Whilst a degree of biological variability is to be expected, especially where individual animals were incubated separately, the respiration rate of an animal is also known to be affected by body size; since a significant correlation was found between length and weight (Figure 4.7), this variability was considered as a function of dry weight (DW). Whilst individual respiration varied significantly with both DW and temperature over the full dataset, weight-specific respiration varied significantly with temperature only, and the effect of size on weight-specific respiration was marginal (Table 4.4). In terms of metabolic theory, this is contrary to what would be expected: a relationship of decreasing weight-specific respiration with increasing body size has been long established for planktonic animals in general (as discussed in Ikeda, 1970) and for euphausiids in particular (Small et al., 1966, Paranjape, 1967, Small and Hebard, 1967). Further, in some of the most influential studies on zooplankton metabolism, Ikeda (1970, 1985), and Ikeda et al. (2001) elaborated on this relationship, showing zooplankton respiration to vary as a function of size and the temperature of habitat, with those two variables alone explaining >90% of the variation in rates. However, the studies of Ikeda (1970, 1985), and Ikeda et al. (2001) incorporated multiple groups of animals spanning four to six orders of magnitude and a temperature range of >30 °C. In contrast, the present study considers a single species, ranging in size within just one order of magnitude (13 to 96 mg) and a temperature range of 4.5 °C. This makes a finding of little significant effect of body size somewhat less surprising since, in narrow body size ranges, the inherent biological variability can effectively mask any relationship (Harris et al., 2000). For the JR15002 experiments, either four or five animals were incubated in the same bottle, and

although efforts were made to minimise the size difference per bottle, one or two bottles contained animals in which the size varied relatively substantially (Figure 4.5). As Lampert (1984) points out, whilst such an approach can be beneficial in terms of reducing the potentially obscuring effect of biological variability, information at the individual level can also be lost. It may therefore be that this muted the effect of size on respiration rate for this experiment, although the extent to which this may be the case cannot be quantified. Since size did not have a significant effect on weight-specific respiration, this did however permit the comparison of weight specific respiration rates across temperature without introducing confounding errors associated with body size (Packard and Boardman, 1999).

4.4.3 Difference in response between years

To further investigate the variability between the data, the two years were also analysed independently (see red and blue data points in Fig 4.10). This revealed a clear relationship between temperature and respiration rate in the second year, yet a somewhat less clear trend in JR304. Applying the same exponential model to the JR15002 data yielded a curve that fell slightly higher to that running through the full dataset but with similar overall coefficients, and producing a Q_{10} of 4.51. On the other hand, the same model applied to the JR304 data produced a much flatter curve and a poor overall fit to the data ($R^2 = 0.032$). Close examination of the JR304 plot suggests that at the lower end of the temperature scale (from ~0 to 2.2 °C), weight-specific respiration rates follow the same pattern as seen in the JR15002 data, increasing from a mean of 0.35 µl O_2 mg DW^{-1} h^{-1} at 0.2 °C to 0.56 µl O_2 mg DW^{-1} h^{-1} at 2.2 °C. However, a cluster of points from ~2.5 to 3.3 °C with lower respiration rates (0.23 to 0.46 µl O_2 mg DW^{-1} h^{-1}) deviates from this trend and flattens out the curve. Whilst certain factors related to different physiological or motile states can likely explain some of the systematic variability in rates at a given temperature (this is also discussed in more detail below), this does not explain the fact that many of the data points obtained in the 2.5 to 3.3 °C temperature range are more comparable to rates obtained between 1.5 and 2 °C. Some light may be shed on this by considering the experimental setup of JR304 and how it differed to JR15002, for which certain modifications were made to provide improved temperature control following some challenges with this during JR304.

The challenges of the first year were two-fold. Firstly, temperature control was provided by a graded incubation tank, with the temperature cooled at one end and rising to a maximum at the other end. In addition, the higher temperature was partially dependent on the ambient temperature of the room. This necessarily created a temperature gradient between the two ends of the tank, however the effect of this on the experiment was minimised by

placing bottles parallel to the ends of the tank and placing solid separators between blocks of experimental bottles. Secondly, due to unavoidable failures of the room thermostat at some points during the cruise, maintaining a stable ambient temperature became difficult. Consequently, this affected the stability of the tank temperature and the cooler was adjusted as described in the methodology to compensate for this. This meant that experiments were carried out at temperatures which ranged between 0.20 °C and 2.20 °C for the lower temperature, T1, and 2.57 °C and 3.35 °C for the higher temperature, T2. This was advantageous in the sense that it increased the range of temperatures that respiration was measured over. However, over the course of individual experiments, T1 varied from as little as 0.04 °C to 0.68 °C and T2 between 0.01 °C and 0.16 °C so it is possible that the measured rates incorporate a degree of error related to the temperature change over time to which the animal had not been acclimated. Similarly, the temperature at which rates are plotted are the mean temperature measured during the incubation, around which the measured variability is as shown in Table 4.1. For the second year, the measurement setup employed separate tanks for the two temperatures, both of which were thermostatically controlled. The tanks were additionally insulated to protect against any influence of ambient temperature. This had the dual benefits of ensuring that the temperature experienced by the animals was not subject to external effects, and also building in redundancy so that, in the event of technical failure of one thermostatic control, the other should not be compromised.

Since the temperature control in JR304 was ultimately reliant on the cooling provided at the cold end of the tank, it was possible for the temperature experienced by *E. triacantha* at the cold end of the tank to have been influenced by the warmer temperatures of the warmer end, but not to have been influenced by colder temperatures. On the other hand, the temperature of the warm end was dependent on the ability of the warm circulator to effectively heat against the colder water propagating from the other end of the tank. The temperature experienced by *E. triacantha* at the warm end therefore had more potential to be lower than that recorded but not higher. It is suggested that the highest rates observed at low temperatures may at most be an artificially high maximum rate for the temperature observed as a physiological response is generated to compensate as the temperature fluctuates slightly above the average temperature. Conversely, the rates observed at the warm end of the tank may be depressed due to the influence of water of a lower temperature. Since this may therefore be reflective of a history of exposure to cooler temperatures than were measured, it probably does not reflect the true aerobic scope of *E.*

triacantha at this temperature and the true rate is more likely to sit somewhere between the slopes running through the full data and the JR15002 data.

In regards to calibration, logistical constraints in the first year meant that oxygen optode sensor spots had not been re-calibrated from the manufacturer's calibration at 20 °C prior to experimentation. For the second year, sensor spots were re-calibrated to 0% and 100% oxygen saturation at temperatures close to the eventual experimental temperature (~4.5 °C). As a result, JR304 data was initially systematically offset from JR15002 data, with JR15002 data being the more reliable. In a study comparing the oxygen data obtained from optodes with water samples analysed with the Winkler method, Uchida et al. (2008) found a similar effect, concluding that the manufacturer's batch calibration was insufficient to achieve high reproducibility of results. Following correction of the JR304 data as described in earlier methods using purpose-built software (Presens GmbH, 2016), data was generally comparable with that of JR15002 in terms of both mean and range of values. Potential calibration error can therefore be eliminated from overall methodological error.

4.4.4 Factors affecting variability in respiration rate

What is common between both datasets is the relatively wide range of respiration rates at a given temperature, with oxygen consumption varying by up to >0.4 µl O_2 mg DW^{-1} h^{-1} at a given temperature, approximately equivalent to the increase in mean oxygen consumption over the experimental temperature range (0.35 µl O_2 mg DW^{-1} h^{-1} at 0.2 °C and 0.70 µl O_2 mg DW^{-1} h^{-1} at 4.7 °C). This variability must be biological since the methodological considerations discussed above were remedied in JR15002 yet the same variation was evident in both years. Beyond size, metabolic rate can also be affected by biological factors such as locomotive activity; feeding (both recent history and general food availability), stage of development, sex or injury; and chemical or physical factors such as pH, oxygen saturation, pressure and light (e.g. Hernández-León and Ikeda, 2005a). In our study, oxygen saturation and pH were never found to be limiting, whilst the effect of pressure is considered to be negligible, especially at low temperatures (Teal and Carey, 1967, Torres and Childress, 1983).

Light may exert an influence on metabolic rate through its control on the circadian rhythm determining many physiological and behavioural processes of animals (e.g. Mortola, 2004), by way of an endogenous clock. Such a circadian rhythm has been found to exist in zooplankton including copepods and euphausiids, and to be linked to fundamental processes such as locomotor activity, diel migrations and, more recently, metabolism (e.g. Aguzzi et al., 2004, Gaten et al., 2008, Teschke et al., 2011, Häfker et al., 2017). In the euphausiid *E. superba*, the highly rhythmic expression of a key clock gene, *cry2*, was found alongside the

similarly rhythmic expression of key metabolic enzymes (Teschke et al., 2011). Such enzymes, involved in aerobic energy metabolism, oscillated over an approximately 9-12 hour time period, and corresponded to oscillations in oxygen consumption over the same timeframe (Teschke et al., 2011), suggesting that oxygen consumption may also be subject to circadian periodicity. Similarly, (Häfker et al., 2017) found evidence of circadian rhythms in core clock genes of the copepod *Calanus finmarchicus*, coinciding with periodicity in DVM and metabolism.

Light was largely controlled for in this study, with the animals kept in the dark throughout, except for when measurements were being taken, and thus all subjected to the same experimental conditions. Furthermore, since all animals used in a given incubation originated from the same net catch, it was assumed that the variability observed in each experiment was individual rather than due to variability in circadian phase between individuals. However, since the timing of individual experiments varied, it is possible that differences in phase of photoperiod may have led to variability in oxygen consumption between experiments, although as discussed by (Teschke et al., 2011), other behavioural rhythms such as locomotor activity may also be related to elevated levels of enzyme expression and associated oxygen consumption. Finally, no obvious effect of injury was observed on any of the animals that were alive at the end of the experiment. With regards to other biological factors, a brief discussion follows.

In a consideration of activity, the distinction between basal, routine and active metabolism is important: basal metabolism represents the minimum level of energy required for maintenance purposes alone; routine metabolism is considered to represent uncontrolled but low levels of motor activity; and active metabolism constitutes maximal activity (Harris et al., 2000). Although it was not possible to fully quantify the effects of activity in the current study, the activity levels of specimens were qualitatively noted at points throughout the experiments and most specimens were found to exhibit a mixture of periods of inactivity interspersed with bouts of active swimming, likely representing a state in between routine and active metabolism. Due to the difficulties in measuring respiration as a function of activity, there is a relative paucity of literature on this subject, although there are a couple of notable exceptions. A study on copepods suggested that temperature did not result in an increased swimming speed and consequently attributed the observed increase in oxygen consumption rate in its entirety to temperature (Hirche, 1987). On the other hand, in a detailed study investigating the effects of temperature, pressure and swimming speeds, Torres and Childress (1983) showed that not only did the respiration rate of the euphausiid *E. pacifica* increase with greater swimming speeds, but that this was further enhanced at

higher temperatures. Given the greater similarities in and control of locomotive physiology between *E. triacantha* and *E. pacifica* compared to copepods, it is possible that values at the higher end of each temperature-specific range represent active metabolism, whereas lower values indicate routine metabolism.

Another important consideration is that of feeding, and the concept of Specific Dynamic Action (SDA) in particular, which represents the additional energy expenditure related to the "ingestion, digestion, absorption and assimilation" of food (Secor, 2009). Peak factorial scopes are typically 2 to 4 times higher than pre-feeding levels (Whiteley et al., 2001) although it is suggested that, in polar ectotherms, a lower peak is compensated for by a longer duration (Peck, 1998). Whilst I am unable to exclude the possibility that some animals had fed more recently than others prior to being caught, the possible effects of post-prandial rises in metabolism were minimised with the experiment setup. The period of time that elapsed between bringing the animals on deck and experiment setup (~2 hours) was likely sufficient for the effects of most recent feeding to subside. In addition, prior to net recovery, animals would have had a period of up to an hour in the net during which feeding, whilst possible, is probably unlikely and it is in fact possible that gut passage would have been expedited as a stress-response. Soon after capture, healthy animals were transferred to separate containers of filtered seawater for inspection where they were thus unable to feed, prior to incubation. Finally, a half hour 'settling' time between incubation and the first oxygen reading, designed to minimise the effect of stress on oxygen uptake measurements, further reduced the possibility of unintended SDA effects. It has been suggested the elevated oxygen consumption associated with SDA is a reflection of the cost of anabolic processes, rather than catabolic processes associated directly with feeding (Kiørboe et al., 1985, Peck, 1998), implying that perhaps there is an extended effect of feeding on metabolism beyond immediate digestion and gut passage. However, since such reports are largely based on studies of benthic animals with characteristically low levels of activity, the same rule may not apply to euphausiids routinely swimming between the meso- and epipelagic. Unfortunately, there is very little extant literature on the effects of SDA in epipelagic crustaceans in general, and euphausiids in particular, although one study by Ikeda and Dixon (1984) concluded that elevated oxygen consumption rates following feeding were the effect of SDA. Whilst they do not calculate the duration of the effect, they do suggest that previous studies on non-feeding krill consequently underestimate the metabolism of wild krill, suggesting the effect to be 1.6 times that of the non-feeding respiration rate.

The respiration rates presented here are based on experiments conducted during late spring. It is important to consider the implications of this to estimates of respiration on a seasonal

scale since, for zooplankton living in high latitude seas in particular, fundamental processes such as metabolism, growth and reproduction of many organisms are closely linked to the spring phytoplankton bloom (Clarke and Peck, 1991). The metabolic rates of epipelagic copepods at high latitudes are known to vary with season (Ikeda et al., 2001) being higher during the phytoplankton bloom than winter. Similarly, the euphausiid *E. superba* is known to cease growth during winter (Siegel, 1987) whilst Meyer et al. (2010) found the metabolism of *E. superba* to be 30-50% lower in autumn-winter compared to late spring. They also found reduced and relatively greater omnivorous feeding, with a greater consumption of lipid reserves in winter. The question is to what extent *E. triacantha* demonstrates a similar seasonal response and associated metabolic slowdown. Siegel (1987) finds *E. triacantha* to display less seasonality in growth than *E. superba*, perhaps also resulting in less variability in metabolic rate. *E. triacantha* is considered to be omnivorous, occupying a higher trophic level than *E. superba* (Stowasser et al., 2012) suggesting that its ecology is not as tightly coupled to phytoplankton production as for more herbivorous species. Ikeda and Kirkwood (1989), considering *E. superba* and *E. crystallorophias* found *E. crystallorophias* to have a higher body carbon content than *E. superba* in winter and to be less affected by low food conditions. Although *E. crystallorophias* have a very different distribution and habitat to *E. triacantha*, they arguably have a more similar feeding ecology in the sense that feeding continues year-round. Since the rates presented here for *E. triacantha* are from spring, if a seasonal difference does exist, these rates likely represent the annual maximal values, although since it exhibits less seasonal variability in growth and is less reliant on phytoplankton as a primary food source, I hypothesise that any seasonal reduction in metabolic rate would be less pronounced in *E. triacantha* compared to *E. superba.*

Lastly, developmental stage or reproductive state can have an effect on oxygen consumption. Higher oxygen consumption has been observed in moulting specimens of *E. pacifica* (Paranjape, 1967) and *E. triacantha* (Ikeda and Mitchell, 1982) whilst gametogenesis requires energy and can also result in increased metabolic rates (Lasker, 1966, Clarke, 1980). No moulting specimens were observed in this study, so it can be concluded that no elevation of oxygen consumption rates occurred as a result of this, although the sizes in this study included both larger sub-adults (17 to 24 mm) and adults (≥24 mm) so some difference in developmental stage is probable. Spawning in *E. triacantha* is thought to occur between October and November (Dzik and Jazdzewski, 1978) so it was considered that any females would have been spent by the time I conducted the experiments. However, the small but nevertheless significant trend of increasing C:N ratio with size (ratio of 3.9 to 4.9, Figure 4.9) shows that some larger animals had greater relative proportions of C than N. Whilst this may

simply be reflective of greater lipid stores of larger animals, it may also indicate the influence of ovarian maturation in larger females. In his seminal work on *E. pacifica,* Lasker (1966) found 9% of assimilated carbon in females to be released as the organic portion of the eggs. Not a great deal of information for the elemental ratios of *E. triacantha* exist so the data presented here represent probably the most comprehensive yet, but comparisons can be made to other well-studied euphausiids. In one study, a high C:N ratio (4.7) was found for a gravid *E. superba* versus ratios of ~4.0 for other *E. superba* in the same study (Ikeda and Bruce, 1986). Marginally lower ratios of 4.0 were also observed for spent *E. crystallorophias* compared to others of the same species who exhibited a ratio of 4.1 to 4.2 (Ikeda and Bruce, 1986). Alternatively, Torres et al. (1994b) found a ratio of 5.0 for *E. superba* in autumn versus 4.2 in winter and, in one of the few examples for *E. triacantha*, a ratio as low as 3.7 during winter although no seasonal comparison was made. In light of the above discussion on seasonality and the fact that *E. triacantha* is assumed to be omnivorous and able to feed year-round, it is perhaps unlikely that it enters a state of quiescence similar to that of *E. superba* during which lipid reserves would be the primary source of energy (Seear et al., 2012). It is hence quite likely that the higher C:N ratios observed here reflect the presence of females. Since in their study of different size ranges of *E. superba*, Ikeda and Mitchell (1982) found the lowest weight-specific respiration rates for gravid krill, it could be hypothesised that values at the lowest extreme of our ranges represent those of females with mature or maturing ovaries.

4.4.5 Overall findings in the context of other studies

In reality it is difficult to separate out biological variability from methodological variability; nevertheless I have shown that *E. triacantha* exhibits an increase in respiration rate with increasing temperature and no obvious evidence of temperature compensation over a short-term migratory timescale. However, to aid the interpretation of the results of this study, it is helpful to place them in the context of respiration rates determined for other species of euphausiid with similar temperature ranges and lifestyles (see Figure 4.11).

Such a comparison shows that the relationship obtained in this study for the dataset as a whole sits on almost an identical slope as rates obtained for *E. crystallorophias* and *Thysanoessa macrura* (Ikeda and Fay, 1981) and *M. norvegica* (Saborowski et al., 2002). These are all omnivorous species and may therefore represent a good analogue for *E. triacantha*. *M. norvegica* is also a known diel migrator and has been found to exhibit elevated metabolic rates during migration (Saborowski et al., 2000). The regression obtained for JR15002 sits slightly higher, yet the rate of 0.36 µl O_2 mg DW^{-1} h^{-1} for *E. triacantha* obtained

by Ikeda and Mitchell (1982) would fall on almost exactly the same slope if it were to be extended and that of Torres et al. (1994a) is only slightly higher.

However, the finding of Donnelly et al. (2004) is markedly different. They calculated a routine respiration rate for *E. triacantha* of 0.72 µl O_2 mg DW^{-1} h^{-1} at 0.5 °C (double that obtained both by Ikeda and Mitchell (1982) and in this study) and a maximum rate of 1.04 µl O_2 mg DW^{-1} h^{-1}. Although the specimens incubated by Donnelly et al. (2004) were obtained from a similar region at a similar time of year, it is unclear how representative the rates are overall since the number of experimental animals was only 2. In contrast, the rates obtained in this study relied on the measurement of 146 animals comprising 76 overall data points which importantly highlighted a degree of variability that is likely to have been missed in a study of only 2 individuals. Even accounting for this, the rate Donnelly et al. (2004) obtained is still greater than the maximum for the same temperature in this study. Notwithstanding this, variability is also a key feature of many of the euphausiids in this comparison: the respiration rate of *E. superba* ranges from 0.38 µl O_2 mg DW^{-1} h^{-1} at -0.5 °C (Ikeda and Fay, 1981) to 0.62 µl O_2 mg DW^{-1} h^{-1} at 0.8 °C (Hirche, 1984) whilst the same authors found a much higher rate of respiration for *M. norvegica* than Saborowski et al. (2002).

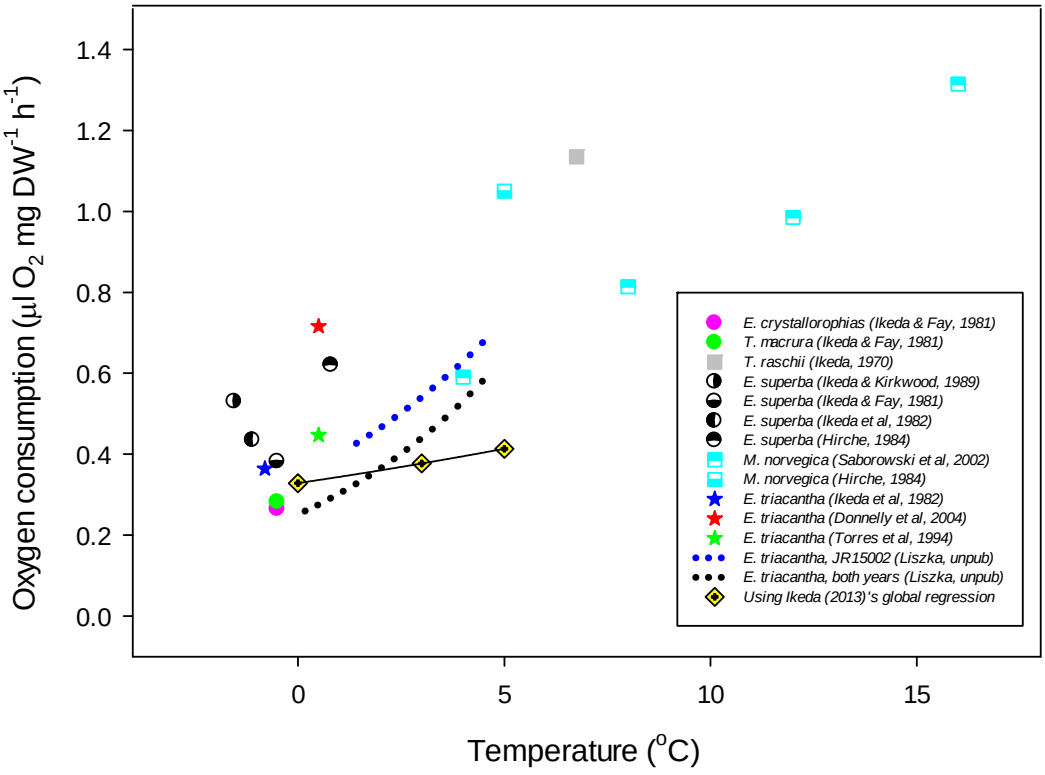

Figure 4.11: Published respiration rates from other authors (converted to µl O_2 mg DW^{-1} h^{-1} when not already published in that unit) for comparative species of euphausiid across temperatures ranging from -1.55 to 16 °C. Most rates correspond to an average of a range of rates provided by the authors so are comparable with the trends obtained in the present study. The points plotted with yellow diamonds are calculated following Ikeda (2013)'s global regression, $lnY = a_0 + a_1 lnX_1 + a_2 X_2 + a_3 lnX_3$, where X_1 was DW (mg), X_2 was temperature (°C) and X_3 was depth (m). Values used were average dry mass for euphausiids in my experiments (34.1 mg DW), temperatures of 0 °C, 3 °C and 5 °C, and a median depth of 370 m.

In addition, a comparison was made with the global-bathymetric model proposed by Ikeda (2013) in which body mass, temperature and depth of occurrence were used in an attempt to describe the global respiration of euphausiids (see Figure 4.11). The curve obtained was flatter, showing a smaller increase in respiration rate with temperature than found here, although the rate at 0 °C fell in between the two regressions and below the other two most comparable rates (Ikeda and Mitchell, 1982, Torres et al., 1994a). It is possible that the global relationship does a relatively good job of enabling comparisons of interspecific variability in mean rates of respiration across temperature of habitat, but does not adequately reflect the full metabolic scope that individual species are capable of, especially at the lowest

temperatures on the spectrum where the curve is flatter than in the middle of the range. As discussed above, variability in size, ontogeny and locomotion may result in intraspecific variability in respiration rate, and animals may also exhibit different responses to short-term temperature change at the molecular level. These results suggest that such intraspecific variation is not reflected in global relationships that span a wide range of species and temperatures. This is also supported with reference to the range of respiration rates of *M. norvegica*, for which a steeper curve, more comparable to that for *E. triacantha* in the present study than the curve based on Ikeda (2013), is obtained. On the other hand, the elevated rates at ~5 °C may also be reflecting the possibility that *E. triacantha* has not evolved to compensate for short-term exposure to the higher end of its range. Despite encountering temperatures as high as this during DVM, the majority of their time is spent at depths between 125-1,000 m with higher temperatures only encountered during ascents to the top ~60 m for feeding. Contrasting Arctic eurytherms with Antarctic stenotherms, Pörtner (2002) suggests that cold-adapted Antarctic species are less efficient during exercise than their Arctic counterparts, leading to a greater metabolic increment with increased effort. It is possible that a similar response is seen in *E. triacantha* when exposed to temperatures above that which they generally experience at depth, and that a short-term loss in metabolic efficiency is minimised by reducing time spent at shallower depths, and offset by food intake. Whilst global relationships have a value in enabling comparisons in physiological response between similar species across a range of habitats, studies of individual species are also needed to determine the potential variability and scope of response at a species-specific level.

4.4.6 Evidence for metabolic cold adaptation?

Over the years, discussion of metabolism in polar ectotherms has often concentrated on the theory of metabolic cold adaptation (MCA). This is a controversial concept which suggests that animals living at colder temperatures have evolved a higher basal metabolism relative to those at warmer temperatures (e.g. Scholander et al., 1953, Wohlschlag, 1960) and that they consequently exhibit a very low Q_{10}. Furthermore, it is posited that this effect is more marked in Antarctic species than Arctic ones due to the greater age of the Antarctic ecosystem relative to the Arctic (Wohlschlag, 1960) although, as for the concept as a whole, there is considerable debate in the academic community as to the veracity of this theory (e.g. Holeton, 1974, Clarke, 1980, Steffensen, 2002). Compared to studies of the benthos, relatively few studies on this subject exist for the zooplankton, part of the problem being that it is near impossible to obtain a true basal metabolic rate due to the problems in controlling for movement of a pelagic animal in a respirometer (Clarke, 1980). In a notable

exception, McWhinnie and Marciniak (1964) provide evidence for low metabolic rates in *E. superba*, with higher oxygen consumption at temperatures of 0 °C than >1.0 °C and lower Q_{10} values over a low-temperature range than a species of decapod obtained from sub-Antarctic waters. However, the results plotted in Figure 4.11 also show considerable variability in rate close to 0 °C, making it difficult to conclude whether this is truly an example of MCA or simply due to other variability, whether biological or methodological. In this study, respiration rates at the lower temperatures are in close agreement with those of Ikeda and Mitchell (1982), Torres et al. (1994a) and the lower value obtained with Ikeda (2013)'s global relationship. In addition, rates subsequently rise relatively substantially with temperature with a Q_{10} of >4. In light of this, based on this study there is currently no evidence in support of MCA in *E. triacantha*. This is in agreement with the body of literature that suggests that elevated metabolic rates at low temperatures are more likely to be an artefact produced by the difficulty in obtaining true basal metabolic rates than a true physiological phenomenon (Clarke, 1980, Hirche, 1984). Nevertheless, it is important to acknowledge the limitations of drawing conclusions in relation to temperature compensation from integrated physiological parameters rather than molecular level responses (Clarke, 1991) and that such efforts may also help to reveal some of the intraspecific variability in *E. triacantha*'s metabolic response to temperature.

4.4.7 Summary and implications

- Oxygen optodes offer a convenient and flexible way to obtain repeatable and reproducible results. However, their accuracy depends on sensor spots being well calibrated to the experimental conditions and a high degree of temperature precision.
- Respiration as a function of temperature yielded a Q_{10} of 4.50 to 4.97, a likely reflection of short-term response to temperature across the range of temperatures encountered over their DVM.
- This showed greater interspecific variation than predicted from global relationships of body size and temperature, suggesting that respiratory flux could be greater for diel migrants than is currently accounted for in models
- As this is a study considering the short-term acclimation to temperature, care should be taken when considering this result in the context of a longer-term response such as responses or adaptations to climate change.
- Despite *E. triacantha* being found in environments with wider ranging temperatures than the ~5 °C range they were exposed to in this study, they have not evolved a

mechanism to compensate for the short-term exposure to the varying temperatures encountered during their migration.

- Variability of up to 0.4 µl O_2 mg DW^{-1} h^{-1} was observed at a given temperature, much of which is accounted for by biological variability.
- No evidence in support of MCA was observed in this study, with low respiration rates at low temperatures and high Q_{10} values.

Chapter 5: Modelling the active carbon flux from the sub-Antarctic krill, *Euphausia triacantha*, in the Atlantic sector of the Southern Ocean

5.1 Introduction

Total global C export is estimated to be between 5 and 20 Gt C y^{-1} (Eppley and Peterson, 1979, Lutz et al., 2007). The Southern Ocean (SO), as one of the world's largest carbon sinks, is responsible for the uptake of up to ~40% anthropogenic carbon (Mikaloff Fletcher et al., 2006, Khatiwala et al., 2009) and carbon export from the mixed layer in the SO is estimated at 1.4 Gt C y^{-1} (Schlitzer, 2002). This is driven largely by the export and sequestration of organic carbon particles, synthesised in the euphotic zone and transported to deeper depths, through the passive sinking of phytoplankton, faecal pellets (faecal pellets) and aggregates and the downward mixing of dissolved organic carbon (DOC).

In addition to passive fluxes, it has long been thought that active flux, driven by the movements of vertically migrating zooplankton and nekton, have the potential to enhance estimated export of carbon by considerable amounts (Angel, 1986) as animals that consume carbon near the surface migrate back across the thermocline after feeding. Longhurst (1990) estimated that the respiration of diel migrants could enhance estimates of C flux between 50° N and 50° S by 5 to 20% of sinking organic carbon flux whilst Steinberg et al. (2000) found that the inclusion of DOC from migrators enhancing vertical fluxes ever further. Others have discussed the role that faecal pellets play as vectors of POC flux to depth (Urrère and Knauer, 1981, Wallace et al., 2013) packaging phytoplankton into heavier, faster sinking particles, and migratory zooplankton may expedite their transport to depth, an idea that has been comprehensively reviewed by Turner (2002). In the Southern Ocean, DVM is considered a likely explanation for fresh faecal pellets found in deep sediment traps at a highly productive site in the Scotia Sea (Manno et al., 2015) and for the change in morphology of faecal pellet with depth (Belcher et al., 2017a).

Resolving the quantity of carbon that is exported to the deep sea, and the role of diel migrants in this process, may help to close the gap between estimates of organic carbon production at the surface, and the heterotrophic demand of organisms in the deeper ocean (Burd et al., 2010, Giering et al., 2014). This in turn will produce better models of the ocean-atmosphere system and how it may respond to future changes in climate. This is particularly true for the SO due to its major role in the uptake of atmospheric CO_2 and in modulating global climate.

However, although widespread, vertical migration is a complex behaviour and the debate around some of the proximate and ultimate drivers of migration is discussed comprehensively by Pearre (2003). These include whether or not (or to what extent) zooplankters migrate in synchrony (Pearre, 1979b), the role that hunger and satiation play in driving migrations (e.g. Pearre, 1979a, Angel, 1986, Tarling and Johnson, 2006), and whether that can override what many believe to be the principal driver of migration, that of light. In addition to these factors, diel vertical migration (DVM) takes place within an abiotic environment, with temperature, seasonal stratification and light conditions varying over the course of the year. Any estimates of active flux from DVM must therefore be made in the context of these additional variables. A recent review that suggests the role of faecal pellets in export to the deep ocean to be lower than previously thought (Turner, 2015) further emphasises the need to better understand the relative contributions of respiratory and egestory C flux from diel migrators.

5.1.1 Purpose of the current study

To address this for the Southern Ocean, I present a model that calculates the relative contributions to active carbon flux from respiration (C_R) and faecal pellet flux (C_E) of a prominent diel vertical migrating species, the euphausiid, *Euphausia triacantha*. The model calculates estimates for active flux over latitude and time of year, and investigates the factors that most affect changes to respiratory and egestory flux. *E. triacantha* is a large, predominantly sub-Antarctic species of euphausiid (Mauchline and Fisher, 1969a, Kirkwood, 1982) that can be locally highly abundant (Piatkowski et al., 1994, Pakhomov and McQuaid, 1996) and thus can be an important contributor to the zooplankton community biomass. The species is known to undergo a substantial vertical migration between the surface layers at night to depths that may reach below 500 m during the day (Baker, 1959). The goals of this study are to understand the potential for DVM to enhance estimated fluxes out of the mixed layer (ML) and assess where future efforts should be focused to better constrain estimates of flux from diel migrators.

5.2 Materials and methods

5.2.1 Model construction

To investigate the role of vertical migration in active carbon flux (C flux) from *E. triacantha,* an individual-based model was constructed. The model, 'BEST', simulated C flux in the Atlantic sector of the Southern Ocean as a function of environmental and hydrographic conditions, and the physiology, feeding and migratory behaviour of the euphausiids. The model calculated total daily respiratory carbon flux (C_R), total daily egestory carbon flux (C_E)

and the sum of these, total daily carbon flux (C_{TOT}), from *E. triacantha* within its south Atlantic distribution. The latitudinal bounds of this distribution were taken as 50° S to 65° S, and longitudinal bounds were 10° E to 100° W, based on historical distributions of *E. triacantha* obtained from the Discovery Investigations of the 1920s and 1930s (Mackey et al., 2012). Seasonal variation in flux was assessed by calculating monthly averages of flux from January through to December. This allowed spatial and seasonal variation in magnitude of, and processes driving, flux to be considered.

For the purposes of this model, C flux was defined as C produced below the mixed layer (ML). This incorporates the assumption that carbon respired or egested below the ML originated in the ML. The model was constructed for one average-sized individual at each latitude and scaled up to the abundance of *E. triacantha* within each degree of latitude within the geographic bounds of the model. A mean size of 34.2 mg dry weight (DW) was calculated from 159 individuals measured and weighed for Chapter 4.

The model (see schematic in Figure 5.1) was constructed to (i) calculate C_R as a function of proximate water temperature; (ii) allow an individual to switch between herbivorous and carnivorous feeding in response to the concentration of surface chl-*a*; (iii) simulate foray-style migration, whereby a euphausiid feeds until the gut is filled, sinks whilst egesting, before repeating the cycle; and (iv) assuming that 100% of the population migrates each day. These elements are further described below. Sensitivity analyses were performed to investigate the influence of different scenarios and model assumptions on estimates of C flux.

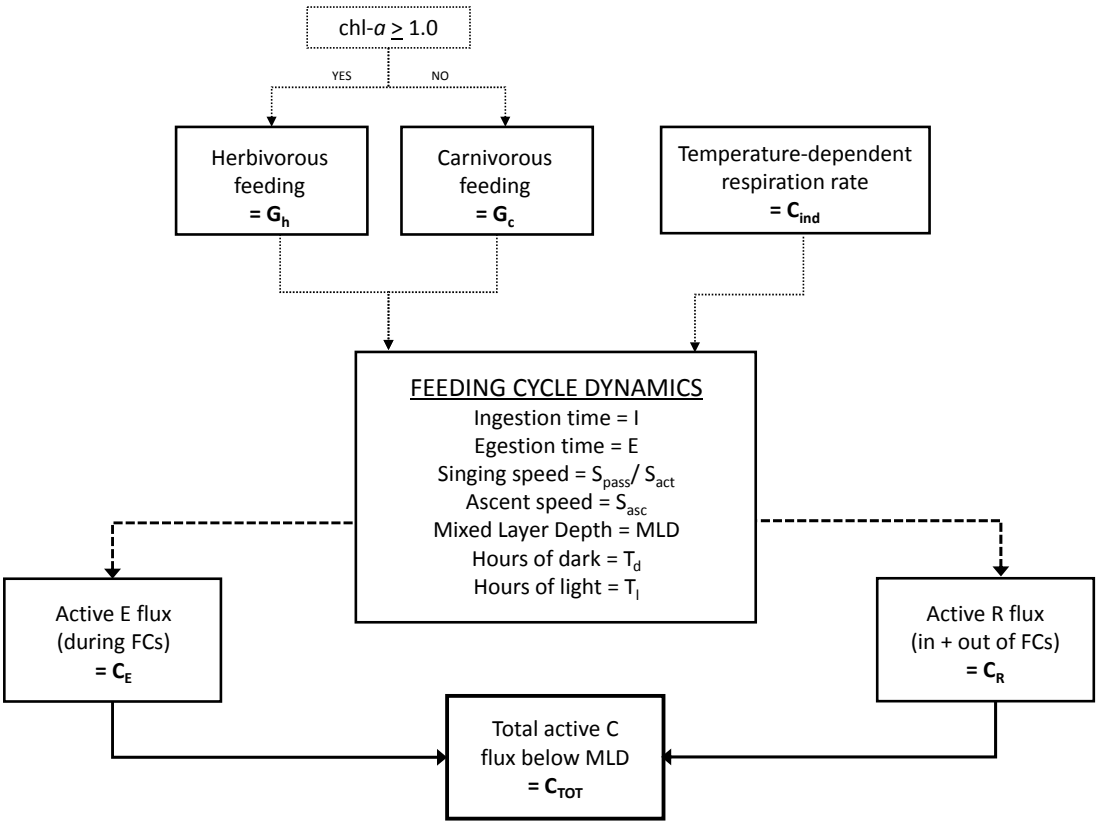

Figure 5.1: Schematic illustrating how the model was constructed, showing key inputs, variables and outputs. All terms are described in Table 5.1

5.2.2 Model inputs and assumptions

Descriptions of the variables and parameters used to initialise the model are given in Table 5.1.

Table 5.1: Table of all the terms used in the construction and description of the model. All terms are further explained in the subsequent text and equations therein.

Parameter	Description	Unit
T*d*	Hours of darkness	Hours
T*l*	Hours of light	Hours
D	Time dark, sunset + 30 mins	Mins
L	Time light, sunrise - 30 mins	Mins
MLD	Mixed Layer Depth	M
MLD_D	Time individual reaches MLD after final descent	mins
MLD_A	Time individual reaches MLD on first ascent	mins
S_{asc}	Ascent speed	m min^{-1}
S_{pass}	Passive sinking speed	m min^{-1}
S_{act}	Active sinking speed	m min^{-1}
G_{chl}	chl-*a* (herbivory) in a full gut	µg
G_h	C (herbivory) in a full gut	mg C
G_c	C (carnivory) in a full gut	mg C
C_I	Copepod ingestion rate	mg C h^{-1}
GER	Gut evacuation rate, *k*	
D_{max}	Maximum depth reached with passive sinking during FC	m
I	Ingestion time	mins
E	Egestion time	mins
A	Time taken to ascend from Dmax	mins
E_R	Egestion time below the MLD spent respiring	mins
A_R	Re-ascent time below the MLD spent respiring	mins
FC	Feeding cycle	
FC_{full}	Number of full feeding cycles	
FC_{part}	Duration of partially complete feeding cycle	Mins
G_{pass}	C egested during passive sinking	mg C
G_{act}	C egested during active sinking	mg C
$C(FC_{full})$	C produced from a complete FC	mg C
$C(FC_{part})$	C produced from a partially completed FC	mg C
Regression 1	Regression obtained from full data, Chapter 4	see Table_coefficients
Regression 2	Regression obtained from JR15002 data, Chapter 4	see Table_coefficients
C_{DW}	Respiratory carbon produced per unit weight	mg C mg DW^{-1} h^{-1}
$C_{ind,day}$	Respiratory carbon produced per individual during day	mg C ind^{-1} min^{-1}
$C_{ind,night}$	Respiratory carbon produced per individual during FCs	mg C ind^{-1} min^{-1}
$C_{R,\ day}$	Respiratory C produced outside of feeding cycles	mg C
$C_{R,\ night}$	Respiratory C produced during feeding cycles	mg C
C_E	Active egestory flux	variable
C_R	Active respiratory flux	variable
C_{TOT}	Total active carbon flux	variable

5.2.2.1 Light

Since light is considered to be a key factor influencing DVM (Forward, 1988, van Haren and Compton, 2013), this was the overriding parameter determining the onset, duration and termination of migration, and hence the length of the feeding period. Upward migration was initiated at the time of sunset and downward migration at the time of sunrise, both of which varied with latitude and time of year. This also determined the duration of feeding time.

Sunrise and sunset times were calculated for every day of the year using the sunrise.set function in the StreamMetabolism package in R for all latitudes from 50° S to 65° S inclusive, and averaged to give a monthly mean for each degree of latitude. Hours of darkness and light were then calculated using Equations 5.1 and 5.2.

$$\mathrm{T}d = \frac{(1440 - D) + L}{60} \qquad \text{Equation 5.1}$$

$$\mathrm{T}l = \frac{D - L}{60} \qquad \text{Equation 5.2}$$

where $\mathrm{T}d$ is hours of darkness, $\mathrm{T}l$ is hours of light, D is time of final darkness (sunset + 30) and L is time of first light (sunrise – 30). 1440 represents the number of minutes in a day and dividing by 60 converted times to hours.

To account for the natural light provided during the twilight period, it was assumed that the response of migrating individuals was to reach their shallowest depth 30 minutes after sunset (D) and to begin their descent 30 minutes prior to sunrise (L). C_E is then calculated as a function of *D*, *L* and MLD, as well as S_{asc}, S_{pass} and S_{act}.

5.2.2.2 Chlorophyll-*a*

E. triacantha is thought to be an omnivorous species (Bernard and Froneman, 2006) and, as such, is able to exploit both herbivorous and carnivorous food sources. To reflect this, the model allowed euphausiids to switch between herbivory and carnivory depending on how favourable environmental conditions were for herbivorous feeding. Above a certain chl-*a* threshold (set at 1.0 µg l^{-1} for the main model run), the individual would select herbivory. Below this threshold, it would switch to carnivory and eat copepods. A key variable for determining feeding preference and duration was thus surface chlorophyll (chl-*a*). Empirically determined chl-*a* (µg l^{-1}) values were taken from Korb et al. (2012) for four groups of stations in the Scotia Sea that clustered together based on phytoplankton assemblages and these were applied to the corresponding latitudes of the model. Korb et al. (2012) station groupings related approximately to latitudes: north-west of South Georgia (zone 1, 50-53° S); south-west of South Georgia to the SACCF (zone 2, 54-55° S); the region between the SACCF and the Southern Boundary (SB) (zone 3, 56-58° S); and south of the SB (zone 4, 60-

65° S) (see Table 5.2). Values were obtained for spring, summer and autumn, whilst winter values were estimated at 0.1 µg l^{-1} for all latitudes as suggested by Park et al. (2010).

Spring included the months of September, October and November; summer, December, January and February; autumn, March, April and May; and winter, June, July and August.

Table 5.2: Table of chl-*a* (µg l^{-1}) values assigned to the model based on latitudinal zones of productivity. Data were calculated as described above, based on Korb et al. (2012) and Park et al. (2010).

Zone	lat	Jan	Feb	Mar	Apr	May	Jun	Jul	Aug	Sep	Oct	Nov	Dec
1	**-50**	3.9	3.9	1.6	1.6	1.6	0.1	0.1	0.1	1.4	1.4	1.4	3.9
1	**-51**	3.9	3.9	1.6	1.6	1.6	0.1	0.1	0.1	1.4	1.4	1.4	3.9
1	**-52**	3.9	3.9	1.6	1.6	1.6	0.1	0.1	0.1	1.4	1.4	1.4	3.9
1	**-53**	3.9	3.9	1.6	1.6	1.6	0.1	0.1	0.1	1.4	1.4	1.4	3.9
2	**-54**	1.6	1.6	0.4	0.4	0.4	0.1	0.1	0.1	0.3	0.3	0.3	1.6
2	**-55**	1.6	1.6	0.4	0.4	0.4	0.1	0.1	0.1	0.3	0.3	0.3	1.6
3	**-56**	0.4	0.4	0.8	0.8	0.8	0.1	0.1	0.1	3.2	3.2	3.2	1.6
3	**-57**	0.4	0.4	0.8	0.8	0.8	0.1	0.1	0.1	3.2	3.2	3.2	0.4
3	**-58**	0.4	0.4	0.8	0.8	0.8	0.1	0.1	0.1	3.2	3.2	3.2	0.4
4	**-59**	1.6	1.6	1.5	1.5	1.5	0.1	0.1	0.1	0.6	0.6	0.6	1.6
4	**-60**	1.6	1.6	1.5	1.5	1.5	0.1	0.1	0.1	0.6	0.6	0.6	1.6
4	**-61**	1.6	1.6	1.5	1.5	1.5	0.1	0.1	0.1	0.6	0.6	0.6	1.6
4	**-62**	1.6	1.6	1.5	1.5	1.5	0.1	0.1	0.1	0.6	0.6	0.6	1.6
4	**-63**	1.6	1.6	1.5	1.5	1.5	0.1	0.1	0.1	0.6	0.6	0.6	1.6
4	**-64**	1.6	1.6	1.5	1.5	1.5	0.1	0.1	0.1	0.6	0.6	0.6	1.6
4	**-65**	1.6	1.6	1.5	1.5	1.5	0.1	0.1	0.1	0.6	0.6	0.6	1.6

5.2.2.3 Temperature

Since the respiration rate of *E. triacantha* is known to be a function of temperature (see Chapter 4), water column temperature was a key variable determining the production of respiratory carbon (C_R). Temperature data were put into the model using the same zones as for chl-*a*. Where possible, data were obtained from full depth CTD (conductivity, temperature and depth) casts deployed in representative locations and seasons. This included data for spring, summer and autumn from RRS James Clark Ross cruises JR161, JR177 and JR200 respectively, for latitudes in zones 1 (52° S), 2 (55° S) and 4 (60° S). Data for

zone 3 were interpolated from zone 2 and 4 data. In the absence of *in situ* measurements for winter, winter temperatures were assumed to be the same as spring: spring exhibited the coldest temperature profiles of the three seasons (Figure 5.2), accordingly providing a conservative estimate of respiration rate during winter.

5.2.2.4 Mixed Layer Depth (MLD)

C flux was also directly related to the MLD which varies both temporally and spatially. This was calculated from NOAA's Monthly Isopycnal & Mixed-layer Ocean Climatology (MIMOC) (https://www.pmel.noaa.gov/mimoc/) using their optimal interpolated mixed-layer monthly MIMOC product (Schmidtko et al., 2013). Data were averaged per degree of latitude and month.

5.2.2.5 Feeding dynamics

DVM has traditionally been thought of as an upward migration of animals to the surface at dusk, feeding in the surface layers throughout the night, followed by a dawn descent. This view is increasingly being challenged and a foray style of DVM is gaining greater recognition (Pearre, 2003), whereby zooplankters feed until satiated, slowly sink whilst egesting the contents of their gut, re-ascend and repeat the cycle until dawn. To simulate this in the model, a number of parameters were required and obtained from literature sources: ingestion time (I), egestion time (E), ascent speed (S_{asc}), passive (egestion) sinking speed (S_{pass}) and active (final) sinking descent speed (S_{act}).

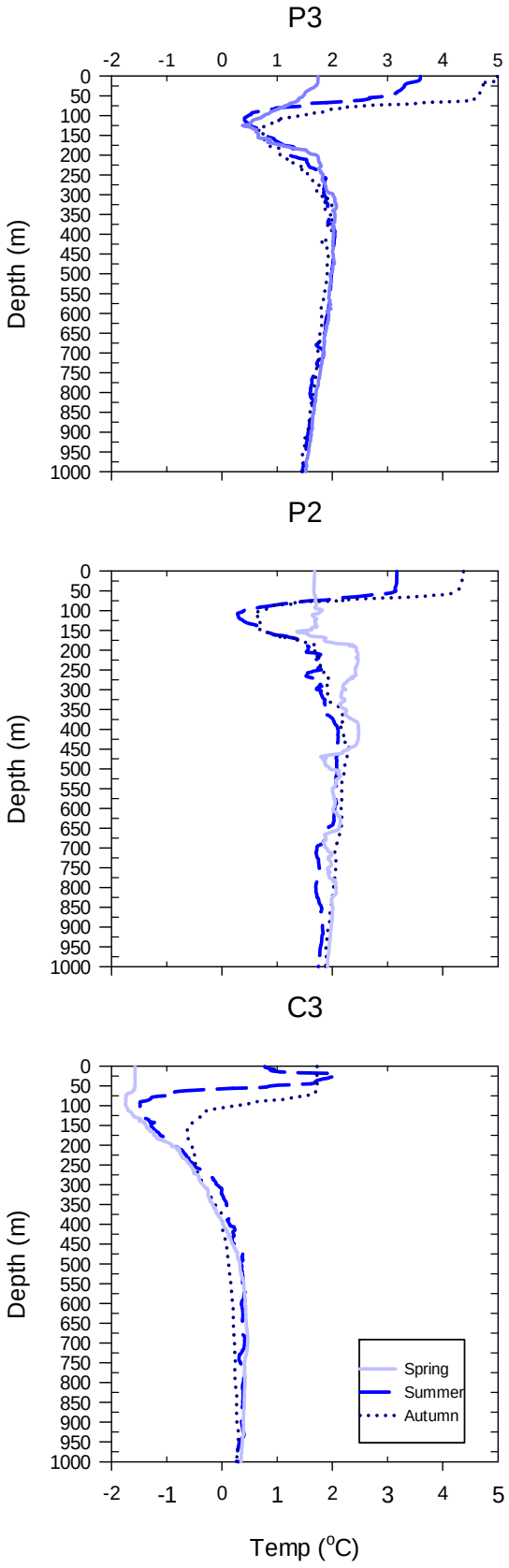

Figure 5.2: Temperature profiles for the vertical distribution of *E. triacantha* at representative latitudes (P3 = 52° S, P2 = 55° S and C3 = 59° S) of the Atlantic sector of the Southern Ocean deployed during JR161, JR177 and JR200.

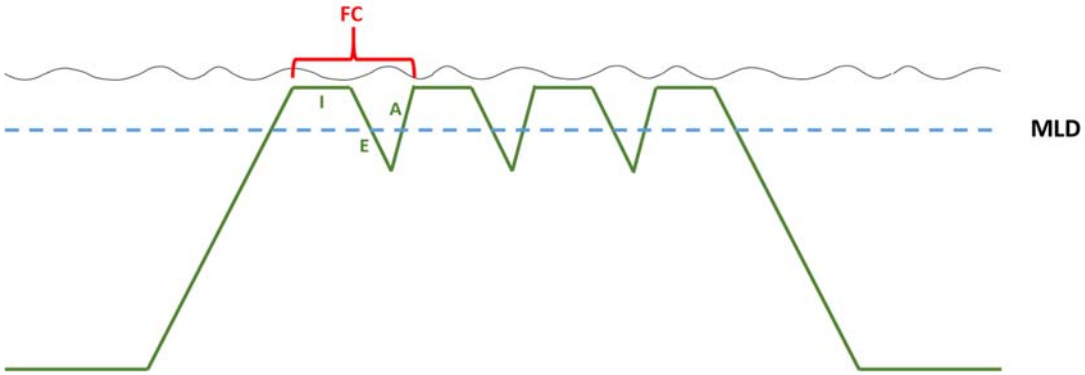

Figure 5.3: Schematic illustrating foray migration and the definition of feeding cycles. FC defines the complete feeding cycle, comprised of Ingestion time (I), Egestion time (E) and Ascent time (A). C_E was comprised of C egested below the MLD only during E. $C_{R,night}$ was comprised of C respired below the MLD during E and A. $C_{R,day}$ was comprised of C respired below the MLD during the non-feeding parts of the day

I (mins) was a function of feeding mode i.e. herbivory vs carnivory, determined as a function of surface chl-*a*, and is described in Equations 5.3 and 5.4 below.

$$I(herbivory) = \left(\frac{G_{chl}}{0.34 \times [chl-a]}\right) \times 60 \qquad \text{Equation 5.3}$$

where G_{chl} is estimated mean chl-*a* in a full gut, from Pakhomov and Froneman (2004a) for summer, and 0.34 is the chl-*a* filtering rate (l h^{-1}), using the mean filtering rate determined for *M. norvegica* by McClatchie (1985), and multiplied by 60 to convert from the filtering rate in hours.

$$I(carnivory) = \left(\frac{G_c}{C_I}\right) \times 60 \qquad \text{Equation 5.4}$$

where G_c is carbon in a full gut from carnivory (mg C), calculated as being 5% of the C body weight of the euphausiid (Båmstedt and Karlson, 1998) and C_I is copepod carbon ingestion rate (mg C h^{-1}).

G_{chl} was then converted into G_h (carbon in a full gut consumed through herbivory) first by multiplying by 1.5 to account for pigment destruction and then by applying a C:chl-a ratio of 50:1 as described by Atkinson et al. (1996).

E (mins) was determined from the gut evacuation rate (GER, *k*). GER was calculated as an average of the GER constants determined by Pakhomov and Froneman (2004a) and Bernard and Froneman (2006) for *E. triacantha*. The maximum depth reached during *E* (D_{max}) was determined from the passive sinking speed, S_{pass}, and re-ascent time (mins, *A*) was determined from the ascent speed, S_{asc}. Both speeds were taken from Tarling et al. (2001) which calculated ascent and sinking speed of *Meganyctiphanes norvegica*, which was used as an analogue in the absence of corresponding data for *E. triacantha*: both are important components of their respective ecosystems, perform substantial diel vertical migrations, and are euphausiids of similar size and ecology.

A full feeding cycle (FC_{full}) was calculated as $I + E + A$ (Figure 5.3). C_E would then be determined by i) whether herbivory or carnivory had been selected; and ii) the proportion of C egested after assimilation, respiration and growth had been accounted for. For this model, it was assumed that 30% of ingested carbon was egested (Lasker, 1966). Final C_E could then be calculated from C egested below the MLD during full and partially completed feeding cycles, according to Equation 5.5.

$$C_E = C(FC_{full} + FC_{part}) \qquad \text{Equation 5.5}$$

C_E from full feeding cycles, $C(FC_{full})$, was defined as:

$$\text{if } D_{max} < MLD, C\left(FC_{full}\right) = 0$$

$$\text{if } D_{max} > MLD, C\left(FC_{full}\right) = FC_{full} * G_{pass}$$

where FC_{full} defined the number of complete feeding cycles and G_P defined the C from a full gut egested below MLD during *passive* sinking.

C_E from an incomplete feeding cycle, $C(FC_{part})$, depended on the amount (in minutes) of a feeding cycle (FC_{part}) remaining at the end of the night, with dawn also stimulating a switch to the active descent rate (S_{act}) (thus a potential increase in the proportion of descent time spent below the MLD). This was therefore further defined as:

$$\text{if } FC_{part} < I, C\left(FC_{part}\right) = (FC_{part}/I) * G_{act}$$

$$\text{if } FC_{part} > I \text{ and } > I + E, C\left(FC_{part}\right) = G_{pass}$$

$$\text{if } FC_{part} > I \text{ and if } < I + E, C\left(FC_{part}\right) = (G_{act} + G_{pass})/2$$

where G_A defined the C from a full gut egested below MLD during *active* sinking.

5.2.2.6 Respiratory carbon function

Respiratory carbon (C_R) was calculated as a function of water temperature (T, °C), MLD (m) and feeding cycle dynamics. All C_R produced below the MLD was assumed to contribute to C flux.

Firstly, oxygen consumption (*R*, µl O_2 mg DW^{-1} h^{-1}) was calculated using Regression 1 which defines the relationship between respiration rate and temperature obtained in Chapter 4 for the full dataset (see Chapter 4, Figure 4.10 and Table 4.5) following Equation 5.6.

$$R\ (\mu l\ O_2\ mgDW^{-1}h^{-1}) = a \times b^T \qquad \text{Equation 5.6}$$

where *T* is temperature, *a* is the regression intercept, 0.29 and *b* is the slope, 1.174.

This was converted into units of carbon (*C*, mg C mg DW^{-1} h^{-1}) following Equation 5.7.

$$C_{DW} = \left(\frac{R}{1000}\right) \times RQ \times \left(\frac{12}{22.4}\right) \qquad \text{Equation 5.7}$$

Where the RQ (respiratory quotient) was calculated as 0.91 (average RQ for lipid, protein and carbohydrate metabolism based on the body composition of an omnivorous euphausiid, (Bämstedt, 1976)) and (12/22.4) represents the amount of C produced from every mole of CO_2.

This was finally converted into C produced per individual per minute (C_{ind}) (Equation 5.8).

$$C_{ind} = \frac{(C_{DW} \times 34.2\ mg)}{60} \qquad \text{Equation 5.8}$$

where 34.2 mg is the weight of an average *E. triacantha* as explained above and the denominator converts production into minutes.

Final C_R was calculated following equation 5.9.

$$C_R = C_{R,day} + C_{R,night} \qquad \text{Equation 5.9}$$

where $C_{R,day}$ is the respiratory C produced below the MLD during daylight hours, outside of feeding cycles, and $C_{R,night}$ is the respiratory C produced during the portions of feeding cycles that occurred below the MLD during the night (see Figure 5.3).

The wide daytime distribution of *E. triacantha* (see Chapter 4, Figure 4.6) suggests a continuous movement of euphausiids throughout the water column. To reflect this in the model, C_R during daylight hours was accordingly calculated to be a function of average temperature between the MLD and 1000 m, and the time spent below the MLD during the day, according to Equation 5.10.

$$C_{R,day} = C_{ind,day} \times (1440 - (MLD_D - MLD_A)) \quad \text{Equation 5.10}$$

where $C_{ind,day}$ is the C produced per individual per minute at daytime depths, 1440 is the number of minutes in a day, and MLD_D - MLD_A is the difference in time between when an individual arrives at the MLD after the final descent, and the time it arrives at the MLD on first ascent respectively. The difference between the two is the time spent feeding.

Under the foray feeding scenario, C_R during the night was additionally dependent on feeding cycle dynamics as described above, with time spent below the MLD during sinking and ascent contributing to C_R. It was thus a function of the average temperature between the MLD and D_{max}, and the time spent between these depths during *E* and *A* (egestion and re-ascent time respectively), according to Equation 5.11. When the MLD was deeper than D_{max}, C_R defaulted to zero.

$$C_{R,night} = \left(C_{ind,night} \times (E_R + A_R)\right) \times FC_{full} \quad \text{Equation 5.11}$$

where $C_{ind,night}$ is the C produced per individual per minute at night time depths, and E_R and A_R are the minutes of E and A spent below MLD, respectively.

5.2.3 Scaling the model up

Once the model was run for an average individual, it was scaled up to the area of the Atlantic sector of the Southern Ocean by calculating the distribution area of *E. triacantha* within the south Atlantic. To do this, the most comprehensive estimate of *E. triacantha* abundance was used based on data from 615 stations sampled during the Discovery expeditions of the 1920s and 1930s and analysed by Mackey et al. (2012). Sampling was conducted with an N100 net, in the top 0-70 m and at all times of day between austral spring and late summer (November to March). The mesh size of the N100 net was 4 mm; marginally finer than that used in the RMT8 nets currently used to collect macrozooplankton (4.5 mm). This may mean that macrozooplankton abundances were slightly reduced due to greater water displacement by the finer mesh and this is therefore a conservative estimate.

Abundance of *E. triacantha* per degree of latitude in the south Atlantic sector was estimated by:

1. Averaging the density of *E. triacantha* (individuals m^{-2}) in each 2 degree latitude x 5 degree longitude grid square (Mackey et al., 2012) (supp. info.)
2. Calculating the area (m^2) of 1 x 2.5 degree grid cells in which *E. triacantha* were encountered

3. Calculating the number of 1 x 2.5 degree grid cells in which *E. triacantha* were encountered (based on the original 2 x 5 degree grid cells) for each degree of latitude
4. Multiplying the number of 1 x 2.5 degree grid cells (3) by the area of grid cell (2) for each degree of latitude, giving area of *E. triacantha* distribution per degree of latitude
5. Multiplying mean density of *E. triacantha* grid cell^{-1} (1) by total area of distribution per degree of latitude (4) of grid cell^{-1}, giving total abundance per degree of latitude

5.2.4 Sensitivity analyses

A number of sensitivity analyses (summarised in Table 5.3) were carried out to investigate how changes to certain assumptions or behaviours in the main ('BEST') model alter the magnitude and distribution of C flux. Only one parameter was changed per run and all other settings remained the same. The results of the sensitivity analyses were ranked in terms of percentage difference to total C flux, relative to the main model run. They were also compared in terms of percentage difference to C_R and C_E.

Table 5.3: Description of all the model runs that were carried out

Scenario	Description
BEST	Main model
JR15002	Respiration flux calculated with Regression 2
NO FORAYS	Animals remain feeding in the surface throughout the night
100% HERB	All individuals feed herbivorously
100% CARN	All individuals feed carnivorously
70% MIGRATING	70% population migrates each day
50% MIGRATING	50% population migrates each day
30% MIGRATING	30% population migrates each day
FULL GUT 75%	Individuals feed to 75% gut fullness
FULL GUT 50%	Individuals feed to 50% gut fullness
FULL GUT 25%	Individuals feed to 25% gut fullness
CHL-A 0.5	chl-*a* threshold is 0.5 µg l^{-1}
CHL-A 2.0	chl-*a* threshold is 2.0 µg l^{-1}

5.2.4.1 Respiration regression

In the main model, the regression used to calculate C_R as a function of temperature was Regression 1, determined in Chapter 4 for the full dataset. To evaluate the difference made

to C flux with the regression obtained for the second year's data (JR15002) alone, C_R was also calculated with Regression 2, reproduced in Table 5.4.

Table 5.4: Table of coefficients to explain the relationship between O_2 consumption and temperature for *E. triacantha*, reproduced from Chapter 4

Oxygen consumption rate (µl O_2)	**a**	**b**	**R^2**
Regression 1: Full dataset	0.290	1.174	0.310***
Regression 2: JR15002 only	0.345	1.163	0.547***

5.2.4.2 Feeding behaviour

In the main model, the feeding ecology of *E. triacantha* was simulated by the individual selecting herbivory above a certain chl-*a* threshold, and carnivory below this threshold. Two sensitivity analyses were run in which the animals fed either (i) 100% herbivorously or (ii) 100% carnivorously. This had the effect of changing both the ingestion time (I) and the total amount of C in a full gut.

5.2.4.3 Chl-a threshold

To instigate switching between herbivory and carnivory, a concentration of 1 µg chl-*a* l^{-1} was set as the threshold above which euphausiids would filter chl-*a* and below which they would feed on copepods. To investigate the effect of this threshold being set at different concentrations, it was altered in two simulations to (i) 0.5 µg l^{-1} and (ii) 2.0 µg l^{-1}. These were selected as they represent approximate lower and upper chl-*a* levels for late autumn to early spring, and for summer respectively.

5.2.4.4 Migration behaviour

To consider how a change to migratory behaviour could alter C flux, a simulation was run in which the euphausiids did not foray throughout the night. Instead, after arriving at the surface they remained there until dawn before actively swimming downwards (S_{act}) and evacuating the contents of a full gut only once.

5.2.4.5 Proportion of population migrating

Finally, in the main model simulation, the C flux pertaining to one individual was scaled up to 100% of the population, thus assuming that 100% of the population were engaged in a simultaneous migration each day. To investigate the effect on C flux from only parts of the population migrating, whilst the rest remained at depth, three further simulations were run in which (i) 70%, (ii) 50% and (iii) 30% of the population migrated each day. The remainder of the population that did not migrate but remained at depth contributed to active flux from

respiration only, under the assumption that the portion migrating is comprised of different individuals each day and thus the carbon respired was obtained from surface feeding during the previous day.

5.3 Results

5.3.1 Mixed layer depths

Mixed layer depths (MLDs) (Figure 5.4) varied from an average of 46 m across all latitudes in January to an average of 142 m in August. The shallowest MLDs were in the highest latitudes (31 m in January to 107 m in August at 65° S), deepening to a maximum at 53° S (55 m in January to 168 m in August), followed by a slight shoaling at the very lowest latitudes (51 m to 153 m from January to August at 50° S). The MLD was deepest at all latitudes during the winter and early spring (June to September) and shallowest in summer and early autumn (December to March).

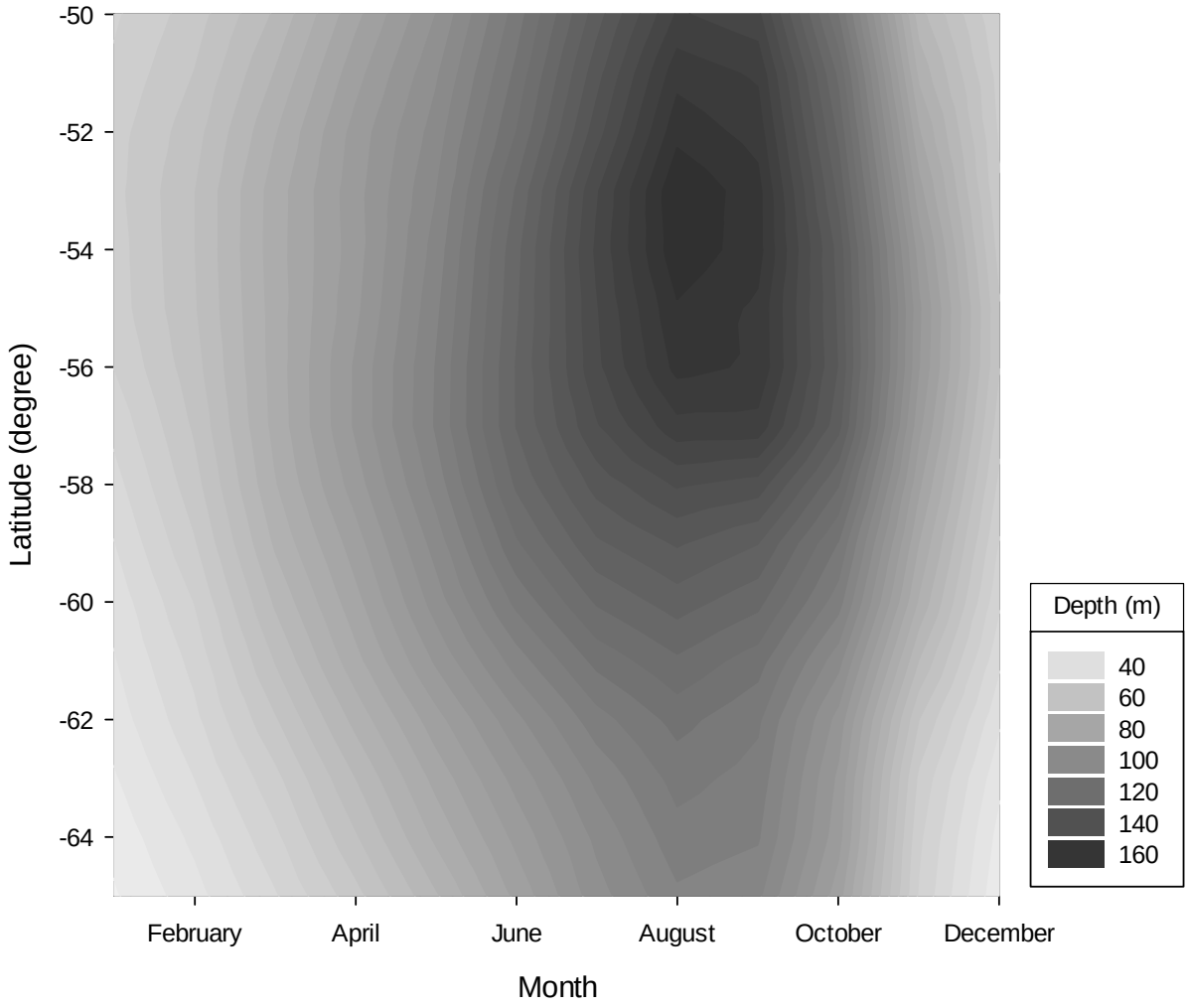

Figure 5.4: Variation of mixed layer depth (MLD, m) with latitude and time of year. Values are taken from NOAA's Monthly Isopycnal & Mixed-layer Ocean Climatology (MIMOC) (https://www.pmel.noaa.gov/mimoc/) using their optimal interpolated mixed-layer monthly MIMOC product. Data were averaged over degree of latitude and month.

5.3.2 *E. triacantha* south Atlantic latitudinal distribution

The density of *E. triacantha* was greatest (5.42 inds m^{-2}) in the most northerly latitudes (50–51° S) and decreased with increasing latitude to a minimum of 0.09 inds m^{-2} at 64–65° S (Table 5.5). The distribution area of *E. triacantha*, defined as the area within the south Atlantic sector containing *E. triacantha* (see section 4.2.3), initially increased from an area of >190,000 km^2 at 50-51° S to a peak at 55° S (>315,000 km^2) with increasing latitude, before decreasing again to a minimum at 65° S of 77,400 km^2. Overall, this resulted in maximum

abundances at 52-53° S (>1,100 billion individuals), to a minimum of 7 billion individuals at 64–65° S.

Table 5.5: Abundance of *E. triacantha* in the south Atlantic from the original Discovery expeditions of the 1920s and 1930s, reproduced from Mackey et al. (2012). Data are based on the mean density (inds m^{-2}) of euphausiids per grid cell of occurrence, number of grid cells euphausiids occurred in, and the area of inhabited grid cells (km^2).

Latitude (° S)	Mean density (inds m^{-2})	# cells with *E. triacantha* degree^{-1}	Distribution area degree^{-1} (km^2)	Billion individuals degree^{-1}
50	5.42	10	197,240	1,068
51	5.42	10	193,080	1,046
52	3.74	16	302,176	1,131
53	3.74	16	295,328	1,105
54	1.98	18	324,414	643
55	1.98	18	316,512	627
56	0.22	12	205,656	44
57	0.22	12	200,244	43
58	0.11	8	129,848	15
59	0.11	8	126,160	14
60	0.36	6	91,818	33
61	0.36	6	88,992	32
62	0.15	6	86,130	13
63	0.15	6	83,250	12
64	0.09	6	80,334	7
65	0.09	6	77,400	7

5.3.3 Main ('BEST') model results

Results from the main model run ('BEST') estimated a total annual active C flux for *E. triacantha* in the south Atlantic sector of the Southern Ocean, of 0.00027 Gt C y^{-1}. Two thirds of this, 0.00018 Gt C y^{-1} came from respiratory flux (C_R) whilst the remaining third, 0.00009 Gt C y^{-1} came from egestory, or faecal pellet, flux C_E).

The model showed considerable variation over latitude and time of year (Figures 5.5 and 5.6). In the highest latitudes, from 56 to 65° S, flux was substantially lower than between 50 to 55° S, with 95% flux originating from between 50 and 55° S and only 5% from 56° S and below (Table 5.6). Separated into the different components, 97% of C_R and 93% of C_E came from 50 to 55° S.

Table 5.6: Contribution to C flux per degree of latitude in the south Atlantic sector of the SO for respiratory flux (C_R), egestory flux (C_E) and total C flux (C_{TOT}) as a % of the total C_R, C_E or C_{TOT} respectively.

Degree of latitude	C_R per degree as % of total C_R	C_E per degree as % of total C_E	C_{TOT} per degree as % of total C_{TOT}
-50	18.7%	11.8%	16.4%
-51	18.1%	11.7%	16.0%
-52	19.3%	12.7%	17.2%
-53	18.8%	12.7%	16.8%
-54	11.1%	22.1%	14.7%
-55	10.8%	21.6%	14.4%
-56	0.6%	1.7%	1.0%
-57	0.6%	1.9%	1.1%
-58	0.2%	0.7%	0.4%
-59	0.2%	0.3%	0.2%
-60	0.4%	0.9%	0.6%
-61	0.4%	0.9%	0.6%
-62	0.2%	0.4%	0.2%
-63	0.2%	0.3%	0.2%
-64	0.1%	0.2%	0.1%
-65	0.1%	0.2%	0.1%

North of 56° S, the magnitude of C flux varied spatially and temporally. Furthest north, between 50 and 53° S, the episodes of highest flux occurred in winter (mean 4.57 Kt C per degree during June/ July/ August) and summer (mean 4.42 Kt C during December/ January/ February), whilst C flux in spring and autumn was relatively low (mean 2.78 Kt C). Between 54 and 55° S, total C flux was highest in March (mean 6.87 Kt C per degree latitude) with a secondary peak in October (mean 4.16 Kt C per degree latitude) but for the rest of the year

decreased to a mean of 2.82 Kt C per degree latitude. Whilst the magnitude of C_R varied across latitude, the pattern of maximal flux in summer decreasing to a winter minima was consistent across latitude (Figure 5.6). C_E was more variable and varied from a short, three month, period of enhanced flux during winter at P3 (52° S) to a sustained duration (nine months) of substantial flux at P2 (55° S).

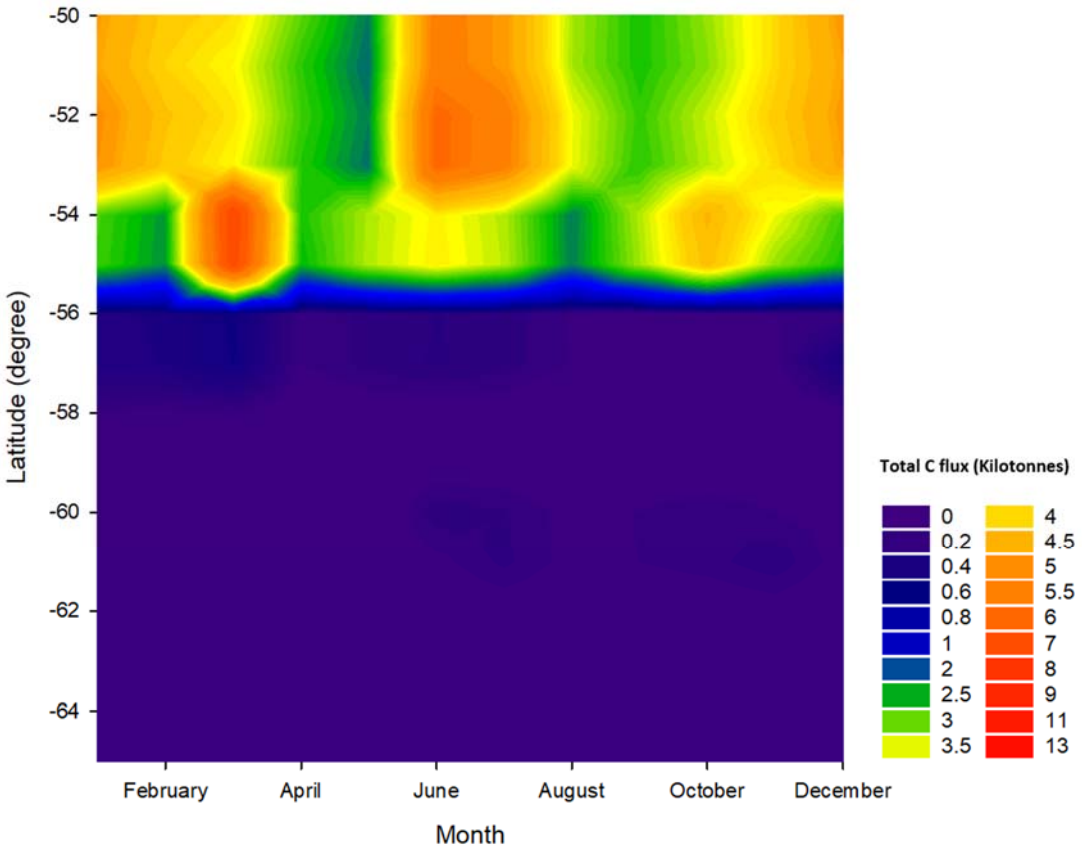

Figure 5.5: Contour plot showing the total C flux (respiration and egestion) from the main model run ('BEST') across the full model extent (latitudes 50 to 65° S) in the Atlantic sector. Values are shown as kilotonnes C produced below the MLD per day for each month of the year at every degree of latitude.

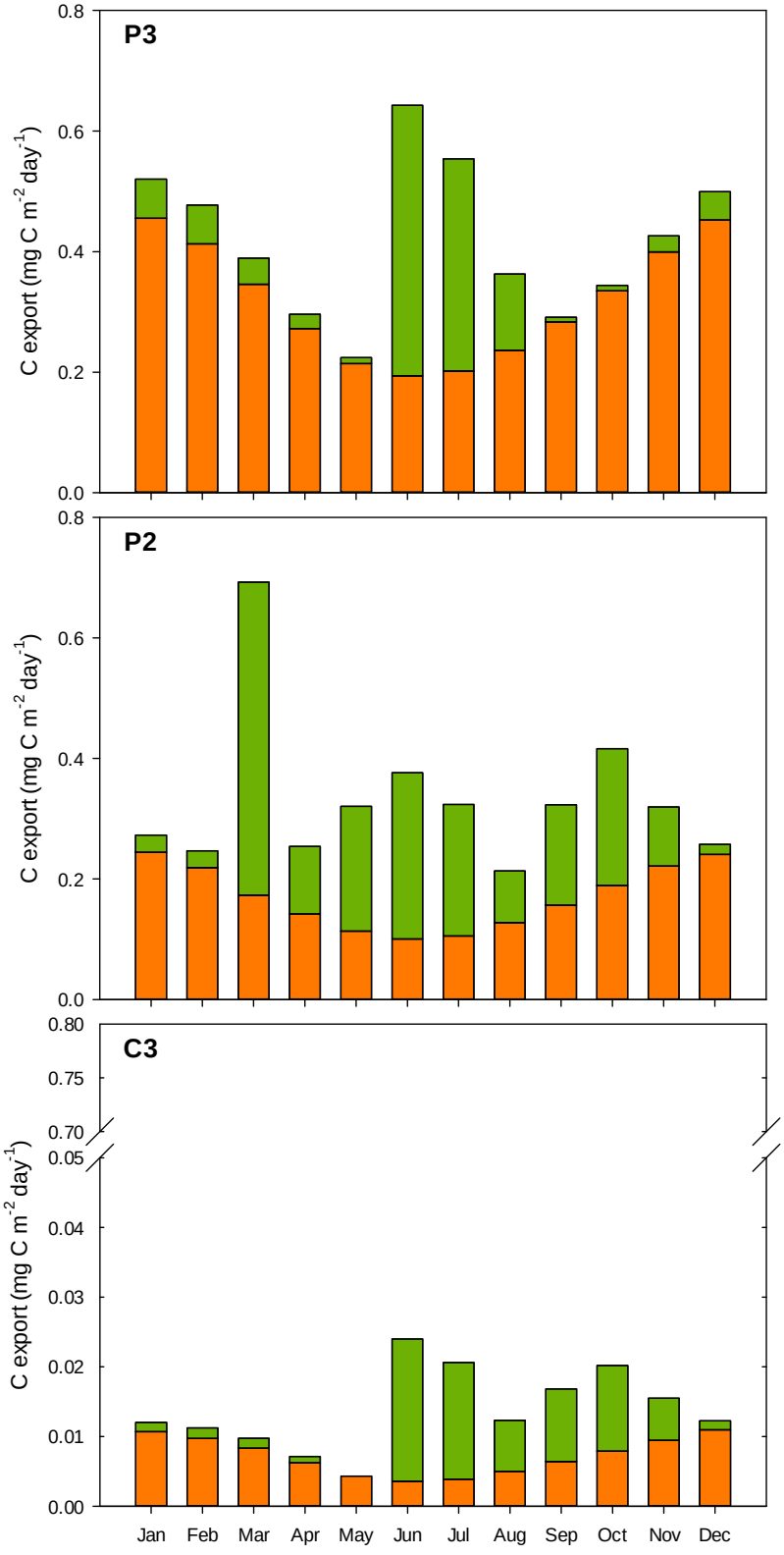

Figure 5.6: Stacked bar plot of the relative contributions of C_R (orange) and C_E (green) to total C flux across the year at stations representative of different latitudes. Top: P3 (52° S); middle: P2 (55° S); and bottom: C3 (59° S). C flux is shown in mg C m^{-2} day^{-1} and thus represents an average for that degree of latitude.

5.3.4 Results of sensitivity analyses

Out of 12 sensitivity runs, seven changed the magnitude of C_R whilst 11 affected C_E. There was a slight inverse correlation in the relative contributions of C_R and C_E to total C flux, with the three scenarios that produced the largest positive effect on C_E i.e. increased C_E relative to 'BEST', corresponding to the three that produced the largest negative effect on C_R i.e. reduced C_R relative to 'BEST'. However, none of these reductions in C_R were substantial, ranging from only 2 to 6%. These three scenarios, '100% CARNIVORY', 'CHL-A 2.0' and 'NO FORAYS' also corresponded to the three that resulted in the greatest positive effect (22 to 66%) on C flux overall (Table 5.7), although changes to flux were not uniform, instead varying with latitude and season (Figure 5.7). Switching to 100% carnivory resulted in increased C flux in spring, summer and autumn in the more northerly latitudes (50-53° S) and in summer at 54-55° S. Increasing the chl-*a* threshold resulted in increased flux from carnivorous feeding during summer at 54-55° S and in spring and autumn at 50-53° S. Eliminating forays and associated satiation sinking substantially increased winter flux at 50-53° S whilst reducing it throughout the rest of the year, and made flux greater and relatively more constant throughout autumn, winter and spring at 54-55° S. No scenario resulted in substantial differences to C flux south of 56° S since fluxes here were already minimal.

In direct contrast to the '100% CARNIVORY' run, changing the feeding behaviour from omnivory to '100% HERBIVORY' resulted in the greatest reduction in overall C flux, again driven almost entirely by changes to C_E. Under this scenario, C_E was almost eliminated during winter at 50-53° S and from early autumn to late spring at 54-55° S. Although C_R increased very marginally as a result of changes to feeding cycle duration, overall C flux dropped by 27% (74 kt C y^{-1}).

The four scenarios resulting in elevated C_R relative to 'BEST' included all three runs in which the proportion of the population migrating was reduced, with C_R increasing as the migrating population diminished from 100% to 30%, and 'JR15002', discussed further below. The three scenarios of reduced % population migrating corresponded to reduced C_E, although total C flux was enhanced overall, from a moderate 6% (17 kt C y^{-1}) under '70% MIGRATING', to 15% (40 kt C y^{-1}) under '30% MIGRATING'. This was reflected in an increasingly even distribution of C flux throughout the year, and export becoming less with increasing latitude. Furthermore, the contribution of C_R to overall flux became increasingly constant throughout the year, in particular enhancing winter C_R fluxes, whilst C_E followed the same pattern as in 'BEST' but with significant reductions in magnitude.

Changing the respiration regression to that derived from JR15002 data (Chapter 4) also resulted in an increase of total C flux of 11% (31 kt C y^{-1}) which came entirely from C_R. No changes to seasonal or temporal distribution of flux resulted.

Reducing the % of gut that was filled before satiation sinking was initiated resulted in progressive decreases to C flux in all cases, with all of the reduction being driven by C_E and offsetting only very slight increases in C_R. The reduction in flux ranged from 11% (29 kt C y^{-1}) in '75% FULL GUT' to 22% (58 kt C y^{-1}) in '25% FULL GUT'. Seasonally, this was manifest in increases to flux during late winter and decreases during early/ mid-winter at the lowest latitudes, whilst at 54-55° S there was a general reduction in flux in early spring, early autumn and early winter, with summer flux not being significantly impacted (Figure 5.7). In '50% FULL GUT' there was a continued decrease in flux in every season apart from summer, and this trend was further continued in '25% FULL GUT', with localised increases in flux e.g. during winter at 50° S, more than offset by increases elsewhere.

Considering C_R and C_E separately, C_R tended to follow a similar pattern of summer maxima and winter minima across all latitudes (Figure 5.8), although the decrease was steepest furthest north, becoming more subtle with increasing latitude. Changes to C_E displayed comparatively more seasonal and latitudinal variation. Seasonally, C_E varied from a maximal summer increase ('100% CARNIVORY') to a maximal winter increase ('NO FORAYS', low latitudes) or increases evenly spread across autumn, winter and spring ('NO FORAYS', mid latitudes). C_E also varied latitudinally, from the same pattern being replicated with different magnitudes e.g. '100% CARNIVORY' to quite different patterns depending on different environmental variables across latitude e.g. 'NO FORAYS' (Figure 5.8).

Table 5.7: Table showing the results of all sensitivity analyses, ranked alongside the results of the main model run ('BEST') in terms of size of difference +ve to -ve). Results are ranked according to the difference to C_{TOT} for each run as a proportion of 'BEST'. Left: C_R, C_E and C_{TOT} (gigatonnes, Gt, C) summed across all latitudes. Right: variation of each sensitivity analysis from 'BEST' for C_R, C_E and C_{TOT}. Cells corresponding to runs showing the three largest +ve differences are shown in red, and those corresponding to the largest -ve differences are shown in blue. The original run 'BEST' is coloured green for clarity.

	Total annual C export in Atlantic sector (Gt y^{-1})			**Difference in C export as proportion of 'BEST'**		
Scenario	**C_R**	**C_E**	**C_{TOT}**	**C_R**	**C_E**	**C_{TOT}**
100% CARN	0.00017	0.00027	0.00045	0.96	3.08	1.66
CHL-A 2.0	0.00018	0.00021	0.00039	0.98	2.35	1.43
NO FORAYS	0.00017	0.00016	0.00033	0.94	1.77	1.22
30% MIGRATING	0.00028	0.00003	0.00031	1.57	0.30	1.15
JR15002	0.00021	0.00009	0.00030	1.17	1.00	1.11
50% MIGRATING	0.00025	0.00004	0.00030	1.41	0.50	1.11
70% MIGRATING	0.00022	0.00006	0.00029	1.24	0.70	1.06
BEST	**0.00018**	**0.00009**	**0.00027**	**1.00**	**1.00**	**1.00**
CHL-A 0.5	0.00018	0.00009	0.00027	1.00	0.97	0.99
FULL GUT 75%	0.00018	0.00006	0.00024	1.00	0.67	0.89
FULL GUT 50%	0.00018	0.00005	0.00023	1.00	0.54	0.85
FULL GUT 25%	0.00018	0.00003	0.00021	1.00	0.34	0.78
100% HERB	0.00018	0.00001	0.00020	1.00	0.17	0.73

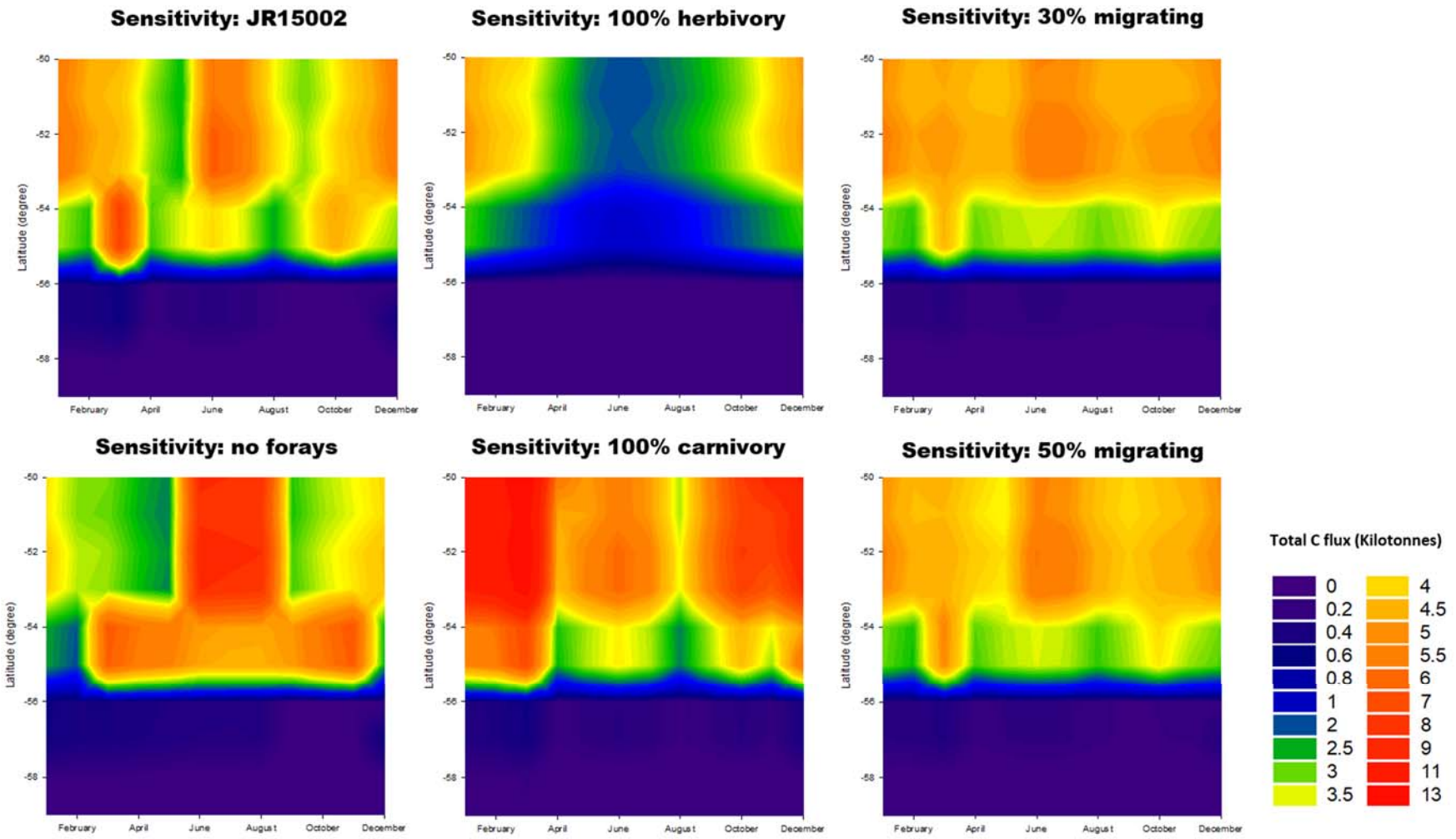

Figure 5.7: Total C flux (kilotonnes) across latitude and month of year for sensitivity analyses. Values represent the sum of C_R and C_E. C flux at latitudes south of 59° S was insubstantial in all model runs so, in the interests of clarity, the model's southerly extent is reduced from 65° S to 59° S.

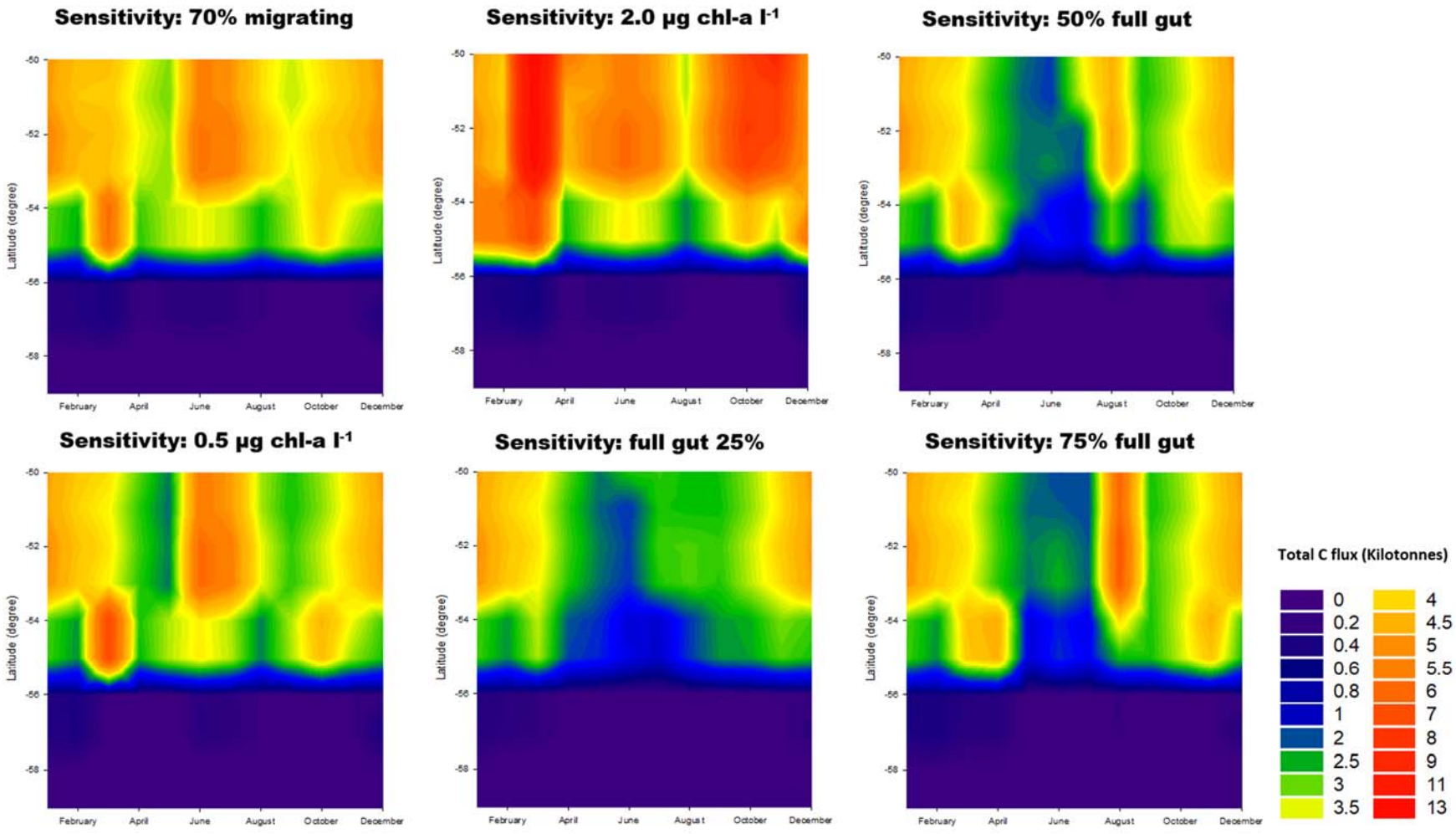

Figure 5.7: plot continued from the previous page.

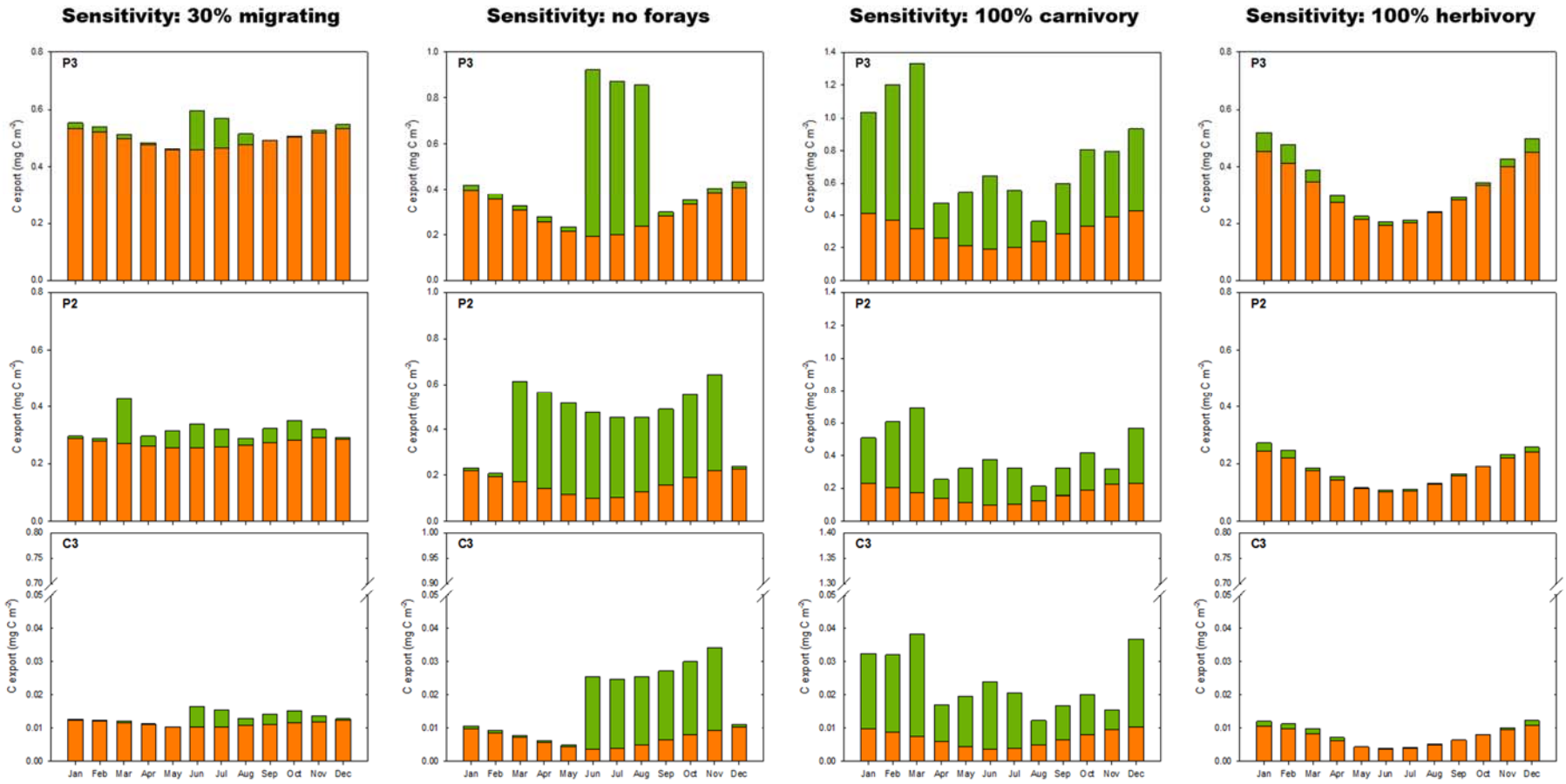

Figure 5.8: Plots of relative C_R (orange) and C_E (green) of selected sensitivity analyses that represent the maximum and minimum difference to C export. From L-R, plots represent the runs in which: C_R varied most compared to 'BEST' (30% migrating); C_R varied least compared to 'BEST' (no forays); C_E and C_{TOT} varied most compared to 'BEST' (100% carnivory); and C_E and C_{TOT} varied least compared to 'BEST' (100% herbivory).

5.4 Discussion

The total C flux calculated from the main model run was 2.7 x 10^{-4} Gt C, of which 95% came from latitudes north of 56° S. This was largely driven by the abundance of *E. triacantha* in the Atlantic sector of the SO, which was essentially defined by three main zones: between 50 and 53° S where abundance was greatest at >1 trillion individuals per degree; 54-55° S, with >0.6 trillion individuals per degree; and 56° S and below, where abundance ranged from >44 to >7 billion individuals per degree. Whilst individual C flux could at times be substantially higher at the mid to high latitudes (for example 0.24-0.30 mg C ind^{-1} day^{-1} in January at 56° S and 58° S respectively, compared to 0.14 mg C ind^{-1} day^{-1} between 50 and 55° S), the magnitude of overall C flux was determined by the abundance and distribution of *E. triacantha*, which is substantially greater in warmer waters of the sub-Antarctic. Despite this, there was a large degree of both seasonal and latitudinal variability in the magnitude of C flux at the higher latitudes, and in the relative contributions of respiration (C_R) and egestion (C_E). Latitudinal variability was also evident in the contribution active flux from *E. triacantha* made relative to passive POC flux. Comparable estimates of passive flux in the Southern Ocean are somewhat sparse but, in their 1991 paper, Wefer and Fischer (1991) present data based on sediment trap samples for passive flux at 100 m at a number of different locations in the Southern Ocean. When fluxes were lower (~1.5 g C m^{-2} y^{-1}), active flux from *E. triacantha* accounted for 8-10% of passive flux in the lower latitudes to the north of the SACCF, but only up to 3% when fluxes were higher (5-9 g C m^{-2} y^{-1}). In higher latitude regions, active flux from *E. triacantha* was negligible in the context of passive fluxes.

To aid the comparison of fluxes between latitudes, three latitudes have been selected that correspond to three study stations considered in previous chapters and to which environmental variables in the model relate: 52° S (P3), 55° S (P2) and 59° S (C3). P3 is found within a naturally iron-fertilised area and is characterised by high productivity; P2 is iron-limited and generally is less productive; whilst C3 is an open ocean, oligotrophic region in the colder waters south of the Southern Antarctic Circumpolar Current Front (SACCF). To reflect the greater contribution of the lower latitudes to C flux overall, the discussion will be primarily focussed most on latitudes north of 56° S.

The *E. triacantha* abundance data that these estimates are based on are the most comprehensive to date for the South Atlantic sector of the Southern Ocean but some limitations to the dataset must be acknowledged. The data originates from the *Discovery* expeditions of the early 20th century and, despite individual reports of *E. triacantha* abundances from later studies, a comprehensive update of the *Discovery* dataset has so far

not been carried out. A key limitation therefore is that the estimates take no account of changes in abundance over the last 100 years. Since the 1970s, a recorded decline in the abundance of *E. superba* has been linked to reductions in winter sea ice extent corresponding to warmer winters (Atkinson, 2004). However, (Tarling et al., 2017) found the spatial distributions of mesozooplankton between the *Discovery* and contemporary periods to be unaffected by recent warming suggesting that the response to increasing temperatures may vary between species. Indeed, the central range for *E. triacantha* has been projected to expand by up to 12 °S with a 1 °C of warming from a century ago (Mackey et al., 2012) with a corresponding increase in abundance in the South Atlantic sector.

A review of existing data reveals a lack of information upon which to assess trends in the abundance of *E. triacantha* over the long term. The KRILLBASE database managed by the British Antarctic Survey for example, is specific to *E. superba* and salps. Data on *E. triacantha* abundances are provided in at least two other datasets, the Southern Ocean Continuous Plankton Recorder (SO-CPR) database and the Palmer Station Long Term Ecological Research (PAL-LTER) current (2009 to present) and historical (1993-2007) datasets on zooplankton off the Western Antarctic Peninsula; however limitations exist for both. For SO-CPR, the data is necessarily biased against larger or migrating zooplankton such as *E. triacantha* as it is limited to the upper 10 m only. It is therefore primarily an indicative record of the calyptopis and furcilia abundance in surface waters but omits information on vertical distribution and juvenile or older stages. In terms of spatial extent, the SO-CPR database is focused predominantly between 60 °E and 160 °E and therefore also not directly comparable to *Discovery* data.

The other limitation of the *Discovery* data is that the majority of records originate from net hauls between 0 and 200 m with only one record to 310 m. Total abundances may therefore be underestimated although, since there was no sampling bias between day and night, this may not be substantial. The PAL-LTER data is limited vertically to the top 120 m and geographically to the area around the Western Antarctic Peninsula, an area where *E. triacantha* abundances are typically low (Kittel et al., 1985, Piatkowski, 1985), thus being representative of a much smaller part of its habitat than the *Discovery* data. A visual comparison of the *Discovery* and PAL-LTER datasets does not suggest substantial change in this region. Further, comparison of the *Discovery* data with that of Piatkowski et al. (1994) and the present study (see Chapter 4) suggests that abundances within the Scotia Sea remain in a similar range. Whilst the *Discovery* data therefore remains the most comprehensive in

terms of geographic and vertical coverage, an accurate assessment of the current status of *E. triacantha* requires more large-scale and full-depth sampling efforts in the future.

5.4.1 Carbon export from respiration is affected by temperature and migrating population

Within the main model run, C_R was found to contribute substantially to C flux, on average contributing more than 50% from September to May and, at selected latitudes, as much as 100%. This was especially pronounced at 50-53° S (P3) where C_R was only exceeded by C_E in the winter months of June and July, and least pronounced at 54-55° S (P2) where C_R was, on average, 42% of total flux between March and October but greater outside of these months. Longhurst (1990) was among the first to highlight the potential importance of respiratory carbon from diel vertical migrants to ocean C flux, suggesting that they could contribute 5 to 20% to estimates of organic C flux sinking across the pycnocline. When scaled up to the entire SO distribution area (based on Mauchline and Fisher (1969a)), C_R from *E. triacantha* in this model equated to 0.16% of the SO POC export at 133 m as estimated by Schlitzer (2002). Although small in absolute terms, these results suggest that, as a single species, *E. triacantha* could be an important local contributor to C flux and is an indication of the contribution other biomass dominant migrators could make. Furthermore, a consideration of the factors affecting the variability in C_R is warranted.

In the original ('BEST') run, O_2 consumption, and subsequently C production from respiration, was calculated using Regression 1, defining the relationship between respiration and temperature (described in Chapter 4). A second regression equation, Regression 2, was also calculated, produced from the second year's data alone ('JR15002'). For Regression 2, both the intercept and the *b* coefficient were slightly higher, resulting in a higher O_2 consumption for a given temperature. Given this, increased C export from respiration was expected as a result of switching to the 'JR15002' regression, although how much this would affect overall C flux was not known. Overall, the change in coefficients resulted in an increase in C_R of 17% and an increase to total C flux of 11% relative to 'BEST', equating to 31 kt C y^{-1}. This was not one of the runs most affecting the magnitude of C flux and, in the context of the range of fluxes (-27% to + 66%) 11% is a relatively modest increase. Nevertheless, since the respiration of *E. triacantha* has been found to vary over periods as short as their diurnal vertical migration (Chapter 4), it indicates that an error of up to 11% total C flux could be introduced when selecting the temperature relationship to describe the response. A more detailed discussion around the determination of each equation is provided in Chapter 4, however the 'JR15002' regression can probably be considered as representing the upper bound of *E.*

triacantha's temperature-dependent respiratory rate, at least within the range of temperatures they are currently exposed to, and any increase to C_R due to error is therefore likely to be somewhere in between these two runs. However, whilst 'JR15002' should not be directly extrapolated to a response under a warmer climate, it does suggest that warmer temperatures may result in an increase in C_R from diel migrants and more work should be done to determine the longer term effects of climate warming on respiratory flux.

Only three out of the 12 sensitivity tests resulted in reductions to C_R, reductions which were also relatively small and are discussed further in later sections. For five of the remaining runs, the increase to C_R was negligible, whilst the three that displayed the greatest increases in C_R (24 to 57% greater flux than 'BEST') came from changes to the proportion of the population migrating, with an inverse relationship between the proportion migrating and C_R. Since C_E is directly related to the number of individuals migrating, it follows that C_E was also negatively correlated to C_R under these scenarios, with the effect on C flux being somewhat muted but overall increased: with 30% of the population migrating per day, C_R was enhanced by 57% and overall C flux increased by 15%, whilst when 70% were migrating per day, overall C flux only increased by 6%. The question of synchrony in zooplankton diel vertical migrations is discussed by Pearre (1979b, 2003), who suggests that synchrony likely depends on whether a light or satiation cue is the proximate driver, with individual differences in satiation considered more likely to result in asynchronous sinking. A bimodal distribution as an indicator of asynchronous migrations is discussed further by Pearre (2003) with suggestions for such a profile ranging from satiation sinking, to different parts of the population migrating on different nights, or separate feeding at depth by the non-migrating part of the population. Such a bimodal distribution is indeed observed for *E. triacantha* and although the exact cause of this cannot be readily determined, the depth of the secondary peak (see Chapter 4, Figure 4.6) is likely deeper than would be reached with satiation sinking as modelled in this study. Assuming therefore that some part of the *E. triacantha* population is not migrating, and that all other variables remain the same, these results suggest that C flux calculated from the 'BEST' run represent an underestimate of total C flux with increases to C_R from the non-migrating portion of the population outweighing losses from C_E from the same individuals. As a conservative estimate, actual fluxes could therefore be enhanced by a further 6% or >17 kt C y^{-1} across the distribution of the model alone, or >150 kt C y^{-1} when scaled to the entire SO distribution area.

These results additionally suggest that a better assessment of the migrating population is necessary to constrain seasonal carbon fluxes since, as the migrating population decreases,

so fluxes during autumn and spring increase (Figure 5.7), most significantly at the lowest latitudes where abundances are highest.

5.4.2 Carbon export from egestion is highly sensitive to feeding behaviour

C_E was generally more variable than C_R over latitude and season, largely as a result of how feeding dynamics responded to environmental and behavioural variables. At P3, corresponding to 52° S in 'BEST', C_E was the dominant contributor to flux during winter, as a result of enhanced carnivory during these months (Figure 5.6) whilst C_E dominated during winter and spring at the more southerly C3 (60° S). At P2 (55° S) however, due to lower chlorophyll and hence greater carnivory, C_E contributed a sustained and substantial amount to flux for most of the year, contributing on average 58% of total flux from March to October (0.6×10^{-4} Gt C y^{-1}). In a study by Manno et al. (2015), the contribution of faecal pellets (faecal pellets) to deep carbon transport at P2 and P3 found fluxes at P3 to be an order of magnitude higher than at P2 (22.91 mg C m^{-2} d^{-1} vs 4.01 mg C m^{-2} d^{-1}) and for seasonality to vary between the sites. A direct comparison cannot be made, since the model results estimate flux out of the ML whilst Manno et al. (2015) estimate fluxes reaching deep-sea sediment traps; however, these results suggest that fluxes out of the ML from the faecal pellets of euphausiids may be relatively more important in terms of overall C flux in areas of lower overall productivity such as P2, and may represent enhanced fluxes in these areas.

However, this model also estimates greater C_E during spring and autumn bloom times at 54-55° S, equivalent to P2, than the 50-53° S region (equivalent to P3) whilst the opposite is observed by Manno et al. (2015). Attenuation processes that are beyond the scope of this discussion (but are discussed in Chapter 3) will likely be responsible for some of this discrepancy, although how estimates of C_E vary under different model assumptions may also shed some light on the processes affecting C_E from diel migrators. It should also be pointed out that C_E produced by these model runs may be conservative estimates of total faecal pellet flux from diel migrators, as they take no account of faecal pellets produced in the ML and sinking out.

5.4.2.1 Implications of foray feeding

In the original model run, export between 54-55° S is characterised by a large peak in C flux in March, driven largely by C_E, and moderate but fluctuating C flux throughout the rest of the year. Both the March peak and subsequent lower flux can be attributed to a combination of feeding cycle (FC) dynamics and seasonal change in the MLD. In terms of the FC, throughout the months of May to November, individuals in the model feed carnivorously as chl-*a* is below the 1 µg l^{-1} threshold that stimulates the switch from herbivory. The direct effects of

a switch to carnivorous feeding are firstly a much longer ingestion period which has knock-on effects to the duration of the feeding cycle and hence how many cycles are completed during the course of the night. Secondly, it results in a gut which contains substantially more C than it would manage to ingest under herbivorous feeding. Since the GER (*k*) is assumed to remain constant between feeding modes, substantially more C is therefore egested over the sinking time which is further enhanced when the sinking rate increases at the end of the night. In this scenario, the increase in sinking speed upon perception of light (Cushing, 1951) has the potential to enhance active flux below the ML. However, this also depends on the depth of the ML, with a deeper ML acting to reduce the amount of C egested below this depth. This has most pronounced effects under the foray feeding scenario of 'BEST', where a deepening of the ML from April to November means most, if not all, egestion during FCs takes place within the ML itself. C_E therefore becomes dependent on how much of a FC remains at the end of the night, hence how full the gut is when the euphausiid is forced by the model to descend. The consequence of this is clearly seen when individuals are prevented from foraying (the 'NO FORAYS' scenario): a higher and more constant C flux between 54° S and 55° S is observed due to individuals actively descending with a full gut upon stimulation by light. During summer, herbivorous feeding results in lower C_E whilst the removal of forays below the ML also reduces the magnitude of C_R.

The same effect is seen between 50 and 53° S, where a region of modest yet variable C flux during winter in 'BEST' is replaced by a region of substantial and sustained export in the 'NO FORAYS' run (Figure 5.7), again driven predominantly by C_E (Fig 5.8). Although this scenario produces the greatest overall reduction in C_R, this is more than offset by the increase in C_E, suggesting that overall C flux could be quite sensitive to changes in feeding and migration behaviour, in particular the demonstration of satiation sinking. However, results from the model suggest that C flux may not necessarily be enhanced by the inclusion of forays as has been previously suggested (Pearre, 2003, Tarling and Johnson, 2006). Specifically, the 'NO FORAYS' run resulted in enhanced C_E during winter at 50-53° S and from autumn to spring at 54-55° S, whilst an already modest C_E decreased outside of these months. As alluded to above, part of this can be attributed to the fact that during the summer at 54-55° S and from spring to autumn at 50-53° S the euphausiids are feeding herbivorously, hence contain less C in their guts, suggesting that feeding preferences may play an important role in determining the magnitude of C_E.

5.4.2.2 Implications of feeding dynamics

The sensitivity of C flux to C_E can therefore also be considered in terms of the C ingested by *E. triacantha* and the assumptions underlying this in the model. I have not attempted to fully

balance the daily ration of *E. triacantha* with night time feeding. With herbivorous feeding this would be impossible and evidence suggests that this is also the case in the environment, both for *E. triacantha* specifically (Bernard and Froneman, 2006) and its northern analogue, *M. norvegica* (McClatchie, 1985). Satisfying a daily ration of 5 to 15% of body weight (Pakhomov et al., 2002) with carnivorous feeding would be dependent on the duration of night and satisfied only when night exceeded 14 hours. Instead, a simple omnivorous behaviour was simulated, with the expectation that additional C requirements were satisfied at depth. This represents current knowledge of the diet of *E. triacantha* (Bernard and Froneman, 2006) and that surface herbivorous feeding does occur during night (Pakhomov and Froneman, 2004b, Bernard and Froneman, 2006). Since this was simulated by using a chl-*a* threshold to determine the preferred mode of feeding, it also reflects the fact that gut pigment in *E. triacantha* varies seasonally, with pigment at night during autumn an order of magnitude lower than during the summer (Bernard and Froneman, 2006). However, a limitation of this model is that it does not allow combined feeding, a scenario which would likely alter ingestion rates, gut content, and ultimate export. Without further knowledge of the feeding regime of *E. triacantha* however, such a scenario would be difficult to model without introducing unsubstantiated assumptions. In addition, the calculation of FC duration is fundamentally dependent on ingestion rate, which is based on either a constant chlorophyll filtering rate (Boyd et al., 1984, McClatchie, 1985) or a constant copepod consumption rate (Båmstedt and Karlson, 1998) which is likely far too simplistic. In the environment, feeding may vary with different prey concentrations or types (Fowler et al., 1971, Frost, 1972, McClatchie, 1985). This may have implications for assimilation efficiencies and egestion rates, with assimilation decreasing as prey concentration increases, although it is not clear that this is the case for euphausiids (Fowler et al., 1971). Additionally, the relative importance of C ingested from herbivorous feeding may vary, for example comprising a greater fraction of ingested food during the night (Sameoto, 1980) or being comparable to that from carnivory during spring despite comprising a minor contribution overall (Kaartvedt et al., 2002).

In the sensitivity analyses, the '100% HERBIVORY' and '100% CARNIVORY' runs resulted in the greatest changes to both C_E and total C flux overall, equating to a reduction of >73 kt C y^{-1} and an increase of >176 kt C y^{-1} respectively. These scenarios essentially provide an upper and lower bound to C flux within the constraints of the model, with the reality likely being somewhere in between. For a comparable species of northern krill, *M. norvegica,* Kaartvedt et al. (2002) found the majority of C to come from carnivorous feeding, with contributions from phytoplankton only reaching comparable levels in spring. The 'CHL-A 2.0' scenario

attempts to simulate this for the SO, further restricting herbivorous feeding to where chl-*a* is maximal. C flux from this is only slightly lower than in '100% CARNIVORY', with export under both scenarios substantially higher during spring and autumn (and summer under '100% CARNIVORY') at 50-53° S (P3) and during summer at 54-55° S (P2). This illustrates that the availability of particular food types and the feeding preferences of *E. triacantha*, may have a substantial impact on C flux. Contradictory effects may also be seen, in that bloom conditions may result in greater herbivorous feeding but consequently reduced C flux, whilst when phytoplankton is limited or euphausiids are feeding carnivorously, the impact on C flux may be enhanced. A final consideration in feeding behaviour is the frequency with which *E. triacantha* acquire a full gut before descending. In a series of sensitivity runs investigating the effect of animals consuming 75%, 50% or 25% of the C required to fill their gut, consequent reductions in C_E were observed, ranging from 11 to 22% of 'BEST'. The implication is that if individuals consume less than the maximum possible C, total C flux may be overestimated.

This study has shown that estimates of active carbon flux from the diel vertical migration of *E. triacantha* are particularly sensitive to factors related to feeding. In particular, the mode of feeding (herbivory, carnivory or indeed omnivory) which may determine the quantity of carbon egested, and factors that influence the surface feeding dynamics of *E. triacantha*. The latter is also linked to migratory behaviour with complex interactions between ingestion and egestion rates, the duration of the nocturnal period, and whether foray feeding is occurring. I have shown how seasonal changes to relatively well constrained parameters of chlorophyll concentration, mixed layer depth and duration of night can exert a considerable influence on export fluxes. Further work to understand the less well constrained components of this model are now required to reduce the error associated with changes to parameters which affect feeding. Some of the immediate questions to answer are i) Is *E. triacantha* predominantly omnivorous or carnivorous and how is that reflected in the carbon content of faecal pellets? ii) How does food concentration or type affect ingestion, gut fullness and egestion rate? iii) How does the feeding ecology and metabolism of *E. triacantha* vary seasonally? iv) How much feeding occurs below the mixed layer depth and how does this affect estimates of carbon flux? Evidence is converging on the idea of considerable variability in DVM so a final question is also posed: v) How is DVM exhibited in *E. triacantha* both individually and at the level of the population? Answers to these questions will reduce the uncertainty around how particulate organic carbon flux associated with DVM in particular varies on temporal and spatial scales and provide insight into how zooplankton dynamics may be better represented in ocean carbon cycling models.

5.4.3 Summary

- Overall C flux from *E. triacantha* for the 'BEST' model run, for the Atlantic sector of the Southern Ocean between 50 and 65° S, equates to 2.7 x 10^{-4} Gt C y^{-1}.
- This is a conservative estimate as it excludes sinking faecal pellet fluxes from within the ML and assumes that faecal pellets are produced at a constant rate from the cessation of feeding.
- 95% of the flux came from lower latitudes where *E. triacantha* abundances and distribution are greater, between 50 and 55° S, where daily fluxes reached as much as 0.91 mg C m^{-2} d^{-1} in winter whilst only 5% came from below 56° S where fluxes were as low as 0.002 mg C m^{-2} d^{-1} in winter.
- In lower latitudes and when passive organic carbon fluxes are higher, *E. triacantha* has the potential to enhance flux by up to 10%, although this contribution is reduced when fluxes are higher. At higher latitudes, *E. triacantha* currently plays a negligible role in flux enhancement, although if the distribution of *E. triacantha* shifts to the south, their relative importance may increase.
- Two thirds of total C flux came from respiration although this varied considerably over the course of the year, generally being highest in summer and lowest in winter, both due to lower temperatures and longer nights.
- C_R is also sensitive to changes in the temperature response function, suggesting that overall C flux from 'BEST' may be an underestimate and that the response of C_R to a warming climate should be further considered.
- The proportion of the population migrating may also affect C_R more than C_E although this is subject to factors affecting the magnitude of C_E.
- C_E was more variable over latitude and season than C_R and particularly sensitive to changes in feeding dynamics, such as whether the euphausiid fed herbivorously or carnivorously, although a dynamic interplay between feeding and abiotic factors such as the depth of the mixed layer or duration of night may also affect the magnitude of flux from DVM.
- C_E from spring and autumn in 'BEST' is therefore likely to be underestimated, since obligate herbivory results in lower egestory fluxes than if the euphausiid consumed a mixed diet.
- Future work to better understand factors affecting the feeding dynamics of *E. triacantha* (ratio of herbivorous to carnivorous feeding; ingestion rate; gut fullness; and egestion rate), and the dynamics of *E. triacantha*'s migratory behaviour are necessary to reduce uncertainty in estimates of C_E from DVM.

Chapter 6: Synthesis

6.1 Overview

The purpose of this thesis was to investigate the role of zooplankton in the export of carbon from the euphotic zone to the mesopelagic in the Scotia Sea, Southern Ocean (SO). Zooplankton-mediated export is a critical component of the biological carbon pump (BCP) but one that is highly variable across space and time. As a result, it is not well constrained in climate models. I was specifically interested in understanding how diel vertical migration (DVM) and faecal pellet production by the zooplankton community may modify fluxes of carbon over upper mesopelagic depths in the Southern Ocean, and I studied this with reference to four contrasting locations in the Scotia Sea. I evaluated the processes responsible for carbon export, quantified export fluxes, and investigated sensitivities in estimates of flux through a combination of approaches that were designed to address this question in a holistic way. These included (i) taxonomic and multivariate analysis of the zooplankton community at diurnal and interannual timescales, the evaluation of DVM and the quantification of biomass and carbon fluxes of interzonal migrations; (ii) analysis and quantification of faecal pellet morphology, size and flux, to determine the processes controlling faecal pellet export over intermediate depths within the mesopelagic; (iii) determination of the influence of DVM on the respiration rate of a widespread, migratory SO euphausiid, *Euphausia triacantha* and implications for respiration carbon flux and (iv) quantification of the total carbon export from *E. triacantha*, the seasonal and latitudinal variation in export, and evaluation of the major sensitivities in export estimates.

The Scotia Sea is unique within the SO because of the diversity of environments within it that are representative of the broader SO, for its important role in the biological carbon pump, and in supporting the ecology of the Antarctic region. These environments were represented in my study across a south-north transect that included (i) an ice-influenced region important in post-larval euphausiid development (ICE)/ R1; (ii) an oligotrophic region typical of the HNLC conditions of much of the SO (C3); (iii) a mid-productivity region upstream of the Scotia Arc (P2); and (iv) a highly productive, naturally iron-fertilised region downstream of the Scotia Arc (P3). The transect crossed the Southern Antarctic Circumpolar Current Front (SACCF) whose influence on the upper mesopelagic separated species-rich, high biomass communities dominated by copepods to the north, from sparser, lower biomass communities characterised by euphausiids and fewer copepod species such as *Metridia* sp. to the south. Abundance rather than absolute taxonomic differences tended to drive the groupings, agreeing with the conclusion that variability in Scotia Sea zooplankton communities occurs at the population rather than the taxonomic level (Ward

et al., 2012a). As a result, this is an area where different influences both on and of the zooplankton community structure can be compared.

In the following section I present the key findings from each chapter. I then draw some overall conclusions and highlight areas of interest for future work.

6.2 Key findings

Chapter 2

1. The Scotia Sea zooplankton community was principally determined by two abiotic variables: latitude and depth. The position of the Southern Antarctic Circumpolar Current Front (SACCF) separated shallower samples (up to ~375 m) north to south: stations to the north were characterised by a diverse zooplankton community with biomass comprised predominantly of copepods and euphausiids, whilst southern stations exhibited reduced diversity dominated more by euphausiids. Increasing homogeneity across latitude with depth was likely due to the influence of colder Circumpolar Deep Water. Deeper communities were characterised by lower biomass, lower species-richness and the presence of principally deep-dwelling species such as *Metridia curticauda*, *Lucicutia* and *Eucalanus* spp. These findings are in broad agreement with the latitudinal groupings of Ward et al. (2012a,b) although it extends the analysis of Ward et al. (2012a) from 400 m to 1000 m, allowing zooplankton vertical community, biomass and flux gradients to be considered across the mesopelagic for the first time.
2. Later stage development, warmer surface water temperatures and differences in preceding ice extent between years explained a reduced diversity and stronger North/ South separation in the autumn compared to the summer, although the communities were not fundamentally different at a taxonomic level. A key feature of this ecosystem was the presence of many of the same species in all groups, with gradients rather than abrupt changes defining vertical community structure.
3. DVM, assessed by calculating the biomass shift of the main body of the population, revealed three types of individual behaviour, DVM, reverse DVM (rDVM) and no migration, combinations of which were exhibited by most zooplankton. Substantial individual behavioural plasticity suggested either that species regularly reverse their migrations, or that foray behaviour is more widespread than currently understood. rDVM was also widely observed at the community level, where there was a net upward migration of zooplankton from night to day, hypothesised to be a community response to predation risk but may also represent the synchronisation

of forays. First order estimations of active flux, from vertical migrations at the community scale across 125 m, resulted in minimum active fluxes of between 0.3 and >22 mg C m^{-2} d^{-1} when considering gut evacuation only for the last hour of the night, and maximum fluxes of 1.6 to 41 mg C m^{-2} d^{-1} when gut evacuation throughout the night was considered. This therefore represents minimum and maximum estimates of export, and the first such estimates of community active flux for the Scotia Sea.

4. Reversals in mode of migration had implications for flux which were most sensitive during summer than autumn due to the shorter nights. This suggests that better quantifying the frequency of rDVM and understanding the processes driving it is especially important at high latitudes when day and night lengths are unequal.

Chapter 3

1. At all stations, the size of faecal pellet was strongly decoupled from predictions of size based on the overlying mesozooplankton community: there were disproportionately fewer of the smallest faecal pellets whilst larger faecal pellets, such as from biomass-dominant copepods and euphausiids, contributed disproportionately to the flux. This suggests that the smallest faecal pellets were highly labile and rapidly lost to zooplankton processes such as coprohexy or coprophagy (Lampitt et al., 1990, Iversen and Poulsen, 2007) and microbial remineralisation (Poulsen and Iversen, 2008), whilst the larger faecal pellets sank deeper into the mesopelagic. At ICE, many of the largest observed faecal pellets were cylindrical and were not predicted from the mesozooplankton community, suggesting that, in this region, mesozooplankton species composition is a poor predictor of faecal pellet flux. This agrees with previous studies that have found euphausiids to be important contributors to carbon flux at the ice edge (Cavan et al., 2015, Belcher et al., 2017b). It also suggests that in such areas, euphausiid faecal pellets are more likely to reach deep export or sequestration depths, whereas mesozooplankton faecal pellets are more likely to be remineralised.
2. There was a difference in faecal pellet morphological type between the stations, from ICE that was dominated by larger cylindrical faecal pellets to P2 and P3 where a more homogeneous mix was observed. This is reflected in the abundance and diversity of mesozooplankton which is greater in the warmer waters north of the SACCF and, when accounting for loss of the smallest faecal pellets, is also better predicted by the overlying mesozooplankton community.

3. faecal pellet flux attenuation was shallower (40 m) and most rapid in the colder waters at ICE, whilst it was substantially deeper and more gradual at P2 and P3 (100 – 200 m) where surface waters are warmer. This contrasts to the model of Marsay et al. (2015) who proposed a shallower remineralisation in warmer waters; this shows that physical models alone are insufficient to explain variation in faecal pellet flux, especially at high latitudes where temperature variability is comparatively low yet fluxes can vary substantially. I suggest that this can be explained by the overlying mesozooplankton community, whose abundance and diversity over depth results in elevated production and repackaging of faecal pellets throughout the upper mesopelagic.
4. A shallow pulse of fresh, dense, mineral ballasted faecal pellets at P2 is accompanied by a deep remineralisation and the highest faecal pellet carbon fluxes of all three stations (67 mg C m^{-2} d^{-1} by 400 m). This compares to 400 m fluxes of 36 mg C m^{-2} d^{-1} at P3 (where mesozooplankton abundance was greatest) and 9 mg C m^{-2} d^{-1} at ICE. The night-time sampling of P2 suggests that DVM plays an important role in the supply of faecal pellet material to the mesopelagic, and that diurnal variability in fluxes may be substantial.

Chapter 4

1. When incubated between 0.2 and 4.7 °C, temperatures within the range experienced over its vertical migration, the short-term respiration rate of *Euphausia triacantha* was found to increase with temperature with a Q_{10} of 4.5 (JR15002 only) to 4.9 (full two-year dataset). These results represent the first comprehensive measurements of the temperature-dependent respiration rate of *E. triacantha*, comprising 159 animals over 2 years, and suggest that DVM may affect the respiration carbon flux from large interzonal migrants. This suggests that, despite the temperature being within the experiential range of *E. triacantha*, the species is not able to compensate for increased temperature during its migration.
2. In contrast to global relationships of respiration with body size and temperature (e.g. Ikeda, 1985) body size was not found to have a significant effect on weight-specific respiration in this study, with temperature being the most significant explanatory variable in a multiple logistic regression. It is suggested that this is due to the relatively narrow range of body sizes in a single-species study (varying within 1 order of magnitude), in contrast to the ~3 orders of magnitude that interspecific studies are based on. When compared with the global bathymetric model of Ikeda (2013), the respiration rates of *E. triacantha* determined in this study were broadly

comparable at the lower end of the range, but were found to be significantly more sensitive to higher temperatures in the experiment than predicted from the Ikeda (2013) global model. In comparison to a study on *M. norvegica* (Saborowski et al., 2002), similar regression slopes are obtained, suggesting that global models may do a good job of representing interspecific relationships spanning wide size and temperature ranges, but fare less well at predicting single-species responses to temperature.

3. In one of the few studies of this nature on epipelagic marine zooplankton, little evidence was found to support Metabolic Cold Adaptation (MCA), as metabolic rates at lower temperatures were comparable both to those of other species measured at similar temperatures, and to predicted rates. Elevated metabolic rates are discussed in terms of a response to higher temperature rather than an adaptation to temperature. Our findings, whilst purely suggestive, are in agreement with those of other authors (e.g. Holeton, 1974, Steffensen, 2002) who believe the concept of MCA to be an artefact induced by measuring the effects of handling stress or activity rather than an inherently raised metabolic rate.

Chapter 5

1. Total active carbon flux from *Euphausia triacantha* for the south Atlantic sector of the SO model region was estimated at 2.7 x 10^{-4} Gt C y^{-1} based on the 'BEST' model run. This was greatest to the north of the model domain, in the sub-Antarctic region where abundances of *E. triacantha* were highest. Overall, two thirds of this was active respiration flux (C_R) and a third was active egestion flux (C_E) although there was significant latitudinal and seasonal variability in the magnitude and relative proportions of flux. Respiration flux was disproportionately concentrated towards summer months, reflecting the longer days, and so greater time spent respiring at depth. Egestion flux was generally greatest during winter months when chlorophyll was too low to support herbivorous feeding and carnivorous feeding was adopted instead. Latitudinal variation in the relative contributions of C_R and C_E was due largely to interactions between feeding cycle dynamics, surface chl-*a* concentrations and the mixed layer depth (MLD) which together determined the carbon that would be egested and respired below the mixed layer during feeding cycles.
2. Active export flux was most sensitive to changes in feeding dynamics: obligatory carnivory resulted in the greatest increase to C_E and, correspondingly, to total flux, whilst the reverse was true of obligate herbivory. Reductions in gut fullness also

reduced C_E suggesting that, under conditions of high food concentration, regular but less efficient feeding may lead to the greater retention of carbon in the mixed layer and a reduction in export flux.

3. An unexpected result was that switching from foray behaviour to 'classical' migration increased egested (and total) flux. This is contrary to recent suggestions of enhanced flux under foray feeding (Tarling and Johnson, 2006, Tarling and Thorpe, 2017) but is reconciled with reference to assumptions within the satiation-sinking model. In particular, under foray migration an individual may reach dawn without a full gut, thus exporting less during egestion than an individual that has remained at the surface all night and has a full gut on descent. Under these conditions and with active sinking at the end of the night, maximal export at dawn can exceed the sum of export during satiation-sinking. This challenges the assumption that foray feeding always results in greater export flux and highlights the need for further work to understand the seasonal dynamics of migration, feeding and mixed layer depths to quantify flux from different migratory behaviours.
4. Export flux also varied with changes in the proportion of the population migrating each day, with increasing flux corresponding to a decreasing proportion of migrators. This was driven by an increase in respiration flux from the non-migrating population which exceeded losses from reduced egestion. This supports the original proposition by Longhurst (1990) that respiratory flux from migrators could account for a significant enhancement to passive flux and lays the foundations for future work to resolve questions of asynchrony in migration so as to understand the relative balance between C_E and C_R and the depth at which carbon is exported.

6.3 Concluding remarks

The Scotia Sea is a physically dynamic and biologically variable region. In oceanographic terms, temperature is relatively stable and varies by only a few degrees, whether over latitude or depth. Other variables, including frontal features, ice extent, physical hydrography, and strong seasonality exert much more influence over the biology, and this is reflected in the biological control over carbon export. As shown in the first chapter of this thesis, the zooplankton community structure of the Scotia Sea can broadly be described in terms of gradients, with zooplankton biomass decreasing as latitude and depth increase. Superimposed on this are the influence of the SACCF and deeper water masses which sharpen latitudinal and vertical gradients, and which are relatively consistent between years and seasons. This influences the zooplankton communities which are found there

and, as shown in this thesis, ultimately has an important influence on the export of carbon from the epipelagic to the mesopelagic. Throughout the chapters of this thesis, I find that the behaviour and physiology of zooplankton can be complex, and this can have a particular influence over flux in regions where the community is abundant and species rich. Chapter 2 allowed three broad groups to be defined based upon zooplankton biomass and diversity: north of the SACCF; south of the SACCF; and deeper than ~500 m, although wide distributions of many species show that these groups are not taxonomically exclusive.

The schematic in Figure 2.10 depicts the relatively greater complexity of the community on the northern side of the SACCF, with a greater species diversity typifying the northern communities. It also illustrates the variability in migratory behaviour at species and community scale, with widespread reverse migrations that may consequently have impacts on flux. Chapter 3 showed how this was reflected in faecal pellet export. The morphology of faecal pellets exported from stations north of the SACCF was highly heterogeneous and the size showed that they originated disproportionately from larger copepods and euphausiids. This influence persisted across the upper mesopelagic, with a mixed morphology over the 400 m sampling depth and deep attenuation of faecal pellet flux which resulted in fluxes at 400 m as large as 67 mg C m^{-2} d^{-1}. On the colder, south side of the SACCF, where biomass was lower, less taxonomically diverse and influenced more by euphausiids, faecal pellet flux was also more dominated by large cylindrical faecal pellets of a euphausiid origin. At the time of sampling, faecal pellet flux attenuation was shallow and by 400 m was only 9 mg C m^{-2} d^{-1} suggesting that fluxes in this region are generally low (although may be periodically high during a swarm event) and that the mesozooplankton plays a relatively small role in the export of faecal pellet carbon over the mesopelagic. The increasing proportion of fast-sinking faecal pellets of euphausiid origin with depth at P3 also indicates their ability to persist despite the relative dominance of copepods in the overlying mesozooplankton. Night-time sampling at P2 (Chapter 3) also revealed the potential for DVM to substantially enhance the supply of large, dense and labile faecal pellets to the upper mesopelagic. Despite being putatively less productive than P3, this station exhibited the highest 20 to 100 m fluxes, although sediment traps show that more faecal pellet carbon reaches 1,500 to 2,000 m depths at P3 (Manno et al., 2015). This suggests that an intense reworking of material occurs in the mesopelagic at P2 and that diel pulses of material may support more microbial and protozooplankton activity in the mesopelagic at such stations.

The importance of respiration in estimates of flux is then addressed in Chapter 4, which represents the first comprehensive study of the effect of DVM on the metabolism of the

euphausiid, *E. triacantha.* Despite the species displaying a vertical distribution and migratory amplitude of up to 1,000 m, results showed that it does not compensate for the temperatures experienced during its migration and is sensitive to higher temperatures over the short term. Comparison with global predictive relationships suggested that intraspecific variability may be greater than would be predicted from interspecific relationships of species with temperature, with the global models smoothing out much of the individual biological variability. Chapter 5 showed the implication of incorporating such a physiological response into active flux estimates, with C_R demonstrating distinct seasonality, in particular at the lower latitudes where greater surface temperature differences are experienced. The sensitivity of combined respiration and egestion export flux to differences in individual or population migratory behaviour shown in Chapter 5 is emphasised by the findings in Chapter 2, which show the regularity with which taxa switch between DVM, rDVM and no migration (or alternatively exhibit foray-style migration). The sensitivity of C_E to prey availability, selection and processing (Chapter 5) raises important questions around the temporal and spatial supply of faecal pellets to the mesopelagic, but is also of direct relevance to C_R, since it defines the time spent respiring in near surface waters. These findings build on decades of work on DVM that document its complexity, in particular in relation to hunger and satiation (comprehensively discussed by Pearre, 1979b, 2003) and suggest some directions for future work that are discussed further in section 6.4.

The conclusions drawn in this thesis also challenge the notion that more rapid attenuation of flux occurs in warmer waters due to the deeper and slower remineralisation in colder waters (Marsay et al., 2015). I found deeper and slower attenuation of faecal pellets to occur in warmer regions where the zooplankton was correspondingly more abundant and I suggest that, particularly in regions of high biological productivity, control of flux by the biota may be more influential than physical controls of temperature. In particular, I find support for Vinogradov (1962)'s 'ladder of migration' theory which proposes the production and successive reworking of faecal pellets by successively deeper communities that can support high fluxes to the deep sea. In areas of intermediate or variable productivity, processes of coprohexy (Iversen and Poulsen, 2007) followed by enhanced microbial remineralisation may dominate in the mesopelagic, reducing particulate fluxes to depth. Along with further work to elucidate the diel variability in faecal pellet supply to the mesopelagic, this may help resolve spatial imbalances in organic supply and heterotrophic demand in the mesopelagic (Burd et al., 2010).

Lastly, I offer some final thoughts on the relative importance of the factors and processes discussed in this thesis, and the extent to which they can be considered influential in the zooplankton-mediated flux of carbon in the Scotia Sea and Southern Ocean.

A key finding in Chapter 2 was the extent of migration throughout the water column and the variability exhibited in its vertical direction. This translated into estimates of active flux of up to 0.3-14.3 mg C m^{-2} d^{-1} in summer, corresponding to between 0-13% of spring/summer POC flux from comparable locations, and 3.0-22.1 mg C m^{-2} d^{-1}, corresponding to 2-19% spring/summer POC flux in autumn. Considering that POC fluxes may in fact be reduced during the autumn, the contribution made by active flux of the migrating community may in fact be higher still during this season and may represent a substantial enhancement to flux. In addition, variability in migration mode was found to be common and may exert an influence on the magnitude of flux, particularly when hours of light and darkness are uneven. Finally, respiration was found to be a major contributor to the overall export flux of the migrating zooplankton community, contributing 79-98% of the total active flux from the migrating biomass under a conservative scenario of FP export yet still contributing between 16-79% under the hypothetical maximum estimate and being more consistent during autumn then summer.

Zooplankton faecal pellet export below the mixed layer was found to be the dominant contributor to POC flux at all stations showing that, for this region, zooplankton play an important role in delivering carbon to intermediate depths. Export from the mixed layer was greater and attenuation deeper in the more productive, copepod dominated waters north of the SACCF. Export was lower south of the SACCF but dominated by faecal pellets of a euphausiid origin, swarms of which may episodically result in substantial export fluxes. Short-term diel variability related to diel vertical migration was also suggested to explain high fluxes at the mid-productivity station, and this may play an important role in exporting carbon and nutrients to the upper mesopelagic where it may fuel microbial and protozooplankton communities.

In terms of respiration, *E. triacantha* was found to be highly sensitive to short-term changes of temperature experienced across its migratory amplitude. A lack of compensation to such temperature gradients suggests that respiration flux may be an important component to consider in fluxes originating from *E. triacantha*, and that further attention should be dedicated to the effect of a warmer or expanded range on respiration flux under a changing climate. A greater amount of individual variability was observed than predicted by global

relationships, indicating that using global relationships may result in missing the full range of physiological response exhibited by an organism undertaking migrations.

The combined effect of respiration and faecal pellet export over the full range of *E. triacantha* was then considered, because of its potential to be a driver of active flux as it exhibits a wide migratory amplitude yet does not swarm. Among many interesting findings were that respiration accounted for a large amount of estimated export flux and should be included in future considerations of flux, and that export flux from the egestion of faecal pellets is highly sensitive to the dynamics of feeding and migration mode. These findings are likely to be unique to *E. triacantha* but may be applicable to larger species that have deep distributions or migratory amplitudes, and that have the potential to pass through the mixed layer during migrations and feeding cycles. Overall flux was generally small in absolute terms, but in areas of high abundance (north of the SACCF) and at times of lower passive flux, active flux from *E. triacantha* enhanced passive fluxes by up to 10%.

6.4 Directions for future work

As well as answering a number of questions related to the zooplankton influence on carbon flux in the Scotia Sea, this thesis has also highlighted a number of areas where further work would be beneficial. A particularly important question to resolve is how variable individual migratory behaviour truly is. This thesis revealed a number of different migratory modes within individual species and the community, with large implications for export flux, but that were limited by their relatively coarse temporal resolution. Linked to this is the suggestion that, within individual species populations, not all of the population is migrating in the same way, or at the same time. The implications of this became clear in Chapter 5 in which fluxes were highly sensitive to different proportions of the population migrating or the migratory behaviour they employ. Part of the problem has been related to the time-consuming nature and logistical effort required to deploy and analyse multiple sets of nets during research cruises with competing demands and tight schedules. However, methods such as the ZooScan are a relatively quick and effective method of obtaining size-fractionated biomass estimates and, with training, can also provide an informative level of taxonomic resolution. In combination with sampling protocols designed to catch both upward and downward swimming animals at multiple times throughout the day, a greater level of temporal insight into the movements of particular populations should be achievable. This will help to answer the question of how often migrations are truly reversed, whether they are in fact an artefact brought about by sampling design, or by foray migrations by different species simply becoming synchronised at the scale of the community. Answering this would also help to understand the regularity of foray

migrations, and whether they occur with a similar frequency during day and night and across wider spatial and temporal scales. This is particularly important for high latitude environments where strong seasonality, combined with the influence of the MLD, could significantly alter fluxes if the migratory mode were to be reversed. Furthermore, the role of the lunar cycle could not be fully considered in this thesis, yet evidence from the Arctic suggests that this may play a role in modifying DVMs (Berge et al., 2009, Tarling, 2015, and Last et al., 2016), especially during the first part of the night, and in stimulating synchronised night-time descents. To date, this has not been explored in the Antarctic but this may also reveal what external factors are controlling rDVM at the community level versus at the individual level, to what degree this can be predicted, and whether this may be significant enough to influence carbon fluxes.

Since these are important questions to resolve in the understanding of flux, another way this could be achieved is through the use of mesocosm or long-term monitoring experiments, in which a suite of approaches could be used to investigate the complexity of zooplankton behaviour including the deployment of optical instruments, regular sampling, and floating sediment traps. This could include high-level temporal monitoring and sampling of zooplankton at times of varying food concentrations, to examine changes in migratory dynamics alongside food availability and gut content, or the deployment of instrumented autonomous vehicles. One of the problems of answering these questions in a region as remote as the open waters of Antarctica is the necessary reliance upon relatively low resolution sampling which effectively provides a snapshot of the system at a single place and point in time. Whilst this has undoubtedly informed a detailed and consistent understanding of much of the system, it is clear that some questions related to zooplankton dynamics require a different approach, as illustrated by the schematic in Figure 6.1 which shows how low-frequency sampling has the potential to miss detail or lead to incorrect conclusions being drawn. As I showed in Chapter 5, different behavioural and feeding patterns can lead to quite different estimates of flux, so sampling designed to answer these questions is an important next step.

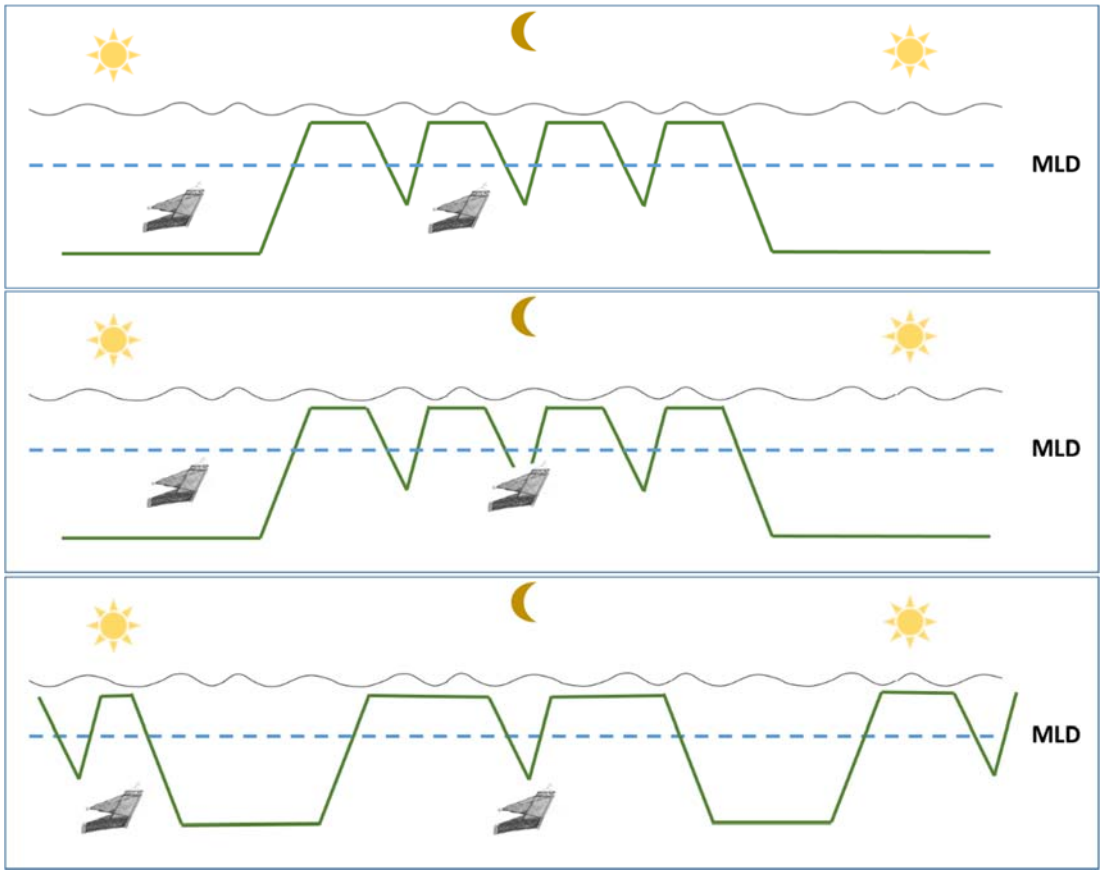

Figure 6.1: Schematic showing how different sampling times or migration patterns may lead to incorrect conclusions when sampled only once during day and night. Top and middle panels: the same migration pattern is shown but with sampling (shown by the position of the MOCNESS net) at slightly different times, leading to a conclusion of normal DVM (Top) or negligible DVM (Middle). Bottom panel: foray migration during day and night may lead to a conclusion of rDVM if sampling resolution is insufficient.

An important question highlighted particularly in Chapter 3 was the possibility for DVM to enhance upper mesopelagic fluxes of carbon over diel timescales. Therefore, in addition to finer resolution zooplankton sampling studies, it would be highly beneficial to conduct more detailed resolution studies of particle flux to temporally constrain carbon fluxes into the mesopelagic and their eventual fate. One approach to this would be to repeat the CTD sampling methodology at more regular time points and additional depths throughout the day and night to reveal patterns of faecal pellet flux over diel timescales. Combining this with emerging developments in optical technologies (e.g. Jouandet et al., 2011, Möller et al., 2012, Schoening et al., 2017) would help to develop methods for characterising particle type and properties, and accelerate progress towards the quantification of fluxes with reduced need for costly and time-intensive ship-based fieldwork.

Beyond larger-scale population dynamics, there are also important questions to answer related to the feeding ecology and physiology of the individual. Chapters 4 and 5 showed that respiration may be a significant component of active flux from diel migrants, and that it may be highly sensitive to temperature. A key question to answer therefore is, how much of the population does this apply to? And, does the fact that *E. triacantha* has a strong short-term response to temperature indicate that DVM is not in fact a daily occurrence by most individuals? Baker (1959) suggests that the population of *E. triacantha* may be split, with part of the population dwelling between 250-500 m during the day and part dwelling deeper, and this may influence the proportion that migrates up into the top 100 m. To better understand the response of the population to short-term temperature changes during DVM, we need to understand which individuals are migrating and how often. Whilst 125 m sampling intervals provided an adequate balance in terms of vertical resolution and species movements, it does not capture many of the finer-scale movements in the top 200 m that are of relevance in carbon flux across the thermocline. Therefore, a finer resolution sampling approach would help resolve the depth individuals reach, and the taxonomic and species-stage structure within the euphotic zone that controls export flux across it.

Finally, feeding cycle dynamics were shown to affect egestion and respiration flux from *E. triacantha*, and to be interdependent on seasonally varying properties of water temperature, mixed layer depth and chlorophyll concentration. To reduce uncertainties associated with the assumptions used for ingestion rate and feeding preference, we therefore need to better understand feeding dynamics diurnally, seasonally and with depth. This could be approached through a series of feeding experiments. However, for establishing feeding preference, this could be a time-consuming task and may have limited applicability depending on the feeding assemblage used. On the other hand, they may be very useful in targeted experiments to establish feeding duration under herbivory or carnivory. A more informative approach for feeding preference at the population level may combine gut content analyses with molecular and isotopic techniques (e.g. Phillips et al., 2009, Bowser et al., 2013). Together, such approaches would enable uncertainty related to complex individual behaviours to be reduced and to better constrain estimates of flux and their seasonal and spatial variability.

Glossary

A09	Autumn 2009
BCP	Biological Carbon Pump
C3	Oligotrophic, open ocean station, Scotia Sea
C	Carbon
chl-*a*	Chlorophyll
CO_2	Carbon dioxide
C_E	Active egestion flux
C_R	Active respiration flux
C_{TOT}	Total active carbon flux
CTD	Conductivity, Temperature, Depth profiler
DIC	Dissolved Inorganic Carbon
DW	Dry Weight
DVM	Diel/ Diurnal Vertical Migration
FP(s)	Faecal Pellet(s)
ICE	Ice Station, Scotia Sea
ML	Mixed Layer
MLD	Mixed Layer Depth
O_2	Oxygen
N	Nitrogen
P2	Time-series/ Process station 2 in the Scotia Sea
P3	Time-series/ Process station 3 in the Scotia Sea
PF	Polar Front
POC	Particulate Organic Carbon
R1	Ice-edge station, Scotia Sea
rDVM	Reverse DVM
RQ	Respiratory Quotient
SACCF	Southern Antarctic Circumpolar Current Front
S08	Summer 2008
SO	Southern Ocean
WW	Wet Weight

Appendix 1: Flow rate data

Table A1.1: Volume of water filtered by MOCNESS deployments on JR177 based on flow rate data which was used to calculate volume filtered on a few occasions when the flowmeter failed. Volume filtered was calculated using the duration of net haul (minutes) and volume filtered (m^3) when known from the flow meter. Missing volumes were then calculated using the known duration of net hauls for which the flowmeter failed. Numbers in blue are those calculated by the equation.

Station	Event #	Net	Net open depth (m)	Net closed depth (m)	Vol filtered (m3)	Duration (mins)
P3 Day	292	9	125	0	544	11
P3 Day	292	8	250	125	560	11.2
P3 Day	292	7	375	250	575	11.5
P3 Day	292	6	500	375	509	10.3
P3 Day	292	5	625	500	513	10.8
P3 Day	292	4	750	625	420	8.9
P3 Day	292	3	875	750	427	9.2
P3 Day	292	2	1000	875	456	15.3
P3 Night	276	9	125	5	361	7.4
P3 Night	276	8	250	125	528	11.2
P3 Night	276	7	375	250	455	9.3
P3 Night	276	6	500	375	477	10.2
P3 Night	276	5	610	500	463	9.2
P3 Night	276	4	750	610	359	7.9
P3 Night	276	3	875	750	653	17.7
P3 Night	276	2	1000	875	463	9.2
P3 Night	276	1	0	1000	1707	61.2
P2 Night	260	9	112	5	500.9	9.3
P2 Night	260	8	250	112	530	12
P2 Night	260	7	375	250	550	10.8
P2 Night	260	6	500	375	452	9.1
P2 Night	260	5	625	500	467	9.5
P2 Night	260	4	750	625	511	10.2
P2 Night	260	3	875	750	492	10.4
P2 Night	260	2	1000	875	214	8.8
P2 Night	260	1	0	1000	1534	62
P2 Day	249	9	125	5	537.6	
P2 Day	249	8	250	125	650	13
P2 Day	249	7	439	250	514	17
P2 Day	249	6	500	429	387	6
P2 Day	249	5	625	500	341	7
P2 Day	249	4	750	625	483	11
P2 Day	249	3	875	750	489	11
P2 Day	249	2	1000	875	207.8	9

C3 Night	143	9	125	4.8	521	10.3
C3 Night	143	8	250	125	522.6	10.6
C3 Night	143	7	375	250	573	11.6
C3 Night	143	6	500	375	511	10
C3 Night	143	5	625	500	676	13.8
C3 Night	143	4	750	625	576	11.9
C3 Night	143	3	875	750	456	9.5
C3 Night	143	2	1000	875	328	7.2
C3 Night	143	1	0	1000	1750	63
C3 Day	137	9	125	5	530	12
C3 Day	137	8	250	125	514	11.3
C3 Day	137	7	375	250	521	11.6
C3 Day	137	6	500	375	485	10.1
C3 Day	137	5	625	500	516	11.4
C3 Day	137	4	750	625	533	12.1
C3 Day	137	3	875	750	466	9.3
C3 Day	137	2	1000	875	444	8.4
C3 Day	137	1	0	1000	1662	59.3
R1 Night	61	9	125	5	499	10.7
R1 Night	61	8	250	125	299.1	5.9
R1 Night	61	7	375	250	558	11.1
R1 Night	61	6	500	375	668	12.8
R1 Night	61	5	625	500	357	6.8
R1 Night	61	4	750	625	502	9.8
R1 Night	61	3	875	750	630.3	12.3
R1 Night	61	2	1000	875	423	7.5
R1 Night	61	1	0	1000	1831	59.9
R1 Day	57	9	125	5	507	11
R1 Day	57	8	250	125	683	12
R1 Day	57	7	375	250	706	12
R1 Day	57	6	500	375	526	9.4
R1 Day	57	5	625	500	597	10.6
R1 Day	57	4	750	625	520	13.1
R1 Day	57	3	875	750	559	13.2
R1 Day	57	2	1000	875	516	11.4

Table A1.2: Volume of water filtered by MOCNESS deployments on JR200 (description as per previous)

Station	Event #	Net	Net open depth (m)	Net closed depth (m)	Volume filtered (m3)	Duration (mins)
P3 Night	183	9	125	5	583	9.4
P3 Night	183	8	250	125	781	12.1
P3 Night	183	7	375	250	735	13.3
P3 Night	183	6	500	375	726	11.7
P3 Night	183	5	625	500	812	13
P3 Night	183	4	750	625	671	11.7
P3 Night	183	3	875	750	651	11.2
P3 Night	183	2	1000	875	667	11.6
P3 Night	183	1	0	1000	2530	73
P3 Day	167	9	125	5	571	9.6
P3 Day	167	8	250	125	658	11
P3 Day	167	7	375	250	726	12.6
P3 Day	167	6	500	375	314	4
P3 Day	167	5	625	500	720	13
P3 Day	167	4	750	625	563	9
P3 Day	167	3	875	750	643	11
P3 Day	167	2	1000	875	762	14
P3 Day	167	1	0	1000	2633	61
P2 Day	152	9	125	5	758	10.4
P2 Day	152	8	250	125	643	11
P2 Day	152	7	375	250	520	9
P2 Day	152	6	500	375	556	8.8
P2 Day	152	5	625	500	501	8
P2 Day	152	4	750	625	484	7
P2 Day	152	3	875	750	484	7
P2 Day	152	2	1000	875	922	18
P2 Day	152	1	0	1000	2484	75
P2 Night	146	9	125	5	550	9.7
P2 Night	146	8	250	125	697	11.5
P2 Night	146	7	375	250	660	11.4
P2 Night	146	6	500	375	744	12.5
P2 Night	146	5	625	500	547	9.6
P2 Night	146	4	750	625	436	7.5
P2 Night	146	3	875	750	747	13
P2 Night	146	2	1000	875	719	12
P2 Night	146	1	0	1000	3781	81
C3 Day	72	9	125	5	765	13
C3 Day	72	8	250	125	601	10
C3 Day	72	7	375	250	704	13
C3 Day	72	6	500	375	717	13
C3 Day	72	5	625	500	723	13

C3 Day	72	4	750	625	689	12
C3 Day	72	3	875	750	684	12
C3 Day	72	2	1000	875	614	12
C3 Day	75	1	0	1000	3150	66
C3 Night	75	9	125	5	719	10.46
C3 Night	75	8	250	125	732	10.36
C3 Night	75	7	375	250	758	12.3
C3 Night	75	6	500	375	957	15.21
C3 Night	75	5	625	500	472	8.02
C3 Night	75	4	750	625	212	3.51
C3 Night	75	3	875	750	366	4.03
C3 Night	75	2	1000	875	1487	25.5
C3 Night	75	1	0	1000	3632	79
R1 Day	26	9	125	5	470	8.8
R1 Day	26	8	250	125	670	12
R1 Day	26	7	375	250	648	11.6
R1 Day	26	6	500	375	649	11.7
R1 Day	26	5	625	500	608	11.4
R1 Day	26	4	750	625	683	12.4
R1 Day	26	3	875	750	771	15
R1 Day	26	2	1000	875	600	11
R1 Day	26	1	0	1000	2762	64
R1 Night	12	9	125	7	495	9.7
R1 Night	12	8	250	125	503	9.6
R1 Night	12	7	375	250	688	12.7
R1 Night	12	6	500	375	581	10.5
R1 Night	12	5	625	500	883	15.9
R1 Night	12	4	750	625	808	14.5
R1 Night	12	3	875	750	557	10.1
R1 Night	12	2	1000	875	419	8.2
R1 Night	12	1	0	1000	2969	64

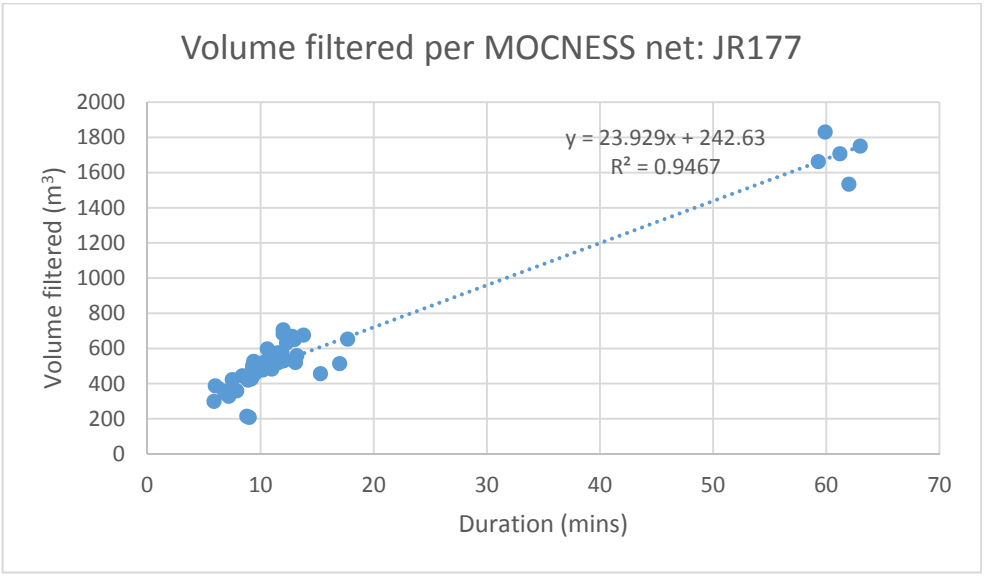

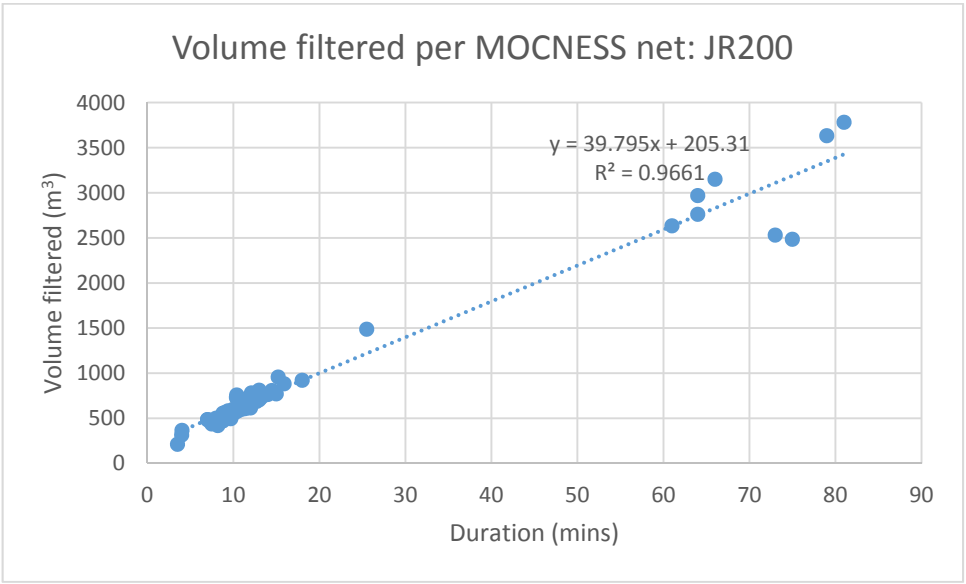

Figure A1.1: Plots of haul duration (minutes) and volume filtered (m^3) with equations used to calculate missing volumes for JR177 (top) and JR200 (bottom)

Appendix 2: Mesozooplankton abundance at individual stations

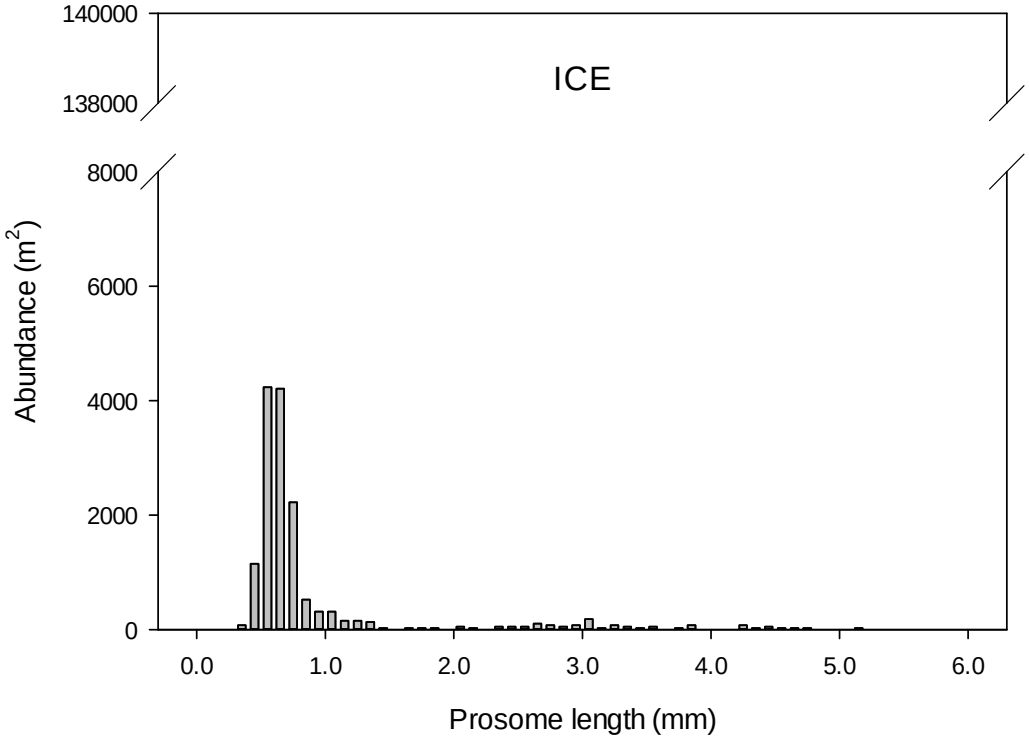

Figure A2.1: Average mesozooplankton abundance and size spectra based on prosome length at ICE

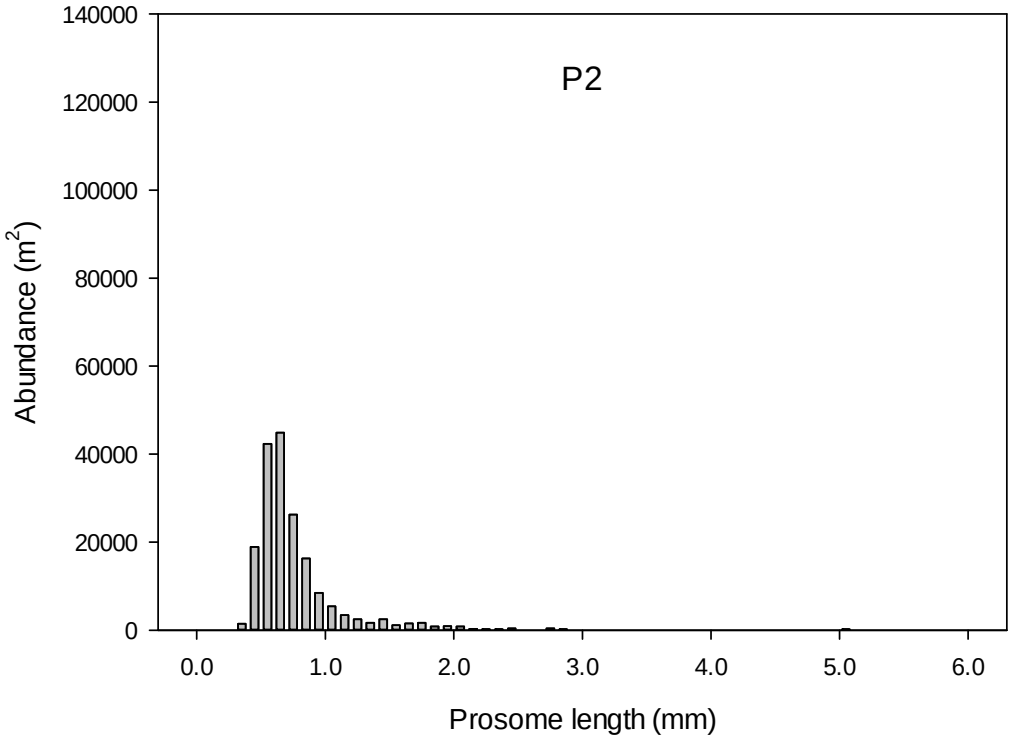

Figure A2.2: Average mesozooplankton abundance and size spectra based on prosome length at P2

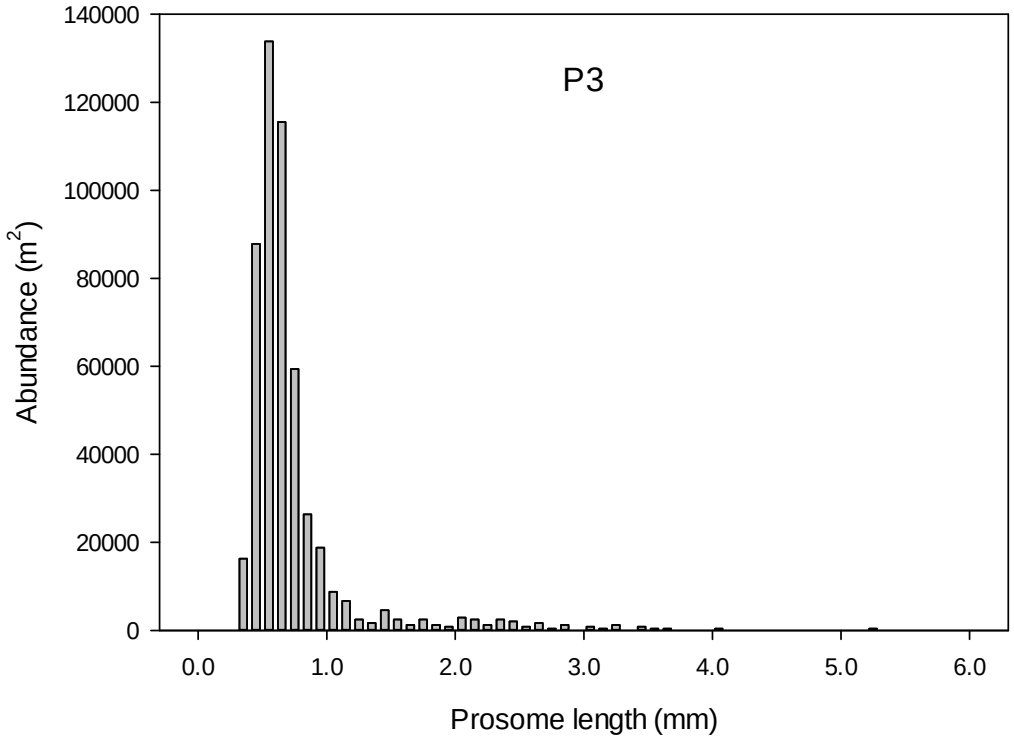

Figure A2.3: Average mesozooplankton abundance and size spectra based on prosome length at P3

Appendix 3: Temperature variation in respiration experiments

Table A3.1: Mean temperature (°C) at T1 for every measuring point for each *Euphausia triacantha* respiration experiment

Temp 1

Cruise	Exp #	T1	T2	T3	T4	T5	T6	T7
JR304	INC3	0.82	0.76	0.65	0.70	0.85	0.78	1.06
JR304	INC4	0.84	0.97	1.06	1.20			
JR304	INC5	-0.66	-0.15	0.47	1.14			
JR304	INC6	1.75	1.82	1.85	1.82			
JR304	INC7	1.44	1.57	1.45	1.70	1.64		
JR304	INC8	2.20	2.19	2.20	2.12	2.29		
JR15002	EXP1	1.43	1.43	1.43				
JR15002	EXP2	1.89	1.69	1.63				

Table A3.2: Mean temperature (°C) at T2 for every measuring point for each *Euphausia triacantha* respiration experiment

Temp 2

Cruise	Exp #	T1	T2	T3	T4	T5	T6	T7
JR304	INC3	3.23	3.32	2.94	3.32	3.36	3.41	3.38
JR304	INC4	2.83	2.91	2.95	2.99			
JR304	INC5	3.27	3.27	3.24	3.62			
JR304	INC6	3.15	3.16	3.13	3.13			
JR304	INC7	2.58	2.56	2.58	2.64	2.49		
JR304	INC8	3.34	3.31	3.16	3.11	3.03		
JR15002	EXP1	4.66	4.65	4.67				
JR15002	EXP2	4.80	4.62	4.77				

Table A3.3: 1 and 2 standard deviations for mean temperatures during each *Euphausia triacantha* respiration experiment

		T1		T2	
Cruise	**Exp #**	**1 s.d.**	**2 s.d.**	**1 s.d.**	**2 s.d.**
JR304	INC3	0.12	0.25	0.15	0.30
JR304	INC4	0.13	0.26	0.06	0.12
JR304	INC5	0.68	1.35	0.16	0.31
JR304	INC6	0.04	0.07	0.01	0.03
JR304	INC7	0.10	0.20	0.05	0.10
JR304	INC8	0.05	0.11	0.12	0.23
JR15002	EXP1	0.00	0.00	0.00	0.01
JR15002	EXP2	0.11	0.22	0.08	0.15

Table A3.4: Percentage of measuring points for each year within 1 and 2 standard deviations

	T1			T2	
	% in 1 s.d.	**% in 2 s.d.**		**% in 1 s.d.**	**% in 2 s.d.**
JR304	52%	97%	JR304	62%	97%
JR15002	67%	100%	JR15002	67%	100%

References

AGUZZI, J., COMPANY, J. B. & ABELLÓ, P. 2004. Locomotor activity rhythms of continental slope Nephrops norvegicus (Decapoda: Nephropidae). *Journal of Crustacean Biology,* 24**,** 282-290.

AL-MUTAIRI, H. & LANDRY, M. R. 2001. Active export of carbon and nitrogen at Station ALOHA by diel migrant zooplankton. *Deep Sea Research Part II: Topical Studies in Oceanography,* 48**,** 2083-2103.

ALCARAZ, M., ALMEDA, R., SAIZ, E., CALBET, A., DUARTE, C. M., AGUSTI, S., SANTIAGO, R. & ALONSO, A. 2013. Effects of temperature on the metabolic stoichiometry of Arctic zooplankton. *Biogeosciences,* 10**,** 689-697.

ANGEL, M. V. 1984. Detrital Organic Fluxes Through Pelagic Ecosystems. *In:* FASHAM, M. J. R. (ed.) *Flows of Energy and Materials in Marine Ecosystems.* New York: Plenum Press.

ANGEL, M. V. 1986. Vertical migrations in the oceanic realm: Possible causes and probable effects. *Contributions in Marine Science,* 27**,** 47-70.

ARIZA, A., GARIJO, J. C., LANDEIRA, J. M., BORDES, F. & HERNANDEZ-LEÓN, S. 2015. Migrant biomass and respiratory carbon flux by zooplankton and micronekton in the subtropical northeast Atlantic Ocean (Canary Islands). *Progress in Oceanography,* 134**,** 330-342.

ARMSTRONG, R. A., LEE, C., HEDGES, J. I., HONJO, S. & WAKEHAM, S. G. 2001. A new, mechanistic model for organic carbon fluxes in the ocean based on the quantitative association of POC with ballast minerals. *Deep Sea Research Part II: Topical Studies in Oceanography,* 49**,** 219-236.

ATKINSON, A. 1991. Life cycles of *Calanoides acutus*, *Calanus simillimus* and *Rhincalanus gigas* (Copepoda: Calanoida) within the Scotia Sea. *Marine Biology,* 109**,** 79-91.

ATKINSON, A. 1995. Omnivory and feeding selectivity in five copepod species during spring in the Bellingshausen Sea, Antarctica. *ICES Journal of marine Science,* 52**,** 385-396.

ATKINSON, A. 2004. Long-term decline in krill stock and increase in salps within the Southern Ocean. *Nature,* 432**,** 100-103.

ATKINSON, A., HILL, S., PAKHOMOV, E., SIEGEL, V., ANADON, R., CHIBA, S., DALY, K., DOWNIE, R., FIELDING, S., FRETWELL, P., GERRISH, L., HOSIE, G., JESSOPP, M., KAWAGUCHI, S., KRAFFT, B., LOEB, V., NISHIKAWA, J., PEAT, H., REISS, C., ROSS, R., LANGDON, B. Q., SCHMIDT, K., STEINBERG, D., SUBRAMANIAM, R., TARLING, G. & WARD, P. 2017. KRILLBASE: a circumpolar database of Antarctic krill and salp numerical densities, 1926-2016. *Earth System Science Data,* 9**,** 193-210.

ATKINSON, A. & PECK, J. 1988. A summer-winter comparison of zooplankton in the oceanic area around South Georgia. *Polar Biology,* 8**,** 463-473.

ATKINSON, A., SCHMIDT, K., FIELDING, S., KAWAGUCHI, S. & GEISSLER, P. A. 2012a. Variable food absorption by Antarctic krill: Relationships between diet, egestion rate and the composition and sinking rates of their fecal pellets. *Deep Sea Research Part II: Topical Studies in Oceanography,* 59–60**,** 147-158.

ATKINSON, A., WARD, P., HUNT, B. P. V., PAKHOMOV, E. A. & HOSIE, G. W. 2012b. An overview of Southern Ocean zooplankton data: abundance, biomass, feeding and functional relationships. *CCAMLR Science,* 19**,** 171-218.

ATKINSON, A., WARD, P. & MURPHY, E. J. 1996. Diel periodicity of subantarctic copepods: relationships between vertical migration, gut fullness and gut evacuation rate. *Journal of Plankton Research,* 18**,** 1387-1405.

ATKINSON, A., WARD, P., WILLIAMS, R. & POULET, S. A. 1992. Diel vertical migration and feeding of copepods at an oceanic site near South Georgia. *Marine Biology,* 113**,** 583-593.

BAKER, A. D. C. 1959. Distribution and life history of *Euphausia triacantha* Holt and Tattersall. University Press.
BÄMSTEDT, U. 1976. Studies on the deep-water pelagic community of Korsfjqrden, Western Norway Changes in the size and biochemical composition of Meganycitiphanes norvegica (Euphausiacea) in relation to its life cycle. *Sarsia,* 61**,** 15-30.
BÅMSTEDT, U. & KARLSON, K. 1998. Euphausiid predation on copepods in coastal waters of the Northeast Atlantic. *Marine Ecology Progress Series,* 172**,** 149-168.
BAYLY, I. 1986. Aspects of diel vertical migration in zooplankton, and its enigma variations. *Limnology in Australia.* Springer.
BAYLY, I. A. E. 1963. Reversed Diurnal Vertical Migration of Planktonic Crustacea in Inland Waters of Low Hydrogen Ion Concentration. *Nature,* 200**,** 704.
BELCHER, A., IVERSEN, M., MANNO, C., HENSON, S. A., TARLING, G. A. & SANDERS, R. 2016. The role of particle associated microbes in remineralization of fecal pellets in the upper mesopelagic of the Scotia Sea, Antarctica. *Limnology and Oceanography*.
BELCHER, A., MANNO, C., WARD, P., HENSON, S. A., SANDERS, R. & TARLING, G. A. 2017a. Copepod faecal pellet transfer through the meso-and bathypelagic layers in the Southern Ocean in spring. *Biogeosciences,* 14**,** 1511.
BELCHER, A., TARLING, G., MANNO, C., ATKINSON, A., WARD, P., SKARET, G., FIELDING, S., HENSON, S. & SANDERS, R. 2017b. The potential role of Antarctic krill faecal pellets in efficient carbon export at the marginal ice zone of the South Orkney Islands in spring. *Polar Biology***,** 1-13.
BENDTSEN, J., HILLIGSØE, K. M., HANSEN, J. L. & RICHARDSON, K. 2015. Analysis of remineralisation, lability, temperature sensitivity and structural composition of organic matter from the upper ocean. *Progress in Oceanography,* 130**,** 125-145.
BERGE, J., COTTIER, F., LAST, K. S., VARPE, Ø., LEU, E., SØREIDE, J., EIANE, K., FALK-PETERSEN, S., WILLIS, K. & NYGÅRD, H. 2009. Diel vertical migration of Arctic zooplankton during the polar night. *Biology Letters,* 5**,** 69-72.
BERNARD, A. & FRONEMAN, P. 2006. Euphausiid population structure and grazing in the Antarctic Polar Frontal Zone—austral autumn 2004. *African Journal of Marine Science,* 28**,** 569-579.
BERNARD, K. S., CIMINO, M., FRASER, W., KOHUT, J., OLIVER, M. J., PATTERSON-FRASER, D., SCHOFIELD, O. M. E., STATSCEWICH, H., STEINBERG, D. K. & WINSOR, P. 2017. Factors that affect the nearshore aggregations of Antarctic krill in a biological hotspot. *Deep Sea Research Part I: Oceanographic Research Papers,* 126**,** 139-147.
BIENFANG, P. 1980. Herbivore diet affects fecal pellet settling. *Canadian Journal of Fisheries and Aquatic Sciences,* 37**,** 1352-1357.
BIGG, G. R., JICKELLS, T. D., LISS, P. S. & OSBORN, T. J. 2003. The role of the oceans in climate. *International Journal of Climatology,* 23**,** 1127-1159.
BORRIONE, I. & SCHLITZER, R. 2013. Distribution and recurrence of phytoplankton blooms around South Georgia, Southern Ocean. *Biogeosciences,* 10**,** 217-231.
BOWSER, A. K., DIAMOND, A. W. & ADDISON, J. A. 2013. From puffins to plankton: a DNA-based analysis of a seabird food chain in the northern Gulf of Maine. *PLoS One,* 8**,** e83152.
BOYD, C. M., HEYRAUD, M. & BOYD, C. N. 1984. Feeding of the Antarctic krill *Euphausia superba*. *Journal of Crustacean Biology,* 4**,** 123-141.
BOYSEN-ENNEN, E., HAGEN, W., HUBOLD, G. & PIATKOWSKI, U. 1991. Zooplankton biomass in the ice-covered Weddell Sea, Antarctica. *Marine Biology,* 111**,** 227-235.
BRIERLEY, A. S. 2014. Diel vertical migration. *Current Biology,* 24**,** R1074-R1076.
BROECKER, W., PEACOCK, S., WALKER, S., WEISS, R., FAHRBACH, E., SCHRÖDER, M., MIKOLAJEWICZ, U., HEINZE, C., KEY, R. & PENG, T. H. 1998. How much deep water is formed in the Southern Ocean? *Journal of Geophysical Research: Oceans (1978–2012),* 103**,** 15833-15843.

BRULAND, K. & SILVER, M. 1981. Sinking rates of fecal pellets from gelatinous zooplankton (salps, pteropods, doliolids). *Marine Biology,* 63**,** 295-300.

BUESSELER, K. O. & BOYD, C. M. 2009. Shedding light on processes that control particle export and flux attenuation in the twilight zone of the open ocean. *Limnology and Oceanography,* 54**,** 1210-1232.

BUESSELER, K. O., LAMBORG, C. H., BOYD, P. W., LAM, P. J., TRULL, T. W., BIDIGARE, R. R., BISHOP, J. K., CASCIOTTI, K. L., DEHAIRS, F. & ELSKENS, M. 2007. Revisiting carbon flux through the ocean's twilight zone. *Science,* 316**,** 567-570.

BURD, A. B., HANSELL, D. A., STEINBERG, D. K., ANDERSON, T. R., ARÍSTEGUI, J., BALTAR, F., BEAUPRE, S. R., BUESSELER, K. O., DEHAIRS, F., JACKSON, G. A., KADKO, D. C., KOPPELMANN, R., LAMPITT, R. S., NAGATA, T., REINTHALER, T., ROBINSON, C., ROBISON, B. H., TAMBURINI, C. & TANAKA, T. 2010. Assessing the apparent imbalance between geochemical and biochemical indicators of meso-and bathypelagic biological activity: What the@ $♯! is wrong with present calculations of carbon budgets? *Deep Sea Research Part II: Topical Studies in Oceanography,* 57**,** 1557-1571.

CADÉE, G. C., GONZÁLEZ, H. & SCHNACK-SCHIEL, S. B. 1992. Krill diet affects faecal string settling. *Polar Biology,* 12**,** 75-80.

CAVAN, E. L., LE MOIGNE, F. A. C., POULTON, A. J., TARLING, G. A., WARD, P., DANIELS, C. J., FRAGOSO, G. M. & SANDERS, R. J. 2015. Attenuation of particulate organic carbon flux in the Scotia Sea, Southern Ocean, is controlled by zooplankton fecal pellets. *Geophysical Research Letters,* 42**,** 1-10.

CHISHOLM, S. W. 2000. Stirring times in the Southern Ocean. *Nature,* 407**,** 685.

CIAIS, P., SABINE, C., BALA, G., BOPP, L., BROVKIN, V., CANADELL, J., CHHABRA, A., DEFRIES, R., GALLOWAY, J., HEIMANN, M., JONES, C., LE QUÉRÉ, C., MYNENI, R. B., PIAO, S. & THORNTON, P. 2013. Carbon and Other Biogeochemical Cycles. *In:* STOCKER, T. F., QIN, D., PLATTNER, G.-K., TIGNOR, M., ALLEN, S. K., BOSCHUNG, J., NAUELS, A., XIA, Y., BEX, V. & MIDGLEY, P. M. (eds.) *Climate Change 2013: The Physical Science Basis. Contribution of Working Group I to the Fifth Assessment Report of the Intergovernmental Panel on Climate Change.* Cambridge, United Kingdom and New York, NY, USA: Cambridge University Press.

CLARK, J. 1956. *Electrochemical device for chemical analysis*. United States patent application US2913386A.

CLARK, P. U., PISIAS, N. G., STOCKER, T. F. & WEAVER, A. J. 2002. The role of the thermohaline circulation in abrupt climate change. *Nature,* 415**,** 863-869.

CLARKE, A. 1980. A reappraisal of the concept of metabolic cold adaptation in polar marine invertebrates. *Biological Journal of the Linnean Society,* 14**,** 77-92.

CLARKE, A. 1991. What is cold adaptation and how should we measure it? *American Zoologist,* 31**,** 81-92.

CLARKE, A. 2017. *Principles of Thermal Ecology: Temperature, Energy and Life*, Oxford University Press.

CLARKE, A. & PECK, L. S. 1991. The physiology of polar marine zooplankton. *Polar Research,* 10**,** 355-370.

CLARKE, K. & GORLEY, R. 2015. *PRIMER v7: User Manual/Tutorial,* Plymouth, PRIMER-E

CONOVER, R. 1978. Transformation of organic matter. *Marine ecology: a comprehensive, integrated treatise on life in oceans and coastal waters,* 4**,** 277-288.

CONSTABLE, A. J., NICOL, S. & STRUTTON, P. G. 2003. Southern Ocean productivity in relation to spatial and temporal variation in the physical environment. *Journal of Geophysical Research: Oceans,* 108.

CUSHING, D. 1951. The vertical migration of planktonic Crustacea. *Biological reviews,* 26**,** 158-192.

CUVIER, G. 1817. Le règne animal, Tome I. *Paris: Deterville*.

CUZIN-ROUDY, J., IRISSON, J. O., PENOT, F., KAWAGUCHI, S. & VALLET, C. 2014. Southern Ocean Euphausiids. *In:* DE BROYER, C., KOUBBI, P., GRIFFITHS, H. J., RAYMOND, B., D'UDEKEM D'ACOZ, C., VAN DE PUTTE, A. P., DANIS, B., DAVID, B., GRANT, S., GUTT, J., HELD, C., HOSIE, G., HUETTMANN, F., POST, A. & ROPERT-COUDERT, Y. (eds.) *Biogeographic Atlas of the Southern Ocean.* Cambridge UK: Scientific Committee on Antarctic Research.

DAGG, M. J., JACKSON, G. A. & CHECKLEY, D. M. 2014. The distribution and vertical flux of fecal pellets from large zooplankton in Monterey Bay and coastal California. *Deep Sea Research Part I: Oceanographic Research Papers,* 94**,** 72-86.

DAGG, M. J. & WALSER, W. E. 1986. The effect of food concentration on fecal pellet size in marine copepods. *Limnology and Oceanography,* 31**,** 1066-1071.

DAHMS, H.-U., TSENG, L.-C. & HWANG, J.-S. 2015. Biogeographic distribution of the cyclopoid copepod genus Oithona – from mesoscales to global scales. *Journal of Experimental Marine Biology and Ecology,* 467**,** 26-32.

DAM, H. G., ZHANG, X., BUTLER, M. & ROMAN, M. R. 1995. Mesozooplankton grazing and metabolism at the equator in the central Pacific: Implications for carbon and nitrogen fluxes. *Deep Sea Research Part II: Topical Studies in Oceanography,* 42**,** 735-756.

DAVID, P. 1965. The Chaetognatha of the Southern Ocean. *Biogeography and ecology in Antarctica.* Springer.

DE BAAR, H. J. W., DE JONG, J. T. M., BAKKER, D. C. E., LÖSCHER, B. M., VETH, C., BATHMANN, U. & SMETACEK, V. 1995. Importance of iron for plankton blooms and carbon dioxide drawdown in the Southern Ocean. *Nature,* 373**,** 412.

DEL GIORGIO, P. A. & DUARTE, C. M. 2002. Respiration in the open ocean. *Nature,* 420**,** 379.

DEMAS, J. N., DEGRAFF, B. A. & COLEMAN, P. B. 1999. Oxygen sensors based on luminescence quenching. *Analytical chemistry,* 71**,** 793A-800A.

DONNELLY, J., KAWALL, H., GEIGER, S. P. & TORRES, J. J. 2004. Metabolism of Antarctic micronektonic crustacea across a summer ice-edge bloom: respiration, composition, and enzymatic activity. *Deep-Sea Research Part II,* 51**,** 2225-2245.

DZIK, J. & JAZDZEWSKI, K. 1978. The euphausiid species of the Antarctic region. *Polaskie Archiwum Hydrobiologii,* 25**,** 589-605.

EGE, R. & KROGH, A. 1914. On the relation between the temperature and the respiratory exchange in fishes. *Internationale Revue der gesamten Hydrobiologie und Hydrographie,* 7**,** 48-55.

EL-SAYED, S. Z. 1994. *Southern Ocean ecology: the BIOMASS perspective*, Cambridge University Press.

EMERSON, C. W. & ROFF, J. C. 1987. Implications of fecal pellet size and zooplankton behaviour to estimates of pelagic-benthic carbon flux. *Marine Ecology Progress Series,* 35**,** 251-257.

ENRIGHT, J. 1977. Diurnal vertical migration: Adaptive significance and timing. Part 1. Selective advantage: A metabolic model 1. *Limnology and Oceanography,* 22**,** 856-872.

EPPLEY, R. W. & PETERSON, B. J. 1979. Particulate organic matter flux and planktonic new production in the deep ocean. *Nature,* 282**,** 677.

FALKOWSKI, P., SCHOLES, R. J., BOYLE, E., CANADELL, J., CANFIELD, D., ELSER, J., GRUBER, N., HIBBARD, K., HÖGBERG, P. & LINDER, S. 2000. The global carbon cycle: a test of our knowledge of earth as a system. *Science,* 290**,** 291-296.

FIELD, J. G., CLARKE, K. R. & WARWICK, R. M. 1982. A Practical Strategy for Analysing Multispecies Distribution Patterns. *Marine Ecology Progress Series,* 8**,** 37-52.

FLORES, H., VAN FRANEKER, J.-A., CISEWSKI, B., LEACH, H., VAN DE PUTTE, A. P., MEESTERS, E. H., BATHMANN, U. & WOLFF, W. J. 2011. Macrofauna under sea ice and in the open surface layer of the Lazarev Sea, Southern Ocean. *Deep Sea Research Part II: Topical Studies in Oceanography,* 58**,** 1948-1961.

FOLT, C. L. & BURNS, C. W. 1999. Biological drivers of zooplankton patchiness. *Trends in Ecology & Evolution,* 14**,** 300-305.
FORWARD, R. B. J. 1988. Diel vertical migration: Zooplankton photobiology and behaviour. *Annual Review of Oceanography and Marine Biology,* 26**,** 361-393.
FOWLER, S., BENAYOUN, G. & SMALL, L. F. 1971. Experimental studies on feeding, growth and assimilation in a Mediterranean euphausiid. *Thalassia jugosl,* 7**,** 35-47.
FOWLER, S. W. & SMALL, L. F. 1972. Sinking rates of euphausiid fecal pellets. *Limnology and Oceanography,* 17**,** 293-296.
FRANCOIS, R., HONJO, S., KRISHFIELD, R. & MANGANINI, S. 2002. Factors controlling the flux of organic carbon to the bathypelagic zone of the ocean. *Global Biogeochemical Cycles,* 16**,** 1087.
FRANGOULIS, C., BELKHIRIA, S., GOFFART, A. & HECQ, J.-H. 2001. Dynamics of copepod faecal pellets in relation to a *Phaeocystis* dominated phytoplankton bloom: characteristics, production and flux. *Journal of Plankton Research,* 23**,** 75-88.
FROST, B. W. 1972. Effects of size and concentration of food particles on the feeding behaviour of the marine planktonic copepod, *Calanus pacificus*. *Limnology and Oceanography,* 17**,** 805-815.
GALLIENNE, C. & ROBINS, D. 2001. Is *Oithona* the most important copepod in the world's oceans? *Journal of Plankton Research,* 23**,** 1421-1432.
GARABATO, A. C. N., POLZIN, K. L., KING, B. A., HEYWOOD, K. J. & VISBECK, M. 2004. Widespread Intense Turbulent Mixing in the Southern Ocean. *Science,* 303**,** 210-213.
GARÇON, V. C., OSCHLIES, A., DONEY, S. C., MCGILLICUDDY, D. & WANIEK, J. 2001. The role of mesoscale variability on plankton dynamics in the North Atlantic. *Deep Sea Research Part II: Topical Studies in Oceanography,* 48**,** 2199-2226.
GATEN, E., TARLING, G., DOWSE, H., KYRIACOU, C. & ROSATO, E. 2008. Is vertical migration in Antarctic krill (*Euphausia superba*) influenced by an underlying circadian rhythm? *Journal of Genetics,* 87**,** 473.
GIERING, S. L., SANDERS, R., LAMPITT, R. S., ANDERSON, T. R., TAMBURINI, C., BOUTRIF, M., ZUBKOV, M. V., MARSAY, C. M., HENSON, S. A. & SAW, K. 2014. Reconciliation of the carbon budget in the ocean's twilight zone. *Nature,* 507**,** 480-483.
GILLOOLY, J. F., BROWN, J. H., WEST, G. B., SAVAGE, V. M. & CHARNOV, E. L. 2001. Effects of size and temperature on metabolic rate. *Science,* 293**,** 2248-2251.
GLIWICZ, M. Z. 1986. Predation and the evolution of vertical migration in zooplankton. *Nature,* 320**,** 746.
GONZÁLEZ, H. E. 1992. The distribution and abundance of krill faecal material and oval pellets in the Scotia and Weddell Seas (Antarctica) and their role in particle flux. *Polar Biology,* 12**,** 81-91.
GONZÁLEZ, H. E., ORTIZ, V. C. & SOBARZO, M. 2000. The role of faecal material in the particulate organic carbon flux in the northern Humboldt Current, Chile (23 S), before and during the 1997–1998 El Niño. *Journal of Plankton Research,* 22**,** 499-529.
GONZALEZ, H. E. & SMETACEK, V. 1994. The possible role of the cyclopoid copepod *Oithona* in retarding vertical flux of zooplankton faecal material. *Marine Ecology Progress Series,* 113**,** 233-246.
GORSKY, G., OHMAN, M. D., PICHERAL, M., GASPARINI, S., STEMMANN, L., ROMAGNAN, J.-B., CAWOOD, A., PESANT, S., GARCÍA-COMAS, C. & PREJGER, F. 2010. Digital zooplankton image analysis using the ZooScan integrated system. *Journal of Plankton Research,* 32**,** 285-303.
HÄFKER, N. S., MEYER, B., LAST, K. S., POND, D. W., HÜPPE, L. & TESCHKE, M. 2017. Circadian Clock Involvement in Zooplankton Diel Vertical Migration. *Current Biology,* 27**,** 2194-2201. e3.

HAGEN, W. & AUEL, H. 2001. Seasonal adaptations and the role of lipids in oceanic zooplankton. *Zoology,* 104**,** 313-326.
HANSEN, F. C., MÖLLMANN, C., SCHÜTZ, U. & HINRICHSEN, H.-H. 2004. Spatio-temporal distribution of *Oithona similis* in the Bornholm Basin (Central Baltic Sea). *Journal of Plankton Research,* 26**,** 659-688.
HARRIS, R., WIEBE, P., LENZ, J., SKJOLDAL, H.-R. & HUNTLEY, M. 2000. *ICES zooplankton methodology manual*, Elsevier.
HAUCK, J. & VÖLKER, C. 2015. Rising atmospheric CO_2 leads to large impact of biology on Southern Ocean CO_2 uptake via changes of the Revelle factor. *Geophysical Research Letters,* 42**,** 1459-1464.
HAUCK, J., VÖLKER, C., WANG, T., HOPPEMA, M., LOSCH, M. & WOLF-GLADROW, D. A. 2013. Seasonally different carbon flux changes in the Southern Ocean in response to the southern annular mode. *Global Biogeochemical Cycles,* 27**,** 1236-1245.
HAUCK, J., VÖLKER, C., WOLF-GLADROW, D. A., LAUFKÖTTER, C., VOGT, M., AUMONT, O., BOPP, L., BUITENHUIS, E. T., DONEY, S. C. & DUNNE, J. 2015. On the Southern Ocean CO_2 uptake and the role of the biological carbon pump in the 21st century. *Global Biogeochemical Cycles,* 29**,** 1451-1470.
HAURY, L., MCGOWAN, J. & WIEBE, P. 1978. Patterns and processes in the time-space scales of plankton distributions. *Spatial pattern in plankton communities.* Springer.
HEINZE, C., MAIER-REIMER, E. & WINN, K. 1991. Glacial pCO_2 Reduction by the World Ocean: Experiments With the Hamburg Carbon Cycle Model. *Paleoceanography,* 6**,** 395-430.
HENSON, S. A., SANDERS, R., MADSEN, E., MORRIS, P. J., LE MOIGNE, F. & QUARTLY, G. D. 2011. A reduced estimate of the strength of the ocean's biological carbon pump. *Geophysical Research Letters,* 38**,** n/a-n/a.
HERNÁNDEZ-LEÓN, S. & GÓMEZ, M. 1996. Factors affecting the respiration/ETS ratio in marine zooplankton. *Journal of Plankton Research,* 18**,** 239-255.
HERNÁNDEZ-LEÓN, S., GÓMEZ, M., PAGAZAURTUNDUA, M. A., PORTILLO-HAHNEFELD, A. N., MONTERO, I. & ALMEIDA, C. 2001. Vertical distribution of zooplankton in Canary Island waters: implications for export flux. *Deep Sea Research Part I: Oceanographic Research Papers,* 48**,** 1071-1092.
HERNÁNDEZ-LEÓN, S. & IKEDA, T. 2005a. A global assessment of mesozooplankton respiration in the ocean. *Journal of Plankton Research,* 27**,** 153-158.
HERNÁNDEZ-LEÓN, S. & IKEDA, T. 2005b. Zooplankton Respiration. *In:* DEL GIORGIO, P. A. & WILLIAMS, P. J. L. B. (eds.) *Respiration in aquatic systems.* Oxford: Oxford Academic Press.
HIRCHE, H.-J. 1984. Temperature and metabolism of plankton—I. Respiration of antarctic zooplankton at different temperatures with a comparison of Antarctic and Nordic krill. *Comparative Biochemistry and Physiology Part A: Physiology,* 77**,** 361-368.
HIRCHE, H.-J. 1987. Temperature and plankton. *Marine biology,* 94**,** 347-356.
HOLETON, G. F. 1974. Metabolic cold adaptation of polar fish: fact or artefact? *Physiological Zoology,* 47**,** 137-152.
HOLOPAINEN, I. & RANTA, E. 1977. Respiration of *Pisidium amnicum* (Bivalvia) measured by infrared gas analysis. *Oikos,* 28**,** 196-200.
HOPKINS, T. L., LANCRAFT, T. M., TORRES, J. J. & DONNELLY, J. 1993. Community structure and trophic ecology of zooplankton in the Scotia Sea marginal ice zone in winter (1988). *Deep Sea Research I,* 40**,** 81-105.
HOPKINS, T. L. & TORRES, J. J. 1988. The zooplankton community in the vicinity of the ice edge, western Weddell Sea, March 1986. *Polar Biology,* 9**,** 79-87.
HORTON, T., KROH, A., BAILLY, N., BOURY-ESNAULT, N., BRANDÃO, S. N., COSTELLO, M. J., GOFAS, S., HERNANDEZ, F., MEES, J., PAULAY, G., POORE, G., ROSENBERG, G., STÖHR, S., DECOCK, W., DEKEYZER, S., VANDEPITTE, L., VANHOORNE, B., VRANKEN, S., ADAMS, M. J., ADLARD, R., ADRIAENS, P., AGATHA, S., AHN, K. J., AHYONG, S.,

ALVAREZ, B., ANDERSON, G., ANGEL, M., ARANGO, C., ARTOIS, T., ATKINSON, S., BARBER, A., BARTSCH, I., BELLAN-SANTINI, D., BERTA, A., BIELER, R., BŁAŻEWICZ, M., BOCK, P., BÖTTGER-SCHNACK, R., BOUCHET, P., BOYKO, C. B., BRAY, R., BRUCE, N. L., CAIRNS, S., CAMPINAS BEZERRA, T. N., CÁRDENAS, P., CARSTENS, E., CEDHAGEN, T., CHAN, B. K., CHAN, T. Y., CHENG, L., CHURCHILL, M., COLEMAN, C. O., COLLINS, A. G., CORDEIRO, R., CRANDALL, K. A., CRIBB, T., DAHDOUH-GUEBAS, F., DALY, M., DANELIYA, M., DAUVIN, J. C., DAVIE, P., DE GRAVE, S., DE MAZANCOURT, V., DEFAYE, D., D'HONDT, J. L., DIJKSTRA, H., DOHRMANN, M., DOLAN, J., DOWNEY, R., DRAPUN, I., EISENDLE-FLÖCKNER, U., EITEL, M., ENCARNAÇÃO, S. C. D., EPLER, J., EWERS-SAUCEDO, C., FABER, M., FEIST, S., FINN, J., FIŠER, C., FONSECA, G., FORDYCE, E., FOSTER, W., FRANK, J. H., FRANSEN, C., FURUYA, H., GALEA, H., GARCIA-ALVAREZ, O., GASCA, R., GAVIRIA-MELO, S., GERKEN, S., GHEERARDYN, H., GIBSON, D., GIL, J., GITTENBERGER, A., GLASBY, C., GLOVER, A., GORDON, D., GRABOWSKI, M., GRAVILI, C., GUERRA-GARCÍA, J. M., et al. 2017. World Register of Marine Species (WoRMS). WoRMS Editorial Board.

ICES. 2018. *Unit Conversion* [Online]. http://ocean.ices.dk/tools/unitconversion.aspx: International Council for the Exploration of the Sea (ICES). [Accessed 29/04/2018 2018].

IKEDA, T. 1970. Relationship between respiration rate and body size in marine plankton animals as a function of the temperature of habitat. *Bulletin of the Faculty of Fisheries Hokkaido University,* 21**,** 91-112.

IKEDA, T. 1985. Metabolic rates of epipelagic marine zooplankton as a function of body mass and temperature. *Marine Biology,* 85**,** 1-11.

IKEDA, T. 2013. Respiration and ammonia excretion of euphausiid crustaceans: synthesis toward a global-bathymetric model. *Marine Biology,* 160**,** 251-262.

IKEDA, T. & BRUCE, B. 1986. Metabolic activity and elemental composition of krill and other zooplankton from Prydz Bay, Antarctica, during early summer (November–December). *Marine Biology,* 92**,** 545-555.

IKEDA, T. & DIXON, P. 1984. The influence of feeding on the metabolic activity of Antarctic krill (*Euphausia superba* Dana). *Polar Biology,* 3**,** 1-9.

IKEDA, T. & FAY, E. 1981. Metabolic activity of zooplankton from the Antarctic Ocean. *Australian Journal of Marine and Freshwater Research,* 32**,** 921-930.

IKEDA, T., KANNO, Y., OZAKI, K. & SHINADA, A. 2001. Metabolic rates of epipelagic marine copepods as a function of body mass and temperature. *Marine Biology,* 139**,** 587-596.

IKEDA, T. & KIRKWOOD, R. 1989. Metabolism and body composition of two euphausiids (*Euphausia superba* and *E. crystallorophias*) collected from under the pack-ice off Enderby Land, Antarctica. *Marine Biology,* 100**,** 301-308.

IKEDA, T. & MITCHELL, A. 1982. Oxygen uptake, ammonia excretion and phosphate excretion by krill and other Antarctic zooplankton in relation to their body size and chemical composition. *Marine Biology,* 71**,** 283-298.

IVERSEN, M. H. & POULSEN, L. K. 2007. Coprorhexy, coprophagy, and coprochaly in the copepods *Calanus helgolandicus*, *Pseudocalanus elongatus*, and *Oithona similis*. *Marine Ecology Progress Series,* 350**,** 79-89.

IVLEVA, I. 1973. Quantitative correlation of temperature and respiratory rate in poikilothermic animals. *Pol. Arch. Hydrobiol,* 20**,** 283-300.

JOHANNES, R. E. & SATOMI, M. 1966. Composition and nutritive value of fecal pellets of a marine crustacean. *Limnology and Oceanography,* 11**,** 191-197.

JOHNSEN, G. H. & JAKOBSEN, P. J. 1987. The effect of food limitation on vertical migration in *Daphnia longispina*. *Limnology and Oceanography,* 32**,** 873-880.

JÓNASDÓTTIR, S. H., VISSER, A. W., RICHARDSON, K. & HEATH, M. R. 2015. Seasonal copepod lipid pump promotes carbon sequestration in the deep North Atlantic. *Proceedings of the National Academy of Sciences,* 112**,** 12122-12126.

JOUANDET, M.-P., TRULL, T. W., GUIDI, L., PICHERAL, M., EBERSBACH, F., STEMMANN, L. & BLAIN, S. 2011. Optical imaging of mesopelagic particles indicates deep carbon flux beneath a natural iron-fertilized bloom in the Southern Ocean. *Limnology and Oceanography,* 56**,** 1130-1140.

KAARTVEDT, S., LARSEN, T., HJELMSETH, K. & ONSRUD, M. S. 2002. Is the omnivorous krill *Meganyctiphanes norvegica* primarily a selectively feeding carnivore? *Marine Ecology Progress Series,* 228**,** 193-204.

KAHRU, M., MITCHELL, B. G., GILLE, S. T., HEWES, C. D. & HOLM-HANSEN, O. 2007. Eddies enhance biological production in the Weddell-Scotia Confluence of the Southern Ocean. *Geophysical Research Letters,* 34**,** n/a-n/a.

KHATIWALA, S., PRIMEAU, F. & HALL, T. 2009. Reconstruction of the history of anthropogenic CO_2 concentrations in the ocean. *Nature,* 462**,** 346.

KING, F. D. & PACKARD, T. T. 1975. Respiration and the activity of the respiratory electron transport system in marine zooplankton. *Limnology and Oceanography,* 20**,** 849-854.

KIØRBOE, T., MØHLENBERG, F. & HAMBURGER, K. 1985. Bioenergetics of the planktonic copepod *Acartia tonsa*: relation between feeding, egg production and respiration, and composition of specific dynamic action. *Marine Ecology Progress Series***,** 85-97.

KIRKWOOD, J. M. 1982. *A guide to the Euphausiacea of the Southern Ocean*, Information Services Section, Antarctic Division, Deptartment of Science and Technology.

KITTEL, W., WITEK, Z. & CZYKIETA, H. 1985. Distibution of Euphausia frigida, Euphausia crystallorophias, Euphausia triacantha and Thysanoessa macrura in the southern part of Drake Passage and in the Bransfield Strait during the 1983-1984 austral summer (BIOMASS-SIBEX). *Polish Polar Research,* 1.

KLEIBER, M. 1932. Body size and metabolism. *Hilgardia,* 6**,** 315-353.

KLEVJER, T. A., TARLING, G. A. & FIELDING, S. 2010. Swarm characteristics of Antarctic krill *Euphausia superba* relative to the proximity of land during summer in the Scotia Sea *Marine Ecology Progress Series,* 409**,** 157-170.

KLIMANT, I., KÜHL, M., GLUD, R. & HOLST, G. 1997. Optical measurement of oxygen and temperature in microscale: strategies and biological applications. *Sensors and Actuators B: Chemical,* 38**,** 29-37.

KNOX, G. A. 2007. Zooplankton. *In:* KNOX, G. A. (ed.) *Biology of the Southern Ocean.* 2 ed. United States of America: CRC Press.

KOMAR, P. D., MORSE, A. P., SMALL, L. F. & FOWLER, S. W. 1981. An analysis of sinking rates of natural copepod and euphausiid fecal pellets. *Limnology and Oceanography,* 26**,** 172-180.

KORB, R. E., WHITEHOUSE, M. J., THORPE, S. E. & GORDON, M. 2005. Primary production across the Scotia Sea in relation to the physico-chemical environment. *Journal of Marine Systems,* 57**,** 231-249.

KORB, R. E., WHITEHOUSE, M. J., WARD, P., GORDON, M., VENABLES, H. J. & POULTON, A. J. 2012. Regional and seasonal differences in microplankton biomass, productivity, and structure across the Scotia Sea: Implications for the export of biogenic carbon. *Deep Sea Research Part II: Topical Studies in Oceanography,* 59–60**,** 67-77.

KRUSE, S., BATHMANN, U. & BREY, T. 2009. Meso- and bathypelagic distribution and abundance of chaetognaths in the Atlantic sector of the Southern Ocean. *Polar Biology,* 32**,** 1359-1376.

KWON, E. Y., PRIMEAU, F. & SARMIENTO, J. L. 2009. The impact of remineralization depth on the air-sea carbon balance. *Nature Geoscience,* 2**,** 630-635.

LAMPERT, W. 1984. The measurement of respiration. *A manual on methods for the assessment of secondary productivity in fresh waters,* 17**,** 413-468.

LAMPERT, W. 1989. The adaptive significance of diel vertical migration of zooplankton. *Functional Ecology,* 3**,** 21-27.

LAMPITT, R. S., NOJI, T. & VON BODUNGEN, B. 1990. What happens to zooplankton faecal pellets? Implications for material flux. *Marine Biology,* 104**,** 15-23.
LANCRAFT, T. M., TORRES, J. J. & HOPKINS, T. L. 1989. Micronekton and macrozooplankton in the open waters near Antarctic ice edge zones (AMERIEZ 1983 and 1986). *Polar Biology,* 9**,** 225-233.
LANE, P., SMITH, S., URBAN, J. & BISCAYE, P. 1994. Carbon flux and recycling associated with zooplanktonic fecal pellets on the shelf of the Middle Atlantic Bight. *Deep Sea Research Part II: Topical Studies in Oceanography,* 41**,** 437-457.
LASKER, R. 1966. Feeding, Growth, Respiration, and Carbon Utilization of a Euphausiid Crustacean. *Journal of the Fisheries Research Board of Canada,* 23**,** 1291-1317.
LAST, KIM S., HOBBS, L., BERGE, J., BRIERLEY, ANDREW S. & COTTIER, F. 2016. Moonlight Drives Ocean-Scale Mass Vertical Migration of Zooplankton during the Arctic Winter. *Current Biology,* 26**,** 244-251.
LE QUÉRÉ, C., ANDRES, R. J., BODEN, T., CONWAY, T., HOUGHTON, R. A., HOUSE, J. I., MARLAND, G., PETERS, G. P., VAN DER WERF, G. R., AHLSTRÖM, A., ANDREW, R. M., BOPP, L., CANADELL, J. G., CIAIS, P., DONEY, S. C., ENRIGHT, C., FRIEDLINGSTEIN, P., HUNTINGFORD, C., JAIN, A. K., JOURDAIN, C., KATO, E., KEELING, R. F., KLEIN GOLDEWIJK, K., LEVIS, S., LEVY, P., LOMAS, M. P., B. , RAUPACH, M. R., SCHWINGER, J., SITCH, S., STOCKER, B. D., VIOVY, N., ZAEHLE, S. & ZENG, N. 2013. The global carbon budget 1959–2011. *Earth System Science Data,* 5**,** 165-185.
LE QUÉRÉ, C., BUITENHUIS, E. T., MORIARTY, R., ALVAIN, S., AUMONT, O., BOPP, L., CHOLLET, S., ENRIGHT, C., FRANKLIN, D. J., GEIDER, R. J., HARRISON, S. P., HIRST, A. G., LARSEN, S., LEGENDRE, L., PLATT, T., PRENTICE, I. C., RIVKIN, R. B., SAILLEY, S., SATHYENDRANATH, S., STEPHENS, N. & VALLINA, S. M. 2016. Role of zooplankton dynamics for Southern Ocean phytoplankton biomass and global biogeochemical cycles. *Biogeosciences,* 13**,** 4111-4133.
LEGENDRE, L. & RIVKIN, R. B. 2002. Fluxes of carbon in the upper ocean: regulation by food-web control nodes. *Marine Ecology Progress Series,* 242**,** 95-109.
LEGENDRE, L., RIVKIN, R. B., WEINBAUER, M. G., GUIDI, L. & UITZ, J. 2015. The microbial carbon pump concept: Potential biogeochemical significance in the globally changing ocean. *Progress in Oceanography,* 134**,** 432-450.
LEVIN, S. A. 1992. The problem of pattern and scale in ecology: the Robert H. MacArthur award lecture. *Ecology,* 73**,** 1943-1967.
LIBES, S. M. 2009. Organic Matter: Production and Destruction. *In:* LIBES, S. M. (ed.) *Introduction to Marine Biogeochemistry.* 2nd ed.: Academic Press.
LOEB, V., SIEGEL, V., HOLM-HANSEN, O., HEWITT, R., FRASER, W., TRIVELPIECE, W. & TRIVELPIECE, S. 1997. Effects of sea-ice extent and krill or salp dominance on the Antarctic food web. *Nature,* 387**,** 897-900.
LONGHURST, A. 1990. Vertical flux of respiratory carbon by oceanic diel migrant biota. *Deep-Sea Research,* 37**,** 685-694.
LONGHURST, A. 1998. The Southern Ocean. *In:* LONGHURST, A. (ed.) *Ecological Geography of the Sea.* London: Academic Press.
LONGHURST, A. R. 2010. *Ecological geography of the sea*, Academic Press.
LONGHURST, A. R. & HARRISON, W. 1989. The biological pump: Profiles of plankton production and consumption in the upper ocean. *Progress in Oceanography,* 22**,** 47-123.
LONGHURST, A. R. & HARRISON, W. G. 1988. Vertical nitrogen flux from the oceanic photic zone by diel migrant zooplankton and nekton. *Deep Sea Research Part A. Oceanographic Research Papers,* 35**,** 881-889.
LUTZ, M. J., CALDEIRA, K., DUNBAR, R. B. & BEHRENFELD, M. J. 2007. Seasonal rhythms of net primary production and particulate organic carbon flux to depth describe the

efficiency of biological pump in the global ocean. *Journal of Geophysical Research: Oceans,* 112.

MACKAS, D. L., DENMAN, K. L. & ABBOTT, M. R. 1985. Plankton patchiness: biology in the physical vernacular. *Bulletin of Marine Science,* 37**,** 652-674.

MACKEY, A. P., ATKINSON, A., HILL, S. L., WARD, P., CUNNINGHAM, N. J., JOHNSTON, N. M. & MURPHY, E. J. 2012. Antarctic macrozooplankton of the southwest Atlantic sector and Bellingshausen Sea: Baseline historical distributions (Discovery Investigations, 1928–1935) related to temperature and food, with projections for subsequent ocean warming. *Deep Sea Research Part II: Topical Studies in Oceanography,* 59–60**,** 130-146.

MAITI, K., CHARETTE, M. A., BUESSELER, K. O. & KAHRU, M. 2013. An inverse relationship between production and export efficiency in the Southern Ocean. *Geophysical Research Letters,* 40**,** 1557-1561.

MANNO, C., STOWASSER, G., ENDERLEIN, P., FIELDING, S. & TARLING, G. A. 2015. The contribution of zooplankton faecal pellets to deep-carbon transport in the Scotia Sea (Southern Ocean). *Biogeosciences,* 12**,** 1955-1965.

MANNO, C., TIRELLI, V., ACCORNERO, A. & UMANI, S. F. 2010. Importance of the contribution of *Limacina helicina* faecal pellets to the carbon pump in Terra Nova Bay (Antarctica). *Journal of Plankton Research,* 32**,** 145-152.

MARRARI, M., DALY, K. L., TIMONIN, A. & SEMENOVA, T. 2011. The zooplankton of Marguerite Bay, western Antarctic Peninsula—Part II: Vertical distributions and habitat partitioning. *Deep Sea Research Part II: Topical Studies in Oceanography,* 58**,** 1614-1629.

MARSAY, C. M., SANDERS, R. J., HENSON, S. A., PABORTSAVA, K., ACHTERBERG, E. P. & LAMPITT, R. S. 2015. Attenuation of sinking particulate organic carbon flux through the mesopelagic ocean. *Proceedings of the National Academy of Sciences***,** 201415311.

MARTIN, J. H. 1990. Glacial-interglacial CO_2 change: The Iron Hypothesis. *Paleoceanography,* 5**,** 1-13.

MARTIN, J. H., KNAUER, G. A., KARL, D. M. & BROENKOW, W. W. 1987. VERTEX: carbon cycling in the northeast Pacific. *Deep-Sea Research* 34**,** 267-285.

MARTÍNEZ-GARCÍA, S., FERNÁNDEZ, E., ARANGUREN-GASSIS, M. & TEIRA, E. 2009. In vivo electron transport system activity: a method to estimate respiration in natural marine microbial planktonic communities. *Limnology and Oceanography: Methods,* 7**,** 459-469.

MAUCHLINE, J. 1980. The Biology of Euphausiids. *Advances in Marine Biology,* 18.

MAUCHLINE, J. 1998. Physiology. *In:* BLAXTER, J. H. S., SOUTHWARD, A. J. & TYLER, P. A. (eds.) *The Biology of Calanoid Copepods.* London: Academic Press.

MAUCHLINE, J. & FISHER, L. 1969a. Distribution and Synomony. *In:* RUSSELL, F. S. & YONGE, M. (eds.) *Advances in Marine Biology.* Academic Press London.

MAUCHLINE, J. & FISHER, L. 1969b. The Species of Krill. *In:* RUSSELL, F. S. & YONGE, M. (eds.) *Advances in Marine Biology.* Academic Press London.

MAYZAUD, P., BOUTOUTE, M., GASPARINI, S., MOUSSEAU, L. & LEFEVRE, D. 2005. Respiration in marine zooplankton—the other side of the coin: CO_2 production. *Limnology and Oceanography,* 50**,** 291-298.

MCCLATCHIE, S. 1985. Feeding behaviour in *Meganyctiphanes norvegica* (M. Sars) (Crustacea: Euphausiacea). *Journal of Experimental Marine Biology and Ecology,* 86**,** 271-284.

MCWHINNIE, M. & MARCINIAK, P. 1964. *Temperature responses and tissue respiration in Antarctic Crustacea with particular reference to the krill Euphausia superba*, Wiley Online Library.

METZ, C. & SCHNACK-SCHIEL, S. B. 1995. Observations on carnivorous feeding in Antarctic calanoid copepods. *Marine Ecology Progress Series***,** 71-75.

MEYER, B., AUERSWALD, L., SIEGEL, V., SPAHIC, S., PAPE, C., FACH, B. A., TESCHKE, M., LOPATA, A. L. & FUENTES, V. 2010. Seasonal variation in body composition, metabolic activity, feeding, and growth of adult krill *Euphausia superba* in the Lazarev Sea. *Marine Ecology Progress Series,* 398**,** 1-18.

MICHAEL, E. L. R. 1911. *Classification and Vertical Distribution of the Chaetognatha of the San Diego Region: Including Redescriptions of Some Doubtful Species of the Group*, The University Press.

MIKALOFF FLETCHER, S. E., GRUBER, N., JACOBSON, A. R., DONEY, S. C., DUTKIEWICZ, S., GERBER, M., FOLLOWS, M., JOOS, F., LINDSAY, K. & MENEMENLIS, D. 2006. Inverse estimates of anthropogenic CO_2 uptake, transport, and storage by the ocean. *Global Biogeochemical Cycles,* 20.

MOCK, T., DIECKMANN, G., HAAS, C., KRELL, A., TISON, J.-L., BELEM, A., PAPADIMITRIOU, S. & THOMAS, D. N. 2002. Micro-optodes in sea ice: a new approach to investigate oxygen dynamics during sea ice formation. *Aquatic Microbial Ecology,* 29**,** 297-306.

MÖLLER, K. O., JOHN, M. S., TEMMING, A., FLOETER, J., SELL, A. F., HERRMANN, J.-P. & MÖLLMANN, C. 2012. Marine snow, zooplankton and thin layers: indications of a trophic link from small-scale sampling with the Video Plankton Recorder. *Marine Ecology Progress Series,* 468**,** 57-69.

MOORE, J. K., ABBOTT, M. R. & RICHMAN, J. G. 1999. Location and dynamics of the Antarctic Polar Front from satellite sea surface temperature data. *Journal of Geophysical Research: Oceans,* 104**,** 3059-3073.

MORATA, N. & SEUTHE, L. 2014. Importance of bacteria and protozooplankton for faecal pellet degradation. *Oceanologia,* 56**,** 565-581.

MORTOLA, J. P. 2004. Breathing around the clock: an overview of the circadian pattern of respiration. *European journal of applied physiology,* 91**,** 119-129.

MURPHY, E. J., WATKINS, J. L., TRATHAN, P. N., REID, K., MEREDITH, M. P., THORPE, S. E., JOHNSTON, N. M., CLARKE, A., TARLING, G. A., COLLINS, M. A., FORCADA, J., SHREEVE, R. S., ATKINSON, A., KORB, R., WHITEHOUSE, M. J., WARD, P., RODHOUSE, P. G., ENDERLEIN, P., HIRST, A. G., MARTIN, A. R., HILL, S. L., STANILAND, I. J., POND, D. W., BRIGGS, D. R., CUNNINGHAM, N. J. & FLEMING, A. H. 2007. Spatial and temporal operation of the Scotia Sea ecosystem: a review of large-scale links in a krill centred food web. *Philosophical Transactions of the Royal Society B: Biological Sciences,* 362**,** 113-148.

NEILL, W. E. 1990. Induced vertical migration in copepods as a defence against invertebrate predation. *Nature,* 345**,** 524-526.

NOJI, T. T., ESTEP, K. W., MACINTYRE, F. & NORRBIN, F. 1991. Image analysis of faecal material grazed upon by three species of copepods: evidence for coprorhexy, coprophagy and coprochaly. *Journal of the Marine Biological Association of the United Kingdom,* 71**,** 465-480.

O'CONNOR, M. P., KEMP, S. J., AGOSTA, S. J., HANSEN, F., SIEG, A. E., WALLACE, B. P., MCNAIR, J. N. & DUNHAM, A. E. 2007. Reconsidering the mechanistic basis of the metabolic theory of ecology. *Oikos,* 116**,** 1058-1072.

OHMAN, M. D. 1990. The demographic benefits of diel vertical migration by zooplankton. *Ecological Monographs,* 60**,** 257-281.

OMORI, M. & IKEDA, T. 1984. *Methods in marine zooplankton ecology*.

ORSI, A. H., WHITWORTH, T. & NOWLIN, W. D. 1995. On the meridional extent and fronts of the Antarctic Circumpolar Current. *Deep Sea Research Part I: Oceanographic Research Papers,* 42**,** 641-673.

PACKARD, G. C. & BOARDMAN, T. J. 1999. The use of percentages and size-specific indices to normalize physiological data for variation in body size: wasted time, wasted effort? *Comparative Biochemistry and Physiology Part A,* 122**,** 37-44.

PACKARD, T. 1971. The Measurement of Respiratory Electron-transport Activity in Marine Phytoplankton. *Journal of Marine Research,* 29**,** 235-244.

PAKHOMOV, E., FRONEMAN, P. & PERISSINOTTO, R. 2002. Salp/krill interactions in the Southern Ocean: spatial segregation and implications for the carbon flux. *Deep Sea Research Part II: Topical Studies in Oceanography,* 49**,** 1881-1907.

PAKHOMOV, E. & MCQUAID, C. 1996. Distribution of surface zooplankton and seabirds across the Southern Ocean. *Polar Biology,* 16**,** 271-286.

PAKHOMOV, E. A. & FRONEMAN, P. W. 2004a. Zooplankton dynamics in the eastern Atlantic sector of the Southern Ocean during the austral summer 1997/1998—Part 1: Community structure. *Deep Sea Research Part II: Topical Studies in Oceanography,* 51**,** 2599-2616.

PAKHOMOV, E. A. & FRONEMAN, P. W. 2004b. Zooplankton dynamics in the eastern Atlantic sector of the Southern Ocean during the austral summer 1997/1998—Part 2: Grazing impact. *Deep Sea Research Part II: Topical Studies in Oceanography,* 51**,** 2617-2631.

PAKHOMOV, E. A., VERHEYE, H. M., ATKINSON, A., LAUBSCHER, R. K. & TAUNTON-CLARK, J. 1997. Structure and grazing impact of the mesozooplankton community during late summer 1994 near South Georgia, Antarctica. *Polar Biology,* 18**,** 180-192.

PARANJAPE, M. A. 1967. Molting and respiration of euphausiids. *Journal of the Fisheries Board of Canada,* 24**,** 1229-1240.

PARK, J., OH, I.-S., KIM, H.-C. & YOO, S. 2010. Variability of SeaWiFs chlorophyll-*a* in the southwest Atlantic sector of the Southern Ocean: Strong topographic effects and weak seasonality. *Deep Sea Research Part I: Oceanographic Research Papers,* 57**,** 604-620.

PARK, T. 1978. Calanoid Copepods (Aetideidae and Euchaetidae) from Antarctic and Subantarctic Waters. *In:* PAWSON, D. L. (ed.) *Biology of the Antarctic Seas VII.* Washington DC: American Geophysical Union.

PARK, T. 1993. Calanoid Copepods of the Genus Euaugaptilus from Antarctic and Subantarctic Waters. *In:* CAIRNS, S. D. (ed.) *Biology of the Antarctic Seas XXII.* Washington DC: American Geophysical Union.

PASSOW, U. & CARLSON, C. A. 2012. The biological pump in a high CO_2 world. *Marine Ecology Progress Series,* 470**,** 249-271.

PEARRE, S. 1979a. On the adaptive significance of vertical migration. *Limnology and Oceanography,* 24**,** 781-782.

PEARRE, S. 1979b. Problems of detection and interpretation of vertical migration. *Journal of Plankton Research,* 1**,** 29-44.

PEARRE, S. 2000. Long-term changes in diel vertical migration behavior: more ups and downs. *Marine Ecology Progress Series,* 197**,** 305-307.

PEARRE, S. 2003. Eat and run? The hunger/satiation hypothesis in vertical migration: history, evidence and consequences. *Biological Reviews,* 78**,** 1-79.

PECK, L. S. 1998. Feeding, metabolism and metabolic scope in Antarctic marine ectotherms. *In:* PÖRTNER, H. O. & PLAYLE, R. C. (eds.) *Cold Ocean Physiology.* Cambridge: Cambridge University Press.

PEINERT, R. 1989. Food web structure and loss rate. *Productivity of the Ocean. Present and Past***,** 35-48.

PHILLIPS, R. A., BEARHOP, S., MCGILL, R. A. & DAWSON, D. A. 2009. Stable isotopes reveal individual variation in migration strategies and habitat preferences in a suite of seabirds during the nonbreeding period. *Oecologia,* 160**,** 795-806.

PIATKOWSKI, U. 1985. Distribution, abundance and diurnal migration of macrozooplankton in Antarctic surface waters. *Meeresforschung-Reports on Marine Research,* 30**,** 264-279.

PIATKOWSKI, U., RODHOUSE, P. G., WHITE, M. G., BONE, D. G. & SYMON, C. 1994. Nekton community of the Scotia Sea as sampled by the RMT25 during austral summer. *Marine Ecology Progress Series,* 112**,** 13-28.

PICHERAL, M., COLIN, S. & IRISSON, J. O. 2017. EcoTaxa, a tool for the taxonomic classification of images. http://ecotaxa.obs-vlfr.fr.
PIERSON, J. J. 2008. *Forays and Foraging in Marine Zooplankton* [Online]. Available: http://www.planktoneer.com/forays.html [Accessed 09/07/2018 2018].
PLOUG, H., IVERSEN, M. & FISCHER, G. 2008. Ballast, sinking velocity and apparent diffusivity in marine snow and zooplankton fecal pellets: Implications for substrate turnover by attached bacteria. *Limnology and Oceanography,* 53**,** 1878-1886.
PÖRTNER, H.-O. 2002. Climate variations and the physiological basis of temperature dependent biogeography: systemic to molecular hierarchy of thermal tolerance in animals. *Comparative Biochemistry and Physiology Part A: Molecular & Integrative Physiology,* 132**,** 739-761.
POULSEN, L. K. & IVERSEN, M. H. 2008. Degradation of copepod fecal pellets: key role of protozooplankton. *Marine Ecology Progress Series,* 367**,** 1-13.
PRESENS GMBH, P. S. G. 2014. Oxygen sensor spots PSt3/Pst6: Instruction Manual. Presens Precision Sensing GmbH.
PRESENS GMBH, P. S. G. 2016. PreSens Oxygen Calculator Software. 3.0.0 ed.: Presens Precision Sensing GmbH.
PUTZEYS, S., YEBRA, L., ALMEIDA, C., BÉCOGNÉE, P. & HERNÁNDEZ-LEÓN, S. 2011. Influence of the late winter bloom on migrant zooplankton metabolism and its implications on export fluxes. *Journal of Marine Systems,* 88**,** 553-562.
QUETIN, L. B. & ROSS, R. M. 1991. Behavioral and physiological characteristics of the Antarctic krill, *Euphausia superba*. *American Zoologist,* 31**,** 49-63.
RASBAND, W. S. 1997-2016. ImageJ. U. S. National Institutes of Health, Bethesda, Maryland, USA.
ROBINSON, C., STEINBERG, D. K., ANDERSON, T. R., ARÍSTEGUI, J., CARLSON, C. A., FROST, J. R., GHIGLIONE, J.-F., HERNÁNDEZ-LEÓN, S., JACKSON, G. A. & KOPPELMANN, R. 2010. Mesopelagic zone ecology and biogeochemistry–a synthesis. *Deep Sea Research Part II: Topical Studies in Oceanography,* 57**,** 1504-1518.
SABOROWSKI, R., BRÖHL, S., TARLING, G. & BUCHHOLZ, F. 2002. Metabolic properties of Northern krill, *Meganyctiphanes norvegica*, from different climatic zones. I. Respiration and excretion. *Marine Biology,* 140**,** 547-556.
SABOROWSKI, R., SALOMON, M. & BUCHHOLZ, F. 2000. The physiological response of Northern krill (*Meganyctiphanes norvegica*) to temperature gradients in the Kattegat. *Hydrobiologia,* 426**,** 157-160.
SAMEOTO, D. 1980. Relationships between stomach contents and vertical migration in *Meganyctiphanes norvegica*, *Thysanoessa raschii* and *T. inermis* (Crustacea Euphausiacea). *Journal of Plankton Research,* 2**,** 129-143.
SAMPEI, M., FOREST, A., SASAKI, H., HATTORI, H., MAKABE, R., FUKUCHI, M. & FORTIER, L. 2009. Attenuation of the vertical flux of copepod fecal pellets under Arctic sea ice: evidence for an active detrital food web in winter. *Polar Biology,* 32**,** 225-232.
SCHLITZER, R. 2002. Carbon export fluxes in the Southern Ocean: results from inverse modeling and comparison with satellite-based estimates. *Deep Sea Research Part II: Topical Studies in Oceanography,* 49**,** 1623-1644.
SCHMIDT, K., SCHLOSSER, C., ATKINSON, A., FIELDING, S., VENABLES, H. J., WALUDA, C. M. & ACHTERBERG, E. P. 2016. Zooplankton gut passage mobilizes lithogenic iron for ocean productivity. *Current Biology,* 26**,** 2667-2673.
SCHMIDTKO, S., JOHNSON, G. C. & LYMAN, J. M. 2013. MIMOC: A global monthly isopycnal upper-ocean climatology with mixed layers. *Journal of Geophysical Research: Oceans,* 118**,** 1658-1672.
SCHNACK-SCHIEL, S. & MUJICA, A. 1994. The zooplankton of the Antarctic Peninsula region. *Southern Ocean ecology. The BIOMASS perspective***,** 79-92.

SCHOENING, T., DURDEN, J., PREUSS, I., ALBU, A. B., PURSER, A., DE SMET, B., DOMINGUEZ-CARRIÓ, C., YESSON, C., DE JONGE, D. & LINDSAY, D. 2017. Report on the Marine Imaging Workshop 2017. *Research Ideas and Outcomes,* 3**,** e13820.

SCHOLANDER, P., FLAGG, W., WALTERS, V. & IRVING, L. 1953. Climatic adaptation in arctic and tropical poikilotherms. *Physiological Zoology,* 26**,** 67-92.

SECOR, S. M. 2009. Specific dynamic action: a review of the postprandial metabolic response. *Journal of Comparative Physiology B,* 179**,** 1-56.

SEEAR, P. J., GOODALL-COPESTAKE, W. P., FLEMING, A. H., ROSATO, E. & TARLING, G. A. 2012. Seasonal and spatial influences on gene expression in Antarctic krill *Euphausia superba*. *Marine Ecology Progress Series,* 467**,** 61-75.

SHARQAWY, M. H., LIENHARD, J. H. & ZUBAIR, S. M. 2010. Thermophysical properties of seawater: a review of existing correlations and data. *Desalination and Water Treatment,* 16**,** 354-380.

SIEFKEN, M. & ARMITAGE, K. B. 1968. Seasonal variation in metabolism and organic nutrients in three *Diaptomus* (Crustacea: Copepoda). *Comparative Biochemistry and Physiology,* 24**,** 591-609.

SIEGEL, D. A., BUESSELER, K. O., DONEY, S. C., SAILLEY, S. F., BEHRENFELD, M. J. & BOYD, P. W. 2014. Global assessment of ocean carbon export by combining satellite observations and food-web models. *Global Biogeochemical Cycles,* 28**,** 181-196.

SIEGEL, V. 1987. Age and growth of Antarctic Euphausiacea (Crustacea) under natural conditions. *Marine Biology,* 96**,** 483-495.

SIMS, D. W., SOUTHALL, E. J., TARLING, G. A. & METCALFE, J. D. 2005. Habitat-specific normal and reverse diel vertical migration in the plankton-feeding basking shark. *Journal of Animal Ecology,* 74**,** 755-761.

SMALL, L., FOWLER, S. & ÜNLÜ, M. 1979. Sinking rates of natural copepod fecal pellets. *Marine Biology,* 51**,** 233-241.

SMALL, L. F. & HEBARD, J. F. 1967. Respiration of a vertically migrating marine crustacean *Euphausia pacifica* Hansen. *Limnology and Oceanography,* 12**,** 272-280.

SMALL, L. F., HEBARD, J. F. & MCINTIRE, C. D. 1966. Respiration in euphausiids. *Nature,* 211**,** 1210.

SMAYDA, T. J. 1969. Some measurements of the sinking rate of fecal pellets. *Limnology and Oceanography,* 14**,** 621-625.

STAMIESZKIN, K., PERSHING, A. J., RECORD, N. R., PILSKALN, C. H., DAM, H. G. & FEINBERG, L. R. 2015. Size as the master trait in modeled copepod fecal pellet carbon flux. *Limnology and Oceanography,* 60**,** 2090-2107.

STEFFENSEN, J. F. 2002. Metabolic cold adaptation of polar fish based on measurements of aerobic oxygen consumption: fact or artefact? Artefact! *Comparative Biochemistry and Physiology - Part A: Molecular and Integrative Physiology,* 132**,** 789-795.

STEINBERG, D. K., CARLSON, C. A., BATES, N. R., GOLDTHWAIT, S. A., MADIN, L. P. & MICHAELS, A. F. 2000. Zooplankton vertical migration and the active transport of dissolved organic and inorganic carbon in the Sargasso Sea. *Deep Sea Research Part I: Oceanographic Research Papers,* 47**,** 137-158.

STEINBERG, D. K., GOLDTHWAIT, S. A. & HANSELL, D. A. 2002. Zooplankton vertical migration and the active transport of dissolved organic and inorganic nitrogen in the Sargasso Sea. *Deep Sea Research Part I: Oceanographic Research Papers,* 49**,** 1445-1461.

STEINBERG, D. K. & LANDRY, M. R. 2017. Zooplankton and the Ocean Carbon Cycle. *Annual Review of Marine Science,* 9**,** 413-444.

STEINBERG, D. K., VAN MOOY, B. A., BUESSELER, K. O., BOYD, P. W., KOBARI, T. & KARL, D. M. 2008. Bacterial vs zooplankton control of sinking particle flux in the ocean's twilight zone. *Limnology and Oceanography,* 53**,** 1327-1338.

STICH, H. B. & LAMPERT, W. 1981. Predator evasion as an explanation of diurnal vertical migration by zooplankton. *Nature,* 293**,** 396.

STOCKER, T. F., QIN, D., PLATTNER, G.-K., ALEXANDER, L. V., ALLEN, S. K., BINDOFF, N. L., BRÉON, F.-M., CHURCH, J. A., CUBASCH, U., EMORI, S., FORSTER, P., FRIEDLINGSTEIN, P., GILLETT, N., GREGORY, J. M., HARTMANN, D. L., JANSEN, E., KIRTMAN, B., KNUTTI, R., KRISHNA KUMAR, K., LEMKE, P., MAROTZKE, J., MASSON-DELMOTTE, V., MEEHL, G. A., MOKHOV, I. I., PIAO, S., RAMASWAMY, V., RANDALL, D., RHEIN, M., ROJAS, M., SABINE, C., SHINDELL, D., TALLEY, L. D., VAUGHAN, D. G. & XIE, S.-P. 2013. Technical Summary. *In:* STOCKER, T. F., QIN, D., PLATTNER, G.-K., TIGNOR, M., ALLEN, S. K., BOSCHUNG, J., NAUELS, A., XIA, Y., BEX, V. & MIDGLEY, P. M. (eds.) *Climate Change 2013: The Physical Science Basis. Contribution of Working Group I to the Fifth Assessment Report of the Intergovernmental Panel on Climate Change.* Cambridge, United Kingdom and New York, NY, USA: Cambridge University Press.

STOWASSER, G., ATKINSON, A., MCGILL, R. A. R., PHILLIPS, R. A., COLLINS, M. A. & POND, D. W. 2012. Food web dynamics in the Scotia Sea in summer: A stable isotope study. *Deep Sea Research Part II: Topical Studies in Oceanography,* 59–60**,** 208-221.

SVENSEN, C., WEXELS RISER, C., REIGSTAD, M. & SEUTHE, L. 2012. Degradation of copepod faecal pellets in the upper layer: role of microbial community and *Calanus finmarchicus*. *Marine Ecology Progress Series,* 462**,** 39-49.

TAKAHASHI, T., SUTHERLAND, S. C., SWEENEY, C., POISSON, A., METZL, N., TILBROOK, B., BATES, N., WANNINKHOF, R., FEELY, R. A., SABINE, C., OLAFSSON, J. & NOJIRI, Y. 2002. Global sea–air CO_2 flux based on climatological surface ocean pCO_2, and seasonal biological and temperature effects. *Deep Sea Research Part II: Topical Studies in Oceanography,* 49**,** 1601-1622.

TALLEY, L. D., PICKARD, G. L., EMERY, W. J. & SWIFT, J. H. 2011. Southern Ocean. *In:* TALLEY, L. D., PICKARD, G. L., EMERY, W. J. & SWIFT, J. H. (eds.) *Descriptive Physical Oceanography : An Introduction.* London, UNITED KINGDOM: Elsevier Science & Technology.

TARLING, G., BUCHHOLZ, F. & MATTHEWS, J. B. L. 1999. The effect of lunar eclipse on the vertical migration behaviour of *Meganyctiphanes norvegica* (Crustacea: Euphausiacea) in the Ligurian Sea. *Journal of Plankton Research,* 21**,** 1475-1488.

TARLING, G., WARD, P. & THORPE, S. 2017. Spatial distributions of Southern Ocean mesozooplankton communities have been resilient to long-term surface warming. *Global Change Biology***,** 1-11.

TARLING, GERAINT A. 2015. Marine Ecology: A Wonderland of Marine Activity in the Arctic Night. *Current Biology,* 25**,** R1088-R1091.

TARLING, G. A., JARVIS, T., EMSLEY, S. M. & MATTHEWS, J. B. L. 2002. Midnight sinking behaviour in *Calanus finmarchicus* a response to satiation or krill predation? *Marine Ecology Progress Series,* 240**,** 183-194.

TARLING, G. A. & JOHNSON, M. L. 2006. Satiation gives krill that sinking feeling. *Current Biology,* 16**,** R83-R84.

TARLING, G. A., MATTHEWS, J. B. L., DAVID, P., GUERIN, O. & BUCHHOLZ, F. 2001. The swarm dynamics of northern krill (*Meganyctiphanes norvegica*) and pteropods (*Cavolinia inflexa*) during vertical migration in the Ligurian Sea observed by an acoustic Doppler current profiler. *Deep Sea Research Part I: Oceanographic Research Papers,* 48**,** 1671-1686.

TARLING, G. A. & THORPE, S. E. 2017. Oceanic swarms of Antarctic krill perform satiation sinking. *Proceedings of the Royal Society B,* 284**,** 20172015.

TARLING, G. A., WARD, P., ATKINSON, A., COLLINS, M. A. & MURPHY, E. J. 2012. DISCOVERY 2010: Spatial and temporal variability in a dynamic polar ecosystem. *Deep-Sea Research Part II-Topical Studies in Oceanography,* 59**,** 1-13.

TAUCHER, J., BACH, L. T., RIEBESELL, U. & OSCHLIES, A. 2014. The viscosity effect on marine particle flux: A climate relevant feedback mechanism. *Global Biogeochemical Cycles,* 28**,** 415-422.

TEAL, J. M. & CAREY, F. G. Effects of pressure and temperature on the respiration of euphausiids. Deep Sea Research and Oceanographic Abstracts, 1967. Elsevier, 725-733.

TENGBERG, A., HOVDENES, J., ANDERSSON, H. J., BROCANDEL, O., DIAZ, R., HEBERT, D., ARNERICH, T., HUBER, C., KÖRTZINGER, A. & KHRIPOUNOFF, A. 2006. Evaluation of a lifetime-based optode to measure oxygen in aquatic systems. *Limnology and Oceanography: Methods,* 4**,** 7-17.

TESCHKE, M., PICCOLIN, F., SCHOLL, A., DE PITTA, C., COSTA, R., KAWAGUSHI, S., BISCONTIN, A., KRAMER, A. & MEYER, B. Biological timing in Antarctic krill: Endogenous clocks and physiological rhythms at the daily and annual scale. Time and Light: Novel Concepts and Models in Sensory and Chronobiology, 2016 Vienna.

TESCHKE, M., WENDT, S., KAWAGUCHI, S., KRAMER, A. & MEYER, B. 2011. A Circadian Clock in Antarctic Krill: An Endogenous Timing System Governs Metabolic Output Rhythms in the Euphausiid Species *Euphausia superba*. *Plos One,* 6.

TORRES, J. & CHILDRESS, J. 1983. Relationship of oxygen consumption to swimming speed in *Euphausia pacifica*. *Marine Biology,* 74**,** 79-86.

TORRES, J. J., AARSET, A., DONNELLY, J., HOPKINS, T. L., LANCRAFT, T. & AINLEY, D. 1994a. Metabolism of Antarctic micronektonic Crustacea as a function of depth of occurrence and season. *Marine Ecology Progress Series***,** 207-219.

TORRES, J. J., DONNELLY, J., HOPKINS, T. L., LANCRAFT, T., AARSET, A. & AINLEY, D. 1994b. Proximate composition and overwintering strategies of Antarctic micronektonic Crustacea. *Marine Ecology Progress Series***,** 221-232.

TRATHAN, P. N. & HILL, S. L. 2016. The importance of krill predation in the Southern Ocean. *Biology and Ecology of Antarctic Krill.* Springer.

TRUDNOWSKA, E., GLUCHOWSKA, M., BESZCZYNSKA-MÖLLER, A., BLACHOWIAK-SAMOLYK, K. & KWASNIEWSKI, S. 2016. Plankton patchiness in the Polar Front region of the West Spitsbergen Shelf. *Marine Ecology Progress Series,* 560**,** 1-18.

TURNER, J. T. 1977. Sinking rates of fecal pellets from the marine copepod *Pontella meadii*. *Marine Biology,* 40**,** 249-259.

TURNER, J. T. 1979. Microbial Attachment to Copepod Fecal Pellets and Its Possible Ecological Significance. *Transactions of the American Microscopical Society,* 98**,** 131-135.

TURNER, J. T. 2002. Zooplankton fecal pellets, marine snow and sinking phytoplankton blooms. *Aquatic Microbial Ecology,* 27**,** 57-102.

TURNER, J. T. 2004. The importance of small planktonic copepods and their roles in pelagic marine food webs. *Zoological Studies,* 43**,** 255-266.

TURNER, J. T. 2015. Zooplankton fecal pellets, marine snow, phytodetritus and the ocean's biological pump. *Progress in Oceanography,* 130**,** 205-248.

TURNER, J. T. & FERRANTE, J. G. 1979. Zooplankton Fecal Pellets in Aquatic Ecosystems. *BioScience***,** 670-677.

UCHIDA, H., KAWANO, T., KANEKO, I. & FUKASAWA, M. 2008. In situ calibration of optode-based oxygen sensors. *Journal of Atmospheric and Oceanic Technology,* 25**,** 2271-2281.

URBAN, J., MCKENZIE, C. & DEIBEL, D. 1993. Nanoplankton found in fecal pellets of macrozooplankton in coastal Newfoundland waters. *Botanica marina,* 36**,** 267-282.

URRÈRE, M. A. & KNAUER, G. A. 1981. Zooplankton fecal pellet fluxes and vertical transport of particulate organic material in the pelagic environment. *Journal of Plankton Research,* 3**,** 369-387.

VAN HAREN, H. & COMPTON, T. J. 2013. Diel vertical migration in deep sea plankton is finely tuned to latitudinal and seasonal day length. *PLoS ONE,* 8**,** e64435.

VENABLES, H., MEREDITH, M. P., ATKINSON, A. & WARD, P. 2012. Fronts and habitat zones in the Scotia Sea. *Deep Sea Research Part II: Topical Studies in Oceanography,* 59–60**,** 14-24.

VERVOORT, W. 1965. Notes of the biogeography and ecology of free-living, marine copepoda. *In:* MIEGHEM, J. V. & OYE , P. V. (eds.) *Biogeography and Ecology in Antarctica.* The Hague, Netherlands: Dr. W. Junk Publishers.

VINOGRADOV, M. E. 1962. Feeding of the deep-sea zooplankton. *Internat. Explor. de la Mer.,* 153**,** 114-120.

VINOGRADOV, M. E. E. 1970. *Vertical distribution of the oceanic zooplankton*, Israel Program for Scientific Translations.

VOLK, T. & HOFFERT, M. I. 1985. Ocean Carbon Pumps: Analysis of Relative Strengths and Efficiencies in Ocean-Driven Atmospheric CO_2 Changes. *In:* SUNDQUIST, E. T. & BROECKER, W. S. (eds.) *The Carbon Cycle and Atmospheric CO_2: Natural Variations Archean to Present.* Washington D.C.: American Geophysical Union.

VORONINA, N. M. 1972. The spatial structure of interzonal copepod populations in the Southern Ocean. *Marine Biology,* 15**,** 336-343.

WALLACE, M. I., COTTIER, F. R., BRIERLEY, A. S. & TARLING, G. A. 2013. Modelling the influence of copepod behaviour on faecal pellet export at high latitudes. *Polar Biology,* 36**,** 579-592.

WARD, P., ATKINSON, A., MURRAY, A., WOOD, A., WILLIAMS, R. & POULET, S. 1995. The summer zooplankton community at South Georgia: biomass, vertical migration and grazing. *Polar Biology,* 15**,** 195-208.

WARD, P., ATKINSON, A. & TARLING, G. 2012a. Mesozooplankton community structure and variability in the Scotia Sea: A seasonal comparison. *Deep Sea Research Part II: Topical Studies in Oceanography,* 59–60**,** 78-92.

WARD, P., ATKINSON, A., VENABLES, H. J., TARLING, G. A., WHITEHOUSE, M. J., FIELDING, S., COLLINS, M. A., KORB, R., BLACK, A., STOWASSER, G., SCHMIDT, K., THORPE, S. E. & ENDERLEIN, P. 2012b. Food web structure and bioregions in the Scotia Sea: A seasonal synthesis. *Deep Sea Research Part II: Topical Studies in Oceanography,* 59–60**,** 253-266.

WARD, P., SHREEVE, R., WHITEHOUSE, M., KORB, B., ATKINSON, A., MEREDITH, M., POND, D., WATKINS, J., GOSS, C. & CUNNINGHAM, N. 2005. Phyto- and zooplankton community structure and production around South Georgia (Southern Ocean) during Summer 2001/02. *Deep Sea Research Part I: Oceanographic Research Papers,* 52**,** 421-441.

WARD, P. & SHREEVE, R. S. 1999. The spring mesozooplankton community at South Georgia: a comparison of shelf and oceanic sites. *Polar Biology,* 22**,** 289-301.

WARD, P., TARLING, G. & THORPE, S. 2014. Mesozooplankton in the Southern Ocean: Spatial and temporal patterns from *Discovery Investigations*. *Progress in Oceanography,* 120**,** 305-319.

WARD, P., WHITEHOUSE, M., BRANDON, M., SHREEVE, R. & WOODD-WALKER, R. 2003. Mesozooplankton community structure across the Antarctic Circumpolar Current to the north of South Georgia: Southern Ocean. *Marine Biology,* 143**,** 121-130.

WARD, P., WHITEHOUSE, M., MEREDITH, M., MURPHY, E., SHREEVE, R., KORB, R., WATKINS, J., THORPE, S., WOODD-WALKER, R. & BRIERLEY, A. 2002. The Southern Antarctic Circumpolar Current Front: physical and biological coupling at South Georgia. *Deep Sea Research Part I: Oceanographic Research Papers,* 49**,** 2183-2202.

WARKENTIN, M., FREESE, H. M., KARSTEN, U. & SCHUMANN, R. 2007. New and fast method to quantify respiration rates of bacterial and plankton communities in freshwater ecosystems by using optical oxygen sensor spots. *Applied and environmental microbiology,* 73**,** 6722-6729.

WATKINS, J., BELCHER, A., DURET, M., ENDERLEIN, P., FIELDING, S., FLOTER, S., GARDNER, J., LA, H. S., LAMPITT, R., LISZKA, C., MIKIS, A., PECK, V., POLFREY, S., ROBST, J., STOWASSER, G., TARLING, G., THOMAS, J., THOMAS, S. & WOOTTON, M. 2015. JR304 Western Core Box & Moorings Cruise Report. British Antarctic Survey.

WEFER, G. & FISCHER, G. 1991. Annual primary production and export flux in the Southern Ocean from sediment trap data. *Marine Chemistry,* 35**,** 597-613.
WEST, G. B., BROWN, J. H. & ENQUIST, B. J. 1997. A General Model for the Origin of Allometric Scaling Laws in Biology. *Science,* 276**,** 122-126.
WESTBERRY, T., BEHRENFELD, M. J., SIEGEL, D. A. & BOSS, E. 2008. Carbon-based primary productivity modeling with vertically resolved photoacclimation. *Global Biogeochemical Cycles,* 22.
WEXELS RISER, C., REIGSTAD, M., WASSMANN, P., ARASHKEVICH, E. & FALK-PETERSEN, S. 2007. Export or retention? Copepod abundance, faecal pellet production and vertical flux in the marginal ice zone through snap shots from the northern Barents Sea. *Polar Biology,* 30**,** 719-730.
WHITEHOUSE, M., PRIDDLE, J. & SYMON, C. 1996. Seasonal and annual change in seawater temperature, salinity, nutrient and chlorophyll-*a* distributions around South Georgia, South Atlantic. *Deep Sea Research Part I: Oceanographic Research Papers,* 43**,** 425-443.
WHITEHOUSE, M. J., KORB, R. E., ATKINSON, A., THORPE, S. E. & GORDON, M. 2008. Formation, transport and decay of an intense phytoplankton bloom within the High-Nutrient Low-Chlorophyll belt of the Southern Ocean. *Journal of Marine Systems,* 70**,** 150-167.
WHITELEY, N. M., ROBERTSON, R. F., MEAGOR, J., EL HAJ, A. J. & TAYLOR, E. W. 2001. Protein synthesis and specific dynamic action in crustaceans: effects of temperature. *Comparative Biochemistry and Physiology Part A: Molecular & Integrative Physiology,* 128**,** 593-604.
WIAFE, G. & FRID, C. L. J. 1996. Short-term temporal variation in coastal zooplankton communities: the relative importance of physical and biological mechanisms. *Journal of Plankton Research,* 18**,** 1485-1501.
WIEBE, P. H., ASHJIAN, C. J., LAWSON, G. L., PIÑONES, A. & COPLEY, N. J. 2011. Horizontal and vertical distribution of euphausiid species on the Western Antarctic Peninsula U.S. GLOBEC Southern Ocean study site. *Deep Sea Research Part II: Topical Studies in Oceanography,* 58**,** 1630-1651.
WILSON, S., RUHL, H. & SMITH JR, K. 2013. Zooplankton fecal pellet flux in the abyssal northeast Pacific: A 15 year time-series study. *Limnology and Oceanography,* 58**,** 881-892.
WILSON, S. E., STEINBERG, D. K. & BUESSELER, K. O. 2008. Changes in fecal pellet characteristics with depth as indicators of zooplankton repackaging of particles in the mesopelagic zone of the subtropical and subarctic North Pacific Ocean. *Deep Sea Research Part II: Topical Studies in Oceanography,* 55**,** 1636-1647.
WOHLSCHLAG, D. E. 1960. Metabolism of an Antarctic fish and the phenomenon of cold adaptation. *Ecology,* 41**,** 287-292.
YOON, W., KIM, S. & HAN, K. 2001. Morphology and sinking velocities of fecal pellets of copepod, molluscan, euphausiid, and salp taxa in the northeastern tropical Atlantic. *Marine Biology,* 139**,** 923-928.